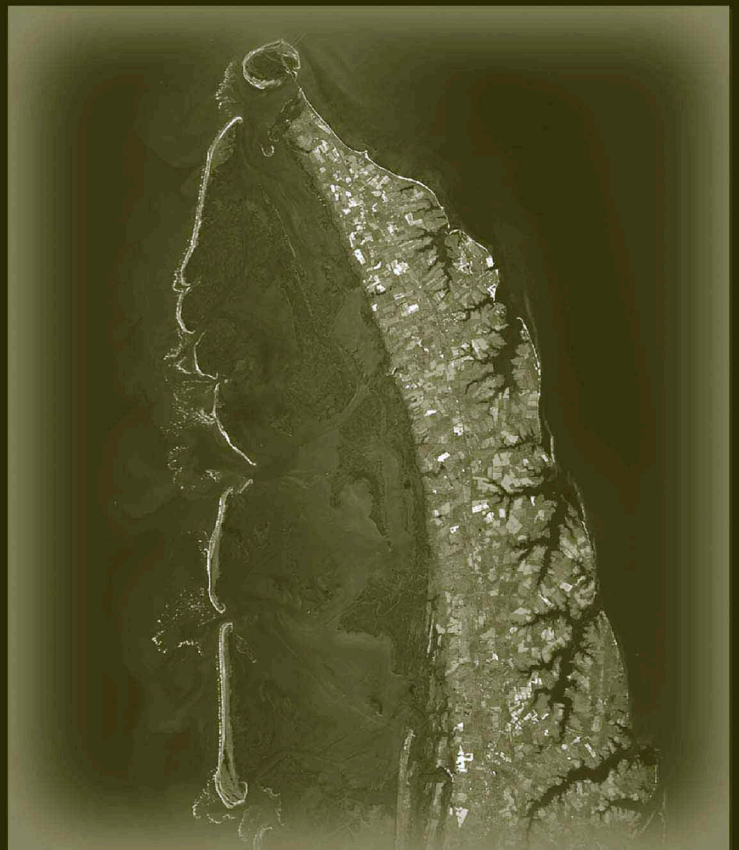




RESEARCH & TECHNOLOGY

NASA AMES RESEARCH CENTER



RESEARCH & TECHNOLOGY
NASA AMES RESEARCH CENTER

2001



NATIONAL AERONAUTICS AND SPACE ADMINISTRATION
AMES RESEARCH CENTER • MOFFETT FIELD, CALIFORNIA

NASA/TM-2003-211405

Notice

The use of trade names and manufacturers in this document does not constitute an official endorsement of such products or manufacturers, either expressed or implied, by the National Aeronautics and Space Administration.

Available from:

NASA Center for AeroSpace Information
7121 Standard Drive
Hanover, MD 21076-1320
(301) 621-0390

National Technical Information Service
5285 Port Royal Road
Springfield, VA 22161
(703) 487-4650

Foreword

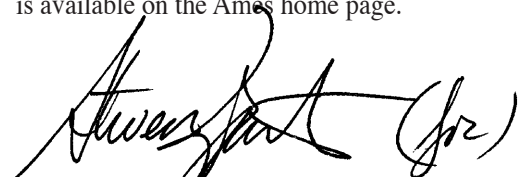
This report highlights the research accomplished during fiscal year 2001 by Ames Research Center scientists and engineers. The work is divided into accomplishments that support four of NASA's Strategic Enterprises: Aerospace Technology, Space Science, Biological and Physical Research, and Earth Science. The key purpose of this report is to communicate information to our stakeholders about the scope and diversity of Ames' mission and the nature of Ames research and technology activities.

Ames Research Center is making significant contributions to the Aerospace Technology Enterprise mission by developing and commercializing high-payoff aeronautics and space transportation technologies. Under NASA's Aviation Systems program, Ames is developing air-traffic management decision-support tools that will significantly improve the productivity of the nation's airports. Ames is a leader in the application of neural networks and genetic algorithms for the real-time reconfiguration of flight controls, and is developing new thermal protection systems that promise radical improvements in vehicle entry performance.

Ames is recognized as a world leader in Astrobiology, the study of life in the Universe and of the chemical and physical forces and adaptations that influence life's origin, evolution, and destiny. Key areas of research include the study of the abundance and distribution of biogenic compounds conducive to the origin of life, the study of life in extreme environments, and modeling of clouds in brown dwarf atmospheres and the thermal properties of dust grains in comets. Ames supports the Office of Earth Science by conducting research in bio-geochemical cycling, ecosystem dynamics, and the chemical and transport processes that determine atmospheric composition, dynamics, and climate. The work supports our astrobiology effort, by studying the physical and biological processes that determine the behavior of the atmosphere on Earth and on solar system bodies. Support for the Biological and Physical Research Enterprise is centered around the role that gravity has played in shaping life on Earth, and what effect its absence has on living systems in space. Research carried out at the sub-cellular level specifically addresses the fundamental biological mechanisms underlying physiological changes in humans caused by the spaceflight environment. Work also continues on developing life-support capabilities for long-duration travel and habitation on other planets, as well as equipment to operate safely and effectively in micro-gravity.

Ames has also been designated the Agency's Center of Excellence for Information Technology. The three cornerstones of Information Technology research at Ames are automated reasoning, human-centered computing, and high performance computing and networking. The mission critical capabilities enabled by NASA's three cornerstones of Information Technology span all of NASA's strategic enterprises.

For further information on Ames' research and technology projects, please contact the person designated as the point of contact at the end of each article. For further information about the report itself, contact Dr. Stephanie Langhoff, Chief Scientist, Mail Stop 230-3, NASA Ames Research Center, Moffett Field, CA 94035. An electronic version of this report is available on the Ames home page.



G. Scott Hubbard
Director, Ames Research Center

Aerospace Technology Enterprise

Overview	1
-----------------------	----------

GOAL 1 - REVOLUTIONIZE AVIATION

OBJECTIVE 1

Intelligent Neural Flight and Propulsion Control System	4
<i>Karen Gundy-Burlet</i>	
Los Angeles International Airport Runway Incursion Studies: Finding Solutions for a Safer Airport	5
<i>Nancy Dorigi</i>	
Computational Modeling of Pilot Taxi Errors	6
<i>Allen Goodman, David C. Foyle</i>	
Opportunities for and Vulnerabilities to Error in Everyday Flight Operations.....	8
<i>Loukia D. Loukopoulos, R. Key Dismukes, Immanuel Barshi</i>	
Risk Assessment and Risk Management in Aviation Decision Making	10
<i>Judith Orasanu, Ute Fischer, Jeannie Davison, Yuri Tada, Lori McDonnell</i>	
Performance Data Analysis and Reporting System	11
<i>Irving C. Statler</i>	
Aviation System Monitoring and Modeling (ASMM): Modeling and Simulation of Clear-Air Turbulence Detection and Response.....	13
<i>Irving C. Statler, Mary Connors</i>	
Scheduling Assistant Software: A Tool for Airline Scheduling	14
<i>Melissa M. Mallis</i>	
Sound Laboratory: A Software-Based System for Interactive Spatial Sound Synthesis	16
<i>Elizabeth M. Wenzel, Joel D. Miller</i>	

OBJECTIVE 2

Computational Simulation of Formation Flight of F-18 Aircraft	17
<i>Steven C. Smith</i>	

OBJECTIVE 3

Boeing 777 Subsonic Transport Aeroacoustic Research	19
<i>Paul T. Soderman, Clifton Horne, Kevin D. James</i>	

Simulation of Aircraft Flightpath Noise and of Noise Abatement Procedures	21
<i>Terrance K. Rager</i>	

O B J E C T I V E 4

Operational Evaluation of the Direct-To Controller Tool	22
<i>David T. McNally</i>	
Neighboring Optimal Wind Routing	24
<i>Matthew R. Jardin</i>	
Probabilistic Forecasting of Air Traffic Demand	25
<i>Larry A. Meyn</i>	
En Route Data Exchange	27
<i>Richard A. Coppenbarger</i>	
Flight Deck Tools for Distributed Air-Ground Decision Making in Future ATM Systems	28
<i>Vernol Battiste, Walter Johnson</i>	
Surface Management System Simulation	30
<i>Stephen C. Atkins</i>	
Virtual National Airspace Simulation System	31
<i>Yuri Gawdiak, Bill McDermott, David Maluf, Peter Tran</i>	

O B J E C T I V E 5

Large-Scale Test Bed Developed for Investigating Tilt-Rotor Aeromechanics and Terminal Area Operation	33
<i>Megan S. McCluer, Jeffery L. Johnson</i>	
A Wind Tunnel Investigation of a Small-Scale Tilt-Rotor Model in Descending Flight ..	34
<i>Anita I. Abrego, Kurtis R. Long</i>	
Wind Tunnel Visualization of Descending Tilt-Rotor Wake Aerodynamics	35
<i>Kurtis R. Long, John Zuk, Robert K. Callaway</i>	
Influence of Wake Models on Calculated Tilt-Rotor Aerodynamics	36
<i>Wayne R. Johnson</i>	
Individual Blade Control for RIA Noise Reduction.....	37
<i>Stephen A. Jacklin, Tom Norman, Patrick Shinoda</i>	
The 7- by 10-Foot Wind Tunnel Investigation of a Ducted Fan System	39
<i>Anita I. Abrego, Robert W. Bulaga</i>	

GOAL 2 - ADVANCE SPACE TRANSPORTATION

OBJECTIVE 6**Updated Displays for the Cockpit of the Space Shuttle 40***Jeffrey W. McCandless, Robert S. McCann*OBJECTIVE 7**Investigation of New Liquefying-Fuel Hybrid Rocket Motors 41***Shane DeZilwa, Gregory G. Zilliac*OBJECTIVE 8**Mars Rotorcraft Scout..... 42***Larry A. Young*

GOAL 3 - PIONEER TECHNOLOGY INNOVATION

OBJECTIVE 9**Pegasus5 Prepares Overset CFD Grids..... 45***Stuart Rogers***The Information Power Grid (IPG) Project 46***Arsi Vaziri, William E. Johnston***Programming Paradigms for Adaptive Applications on SGI Origin 48***Rupak Biswas***Facilitating Human Performance Modeling 49***Alonso Vera, Roger Remington, Michael Matessa, Michael Freed***Subjective Estimation of Visual Quality..... 51***Andrew B. Watson***Text Readability Metric Validated for Transparent Text 53***Albert Ahumada***Computational Modeling of Hovering Rotors and Wakes..... 54***Roger C. Strawn***Unsteady Pressure-Sensitive Paint Measurements on an Oscillating Airfoil 55***Edward T. Schairer, Lawrence A. Hand***Wind Tunnel Tests to Determine the Air-Wake Characteristics of U.S. Navy Ships..... 57***Kurtis R. Long, James T. Heineck*

OBJECTIVE 10

Semiconducting Nanotube—Electrode Contact Modeling.....	59
<i>Toshishige Yamada</i>	
Current Carrying Capacity of Carbon Nanotubes.....	61
<i>M. P. Anantram</i>	
Protein Nanotechnology	62
<i>Jonathan Trent, Andrew McMillan, Chad Paavola</i>	
Nanostructured Skin Effect: Anisotropic Plasticity of Boron-Nitride Nanotubes	64
<i>Deepak Srivastava</i>	
Ultrafast Modulation of Coupled Surface-Emitting Lasers.....	66
<i>Cun-Zheng Ning, Peter Goorjian</i>	
Expanding the Envelope for Shared Memory High-Performance Computing	67
<i>James Taft</i>	
Using Electromyography to Predict Head Motion for Virtual Reality Applications	68
<i>Yair Barniv</i>	
A Real-Time System for Unobtrusive Gaze Tracking.....	69
<i>Jeffrey B. Mulligan</i>	
Kinesthetic Compensation for Rotational Misalignment of Cameras Used for Teleoperation.....	71
<i>Stephen R. Ellis, Bernard D. Adelstein, Robert B. Welch</i>	

Space Science Enterprise

Overview	75
-----------------------	-----------

ASTROPHYSICS

Organic Solids Color the Icy Bodies in the Outer Solar System.....	78
<i>Dale P. Cruikshank, Bishun N. Khare</i>	
A Cryogenic Multiplexer for Far-infrared Astronomy	79
<i>Jessie L. Dotson, Edwin Erickson, Chris Mason</i>	
Scientific Requirements of the NGST Mid-IR Instrument	80
<i>Thomas Greene</i>	

An Interstellar Rosetta Stone: A Database of the Infrared Spectra of Polycyclic Aromatic Hydrocarbons (PAHs)	81
<i>Douglas M. Hudgins, Louis J. Allamandola</i>	
The SOFIA Water-Vapor Monitor Nears Completion.....	83
<i>Thomas L. Roellig, Robert Cooper, Brian Shiroshima, Regina Flores, Lunming Yuen, Allan Meyer</i>	
Using Deuterium to Trace the Links Between Interstellar Chemistry and the Organics that Seeded the Early Earth.....	84
<i>Scott A. Sandford, Louis J. Allamandola, Max P. Bernstein, Jason P. Dworkin</i>	

E X O B I O L O G Y

EMERG Greenhouse One: Simulations of Remote and Ancient Earth Environments at Ames	86
<i>Brad M. Bebout</i>	
A Terrestrial Analog for the Martian Meteorite ALH84001	86
<i>David Blake, Allan H. Treiman, Hans E.F. Amundsen, Ted Bunch</i>	
Microbial Mats and the Origins of Photosynthesis	88
<i>David J. DesMarais, Dan Albert, Brad M. Bebout, Mykell Discipulo, Tori M. Hoehler, Kendra Turk</i>	
Large-Magnitude Biological Input of Hydrogen to the Archaean Atmosphere	89
<i>Tori M. Hoehler, Brad M. Bebout, David J. DesMarais</i>	
Analysis of the Tagish Lake Meteorite	90
<i>Sandra Pizzarello, Yongsong Huang, Luann Becker, Robert J. Poreda, Ronald A. Nieman, George W. Cooper, Michael Williams</i>	
Computational Modeling of Regulatory Networks in Cells.....	91
<i>Andrew Pohorille, Stephen Bay, Pat Langley, Jeff Shrager</i>	
A High-Performance, Low-cost Linux Cluster for Genomics	92
<i>Karl Schweighofer, Rick Graul</i>	

P L A N E T A R Y S C I E N C E

Organic Chemistry Leading to Life	94
<i>Emma Bakes, Alexander Tielens, Charles Bauschlicher, C. P. McKay, Stephen Walch, William J. Borucki, Robert C. Whitten, Bishun Khare, Louis Allamandola, Douglas Hudgins, Sebastien Lebonnois, Hiroshi Imanaka</i>	
Probing Dust Processing Events in Accretion Disk Atmospheres Using Two-Dimensional Radiative Transfer Models	95
<i>K. Robbins Bell, Diane Wooden, David Harker, Charles Woodward</i>	

The Kepler Mission: A Photometric Mission to Determine the Frequency of Earth-Size Planets in the Habitability Zone of Solar-Like Stars.....	96
<i>William J. Borucki, David G. Koch</i>	
Effect of Negative Ions on the Conductivity of Titan's Lower Atmosphere	97
<i>William J. Borucki, E. L. Bakes, Robert C. Whitten</i>	
The Vulcan Photometer: A Dedicated Photometer for Extrasolar Planet Searches	98
<i>William J. Borucki, Douglas A. Caldwell, David G. Koch, Jon Jenkins</i>	
Extrasolar Planet Detector for the South Pole	98
<i>Douglas A. Caldwell, Robert L. Showen, Kevin R. Martin, William J. Borucki, Zoran Ninkov</i>	
Circumstellar Carbonaceous Dust	99
<i>Jean E. Chiar, Alexander G.G.M. Tielens</i>	
Organics and Ices Toward the Galactic Center	100
<i>Jean E. Chiar, Andrew J. Adamson, Yvonne J. Pendleton, Douglas C. B. Whittet</i>	
Artificial Intelligence Techniques for Large-Scale Surveys of Space Science Data	102
<i>Paul R. Gazis, Aaron Barnes, Clark Glymour</i>	
Origin of the Thermal Inertia Continents on Mars	102
<i>Robert M. Haberle</i>	
The Center for Star Formation Studies	104
<i>D. Hollenbach, K. R. Bell</i>	
Understanding the Cloudy Skies of Brown Dwarfs	105
<i>Mark Marley, Andrew Ackerman, Richard Freedman</i>	
The Ultraviolet Photodecomposition of Martian Carbonates	106
<i>Richard C. Quinn, Aaron P. Zent, Christopher P. McKay</i>	
Reflectance Spectra of Titan Tholins at Cryogenic Temperatures	107
<i>T. L. Roush, J. B. Dalton</i>	
New Algorithms for Mining Time Series and Image Databases.....	108
<i>Jeffrey D. Scargle</i>	
Grain Properties of Solar System Comets.....	109
<i>Diane Wooden, David Harker, Charles Woodward</i>	
Static Stability of Jupiter's Atmosphere	109
<i>Richard E. Young, Julio A. Magalhães, Alvin Seiff</i>	
Carbon Dioxide Cycling and the Climate of Early Earth	111
<i>Kevin Zahnle, Norm Sleep</i>	

The Martian Regolith and Climate.....	112
<i>Aaron P. Zent, Richard C. Quinn</i>	

SPACE TECHNOLOGY

Focal-Plane Detector Array Development for Astronomy in Space	113
<i>Mark E. McKelvey, Kimberly A. Ennico, Roy R. Johnson, Robert E. McMurray, Jr., Craig R. McCreight</i>	
A Lightweight, High-Efficiency Pulse Tube Cryocooler for Spaceflight Applications ...	115
<i>Louis J. Salerno, Peter Kittel, Ali Kashani, Ben Helvensteijn</i>	

ADVANCED COMPUTER SCIENCE TECHNOLOGY

K9 Planetary Exploration Rover Prototype	117
<i>Maria Bualat</i>	
NASA IVHM Technology Experiment for X-Vehicles (NITEX) Propulsion IVHM Technology Experiment (PITEX)	118
<i>Howard Cannon</i>	
A Collaborative Web Facility for Mars Data Analysis	119
<i>Glenn Deardorff</i>	
A Planner-Based Software Agent for Data Management	121
<i>Keith P. Golden</i>	
PathExplorer: A Runtime Verification Tool	122
<i>Klaus Havelund, Grigore Rosu</i>	
Clickworkers Project	123
<i>Bob Kanefsky</i>	
ScienceOrganizer	125
<i>Richard Keller</i>	
Livingstone Qualitative Modeling Development Software Tools	126
<i>Mark Shirley</i>	
Quantum Optimization Algorithms	127
<i>Vadim Smelyanskiy, Dogan Timucin</i>	
Human-Centered Computing for the Mars Exploration Rover 2003 Mission	128
<i>Jay Trimble</i>	
Autofilter: Generation of Trusted State Estimation Code from Mathematical Models.....	129
<i>Jonathan Whittle</i>	

Designing Collectives for Distributed Control	130
<i>David Wolpert, Kagan Tumer</i>	

Biological and Physical Research Enterprise

Overview	133
-----------------------	------------

A P S S Y S T E M S A N A L Y S I S

Flow Field Measurements in a Cell Specimen Chamber	135
<i>Stephen Walker, Michael Wilder</i>	

International Space Station Module Noise Control.....	137
<i>Nathan J. Burnside, Paul T. Soderman</i>	

S L R G R A V I T A T I O N A L R E S E A R C H

SPRING: A Surgical Simulator Adapted to Astronaut Training for Space Life Sciences Research.....	139
<i>Richard D. Boyle, Jeffery D. Smith</i>	

Skeletal Unloading in a Salt-Sensitive Hypertension Model.....	141
<i>Sara B. Arnaud</i>	

Computed Tomography X-ray Beam Spectrum Estimation	142
<i>Robert Whalen, Tammy Cleek, Miki Matsubara</i>	

Accurate Measurement of Bone Density with Quantitative Computed Tomography.....	144
<i>Robert Whalen, Tammy Cleek, Miki Matsubara, Gary Beaupré, Chye Yan</i>	

Mechanical and Gravitational Loading of Osteoblasts.....	146
<i>Nancy D. Searby, Ruth K. Globus</i>	

Molecular and Cellular Characterization of a Mitotic Checkpoint Gene during Zebrafish Development: Implications for the Responses to Space Radiation and Human Breast Cancer	148
<i>Gregory Conway</i>	

Cell Culture Unit Development for the International Space Station	151
<i>Nancy D. Searby, Donald P. Vandendriesche</i>	

Tissue-Level and Whole Animal Responses to Altered Gravity	153
<i>Catharine A. Conley</i>	

Insertional Mutagenesis Screen for Otic and Other Genes in <i>Xenopus Tropicalis</i>.....	154
<i>Marcela Torrejon, Sigrid Reinsch</i>	

Toward the First Mammalian Birth in Space: Insights Derived from Hypergravity	156
<i>April E. Ronca, Lisa A. Baer, Charles E. Wade</i>	

Chronic Acceleration (Hypergravity) Influences the Circadian System of the Rat	160
<i>Charles W. DeRoshia, Daniel C. Holley, Margaret M. Moran, Charles E. Wade</i>	

S S R A S T R O B I O L O G Y T E C H N O L O G Y

Atmospheric Resources for Exploration of MARS.....	163
<i>John Finn, Dave Affleck, Lila Mulloth</i>	

Rotating-Disk Analytical System (R-DAS)	164
<i>Michael Flynn, Bruce Borchers</i>	

Clean Incineration for Space Missions	165
<i>John W. Fisher, Suresh Pisharody</i>	

S L O S C I E N C E P A Y L O A D S O P E R A T I O N S

Cooperative Approach to Commercial Biomedical Testing in Space	167
<i>Beverly Girten</i>	

S F D S Y S T E M S D E V E L O P M E N T

Passive Dosimeter System	169
<i>Nina Scheller, Kristofer Vogelsong</i>	

Earth Science Enterprise

Overview	173
-----------------------	------------

A I R B O R N E S E N S O R F A C I L I T Y

The Airborne Sensor Facility - 2001	176
<i>Jeff Myers, Bruce Coffland, Pat Grant, Ted Hildum, Mike Fitzgerald, Rose Dominguez</i>	

S G E - E C O S Y S T E M S C I E N C E T E C H N O L O G Y B R A N C H

Development of a Tactical System for Fire Management and Prediction	179
<i>James Brass, Steve Wegener, Donald Sullivan, Vince Ambrosia, Bob Higgins, Philip Hammer, Ted Hildum, Roy Vogler</i>	
Ecoinformatics: Aerospace Technologies in the Service of Global Health	180
<i>Byron Wood, Brad Lobitz</i>	
Land-Use Effects on Biogeochemistry in the Amazon.....	183
<i>Liane Guild, Christopher Potter</i>	
Modeling Terrestrial Ecosystem Processes	184
<i>Christopher Potter, Liane Guild, Steven Klooster, Vanessa Brooks Genovese, Kelly Decker, David Bubenheim, Hanwant Singh</i>	
On the Feasibility of Using Support Vector Machines to Automatically Extract Open Water Signatures from POLDER Multiangle Data over Boreal Regions	185
<i>V. C. Vanderbilt</i>	
Oxidative Damage in Nature	186
<i>Lynn J. Rothschild</i>	
Past Sea Surface Temperature Derived from Tree Rings.....	187
<i>Hector L. D'Antoni, Ante Mlinarevic</i>	
Planning and Scheduling of Earth-Observing Satellites.....	187
<i>Jennifer Dungan</i>	
Quantifying Uncertainty About Earth Science Information	188
<i>Jennifer Dungan</i>	
Space Solar Power—2001	190
<i>J. W. Skiles</i>	
UAV Remote-Sensing Technology for Agricultural Monitoring	191
<i>Stanley R. Herwitz, Stephen E. Dunagan, Lee F. Johnson, Robert E. Slye, Donald V. Sullivan, Jian Zheng, Robert Higgins</i>	

S G G - A T M O S P H E R I C C H E M I S T R Y A N D D Y N A M I C S B R A N C H

Airborne Measurements of Aerosols and Water Vapor in Support of the Chesapeake Lighthouse and Aircraft Measurements for Satellites (CLAMS) Experiment, 2001	193
<i>Jens Redemann, Beat Schmid, John Livingston, James Eilers, Ric Kolyer, Stephanie Ramirez, Phil Russell</i>	

Airborne Tracking Sunphotometry and Related Studies of Aerosols and Trace Gases.....	194
<i>Philip B. Russell, Beat Schmid, Jens Redemann, John Livingston, Robert Bergstrom, James Eilers, Richard Kolyer, Duane Allen, Stephanie Ramirez, Dawn McIntosh</i>	
Direct Measurements of Stable Isotope Ratios in Nitrous Oxide in Air	196
<i>Hansjürg Jost, James R. Podolske</i>	
Evolution of an Unmanned Aerial Vehicle Science Mission Capability	197
<i>Steven S. Wegener</i>	
Fourth Convection and Moisture Experiment (CAMEX 4): 15 August - 26 September 2001	198
<i>R. Stephen Hipskind, Michael S. Craig</i>	
Global Distribution and Sources of Volatile and Nonvolatile Aerosol in the Remote Troposphere.....	200
<i>Hanwant B. Singh, W. Viezee, Y. Chen, A. Tabazadeh, R. Pueschel</i>	
Laboratory Studies of Atmospheric Heterogeneous and Multiphase Chemistry	201
<i>Laura T. Iraci, Samantha Ashbourn</i>	
Open-Path Diode Laser Hygrometer Instrument for Tropospheric and Stratospheric Water-Vapor Studies	202
<i>James R. Podolske</i>	
Thin Cirrus and Horizontal Transport Studies.....	203
<i>Henry Selkirk, Leonhard Pfister, Marion Legg, Eric Jensen</i>	
Transport and Meteorological Analysis	203
<i>Leonhard Pfister, Henry Selkirk</i>	

S G P - A T M O S P H E R I C P H Y S I C S B R A N C H

Climate Forcing by Clouds and Aerosols: Two Years of Field Studies	206
<i>Peter Pilewskie, Warren Gore, Larry Pezzolo</i>	
Discriminating Type Ia and Ib Polar Stratospheric Clouds in POAM Satellite Data	208
<i>Anthony W. Strawa, Katja Drdla, Rudolf F. Pueschel</i>	
Evidence for the Widespread Presence of Liquid-Phase Particles During the 1999-2000 Arctic Winter.....	209
<i>Katja Drdla, T. P. Bui, H. Jost, J. Greenblatt</i>	
Ice Cloud Formation and Dehydration Along Parcel Trajectories in the Tropical Tropopause Layer.....	209
<i>Eric Jensen, Leonhard Pfister</i>	

In Situ Measurement of Particle Extinction	211
<i>Anthony W. Strawa</i>	
Intensity Measurements of CO₂ Absorption Bands Between 5218 and 5349 cm⁻¹	212
<i>Lawrence P. Giver, Charles Chackerian, Jr., Richard S. Freedman</i>	
Laboratory Measurements of Near-Infrared Water Vapor Bands Using the Solar Spectral Flux Radiometer	212
<i>Lawrence P. Giver, Peter Pilewskie, Warren J. Gore, Charles Chackerian, Jr., Richard S. Freedman</i>	
Microphysical Modeling of Chlorine Activation and Ozone Depletion.....	213
<i>Katja Drdla</i>	
Microphysical Modeling of Polar Stratospheric Clouds, Denitrification, and Dehydration.....	214
<i>Katja Drdla</i>	
Precipitation Condensation Clouds in Substellar Atmospheres	215
<i>Andrew Ackerman</i>	
Quantitative Spectroscopy of Minor Constituents of the Earth's Stratosphere	216
<i>Charles Chackerian, Jr., Lawrence P. Giver</i>	
The Effect of Large Volcanic Eruptions on Arctic Ozone Loss and Recovery	217
<i>Azadeh Tabazadeh, Katja Drdla</i>	
The Effect of Nitric-Acid Uptake on the Deliquescence and Efflorescence of Binary Ammoniated Salts in the Upper Troposphere	219
<i>Jin-Sheng Lin, Azadeh Tabazadeh</i>	
The Runaway Greenhouse Effect on Earth and Its Implication for Other Planets	222
<i>Maura Rabbette, Peter Pilewskie, Christopher McKay (Code SST), Richard Young (Code SST)</i>	

Aerospace Technology

Enterprise





Overview

NASA's mission for the Office of Aerospace Technology (OAT) Enterprise is to pioneer the identification, development, application, and commercialization of high-payoff aeronautics and space-transportation technologies. The Enterprise's research and technology programs promote economic growth and contribute to the national security through advances that will lead to a safe and efficient national aviation system, affordable and reliable space transportation, and improved information-management systems.

Research and development conducted by the OAT Enterprise is led by individual NASA research centers according to primary roles and core competencies. Ames Research Center utilizes its core competencies and its areas of unique expertise to lead research and technology development activities to achieve the OAT Enterprise goals. Those goals are to:

- Develop an environmentally friendly global air-transportation system for the next century that will provide unquestioned safety and improve the Nation's mobility
- Revolutionize air travel and the way in which air and space vehicles are designed, built, and operated
- Achieve the full potential of space for all human endeavors through affordable space transportation

The OAT Enterprise manages through a carefully defined set of technology areas that are aligned with designated Center Missions. Lead Centers have the responsibility to manage the implementation and execution phases of technology programs. To achieve this mission, NASA has designated Ames Research Center as the Center of Excellence for Information Technology and has delegated to Ames the lead role for basic research in Aviation Operations Systems, Information Systems Technology, and Rotorcraft. Ames is also the NASA Lead Center for focused

A controller using the Surface Management System (SMS) during a simulation in FutureFlight Central.

programs in Aviation System Capacity and High-Performance Computing and Communications. To perform these leadership roles, Ames maintains Agency leads in the core competencies of information technology, biotechnology, nanotechnology, and aerospace operations systems, with unique expertise areas in vertical flight and in thermal protection systems.

The goals and plans of the OAT Enterprise directly support national policy in both aeronautics and space, as those goals and plans are documented in “Goals for a National Partnership in Aeronautics Research and Technology” and the “National Space Transportation Policy,” respectively. The following paragraphs highlight Ames Research Center’s accomplishments in FY01 toward achieving the goals of the Enterprise.

Global Civil Aviation

Air transportation is an essential component of the economic progress of the United States. Efficient aviation operations assist in domestic industrial progress and help U.S. businesses compete in the increasingly global marketplace. Aviation products are also a major contributor to a positive U.S. industrial balance of trade. Projections linked to world economic growth suggest that air travel demand will double over the next 20 years.

To preserve the Nation’s economic health and the welfare of the traveling public, NASA must provide technology advances that contribute to safer, cleaner, quieter, and more affordable air travel. Ames has unsurpassed expertise in key disciplines that are requisite to addressing these challenges. These disciplines include human-centered air-traffic management automation tools, innovative rotorcraft and short takeoff vehicles, integrated design-automation tools, and technologies for managing and communicating information on every level. Ames maintains key national facilities that are crucial for performing the basic and applied research needed to support the U.S. aerospace industry. These efforts are all part of Ames’ contribution to safety, capacity, and affordability objectives.

Airlines and other businesses lose billions of dollars annually as a result of delays and lost productivity owing to weather and traffic congestion in the current airspace system. Under the Aviation Systems program, Ames has developed air-traffic management decision-support tools such as the Direct-To (D-2) component of the Center/ TRACON Automation System (CTAS). The success of the CTAS has led to its widespread FAA acceptance, including fielding the system at numerous major airports across the country. During FY01, the installation of these tools was continued at several U.S. sites under the FAA’s “Free Flight Phase 1” program. Ames also leads in the development of innovative air vehicles, such as the Civil Tiltrotor transport, that can lay the foundation for changes in airport operations that will help decrease aviation congestion.

While increasing the capacity and affordability of the aviation system, Ames is improving safety with innovative research into new aircraft crew station designs and display systems and into human-centered air-traffic controller station design. In addition, advanced neural network control systems promise the ability to autonomously reconfigure a vehicle so that it can survive the failure of virtually any of its systems. An example of this reconfiguration capability was flight tested in conjunction with the Dryden Flight Research Center.

A major challenge associated with the more extensive use of rotorcraft in alleviating air-traffic congestion is noise abatement. Ames projects are providing revolutionary technology advances in aeroacoustics, including Higher Harmonic Control (HHC) for blade-vortex-interaction noise reduction, phased microphone-array technology, and development of a Tilt Rotor Aeroacoustic Model (TRAM). Some early results indicate that HHC might reduce rotor noise by a factor of 4 at certain frequencies.

Revolutionary Technology

NASA’s charter is to explore high-risk technology areas that can revolutionize air travel and create new markets for U.S. industry. The technology challenges for NASA include eliminating the barriers to affordable and environmentally friendly high-speed

travel, expanding general aviation, and accelerating the application of technology advances to increase design confidence and decrease design cycle time. Next-generation design tools will revolutionize the aviation industry and benefit all three OAT Enterprise goals, contributing to every technology objective. Ames' aerospace and information technology research programs are developing aerospace-vehicle design tools that integrate the design system with performance analysis and high-accuracy computational and wind-tunnel performance testing. These Ames-developed systems have demonstrated order-of-magnitude improvements in the time required to develop and validate a successful design. The Control Designer's Unified Interface (CONDUIT) technology, developed at Ames to greatly reduce the time required to design control systems, is now in widespread use in both government and industry. Additional research at Ames in information technology will elevate the power of computing tools to that of artificial domain experts through the application of fuzzy logic, neural networks, and other new artificial intelligence methods. New tools will integrate multidisciplinary product teams, linking design, operations, and training databases to dramatically cut design-cycle times and improve operational efficiency. Ames' accomplishments include applying neural networks and genetic algorithms for real-time reconfiguration of integrated flight controls to alleviate system failures, aerodynamic optimization design and analysis tools, and the Environmental Research Aircraft and Sensor Technology (ERAST) flight program. Additionally, in FY01 Ames made significant progress in the application of nanotechnology, including demonstration of the ability to create nano-scale electronic devices utilizing carbon nanotubes.

Access to Space

Low-cost access to space is key to realizing the commercial potential of space and to greatly expanding space research and exploration. Through integration of aviation technologies and flight operations principles with commercial launch vehicles, a tenfold reduction in the cost of placing payloads in low-Earth orbit is anticipated within the next decade. High reliability and rapid turnaround are the first steps to increased confidence in delivering payloads on

time with smaller ground crews. NASA has initiated research on a broad spectrum of technology advancements that have the potential to reduce costs well beyond the initial reusable launch vehicle goals. This involves new technologies and the integration of aeronautical principles such as air-breathing propulsion and advanced structures. This will enable a cost-to-orbit measured in hundreds, not thousands, of dollars per pound. Additional innovative work in interplanetary spacecraft thermal protection and autonomous vehicle systems promises to decrease the mass of interplanetary spacecraft while dramatically improving their reliability and performance.

Ames is developing new thermal protection systems that will enable radical improvements in vehicle entry performance. If forced to de-orbit in an emergency, current spacecraft, such as the space shuttle, have very limited cross-range capability; consequently, the crew has very few available landing sites. Dramatic improvements in thermal protection technology, such as the SHARP (Slender Hypervelocity Aerothermodynamic Research Probe), will allow radically different aerodynamic shapes that will lead to dramatic improvements in cross-range capability. A flight test of some of these technologies, conducted aboard a rocket in the B-2 experiment, is yielding data that will be helpful in understanding more completely the ways in which these new materials must be developed. Advanced sensor technology and intelligent vehicle health management research will provide order-of-magnitude decreases in the cost and time required to inspect and refurbish reusable launch vehicles. These Ames technologies are at the heart of system-wide improvements in the launch-to-low-Earth-orbit space transportation market.

Aviation and space transportation have been exciting and challenging areas of scientific and engineering endeavor since their inception. The basic aerospace paradigm is shifting from large hardware developments to information-based design and data system management. As NASA's Center of Excellence for Information Technology, Ames Research Center's contribution will continue to grow throughout the new century.

Intelligent Neural Flight and Propulsion Control System

Karen Gundy-Burlet

Modern commercial aircraft constitute one of the safest transportation systems ever designed. But even with their track record of successful operation, aircraft remain vulnerable to failures of flight-control systems, whether because of accident or equipment malfunction. Post-accident analyses of catastrophic flight-control accidents show that stricken aircraft usually retain some working control surfaces at the time of the crash. Given enough time, a skilled pilot can often determine how to compensate for the loss of a control surface, but there is usually not enough time during an aircraft emergency for a human pilot to determine the nature of the failure and learn how to compensate for the loss. The objective of this program is to develop next-generation neural flight controllers using enhanced neural network adaptive-control algorithms and interface technologies to automatically compensate for a broad spectrum of damage or failures, to control remote or autonomous vehicles, and to reduce costs associated with flight-control law development.

The Intelligent Neural Flight and Propulsion Control System (INFPCS) was successfully demonstrated in 2000 on a modern fly-by-wire concept transport-class aircraft. As a result of the success of the INFPCS experiment, the question arose as to whether or not the concept could be retrofitted onto today's transport fleet, which mostly utilizes hydraulics and cables to drive the control surfaces. One major issue in evaluating a potential retrofit solution was measuring the trade-off between benefit and cost. The objective of the study was to find the lowest cost implementation that had significant benefit potential.

The test platform selected for the retrofit study was the B747-400 Level-D certified flight simulator at Ames Research Center (figure 1). Like many aircraft, the B747-400 is equipped with a hydraulic actuator control system, yaw-damper, and simulated force-feel steering column/wheel interface. The throttles could not be individually driven in this aircraft, so propulsion control was not utilized in the retrofit experiment. However, the resulting Neural Flight Control System (NFCS) still provides handling qualities that can be shaped for different flight conditions and aircraft configurations. These handling qualities are shaped with the use of a neural adaptive rate-command-attitude-hold (RCAH) system. Most commercial aircraft are designed to provide adequate flying performance with only a yaw-damper, but advanced aircraft such as the B777 incorporate full-stability-augmentation systems on every axis, and Airbus even provides full RCAH



Fig. 1. Ames Research Center Boeing 747-400 Level D flight simulator.

capability. Although RCAH and stability-augmentation system benefits can be achieved through conventional control-system technology, another benefit of the NFCS system is that handling qualities can be maintained in the event of damage or failures, while sufficient control authority remains available.

In FY01, several different retrofit options were considered, and two specific options (lower and higher cost) were implemented on the Boeing 747-400 Level D certified simulator. For the lower-cost option investigated, the axes in the NFCS were decoupled, allowing for the possibility that the system could be independently and locally applied to each of the pitch, roll, and yaw axes. With the other

option, the roll and yaw axes were coupled and daisy-chaining of pitch control into the ailerons was allowed. Both of the options that were investigated provided RCAH capability but different levels of damage-adaptive capability to the aircraft. Piloted flight simulations in FY01 showed that the NFCS significantly improved the handling qualities of the aircraft, for both normal flight conditions and for a variety of failure scenarios, such as engine out, jammed stabilizer, and rudder hard-over scenarios.

Point of Contact: K. Gundy-Burlet
(650) 604-3603
Karen.L.Gundy-Burlet@nasa.gov

Los Angeles International Airport Runway Incursion Studies: Finding Solutions for a Safer Airport

Nancy Dorighi

Ames' FutureFlight Central (FFC), a virtual air-traffic control tower, was designed to realistically model a complete airport environment, providing a way to safely assess (1) changes to airport procedures and physical layout, and (2) new technologies. In the Los Angeles International Airport (LAX) Runway Incursion studies, Ames staff used FutureFlight Central to recreate the complex work environment of controllers at LAX and tested ways to improve runway safety. Integral to the study was the participation of LAX controllers who served as test subjects. Based on the study results, LAX management is proceeding with steps toward implementation of a taxi extension at the end of the 25R/25L runways.

The overall objective of the Runway Incursion studies was to assess alternative changes to either the airport layout, operational procedures, or both, which could reduce the possibility of runway incursions. A runway incursion is a loss of separation between aircraft on approach or taking off, resulting in a colli-

sion hazard with another aircraft (or vehicle) on the runway. The Federal Aviation Administration (FAA) has declared reducing runway incursions a top priority. Because LAX led U.S. airports in the number of runway incursions in both 1999 and 2000, an FAA task force proposed a set of alternatives that could potentially improve safety at LAX. Ames staff conducted two simulation studies of LAX in FutureFlight Central: the first, a baseline to validate the facility's accurate representation of LAX operations, and the second, a simulation to evaluate six alternatives for their effect on safety and capacity.

In the first simulation, Ames staff demonstrated that FFC could represent the LAX operational environment with sufficient realism. To do so, simulation engineers created peak arrival and departure traffic scenarios which LAX controllers managed in real-time under visual and instrument flight rules. Figure 1 shows an LAX local controller managing virtual LAX traffic at FFC. The facility depicted an

accurate 360-degree view from the control tower including reduced visibility, moving aircraft, engine noise, and simulated controller-pilot radio communications. Three types of measurements were used to validate the facility: controller surveys, aircraft surface movement metrics, and voice communication recordings.



Fig. 1. LAX air traffic controller working virtual traffic in Future-Flight Central.

In the second simulation, LAX controllers tested the following alternatives: swapping runways used for arrivals and departures, adding an additional controller in the tower, and four variations utilizing the

proposed B-16 taxiway extension under different sets of procedural rules with or without an additional controller. All alternatives were tested with peak arrival and peak departure scenarios under visual flight rules.

An LAX air-traffic tower manager summed up the value of the simulation for the airport: “The NASA simulation was remarkably similar to LAX in real life. ... Simply put: If we could not get it to work in the simplified version of LAX airport, then it was clearly not going to work at real LAX. This saved the airport a lot of time (and money) in eliminating those untenable procedures and/or options.”

In conclusion, because airports intrinsically involve multiple stakeholders, the project is a model for future airport research. The FAA, Los Angeles World Airports (LAWA), and United Airlines jointly sponsored the LAX Runway Incursion studies. By including airline and air-traffic control involvement in the design and execution of the study, this study cultivated a greater consensus for the outcome and built support toward an eventual solution.

Point of Contact: Nancy Dorigi
(650) 604-3258
Nancy.S.Dorigi@nasa.gov

Computational Modeling of Pilot Taxi Errors

Allen Goodman, David C. Foyle

Five human-performance models differing in architecture, fidelity, and prior application were applied to taxi navigation. Each model was assessed for its utility in generating and explaining a subset of the 12 navigation errors that were actually committed by airline pilots participating in a simulation. These errors are examples of the type of human error cited

as causing 60% to 80% of aviation accidents. Efforts to improve the safety of the civil aviation system and reduce accident rates must address the underlying causes of human error and develop strategies for prevention and mitigation. Effective human modeling and simulation can flag error-prone designs before expensive prototypes are built or sys-

tems fielded. Human-performance modeling tools can evaluate the performance implications of new design concepts early in the development process.

A formal review of human-performance models revealed a variety of architectures and approaches, but few that had attempted to predict errors. Since many were developed and validated primarily with laboratory data, it was a challenge to apply them to the dynamic, interactive complexities of aviation. Each type of model emphasized certain aspects of human perception, cognition, and behavior, and did so with varying fidelity; thus, no one approach would be likely to capture all of the behaviors and failures inherent to the domain. To gain a better understanding of the capabilities and limitations of human performance models, five approaches were selected for development and application to a specific aviation problem: (1) ACT-R/PM (Atomic Components of Thought-Rational/Perceptual Motor) is an activation-based production system architecture of cognition with enhanced perceptual and motor processes; (2) Air MIDAS (Air Man-Machine Interface Design Analysis System) is an integrative model of a goal-seeking human(s) immersed in a context-rich environment; (3) A-SA (Attention and Situational Awareness Model) is a computational model of attention and level of situational awareness; (4) D-OMAR (Distributed Operator Model Architecture) is a general purpose, event-based simulation development environment; and

(5) IMPRINT/ACT-R (Improved Performance Research Integration Tool/Atomic Components of Thought) is a procedural task network model linked with an activation-based production system architecture of cognition. All but one (A-SA model) was well-established with numerous prior applications and validation efforts.

Each modeling team constructed a dynamic representation of the taxi-navigation portion of a recently conducted, high-fidelity, full-mission simulation. These deviations from the assigned course as pilots taxied after landing were seen as especially useful because the errors were clearly specified, well-documented, and very realistic. In Figure 1, a screen capture from a D-OMAR animated runtime display shows the movements of two conflicting aircraft on taxiways, along with model-generated pilot and ATC communications. Explanations derived from the models included instances of decision errors resulting from poor situational awareness, crew coordination problems caused by distraction and workload, and execution errors based on heuristic biases invoked by time pressure. Predictive capabilities were demonstrated by some of the models (e.g., new errors were generated that extended and slightly varied the original taxi conditions and events). The modeling results confirmed the promise of human performance modeling and also demonstrated the challenges.

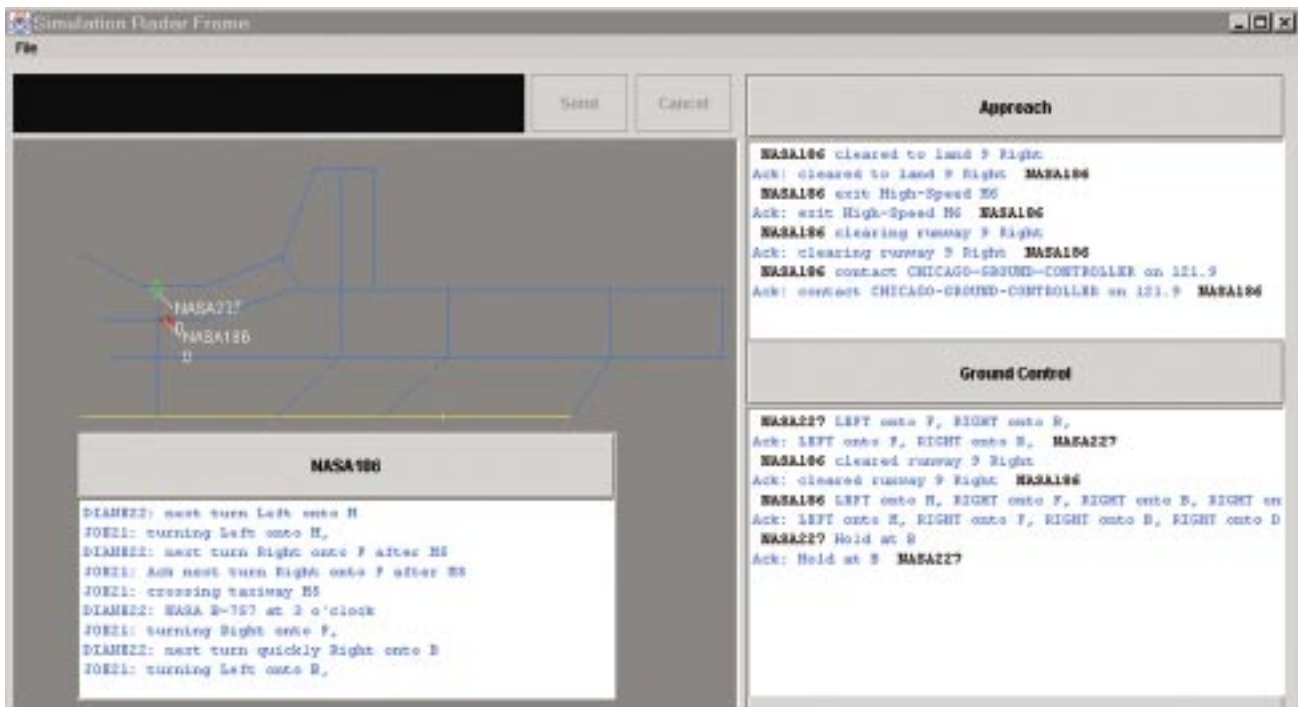


Fig. 1. A screen capture from a D-OMAR animated runtime display shows the movements of two conflicting aircraft on taxiways and the model-generated pilot and ATC communications.

Point of Contact: Allen Goodman
 (650) 604-5692
agoodman@mail.arc.nasa.gov

Opportunities for and Vulnerabilities to Error in Everyday Flight Operations

Loukia D. Loukopoulos, R. Key Dismukes, Immanuel Barshi

Analyses of incident reports, jump-seat observations of line operations, and task analyses were performed in an effort to better understand the causes of pilot error and develop defenses against consequential errors. Between 60% and 80% of aviation accidents and incidents can be attributed, at least in part, to human error. Most incident reports submitted to the Aviation Safety Reporting System are written by experienced, skilled, well-trained, and conscientious pilots. Sheer probability could block such incidents from evolving into accidents since performance er-

rors occur on a daily basis in the course of everyday flight operations. Our effort is to move beyond the traditional view of errors as a source of failure toward a better understanding of the root causes of system failures.

Pilot errors are naturally and predictably occurring events often attributable to many opportunities in the operating environment and to human cognitive vulnerabilities. On the operational side, inter-

observed events typically carries a workload cost (in yellow) in the form of additional activities that have to be performed either immediately or deferred until some later time. The workload cost is assimilated by the pilot who is forced to “navigate” through a complex and dynamic flurry of activities without making a single error.

Expecting to eliminate interruptions and distractions or mitigate cognitive vulnerabilities is unrealistic. Observations from line operations coupled with task analyses can contribute significantly to a better

understanding of the causes for pilot error and aid in the design of robust procedures that offer multiple layers of defense against error. Understanding cockpit interruptions and distractions will enhance existing training programs by aligning the realities of routine line operations with consequences for human error.

Point of Contact: Loukia Loukopoulos
(650) 604-2843
Loukia.D.Loukopoulos@nasa.gov

Risk Assessment and Risk Management in Aviation Decision Making

Judith Orasanu, Ute Fischer, Jeannie Davison, Yuri Tada, Lori McDonnell

Two studies were conducted to determine the types of risk that are of greatest concern to pilots (and thus most influence the perceived difficulty of making a decision) and how they manage such risks. Analyses of air carrier accidents have found that most errors related to the flight crews involve faulty decision making. A common pattern was a crew continuation of an original plan even in the face of changed conditions that suggested another course of action might be more prudent. Many accidents reflected what appeared to be inadequate risk assessment by the crew that led to a decision to take an inappropriate action. Additional factors that might have worked against making safe decisions included organizational and social pressures about fuel economy and maintaining on-time departures and arrivals and peer judgments about professional competence. Risk assessments influence crews’ decision-making during their assessment of a perceived threat that may require intervention and during their evaluation of potential responses to that threat. However, despite its important role in aviation decision making, there has been surprisingly little research on pilots’ risk assessment.

Two studies were conducted to examine this topic. In the first, 119 airline pilots were asked about their everyday experience with five types of risk: economic (dollar costs to the company), physical (safety), productivity (disruption of the schedule), professional (possible job loss), and social (others’ impressions). Their responses indicated that pilots are most concerned with threats to flight safety, which accounted for 79% of their responses. Figure 1 illustrates the types of physical threats that were mentioned. However, pilots reported encountering economic and productivity risks most often. Social and safety risks were rated as least often encountered. Both captains and first officers mentioned that conflicts between safety-related goals and other types, especially customer satisfaction, were most difficult to resolve. Lack of any good options also increased the perceived difficulty of decisions. For captains, difficult decisions were associated with high levels of ambiguity and uncertainty in the decision situation. First officers, on the other hand, attributed greater decision difficulty to the possibility that a poor decision would have negative professional consequences.

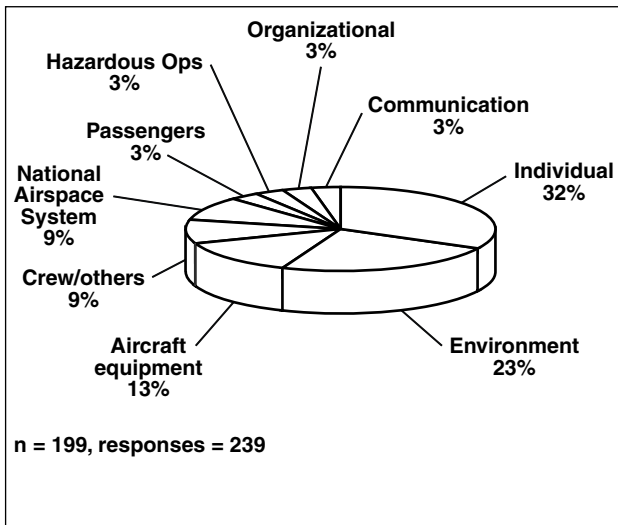


Fig. 1. Physical risk issues cited by pilots.

A second study examined how pilots respond to goal conflict, ambiguity, and uncertainty in dynamic flight situations. Two evolving decision scenarios were presented to each of 30 pilots who were asked to “think aloud” as they decided what to do. In both scenarios, continuing with the original plan to take off would pose a threat to flight safety but bring economic gains if successful. On the other hand, changes to the original plan would enhance

safety but result in economic or other losses. In both scenarios, pilots chose the riskier (in terms of safety) option 50% of the time. Analyses of pilots’ verbalized decision-making processes indicated that they did not weigh the consequences of options, but rather tried to control the safety risk associated with their choices. Those who selected “riskier” options invented solutions that allowed them to minimize the safety risk while also achieving productivity goals. Those who took the conservative option avoided the safety risk.

These two studies are initial efforts toward understanding the risks that pilots face and why they make decisions as they do. The inherently subjective nature of risk assessment was evident in the differences between captain and first officer responses in the risk survey, and in the different interpretations of cues used by pilots in the second study. Subsequent research will seek to improve decision making by developing effective risk-management and decision-making strategies and support tools.

Point of Contact: J. Orasanu
(650) 604-3404
Judith.M.Orasanu@nasa.gov

Performance Data Analysis and Reporting System

Irving C. Statler

The first step in nationalizing the Performance Data Analysis and Reporting System (PDARS) was accomplished by demonstrating its feasibility and value in six air-traffic management facilities in the Western Pacific Region for the past 2 years. Preparations were completed to extend PDARS into the Southwest Region in the first quarter of 2002 (figure 1). The PDARS provides decision-makers with a comprehensive, accurate, and insightful method

for routinely monitoring the operational health, performance, and safety of the National Airspace System (NAS). It was designed to develop technologies to enable a change from the current reactive culture to a more proactive identification and alleviation of life-threatening aviation conditions and events while meeting the projected requirements of increasing air traffic.

The PDARS pursues this objective by establishing

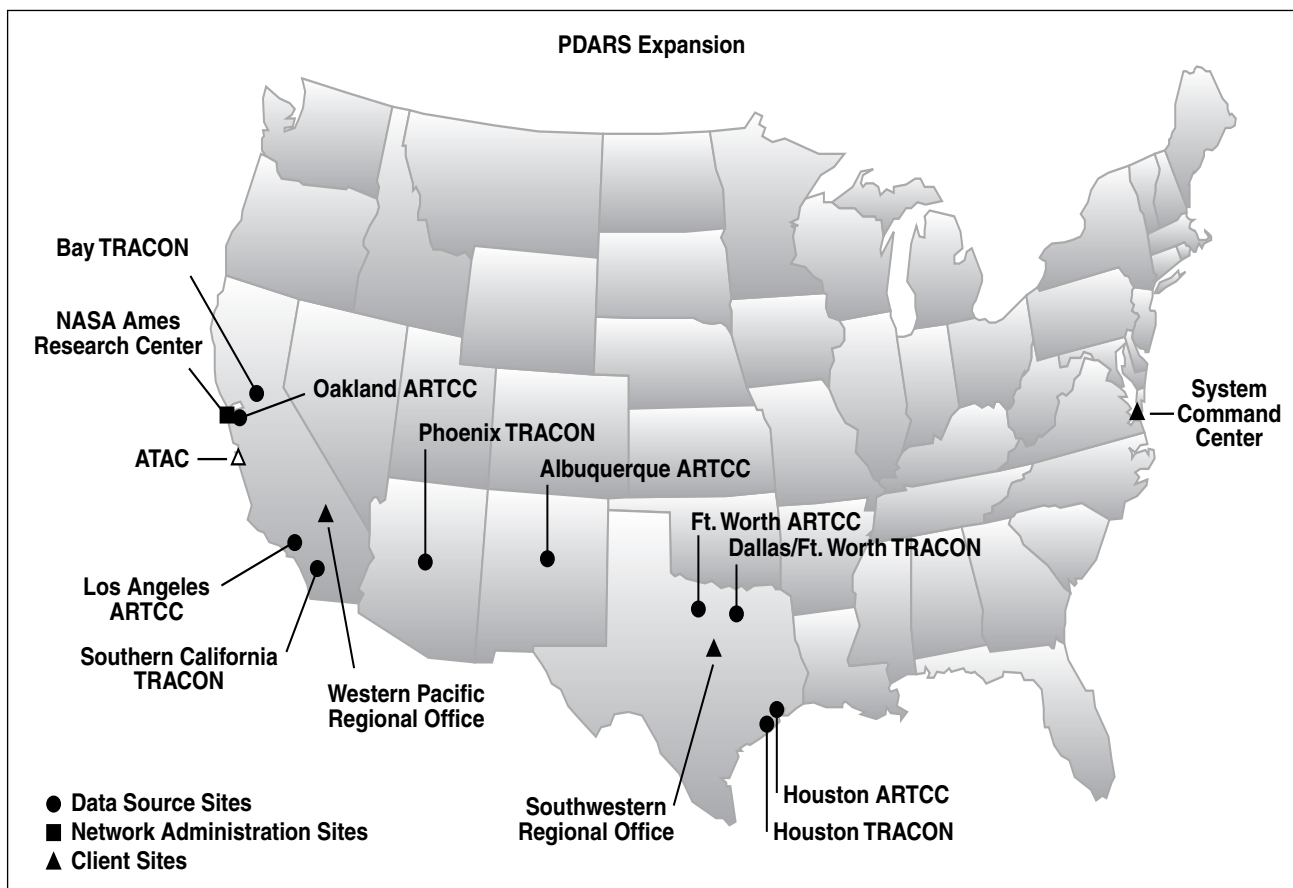


Fig. 1. Facilities operational upon completion of the expansion to the Southwest Region.

new capabilities for managers of air traffic control (ATC) facilities to use in monitoring ATC performance in the NAS (e.g., identifying and analyzing operational performance problems and designing and evaluating improvements). The PDARS incorporates innovative technology for the real-time collection and rapid processing of large volumes of complex data and state-of-the-art tools for extracting, presenting, and visualizing information, including radar flight tracks. Data are accessed daily from all sites and processed overnight. Reports are delivered to each of the participating facilities each morning.

The PDARS accomplished several key milestones in the process of developing a national system, including installation of networking capabilities for seven facilities in the FAA Southwest Region and negotiating an agreement with the FAA to further extend the network to the South and Northwest regions.

Point of Contact: I. Statler
(650) 604-6654
Irving.C.Statler@nasa.gov

Aviation System Monitoring and Modeling (ASMM): Modeling and Simulation of Clear-Air Turbulence Detection and Response

Irving C. Statler, Mary Connors

An operationally interesting scenario within the aviation system was modeled successfully, linking a simulation of air traffic in a given region of airspace with models of multiple pilots and controllers. Textual and quantitative data, collected through intramural and extramural monitoring, were used to support the development and validation of models of causal relationships and predictions in order to support safety risk assessment. The technologies demonstrated by this accomplishment will enable aviation safety predictions and risk assessments through the development and validation of system-wide models and simulations.

The model included 12 aircraft operating in an en route sector with clear-air turbulence (CAT). It specified an experimental design of simulation runs to assess the effects of CAT sensor technology in

that sector. Traffic volumes and routes for the scenario were derived from Enhanced Traffic Management System (ETMS) data for an en route sector in the Boston Air Route Traffic Control Center (ARTCC). These data specified flight crew and controller procedures and communications related to transiting the sector with CAT events. An agent-based model of the scenario was developed in which each agent acted and interacted in accordance with its own internal rules and conditions (figure 1). The model included agents for controllers, flight crews, aircraft, radar surveillance, communication channels, CAT weather events, and sensors. It demonstrated the feasibility of the overall approach to airspace modeling based on agent-based simulation and event-driven, asynchronous modeling with selective resynchronization for fast-time simulation.

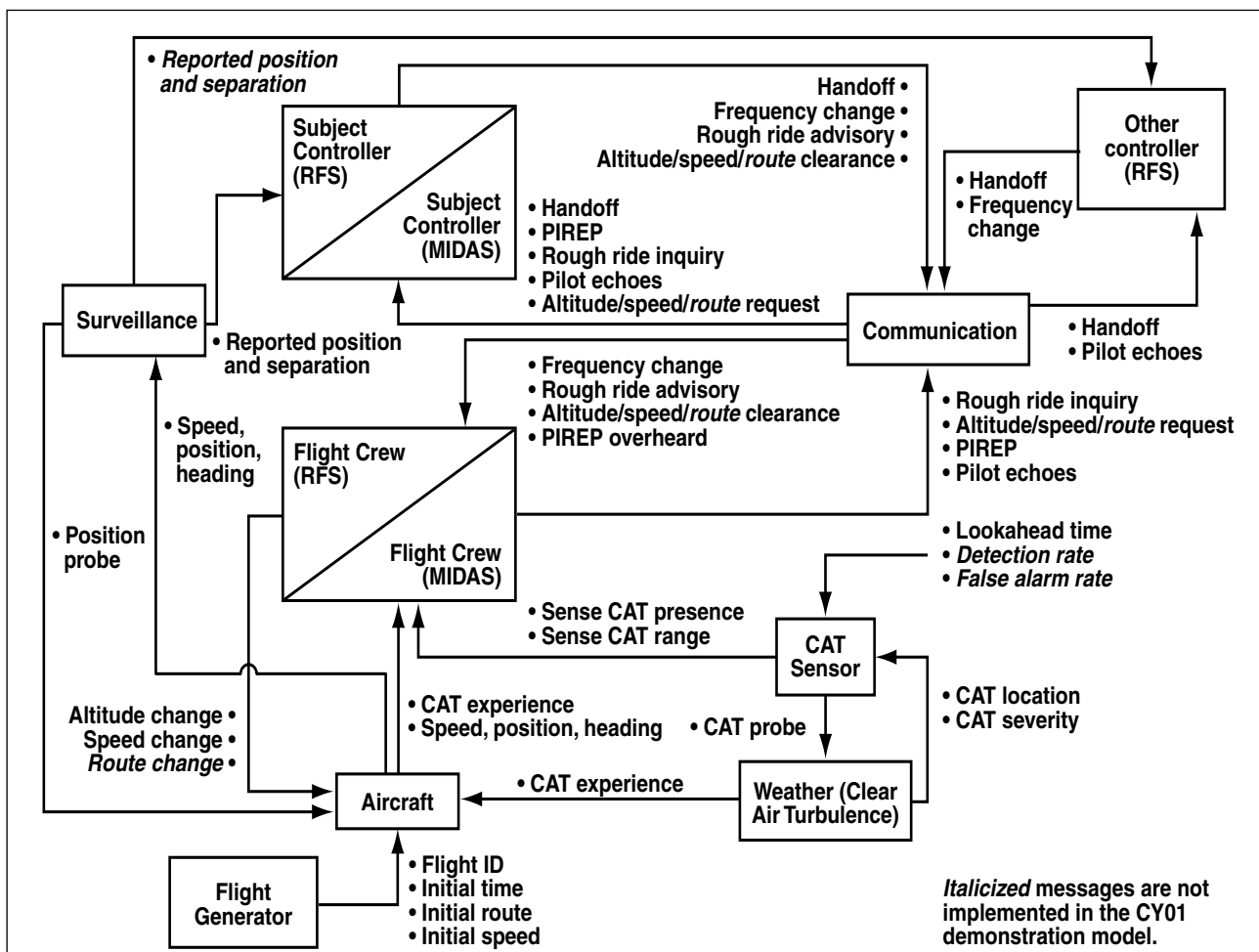


Fig. 1. Modeling the CAT scenario: agent information flows.

Point of Contact: I. Statler
 (650) 604-6654
 Irving.C.Statler@nasa.gov

Scheduling Assistant Software: A Tool for Airline Scheduling

Melissa M. Mallis

An initial biomathematical model capable of predicting alertness and performance specific to the aviation environment was used as the foundation for the development of the Scheduling Assistant Software, a software package to aid airline scheduling. The misalignment of the light/dark cycle and the sleep/wake cycle is often accompanied by increased

subjective and physiological fatigue, adverse health effects, performance decrements, and errors. These effects have been well documented and continue to be a safety concern in flight operations. Pilots on long-haul flight schedules with multiple flight legs and layovers often experience such misalignment of the light/dark cycle and sleep/wake cycle (circadian

desynchrony). This desynchronization between the sleep/wake cycle and the local time zone coupled with fluctuations in the amount and timing of light exposure can affect the ability of pilots to fall asleep, thus reducing sleep efficiency and resulting in fatigue and performance decrements.

One method of predicting sleep/wake cycle and circadian rhythm misalignment effects is through a biomathematical model of the various factors that affect sleep and waking neurobehavioral performance. If packaged in user-friendly software, it could be used as a tool to design flight schedules and assist pilots in scheduling rest and sleep periods during layovers and long-haul flights. However, there have been few attempts to develop such biomathematical models capable of quantifying the effects of circadian and sleep/wake processes in the regulation of alertness and performance.

At Harvard Medical School Brigham & Women's Hospital, Dr. Megan Jewett and colleagues developed biomathematical modeling software that is capable of making such alertness and performance predictions by using light exposure measurements and habitual, circadian, homeostatic, and sleep inertia components. A collaboration between this group and Ames resulted in the initial version of Scheduling Assistant Software, a biomathematical model that incorporates experimentally obtained data on sleep timing, quantity, and quality; length of wake episodes; light exposure; circadian phase; and neurobehavioral and operational measures. The Scheduling Assistant Software is based on neurobehavioral, subjective, operational measurements collected during commercial long-haul flights. Light measurements collected in the cockpit were also used for algorithm development. These light data represent typical exposures for pilots at varying times throughout a long-haul flight, a fundamental component of the model. Based on the combined data, it will be possible to predict the effect of acute

sleep loss, cumulative sleep loss, and circadian desynchrony on waking performance and to provide indications for work/rest schedules that could minimize in-flight fatigue-related problems.

The final version of the Scheduling Assistant Software will be a developed, refined, and validated biomathematical model in a user-friendly interface to be used as an aide in predicting pilots' levels of alertness and neurobehavioral performance under various schedules (figure 1). In addition, this software can be used to estimate the best timing of in-flight rest; to indicate layover sleep conditions that mitigate sleepiness and fatigue in operational duty conditions; and to assist airlines in scheduling flights that take into consideration pilots' circadian rhythms, flight duration, duties, and the light/dark cycle at destinations. Inevitably, as the aviation industry grows, the length of long-haul flights will increase. The Scheduling Assistant Software will serve as an effective assistant that can be used to help promote natural sleep that is closer to pilots' homeostatic sleep schedule, thus reducing fatigue and neurobehavioral performance decrements in aviation, and increasing the safety margin.

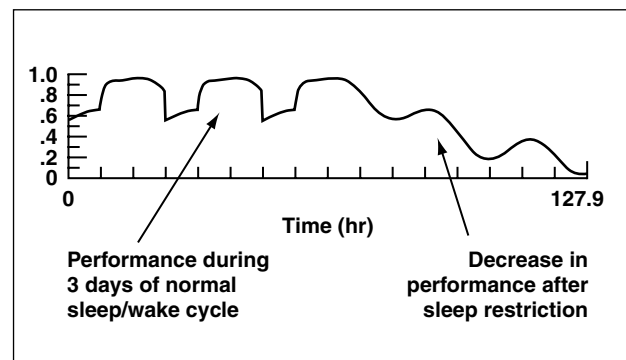


Fig. 1. Sample output from the Scheduling Assistant Software predicting performance levels after 72 hours of wakefulness.

Point of Contact: M. Mallis
(650) 604-3654
Melissa.M.Mallis@nasa.gov

Sound Laboratory: A Software-Based System for Interactive Spatial Sound Synthesis

Elizabeth M. Wenzel, Joel D. Miller

The primary goal of the Sound Laboratory (SLAB) system is to provide an experimental platform for developing and validating advanced spatial auditory displays for aerospace applications. The aviation environment contains multiple channels of auditory and visual information that must be accessed under high-stress, high-workload conditions. Spatialized audio displays will increase the intelligibility of simultaneous verbal communications and auditory alerts in noisy conditions. The use of visual displays, such as those used for collision avoidance, may be improved by assigning some situational awareness and alerting functions to a spatial auditory display that allows the pilot's gaze to remain out the window. Spatialized audio displays could enhance the realism and presence of virtual-reality-based displays, such as those proposed for air-traffic control. Efficient synthesis techniques and environmental modeling will also benefit from further research that specifies the computational fidelity required for perceptually viable displays. The SLAB software is being released under a free public license for noncommercial use. It is our hope that researchers will find it useful in conducting studies of advanced audio displays and that they will also add their own modules to the software to provide additional functionality.

The SLAB system enables individual control of signal-processing parameters to conduct such studies (e.g., the number, fidelity, and positioning of sound sources and environmental reflections, system latency, and update rate). SLAB also provides the basis for a low-cost, software-based system for dynamic synthesis of virtual audio over headphones that does not require an array of special-purpose, signal-processing hardware. SLAB features a modular, object-oriented design that provides the flexibility and extensibility needed to accommodate a wide range of experiments. It can readily take advantage of improvements in processing power without extensive software revisions.

The physical world to be rendered is composed of a source, environment, and listener, as illustrated in figure 1(a). A source, characterized by its waveform, level, radiation pattern, size, and dynamic quantities including position and orientation, radiates into an environment. The source signal propagates through the environment and arrives at a listener characterized by a previously-measured head-related impulse response (HRIR) and interaural time delay (ITD), as well as a dynamically changing position and orientation. The SLAB signal flow (figure 1(b)) implements these physical effects in an easily maintained, efficient architecture that consists of parallel signal paths from each rendered source to a listener's ears. Static effects along each path, such as materials reflection filtering, are combined and implemented as an infinite impulse response (IIR) filter. A finite impulse response (FIR) filter implements dynamic effects like head-related impulse responses and the source radiation pattern.

One of the major implementation hurdles has been achieving adequate dynamic performance in the Windows environment. A preliminary estimate of the internal latency of the system (24 milliseconds) provided an encouraging assessment of the dynamic performance of SLAB, considering the inherent difficulties in managing low-latency Windows audio output. Informal listening tests indicate that the dynamic behavior of the system is both smooth and responsive. The smoothness is enhanced by the 120-hertz (Hz) scenario update rate, as well as a parameter tracking method that produces rather high parameter update rates; that is, time delays are updated at 44.1 kilohertz (kHz) and the FIR filter coefficients are updated at 690 Hz. The responsiveness of the system is enhanced by the low latency of 24 milliseconds. The scenario update rate, parameter update rates, and latency all compare favorably with those of other, more expensive virtual audio systems.

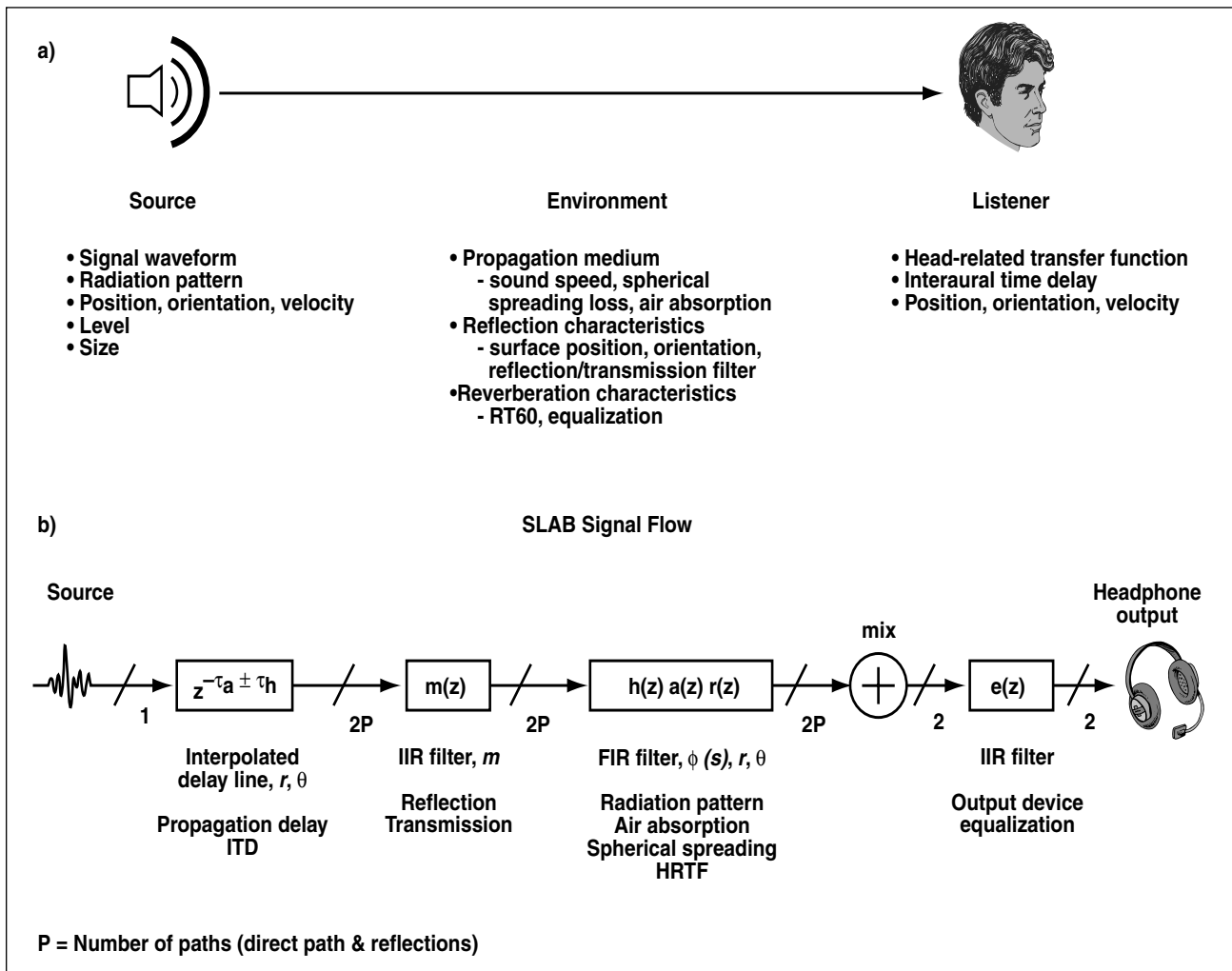


Fig. 1. (a) The physical scenario simulated in the Sound Lab system. (b) The SLAB signal flow partitions the scenario into signal processing components as implemented in system architecture.

Point of Contact: E. Wenzel
(650) 604-6290
Elizabeth.M.Wenzel@nasa.gov

Computational Simulation of Formation Flight of F-18 Aircraft

Steven C. Smith

In support of the Autonomous Formation Flight project at the Dryden Flight Research Center, a computational study is under way here at Ames Research Center to demonstrate the expected formation-flight

drag savings and to define the induced forces and moments on trailing aircraft. Formation flight can produce significant fuel savings by reducing the drag on a trailing aircraft, if it is positioned cor-

rectly relative to the trailing-vortex wake of the lead aircraft. The drag benefit comes from the favorable influence of the wake-vortex flow field on the induced drag of the trailing aircraft. Unlike geese, which fly in a close “V” formation to share the drag benefits mutually, practical aircraft formation flight is a benefit to only the following airplane, positioned many body lengths behind the leader. To achieve these drag benefits, while maintaining safety and normal workload levels, the overall project objectives are to develop and demonstrate a formation-flight control system capable of establishing and holding formation flight position, to measure the drag benefit, and to assess pilot/control system workload and airframe loads in the formation-flight environment.

The computational simulations, using a pair of F-18 aircraft, are performed using the Boeing A502 high-order panel code, which solves the linear potential equations describing the flow over the aircraft. Potential-flow methods compute the induced drag on an aircraft that results from the influence of its own trailing-wake vorticity, but they do not compute the viscous drag (skin friction). This level of flow physics is appropriate to properly capture the influence of the lead aircraft’s wake vortex on the following aircraft. Figure 1 illustrates the input geometry of two F-18 aircraft in formation. The geometry has been



Fig. 1. F-18 aircraft flying in formation.

simplified by omitting the canopy, inlets, and nozzles since these components have no significant effect on the change in aerodynamics associated with formation flight. Panel codes normally require that the trailing-wake location be specified as part of the input. For these studies, the trailing wake was modeled as a straight vortex sheet in the free-stream direction. This model results in some error in vortex position compared with the actual physical wake, which tends to roll up along its free edge downstream of the wing. Future studies are planned that will model the rolled-up wake shape correctly.

Figure 2 shows the predicted induced-drag benefit as a function of the relative flight position of the trailing aircraft. The contour lines indicate values of the ratio of induced drag in formation flight to induced drag in solo flight. The silhouette outline shows the position of the lead airplane, and the vertical and lateral position on the contour plot corresponds to the position of the nose of the following aircraft. All results were generated with a longitudinal spacing of 5 body lengths. It is evident from the figure that induced drag reductions of about 40% (a drag ratio of 0.6) are obtained over a significant region. Adding in the viscous drag, which is unaffected by the formation flight, results in a 15%-20% reduction in total drag for the following aircraft. In addition to these estimates of the potential drag benefit, the computational results provide predictions of the incremental forces and moments induced on the following aircraft. The database of these incremental loads provides a model of how the airplane behavior is influenced by the presence of the trailing-vortex wake of the lead aircraft. This database is used in the design of the flight-control system in order to anticipate the dynamic response of the airplane as it flies in various formation positions. Initial flight test results from Dryden Flight Research Center indicate very close agreement with these predictions, although some position error is evident because of the simplified modeling of the wake shape.

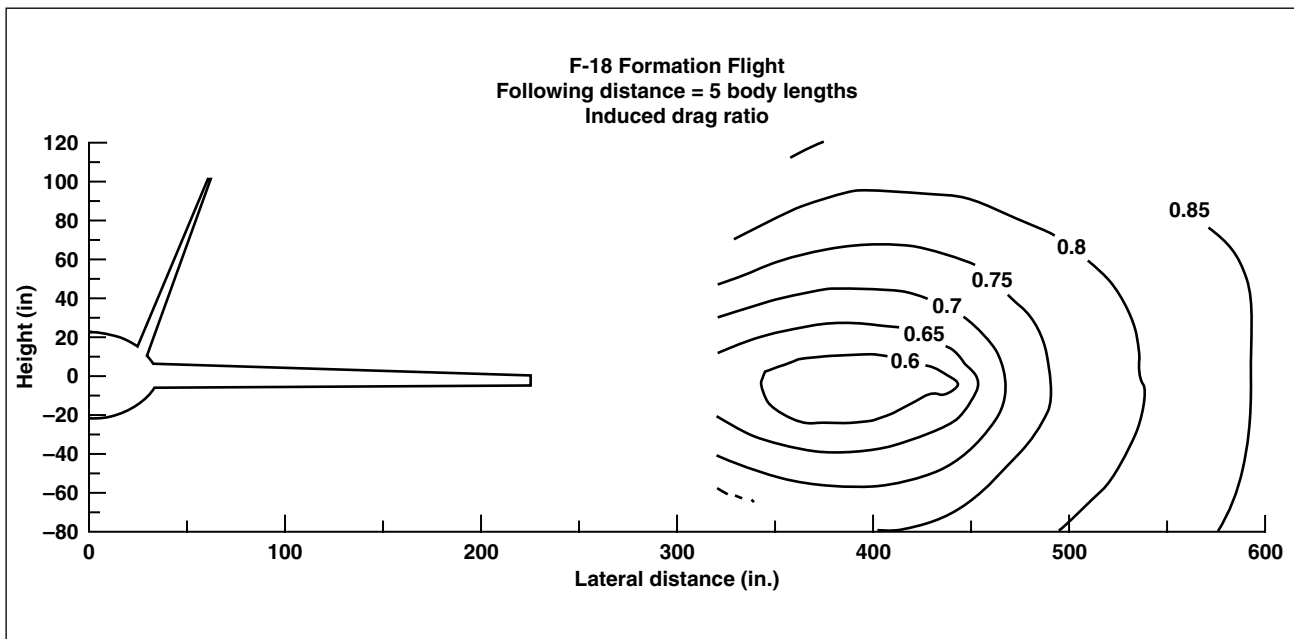


Fig. 2. Formation flight induced-drag benefit.

Point of Contact: S. Smith
(650) 604-5856
Steven.C.Smith@nasa.gov

Boeing 777 Subsonic Transport Aeroacoustic Research

Paul T. Soderman, Clifton Horne, Kevin D. James

One of NASA's principal aeronautical research goals is to reduce the level of community noise around airports. During the approach and landing of transport aircraft, the wing leading-edge slats and trailing-edge flaps are deployed along with the landing gear. These aircraft components, enveloped by high-velocity energetic turbulent flows, generate airframe noise levels that are comparable to the engine noise at these conditions. In an effort to reduce airframe noise, Ames has developed advanced measurement techniques to locate and quantify the individual noise sources. In addition, it has conducted experimental validation tests of concepts that mitigate the sources of airframe noise.

As an overall system validation, Ames Research

Center, in collaboration with its principal partners, Langley Research Center and the Boeing Airplane Company, recently conducted a research program using a large-scale, high-fidelity model of the Boeing 777. This 26%-scale semispan was tested in the Ames 40- by 80-Foot Wind Tunnel (figure 1). The large-scale three-dimensional high-fidelity model provided a unique high Reynolds number aeroacoustic simulation of an actual aircraft, complete with high-lift and landing gear components.

A key element of this test program was the use of the Ames-developed in-flow phased microphone array technology that enabled the measurement and visualization of the noise sources generated by indi-



Fig. 1. 26% scale model of a Boeing 777 in the Ames 40- by 80-Foot Wind Tunnel.

vidual components of the airframe. Figure 2 shows an example of an array survey. The bright areas indicate a noise source, with the sound pressure level being color-coded. Flyover noise was measured using one large fixed array of microphones that provided very high spatial resolution and good resolution of low-frequency noise, and a second smaller mobile array, which traversed the length of the test section, and provided source directivity and good spatial resolution of high-frequency sources. The arrays are identified in figure 1. In addition to acoustic measurements, detailed aerodynamic data, including forces and moments and time-averaged and dynamic pressures, were also obtained. The combination of acoustic and aerodynamic measurements facilitates the understanding of the aeroacoustic phenomena and provides a basis for trade-offs between noise reduction and aerodynamic performance for proposed noise-mitigation concepts. Measurements were obtained over a range of angles of attack and flight Mach number; analysis of the aerodynamic data confirmed proper simulation of aircraft operating conditions and flow fields. Preliminary data

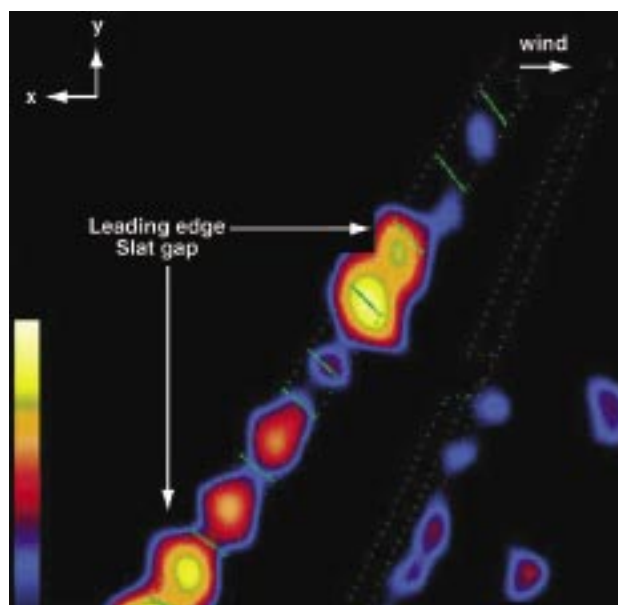


Fig. 2. Microphone array image of noise sources near leading-edge slat.

analyses have documented the location and relative strength of numerous noise sources associated with the edges, gaps, cavities, and protuberances of the high-lift and landing gear systems. To mitigate these noises, many flow-control and sound-absorption devices were tested that had been previously evaluated computationally or tested in small-scale facilities at NASA or industry research laboratories. Several of the devices proved effective whereas others, which showed promise in earlier evaluations, did not perform well at large scale in the full three-dimensional flow environment. Analysis of the data is continuing, focusing on the effects of the acoustic modifications on aircraft performance and the generation of the large aeroacoustic database. This comprehensive database will improve the understanding of airframe noise and enable the development of community noise-reduction strategies in the design of future aircraft.

Point of Contact: C. Horne
(650) 604-4571
Clifton.C.Horne@nasa.gov

Simulation of Aircraft Flightpath Noise and of Noise Abatement Procedures

Terrance K. Rager

The effect of aircraft noise on communities has become a major element of consideration in airport operations. To address community concerns some airports have established special noise-abatement protocols that modify existing instrument flight procedures to minimize noise effects. This study was an attempt to demonstrate that noise issues can be successfully studied in a simulation environment.

In the first experiment phase, a computer model that calculates aircraft noise at ground level positions near the flightpath was integrated into a B747-400 aircraft simulation utilizing runway 28R at San Francisco International Airport (figure 1). Ninety simulation runs were conducted consisting of Standard Instrument Departures and Instrument Approach Procedures. Parameters collected included lateral offset relative to the flightpath, altitude, equivalent airspeed, net thrust, net-corrected high pressure rotor speed, time into the flight, engine pressure ratio, and pitch Euler angle. These aircraft flightpath data and the resulting noise levels were then inserted into an Integrated Noise Model that generated a noise-contour footprint. The calculated noise-contour

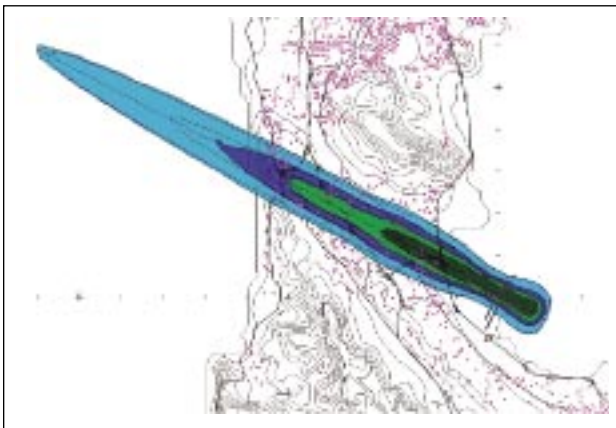


Fig. 1. Noise footprint calculated for runway 28R departure from SFO; colors show ground-level sound intensities.

levels were displayed in the cockpit. These outputs proved to be a useful tool in studying the noise effect on communities adjacent to airports.

The second phase of the experiment used this newly developed tool to help look at human factors issues during Noise Abatement Procedures (NAPs) as they are specified or proposed at noise-sensitive airports. Flight crew performance as well as the effect of the NAPs on noise reduction was examined. Using the B747-400 flight simulator, departure and arrival NAPs were evaluated. London Heathrow Airport was chosen for this phase of the experiment because of its highly stringent noise-effect policy and monitoring plan. Aircraft flightpath data, resulting noise levels, and 69 additional variables were collected during 318 runs. Statistical data for specific aircrew activities, such as aircraft systems activation and initiation of turns, climbs, and descents were also gathered and analyzed. These human factors results are being incorporated in a statistical model to study aircraft separation in a “noise flight procedure” and heavy workload situations for aircrews.

It was determined that only certain NAPs were useable with current Air Traffic Management (ATM) and Flight Management Systems (FMSs). Modern ATM and FMSs can increase the feasibility of utilizing additional NAPs, but the new NAPs must be evaluated before they can be implemented. By using the noise analysis tools integrated with the simulator, researchers can now have a controlled environment for studying human factors with regards to noise abatement.

Both phases of this study were conducted in collaboration with the Boeing Company, Massachusetts Institute of Technology (MIT), and the NASA Quiet

Aircraft Technology Program. Representatives from United Airlines, the Coalition for San Francisco Neighborhoods, and the SFO Aircraft Noise Abatement office attended demonstration runs of the simulation.

Point of Contact: T. Rager
(650) 604-3127
Terrance.K.Rager@nasa.gov

Operational Evaluation of the Direct-To Controller Tool

David T. McNally

Under today's air traffic control system, aircraft fly on fixed airways and air-traffic controllers have limited automation to help identify opportunities for more efficient flight routes. Direct-To (D2) is a tool for en route radar controllers that automatically computes a wind-route and traffic-conflict analysis on all aircraft to identify those that can save at least 1 minute by flying direct to a downstream fix on their route of flight. D2 includes a highly automated "what if" trial planning function that allows controllers to quickly evaluate and input route and altitude changes. D2 functionality is integrated with the controller's radar display in such a way that controllers can use it without being distracted from their primary responsibility for aircraft separation (figure 1). Controllers may bring up a graphic display of a D2 route, activate a fast-loop conflict analysis, modify the route if necessary, and input a D2 flight plan amendment, all with just 2-3 mouse clicks, and within a few seconds, while keeping their eyes on the traffic display. D2 has previously been evaluated in the laboratory and through controller simulations. The objective of this phase of the research was to conduct an operational evaluation of the D2 Tool.

An operational field-test evaluation of D2 was conducted at the FAA's Fort Worth Air Route Traffic Control Center (Center) from 21 May–14 June 2001. D2 is based on the Center/TRACON Automation System (CTAS) trajectory analysis method and software. All CTAS tools use common software for input data processing and four-dimensional (4D) trajectory modeling. Consequently, the D2 func-

tionality was implemented by connecting one additional software module to the daily-use operational Traffic Management Advisor system at Fort Worth Center. The D2 user interface prototype (figure 1) was installed on 15-inch flat-panel auxiliary display monitors (figure 2, right) at three high-altitude sectors. A team of nine full-performance-level controllers participated in the field-test evaluation. Controllers evaluated 3,204 D2 routes and issued 1,198 D2 flight plan amendments to revenue flights during 136 sector-hours of operational testing.

Controller acceptance of the D2 Tool was very high. Controller commentary and written feedback suggest that significant controller benefit could be achieved if D2 functionality were integrated with the radar controller's traffic display. The test data show consistent levels of D2 use through all traffic levels— even the busy periods. Severe weather in and around Fort Worth Center resulted in weather-avoidance routes during 8 of 16 field test days. D2 provided a means of dynamically identifying those weather-avoidance routes that had become obsolete because of changing weather patterns.

An average savings of 9.4 minutes per flight was realized for 27 flights that were on weather-avoidance routes prior to receiving a D2 flight-plan amendment. Analysis of the test data show an average flying time savings of about 1 minute per flight during D2 operations compared with baseline (no-D2) operations. Results also suggest that about 50% of laboratory-derived estimates of flying-time

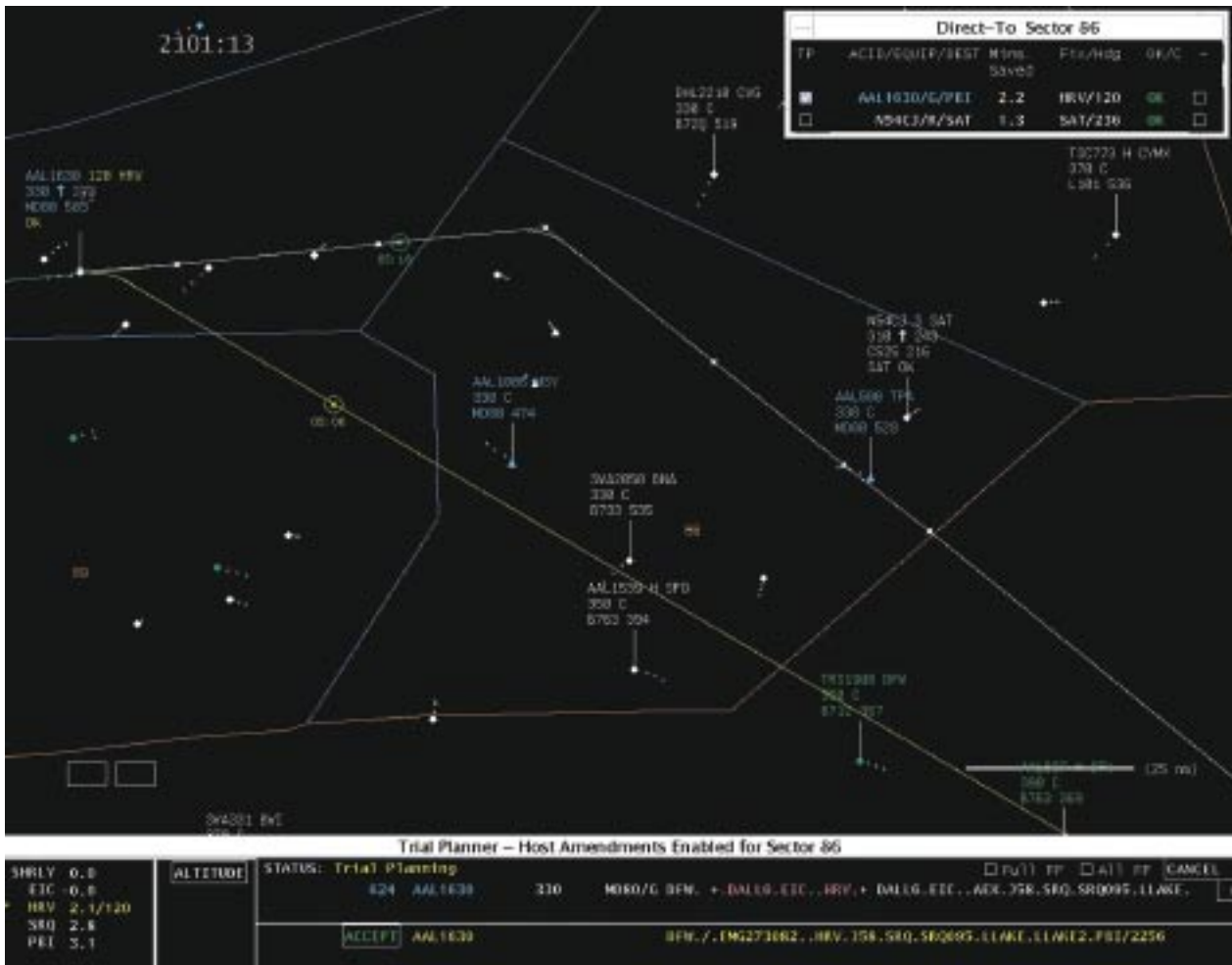


Fig. 1. Direct-To controller tool.



Fig. 2. Direct-To prototype installed at Fort Worth Center sector, May/June 2001.

savings could be achieved if D2 were in operation throughout Fort Worth Center. This equates to a savings of 900 flying minutes per day or \$9,000,000 per year. The D2 field-test operations and results are fully documented in the paper, "Operational Evaluation of the Direct-To Controller Tool," presented at the 4th USA/Europe ATM R&D Seminar, Santa Fe, New Mexico, 3-7 December 2001. Ames is currently working with the FAA and its contractors to implement D2 functionality on the controller's primary radar display. A simulation is planned for April 2002.

Point of Contact: Dave McNally
(650) 604-5440
B.D.McNally@nasa.gov

Neighboring Optimal Wind Routing

Matthew R. Jardin

Cross-continent optimal wind routes can deviate from great-circle (direct) routes by hundreds of miles and can result in time savings of more than 30 minutes. Ideally, simulation tools such as the Future ATM Concepts Evaluation Tool (FACET) and real-time air-traffic management decision-support tools like Direct-To (D2) would utilize wind-optimal routes in simulation and route planning, but current methods for computing wind-optimal routes (e.g., dynamic programming or genetic algorithms) are too computationally intensive for this purpose. To solve this problem, Ames Research Center has developed an algorithm called Neighboring Optimal Wind Routing (NOWR). The objectives of this work were to develop a practical optimal wind-routing algorithm, to implement this algorithm within air traffic control software automation tools, and to estimate the potential savings to air carriers by using real air traffic data.

The NOWR algorithm is based on a feedback technique called neighboring optimal control (NOC). In traditional NOC, one computes an optimal route and a set of regulator coefficients for nominal conditions. The regulator coefficients translate perturbations from the nominal route into optimal-heading perturbations. The heading perturbations are easy to compute, but the nominal optimal route must be obtained using computationally intensive variational calculus methods. Nominal optimal routes would have to be computed for each specific route, and would have to be updated as wind conditions changed. This means that nominal optimal routes must be computed for every flight, which would be computationally prohibitive.

The NOWR algorithm was derived by extending NOC to account for perturbations in the wind field in addition to perturbations from the nominal route. Because of this extension, the nominal optimal route can be computed for the case of zero winds,

the solution to which is simply a great circle route. After applying coordinate rotations, the great-circle nominal optimal solution is geometrically similar for all flight routes. Therefore, a single NOWR solution can be normalized and applied to any flight route and to a wide range of wind conditions. Because the implementation is so simple, NOWR produces optimal wind routes in a fraction of a second on current-day computer hardware (e.g., 750 MHz PIII laptop). By contrast, to obtain routes of similar performance using dynamic programming or genetic algorithms, between 10 seconds and several minutes would be required.

Strong wind-shear conditions typically occur from November through April in the United States. Wind data from the Rapid Update Cycle (RUC) were collected for six different days in February, and both the NOWR and great-circle routes were integrated through these different wind fields for 42 different cross-country routes. On one particular day, the neighboring optimal wind route from Boston to San Francisco was shown to save nearly 40 minutes over the great circle route (figure 1). For the days considered in the study, the maximum flight time savings

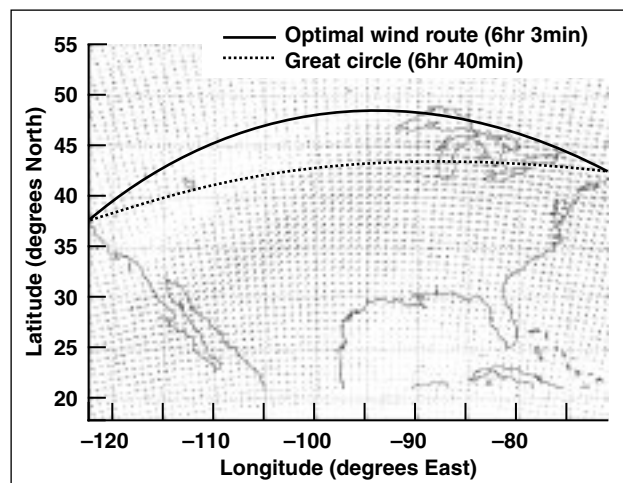


Fig. 1. Neighboring Optimal Wind Route: Boston to San Francisco, 14 February 2001, 2 p.m. PST.

of the optimal routes over the great circle routes was about 10%, with the average savings being of the order of 2%. Optimal wind routes are also geometrically different from great-circle routes so that very different conflict scenarios would develop. Clearly, the use of wind-optimal routes in simulation and analysis of free-flight concepts is important.

The derivation of the NOWR algorithm was published in the July-August 2001 issue of the *AIAA Journal of Guidance, Control, and Dynamics*, and a patent application was filed for NOWR in August 2001 after it was determined that commercial organizations might be interested in using NOWR.

Point of Contact: Matt Jardin
(650) 604-0724
Matthew.R.Jardin@nasa.gov

Probabilistic Forecasting of Air Traffic Demand

Larry A. Meyn

Air traffic managers use predictions of the number of aircraft arriving at an airport or passing through an airspace sector to determine if actions are necessary to limit the number of aircraft to levels that are safe and efficient. However, these actions, such as delaying or rerouting aircraft, should be avoided if they are not necessary, because they degrade the efficiency of the air traffic system. Because of this, the accuracies of airport and sector demand predictions are important factors in the overall efficiency of the national air traffic system. To address this issue, Ames Research Center has developed probabilistic forecasting methods that significantly improve the accuracy of air-traffic-demand forecasts, without requiring any improvement in the accuracy of the data used in calculating demand predictions.

Air-traffic-demand predictions are based on predictions of where aircraft will be located during the time period of the forecast. These predictions have inaccuracies because of uncertainties in weather, airspeed, departure times, and other factors. Current demand forecasting methods include an aircraft if its predicted location places it within the sector or has it arriving at the airport during the forecast period; otherwise the aircraft is not counted. The probability of the predicted location is not

considered. In the probabilistic approach, estimates of each aircraft's location uncertainty are used to determine fractional probabilities that each aircraft should be included in the demand count. Two forecasting methods were developed to utilize these fractional probabilities: the mean probable count, which is a simple sum of the probabilities in order to estimate the demand count, and a new, computationally practical method for calculating the probabilities of all possible demand counts.

The mean probable count was compared with the deterministic method for forecasting airport arrival demand in a series of Monte Carlo simulations. The comparison, presented in figure 1, indicates that the standard deviation in demand-count errors for the probabilistic, mean probable count method is 15% to 20% lower than those produced by the deterministic method, a reduction that is equivalent to what could be achieved deterministically by reducing aircraft location uncertainties by 25% to 35%. However, the mean probable count does not provide any indication of the range of possible demand counts.

The lack of demand-count range indication for the mean probable count is clearly shown in figure 2,

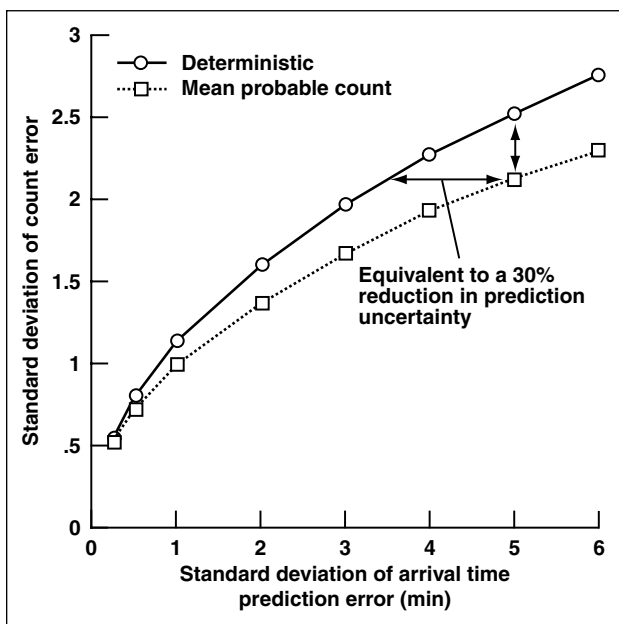


Fig. 1. Count prediction error for airport arrival rate.

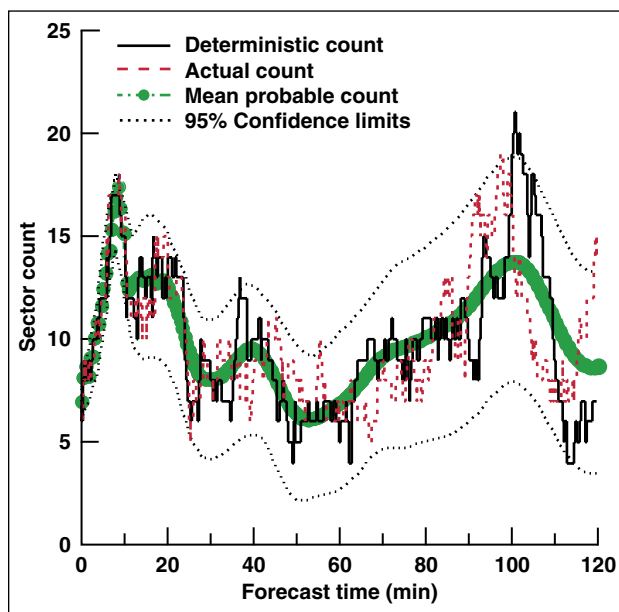


Fig. 2. Probabilistic and deterministic predictions of sector demand.

which depicts the results of a simulation of probabilistic and deterministic sector demand forecasting. In this simulation, aircraft location uncer-

tainty increases with increasing forecast time. Both the deterministic count and the mean probable count follow the actual count closely in the first few minutes. Beyond that point, the deterministic prediction is very similar, in its detail and variation, to the actual count history, but it often does not coincide with the actual count. Unfortunately, traffic-flow modifications based on out-of-step predictions may be unnecessary or may even exacerbate potential sector-loading problems. In contrast, the mean probable count has less overall deviation from the actual count than the deterministic count, but it lacks information about the variability and range of the actual count. The reason for these differences between the deterministic count and mean probable count is that the deterministic prediction produces just one of an infinite number of potential count histories, whereas the mean probable count is the average of all the potential count histories. It is this averaging effect that eliminates the sharp peaks and valleys that are present in an actual count history.

A probabilistic indication of the range of variation in the actual count can be provided by confidence limits, as shown in figure 2. Confidence limits of this type are determined from a count probability distribution. Calculating this distribution has been deemed impractical in the past because the number of calculations needed to directly calculate the distribution increases more than exponentially with the number of aircraft involved. For 25 aircraft, nearly one billion floating-point operations are needed. However, Ames has developed a new calculation method in which the number of calculations needed only increases as the square of the number of aircraft. For 25 aircraft, this new calculation method requires less than 1,000 floating-point operations. Using this new method, it is now practical to predict the range of potential air-traffic-demand counts as well as the most probable count.

Point of Contact: Larry Meyn
(650) 604-5038
Larry.A.Meyn@nasa.gov

En Route Data Exchange

Richard A. Coppenbarger

Software tools that support decision making by air traffic controllers require an ability to accurately predict future aircraft positions during flight. This trajectory-prediction capability is especially important to tools within the Center-TRACON Automation System (CTAS), since they are designed to support strategic controller decisions involving time-horizons of up to 25 minutes. The error between actual and predicted trajectories during climbs can be as much as 2,000 feet vertically in “baseline” CTAS. Similar errors are observed during descent and to a lesser extent during cruise. Horizontal errors can exceed 5 nautical miles. To perform long-range trajectory predictions, CTAS relies on the availability of aircraft state, aircraft performance, flight-plan intent, and atmospheric data. Ames has demonstrated, in a joint flight evaluation with United Airlines, that these errors can be largely eliminated through the transmittal of aircraft data over a real-time data link.

The flight evaluation was completed with assistance from the Federal Aviation Administration (FAA), Honeywell, and United Airlines. The evaluation involved the automatic transfer of more than 40 individual data parameters to CTAS from Boeing 777 airplanes operating within the Denver Air-Route Traffic Control Center (ARTCC). A total of 50 Boeing 777 airplanes received software modifications that allowed the automatic delivery of data parameters over a VHF data link known as the Aircraft Communications and Reporting System (ACARS). Over an 8-month period in FY01, data were collected for over 1,000 operations consisting of 288 departures, 372 over-flights, and 341 arrivals. Data-link messages were transmitted automatically to CTAS operating in the laboratory at Ames Research Center.

Data analysis was carried out to examine the effect of En Route Data Exchange (EDX) parameters, such as weight, speed, and route intent, on CTAS trajectory predictions and subsequent advisories. Errors in CTAS input data were first examined by comparing EDX parameters with corresponding parameters derived from non-aircraft data sources (i.e., FAA radar and flight-plan processing, weather models, and aircraft/pilot performance models). Over all operations, the average errors in aircraft weight and airspeed estimates were measured to be 36,000 pounds and 20 knots, respectively. It was shown that errors of these magnitudes have a substantial effect on CTAS trajectory prediction accuracy over a 20-minute look-ahead time. This is particularly true during climbs, as illustrated by the altitude-prediction example shown in figure 1,

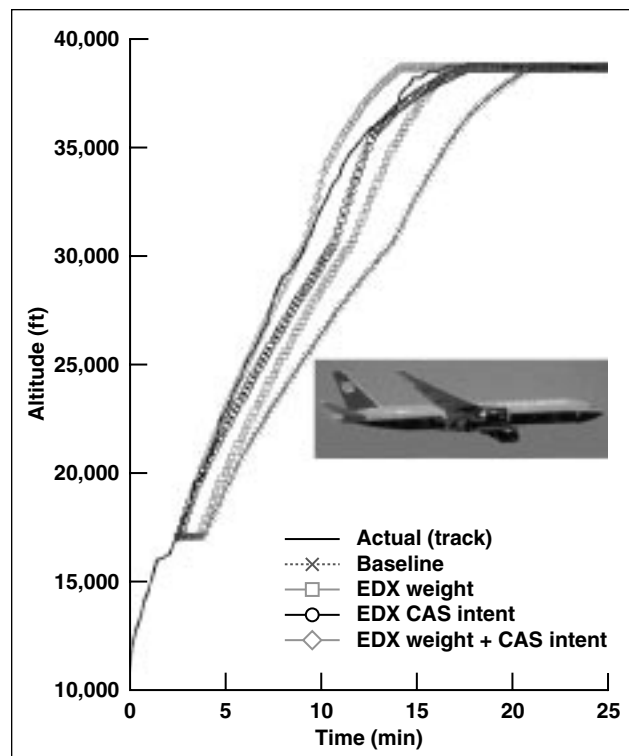


Fig. 1. Impact of EDX weight data on climb trajectory prediction.

where it is shown that EDX reduced the “baseline” errors by more than 2,000 feet vertically. As shown in figure 2, EDX data reduced the overall horizontal errors by more than 5 nautical miles (nmi), which is in excess of current en route separation standards. The effect of EDX-enhanced trajectory predictions on CTAS advisories was examined by considering the effect of aircraft speed and route intent on conflict detection. Aircraft-derived route intent was supplied in the form of way-point identifiers used for guidance and control within the Flight Management System (FMS). Analysis showed that the improved position certainty afforded by EDX data can reduce the false-alarm and missed-alert rates associated with conflict detection by as much as 50% over a 20-minute look-ahead time.

Point of Contact: R. Coppenbarger
(650) 604-6440
Richard.A.Coppenbarger@nasa.gov

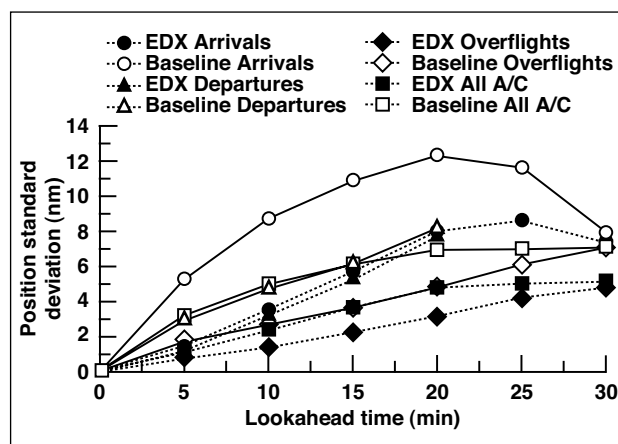


Fig. 2. Position uncertainty as a function of prediction look-ahead time for EDX and non-EDX host data sources.

Flight Deck Tools for Distributed Air-Ground Decision Making in Future ATM Systems

Vernol Battiste, Walter Johnson

Cockpit Situation Display (CSD) tools designed to maintain pilots’ awareness of surrounding aircraft, alert them of impending conflicts, and aid them in developing de-conflicted flight plans were evaluated in an air/ground simulation. The aviation community is exploring new concepts of operations to address saturation of the air traffic management (ATM) system. “Free Flight” concepts decentralize and distribute flightpath management control and responsibility, and information unique to the flight deck and flight dispatchers is included in the ATM decision-making process. All participants must have access to needed information in real time to generate the anticipated benefits. However, a shift away from the current centralized system must not occur at the cost of safe separation between aircraft

and acceptable workload levels. To address these issues, the Advanced Air Transportation Technologies Program is demonstrating new distributed air-ground (DAG) concepts in a series of full-mission, distributed air-ground simulations.

The DAG concept underlying the current effort was based on three principles: (1) current flight-plan information on all aircraft will be updated and broadcasted in real-time; (2) all aircraft will de-conflict their flightpath to the maximum extent possible (within the current 120-nautical-mile-range limit of the Automatic Dependent Surveillance-Broadcast (ADS-B)); and (3) flight-deck display tools will reduce crew workload and head-down time through the use of natural graphical display

interfaces. Airline and general aviation pilots utilized an advanced CSD system to remain clear of conflicting traffic and submit flight-plan revisions to air traffic controllers (ATCs). These flight-plan revisions allowed ATCs to accommodate airline preferences while managing and de-conflicting arrival traffic in a simulation of Dallas/Fort Worth Airport. The CSD depicted the location, heading, and flight plans of surrounding traffic; dynamic four-dimensional (4-D) predictors; and alerted crews to impending losses of separation (see figure 1). A graphical route assessment tool (RAT) was used to develop alternative de-conflicted flight plans and to submit them to ATC for approval, while automatically uploading approved plans into the flight management system and then data-linking them to surrounding aircraft. An advanced spacing tool was used to maintain ATC-assigned intervals behind a leading aircraft after arriving at the final approach fix (figure 2). The autopilot system maintained the specified interval with only minor energy management input from the flight crew.



Fig. 1. Detection and resolution of conflict (inserting climb) with RAT.

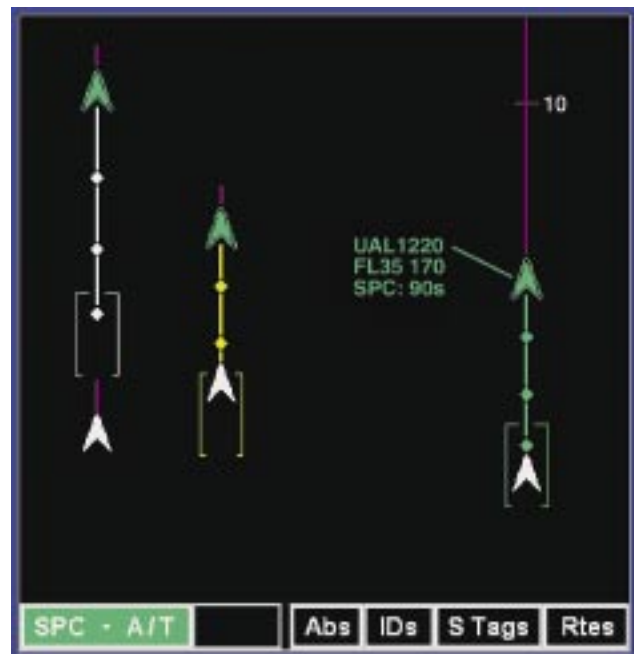


Fig. 2. Approach spacing display symbology of Own-ship at 90 seconds (green), 10 seconds ahead (yellow), and more than 20 seconds behind (gray) another aircraft.

Flight crews reported that the CSD tools were excellent aids for conflict detection and resolution during the free-flight (en route) phase, as well as during the controlled (approach) phase. Further, they agreed that the tools were excellent for self-spacing and maintaining situation awareness. Based on this preliminary demonstration, both controller and pilot comments indicate that the evaluated DAG concepts are feasible.

Point of Contact: V. Battiste
(650) 604-3666
Vernol.Battiste-1@nasa.gov

Surface Management System Simulation

Stephen C. Atkins

Ames Research Center (ARC), in cooperation with the Federal Aviation Administration (FAA), is studying automation for aiding airport surface-traffic management. The Surface Management System (SMS) is a decision-support tool that provides information and advisories to help air traffic controllers and air carriers collaboratively manage the movements of aircraft on the surface of busy airports, thereby improving capacity, efficiency, flexibility, and safety. Detailed information about future departure demand on airport resources is not currently available, which limits the ability to plan and coordinate efficient traffic-management strategies in advance. The SMS provides operational specialists at air-traffic control (ATC) facilities and air carriers with accurate predictions of the future departure demand and of how the situation on the airport surface (e.g., the aircraft queues and delays at each runway) will evolve in response to that demand. Both near-term predictions to support tactical control of surface operations and longer time-horizon forecasts to support strategic planning are provided by the SMS. In addition to the ATC tower and airline ramp towers, SMS information will be used by the TRACON and Center Traffic Management Units, Airline Operations Centers (AOCs), and the ATC System Command Center.

To predict the future state of the surface, the SMS uses real-time surface surveillance, air-carrier predictions of when each flight will want to push back, and a surface trajectory synthesis algorithm that accurately predicts the movement of aircraft on the surface. The initial implementation of this algorithm, which determines efficient and conflict-free taxi paths for every aircraft, has been completed. The ability to predict how the state of the airport surface will evolve enables the SMS to evaluate the effect of various traffic-management decisions in advance of implementing them. The SMS uses this

capability to advise how to best manage departure operations and other surface movements in order to minimize delays.

A 6-day simulation was conducted in the Future-Flight Central (FFC) ATC tower simulator at ARC to solicit feedback on the current SMS design (i.e., the capabilities, interfaces, and algorithm performance) from the future users of the system. Five active controllers from Dallas/Fort Worth airport (DFW) controlled simulated aircraft during the simulation. Representatives from several air carriers (FedEx, UPS, Northwest Airlines, United Airlines, and American Airlines) provided additional feedback. Figure 1 shows a controller using the SMS displays during the simulation in FFC. Three experimental conditions were tested during multiple simulation runs, in which the controllers rotated among the positions in the tower; several traffic scenarios, based on actual traffic observed at DFW and programmed into FFC, were used. The SMS was well received by all of the participants, and simulation results are being used in its further refinement. Through close interactions with the



Fig. 1. SMS displays during the simulation.

participants, data were gathered about how controllers and air carriers currently manage surface operations and how SMS can assist them in these tasks.

The simulation also studied the opportunity for interaction between SMS and the Ames-developed Center-TRACON Automation System (CTAS) Traffic Management Advisor (TMA). The goal of SMS-TMA interoperability is to more effectively manage the trade-off between arrival and departure capacities in response to the time-varying demands for arrivals and departures. Results demonstrated that SMS-provided information can enable better coordination of arrival and departure management. Other opportunities for decision support to help with strategic departure management were identified, and will be pursued as SMS development continues.

Experience has shown that involving the eventual users throughout the development process significantly benefits the quality, operational applicabil-

ity, and usefulness of the final product. ARC will continue to solicit input from both controllers and air carriers throughout the development of the SMS. In the summer of 2002, the SMS will be deployed in an air carrier ramp tower. Following “shadow-mode” testing by controllers in the fall of 2002, a demonstration of the SMS being used operationally in an ATC tower is planned for the summer of 2003. Field-testing of the SMS is expected to be conducted at Memphis airport, to take advantage of the FAA’s Safe Flight 21 experience and infrastructure there. ARC will continue to work with the FAA to prepare the mature SMS technology for transfer to the FAA’s Free Flight Phase 2 Program.

Point of Contact: Stephen Atkins
(650) 604-3577
satkins@mail.arc.nasa.gov

Virtual National Airspace Simulation System

Yuri Gawdiak, Bill McDermott, David Maluf, Peter Tran

In order to fully conduct research that will support the far-term concepts, technologies, and methods required to fix problems with the current air transportation system, a simulation environment of the requisite degree of fidelity must exist. The Virtual National Airspace Simulation System’s suite of tools supports the management of information associated with this complex and critically important operational environment (figure 1). The project’s main objectives are to develop a near real-time, distributed modeling and simulation capability; and to improve the quality of human models and simulations of engines, wings, control surfaces, landing gear, and airframes.

The system consists of a suite of simulation tools, working in conjunction with a distributed network of supercomputers to run simulation software, along with high-speed network connections to aircraft, to the Federal Aviation Administration (FAA), and to airline data sources. Collectively, this system will enable the aviation community to integrate models of varying fidelity into an overall model of the national airspace.

In order to identify the underlying technological issues involved, it was necessary to build a prototype system that would demonstrate the capability for integrating monitoring and simulation data, which

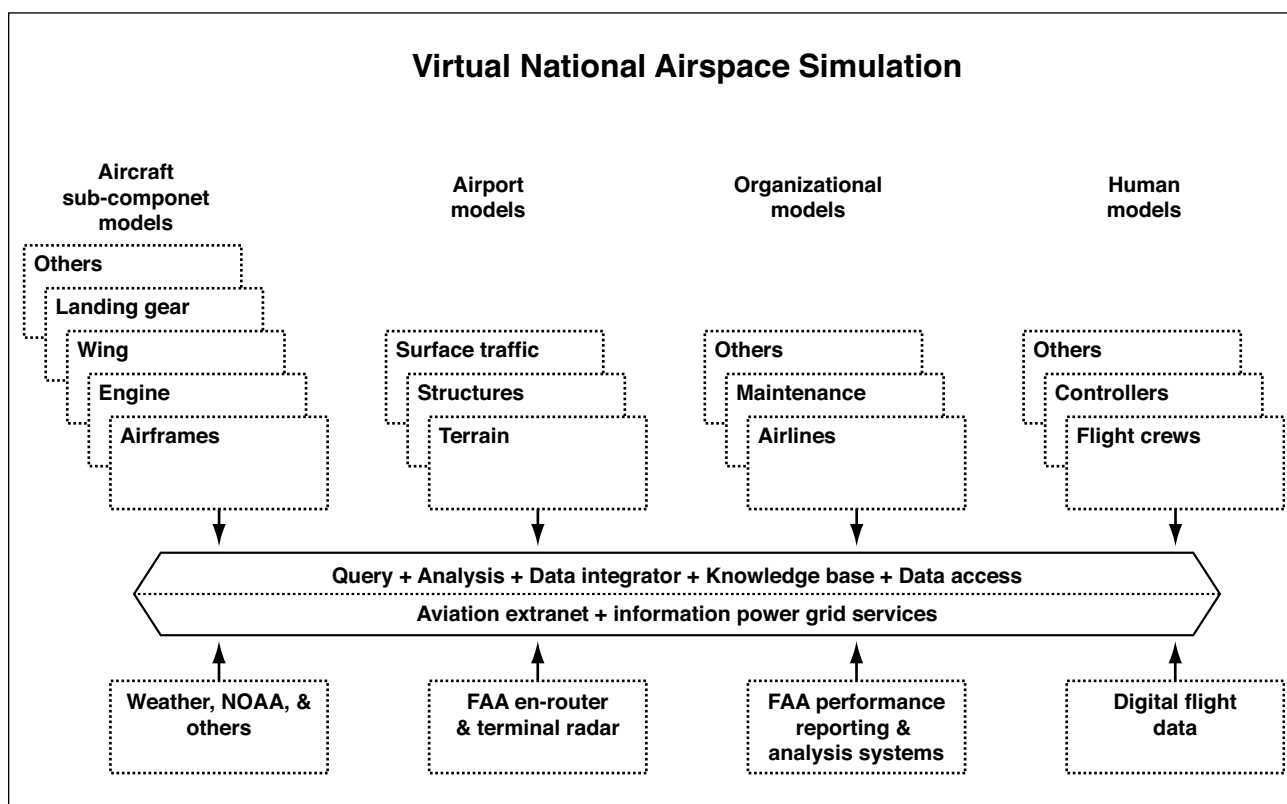


Fig. 1. Tools for information integration and management in complex operational environments.

in this case would encompass real-time operational airport data and aircraft subassembly simulations.

In FY01 a Virtual National Airspace Simulation (VNAS) prototype was successfully demonstrated, using a web browser as a graphical user interface and running on Information Power Grid computers at the Ames and Glenn Research Centers. The VNAS prototype downloads daily operational aircraft arrival and departure data from Atlanta's Hartsfield International Airport, and integrates those data with distributed simulation capabilities from three NASA Centers: an aircraft engine simulation at Glenn Research Center, a landing gear simulation developed at Langley Research Center, and aircraft wing simulations located at Ames.

The resulting simulation allows real-time operational airport data to be batch-processed and run through the distributed simulations, providing a new method of addressing maintenance and operational issues. For example, the maintenance history of a major subcomponent, such as a turbofan engine, when combined with simulation parameters from large numbers of simulated flight operations, would support early identification of engine-components that might be damaged or worn, thus possibly avoiding a delayed or canceled flight. Similarly, fast-time emulation of thousands of flights of a particular aircraft-type will help test new procedures or identify trends in existing procedures for maintenance and airline operations that may be indicative of unsatisfactory performance. In conjunction with other

tools, the Virtual National Airspace Simulation will improve the operation and safety of the National Airspace and will support new technologies that address design, safety, and operational issues in the future air transportation system.

Point of Contact: D. Maluf
(650) 604-0611
dmaluf@mail.arc.nasa.gov

Large-Scale Test Bed Developed for Investigating Tilt-Rotor Aeromechanics and Terminal Area Operation

Megan S. McCluer, Jeffery L. Johnson

The Full-Span Tilt-Rotor Aeroacoustic Model (FS TRAM) is a dual-rotor, powered wind-tunnel model with extensive instrumentation for high-resolution measurement of structural and aerodynamic loads. The model has been developed to investigate tilt-rotor aeromechanics (aerodynamics, dynamics, aeroelasticity, and acoustics), to generate a comprehensive database for validating analyses, and to serve as a research platform for studying current and future tiltrotor designs. The FS-TRAM test stand was brought to operational status, and an initial test campaign was conducted in Ames Research Center's 40- by 80-Foot Wind Tunnel in late 2000. Figure 1 shows the Full-Span TRAM installed in the 40- by 80-Foot Wind Tunnel.

The data were reviewed, analyzed, and presented to the rotorcraft community. The wind-tunnel test results compared well with other small-scale experimental data and confirmed the significant loss of hover performance for the full-span tilt-rotor compared to the isolated rotor configuration. The FS TRAM is currently being prepared for a test entry in the 80- by 120-Foot Wind Tunnel to investigate tilt-rotor interactional aerodynamics and terminal-area operations issues.



Fig. 1. The Full-Span TRAM mounted in the Ames 40- by 80-Foot Wind Tunnel.

Point of Contact: Jeffrey L. Johnson/Megan S. McCluer
(650) 604-6976/(301) 342-8558
jljohnson@mail.arc.nasa.gov
mccluerms@navair.navy.gov

A Wind Tunnel Investigation of a Small-Scale Tilt-Rotor Model in Descending Flight

Anita I. Abrego, Kurtis R. Long

A small-scale tilt-rotor model was tested in the 7- by 10-foot Wind Tunnel at Ames Research Center, with the goal of gaining a better understanding of the effects of vortex ring state (VRS) on tilt-rotor aircraft. Test objectives were to obtain performance data of a tilt-rotor model over a wide range of descent conditions, to explore the effects of sideslip at these descent conditions, and to investigate the validity of using a single-rotor with a physical image plane to simulate dual-rotor performance characteristics. The model consisted of a pair of two-bladed teetering rotors with untwisted, 11.125-inch diameter, rectangular planform blades (figure 1). Model configuration variations included a dual-rotor, an isolated-rotor, and a single-rotor with a physical image plane. Rotor performance data were obtained for the dual-rotor configuration operating over a wide range of descent and sideslip conditions. Isolated-rotor



Fig. 1. Tilt-rotor descent aerodynamics test in the Ames 7- by 10-Foot Wind Tunnel.

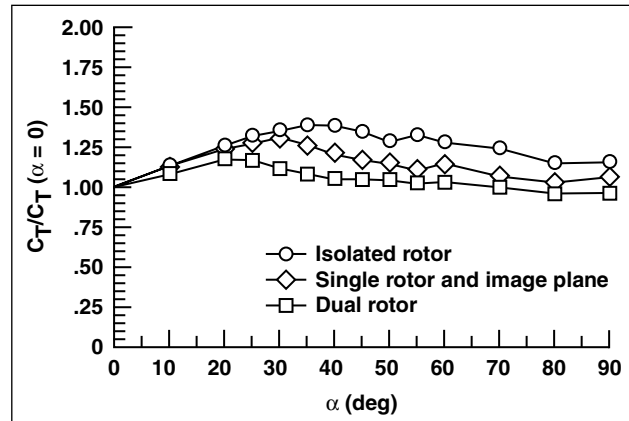


Fig. 2. Effect of image plane on mean thrust coefficient, $V/V_{tip} = 0.08$, $q = 12^\circ$.

and single-rotor-with-image-plane configurations were tested over an abbreviated range of descent conditions. The results of this investigation revealed mean thrust reductions in the region of VRS for each model configuration. Figure 2 shows thrust coefficient (C_t) versus descent angle (α) at an advance ratio of 0.08 and a collective pitch (θ) of 12 degrees for each of the model configurations. Thrust results were similar in trend but different in magnitude. In comparison with the dual-rotor configuration, the isolated-rotor and single-rotor-with-image-plane configurations produced thrust results similar in trend but different in magnitude.

Point of Contact: Anita Abrego
(650) 604-2565
Anita.I.Abrego@nasa.gov

Wind Tunnel Visualization of Descending Tilt-Rotor Wake Aerodynamics

Kurtis R. Long, John Zuk, Robert K. Callaway

Recent assessments of tilt-rotor technology have highlighted a lack of understanding of the complicated aerodynamic environment associated with tilt-rotor aircraft during descending flight conditions. In particular, the descent condition known as vortex ring state (VRS), which occurs when the aircraft descends at speeds comparable to the aircraft's average hover downwash speed, is not thoroughly understood. A wind tunnel test at Ames Research Center investigated the effects of vertical descent rate on the flow field of a twin-rotor tilt-rotor model. Although similar investigations have been conducted for conventional rotorcraft, few if any investigations of tilt-rotor flow patterns have been conducted. This effort is one of the first to document VRS conditions for a tilt-rotor aircraft.

The wind tunnel effort employed a locally manufactured model tilt-rotor apparatus with two, 5-inch-diameter, three-bladed rotors, driven by belts attached to an electric motor. The details of the model are shown in figure 1. The model was mounted such that the rotors were perpendicular to the flow with the downwash directed upstream; the tunnel speed was varied between 40 and 170 feet per second (fps) to simulate varying vertical descent rates. The rotor speed was approximately 12,000 revolutions per minute (rpm), producing a tip speed of approximately 260 fps. Smoke was introduced upwind of the tunnel test section in order to visualize the resultant flow patterns. The development of the flow structure was documented with both still and video imagery.

The flow-visualization results provided considerable insight into tilt-rotor descent flow patterns. Data analysis employed a parameter known as the descent speed ratio (DSR), defined as the dimensionless ratio of tunnel speed (descent speed) to



Fig. 1. Tilt-rotor models (with V-22 shell enclosing gears).

average hover downwash speed. A DSR near unity represents descent speeds at which VRS conditions might be experienced. Figure 2 summarizes the more significant VRS flow-visualization results. High descent speed ($DSR > 1.0$) sequences produced flow patterns that are typical of rotors in autorotation, which include smooth steady flow streamlines

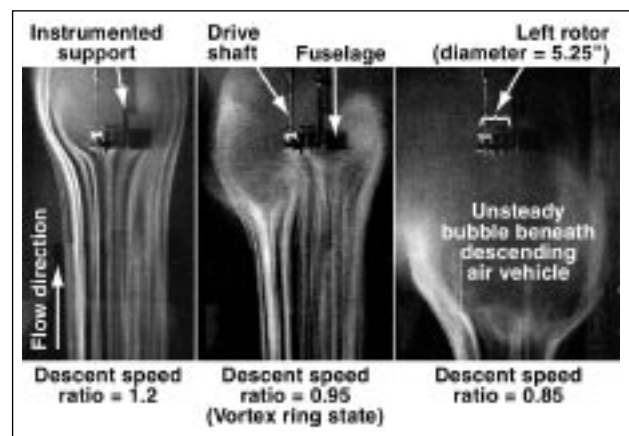


Fig. 2. Effect of tilt-rotor descent speed on flow patterns (tilt-rotor model in side view).

below the descending rotor, and streamlines that expand outward as they travel above the rotor disk. VRS descent speed ($DSR \sim 1.0$) conditions produced smooth flow streamlines below the rotor; these streamlines broke down into less steady, fluctuating patterns just below and adjacent to the rotor system. Conditions that were just slightly lower than those of VRS ($DSR \sim 0.85$) produced a very large unsteady flow region, which extended outward

and below the rotor system. The unsteadiness depicted in this region provides one possible explanation for prior real-world pilot observations of unsteady vehicle response when operating near VRS conditions.

Point of Contact: K. Long
(650) 604-0613
Kurtis.R.Long@nasa.gov

Influence of Wake Models on Calculated Tilt-Rotor Aerodynamics

Wayne R. Johnson

Comparisons of the measured and calculated aerodynamic behavior of a tilt-rotor model have been completed. The test of the Tilt Rotor Aeroacoustic Model (TRAM) with a single, 1/4-scale V-22 rotor in the German-Dutch Wind Tunnel (DNW) provides an extensive set of aeroacoustic, performance, and structural loads data. The calculations were performed using the rotorcraft comprehensive analysis CAMRAD II. The focus of this phase of the work has been the further development of wake models for tilt rotors in helicopter-mode operation. Three tilt rotor wake models were considered, characterized as the rolled-up, multiple-trailer, and multiple-trailer-with-consolidation models. Figure 1 illustrates the calculated wake geometry of the TRAM using the multiple-trailer-with-consolidation model. By using a free-wake geometry calculation method that combines the multiple-trailer-wake model with a simulation of the tip-vortex formation process (consolidation), good correlation of the calculations with TRAM measurements is obtained for both performance and for air loads. Figure 2 is an example of the correlation between measured and calculated blade-section air loads.

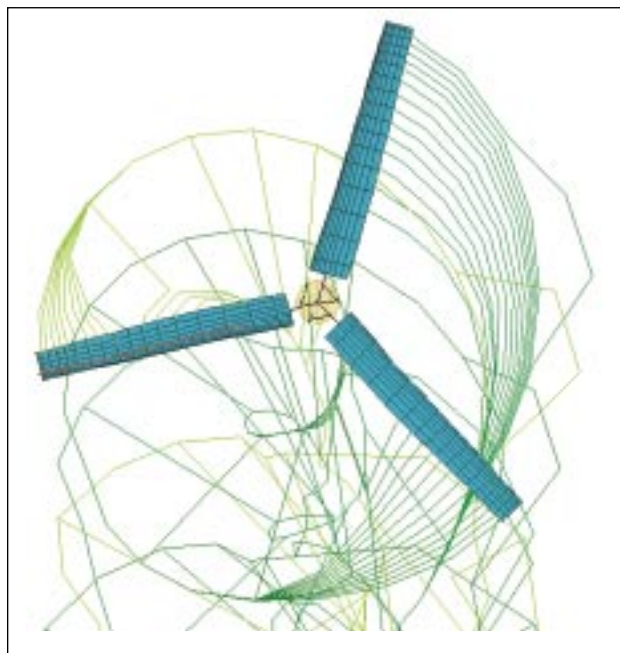


Fig. 1. Calculated wake geometry of Tilt Rotor Aeroacoustic Model (TRAM) in helicopter-mode operation, using the multiple-trailer with consolidation wake model.

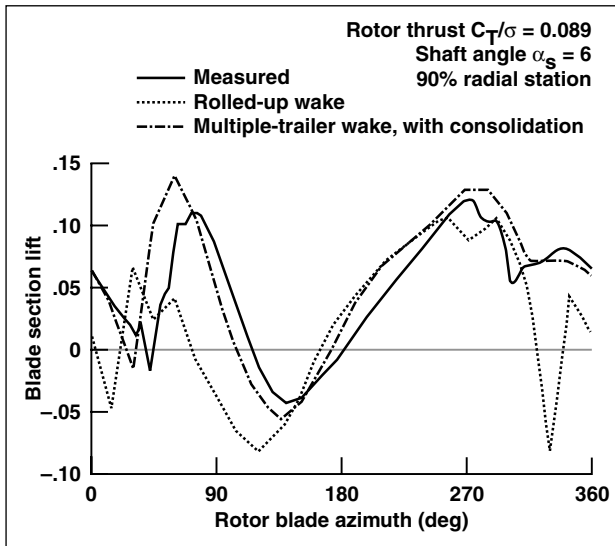


Fig. 2. Comparison of measured blade-section lift with calculations using rolled-up wake model, and the multiple-trailer with consolidation wake model.

The rolled-up-wake model for tilt rotors evolved from the typical helicopter wake model, and features a fully developed tip vortex (and an inboard vortex when there is negative loading of the blade tip). A major difference between this model and the corresponding wake model that has been established for helicopter rotors is that the tilt-rotor model does not use complete entrainment of the tip vortex. The multiple-trailer-wake model has a discrete trailed vortex line emanating from each of the wing aero-

dynamic panel edges. The calculation of the free-wake geometry includes the distortion of all trailed lines, but because of the low spanwise resolution and the absence of viscous effects, a highly concentrated tip vortex is not produced. Good performance correlation is achieved using the rolled-up-wake model, but the calculated air loads are not accurate. Good air-loads correlation is achieved using the multiple-trailer-wake model, but the calculated power is too large.

By using the free-wake geometry calculation method of CAMRAD II that combines the multiple-trailer wake model with a simulation of the tip-vortex formation process (consolidation), good correlation of the calculations with TRAM measurements is obtained for both performance and air loads. With the consolidation model, the trailed lines at the wing panel edges are combined into rolled-up vortices, using the trailed vorticity moment to scale the rate of roll-up. All the vorticity in adjacent lines that have the same sign (bound circulation increasing or decreasing) eventually rolls up into a single vortex, located at the centroid of the original vorticity distribution.

Point of Contact: W. Johnson
(650) 604-2204
Wayne.R.Johnson@nasa.gov

Individual Blade Control for RIA Noise Reduction

Stephen A. Jacklin, Tom Norman, Patrick Shinoda

A full-scale wind tunnel test of an individual blade control (IBC) system showed that active blade-pitch control can lower helicopter blade-vortex-interaction (BVI) noise by 75%. BVI noise reduction is a critical runway-independent-aircraft (RIA) technology that will facilitate aircraft operation in urban areas. The IBC test was performed as part of the Black Hawk helicopter rotor test in the

Ames 80- by 120-Foot Wind Tunnel (figure 1) and conducted under a space-act agreement between Ames/Army, Sikorsky Aircraft Corp., and ZF Luftfahrttechnik (ZFL) GmbH.

A revolutionary concept in active control technology, the rotating blade-pitch-control links of the Black Hawk rotor were replaced by hydraulic



Fig. 1. Large Rotor Test Apparatus and UH-60 rotor installed in the Ames 80- by 120-Foot Wind Tunnel.

actuators. The actuators were manufactured by ZFL to superimpose up to ± 6.0 degrees (deg) of blade pitch on the normal flight controls. Figure 2 shows one IBC actuator as installed in the Black Hawk rotor hub. In the first test phase, the maximum control authority tested was ± 3.0 deg.

The IBC inputs produced substantial noise and vibration reductions. At descent flight conditions typical of noisy landings, BVI noise reductions of over 12 decibels (dB) (75%) were obtained using ± 3.0 deg of 2/rev IBC. Moreover, by using only about ± 1.0 deg of 3/rev blade-pitch control, IBC also



Fig. 2. IBC actuator installed in the Black Hawk rotor system.

eliminated up to 75% of the total vibration. Adaptive IBC control technology holds the promise to meet or exceed the RIA noise and vibration suppression goals. The ability of IBC to positively effect lift capability and high-speed performance of RIA will be evaluated in the Ames 40- by 80-Foot Wind Tunnel using the Sikorsky Growth (S-92) rotor.

Point of Contact: Stephen Jacklin
(650) 604-4567
Stephen.A.Jacklin@nasa.gov

The 7- by 10-Foot Wind Tunnel Investigation of a Ducted Fan System

Anita I. Abrego, Robert W. Bulaga

An experimental investigation was completed in the Ames 7- by 10-Foot Wind Tunnel with the objective of determining the performance characteristics of a ducted fan. The model (figure 1) was an annular duct with a 38-inch-diameter, 10-inch-chord, and a five-bladed fixed-pitch fan. Model variations included duct angle of attack, exit vane flap length, flap-deflection angle, and duct chord length. Duct performance data were obtained for axial and

forward flight-test conditions. Axial-flow test data showed figure-of-merit decreases with increasing advance ratio. Forward flight data, shown in figure 2, indicate increasing propulsive force (C_x) with decreasing duct angle of attack (α). Exit vane flap-deflection angle and flap chord length were shown to be an effective way of providing side force. Extending the duct chord did not affect the duct performance.

Point of Contact: A. Abrego

(650) 604-2565

Anita.I.Abrego@nasa.gov



Fig. 1. Ducted fan test in the Ames 7- by 10-Foot Wind Tunnel.

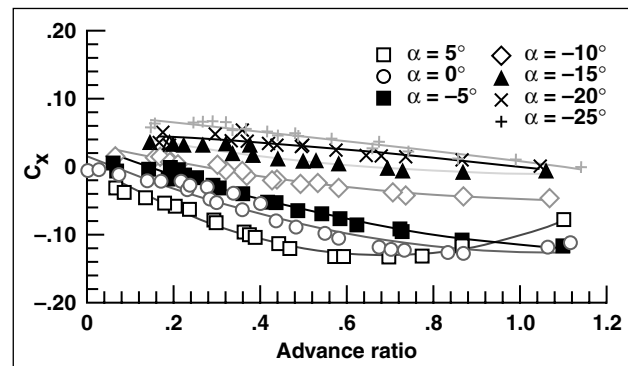


Fig. 2. Forward flight propulsive force coefficient versus advance ratio: baseline configuration, wind axis plus forward component of lift.

Updated Displays for the Cockpit of the Space Shuttle

Jeffrey W. McCandless, Robert S. McCann

Ames Research Center has contributed to the Shuttle Upgrade Program by providing human factors guidance to astronauts, engineers, and programmers in order to ensure that the shuttle displays present complex information effectively. There have been dramatic advances in user interface design and display technology during the two decades that the space shuttles have been operating. Thus, NASA is in the process of redesigning the formats on the liquid crystal displays (LCDs) in the shuttle cockpit to capitalize on these advances.

The existing display formats in the space shuttle cockpit are limited in several ways. For example, the displays are primarily monochromatic, as shown in figure 1, making it difficult for astronauts to locate and focus their attention on a critical piece of information, such as an off-nominal parameter. The

proposed display formats include a systematic and logical use of color. An example of the proposed color-coding logic is illustrated in figure 2. Critical parameters (such as the status of a jet manifold) turn red when the value is off nominal. The letters representing status ("CI" for a closed valve in this example) become a color singleton that draws the viewer's attention automatically.



Fig. 1. Current display for the reaction control system.

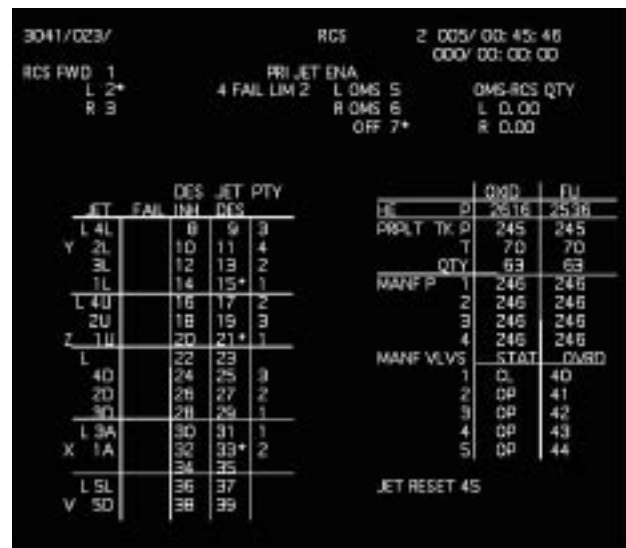


Fig. 2. Proposed display for the reaction control system.

Another limitation of the current displays is that they make only limited use of graphics. The proposed displays have expanded graphics to provide a closer match between the display and the mental models that crew members have of the system being depicted. For example, the proposed reaction control system display (figure 2) provides a graphic depiction of jet availability, enabling the crew to tell at a glance which jets can be fired. These improved display formats should give future shuttle crews

the capability to make better and more rapid decisions under off-nominal conditions, enhancing flight safety and crew member's abilities to meet mission objectives.

Point of Contact: J. McCandless
(650) 604-1162
jmccandless@nasa.gov

Investigation of New Liquefying-Fuel Hybrid Rocket Motors

Shane De Zilwa, Gregory G. Zilliac

The study of hybrid rocket motors is motivated by the need to improve safety, reduce costs, and enhance operational flexibility of rocket-based vehicles. Typical hybrid rocket motors use one propellant that is solid (generally the fuel) and another that is either liquid or gaseous (generally the oxidizer). Potential advantages of hybrids over conventional all-solid or all-liquid/gaseous motors are safety, throttleability, and cost of operations. Historically, the performance of hybrid systems has been limited by the low burning rates of the solid propellants. Recently, Stanford University, through a series of small-scale laboratory experiments, developed a family of paraffin waxes that have burning rates over three times greater than those of any hybrid propellants used previously. The primary objective of this activity was to develop the scaling characteristics of these waxes and demonstrate their potential as a feasible fuel for large-scale systems. If paraffin waxes perform as well at higher values of oxidizer mass flux, hybrid motors fueled with these waxes will also, in addition to the advantages mentioned above, be able to compete with conventional motors in terms of thrust capability.

To address the scaling issue, a facility for delivering up to 16 kilograms of gaseous oxygen per second to a hybrid motor capable of operating at combustion chamber pressures of up to 6,895 kiloPascals (1,000 pounds per square inch) has been built at Ames. During a firing, gaseous oxygen is delivered from a storage tank to the combustion chamber

through a closed-loop control system. Combustion of the wax is initiated by a spark-ignited methane-oxygen stream that is switched off once the wax begins to burn. A typical firing lasts about 10 seconds. A photograph of a firing is shown in figure 1. Important parameters measured during a firing include the supply and chamber pressures and the oxygen mass flow rate. A set of typical results is shown in figure 2(a). The most important parameter, the burning rate of the wax, is determined by measuring the mass loss from the fuel grain during the firing.

The experiments at Stanford University investigated oxygen mass fluxes of up to 10 grams per square centimeter per second ($\text{g}/\text{cm}^2/\text{s}$). To date, the tests at Ames have extended this range up to $50 \text{ g}/\text{cm}^2/\text{s}$, which is comparable with that required for practical



Fig. 1. Photograph of a firing.

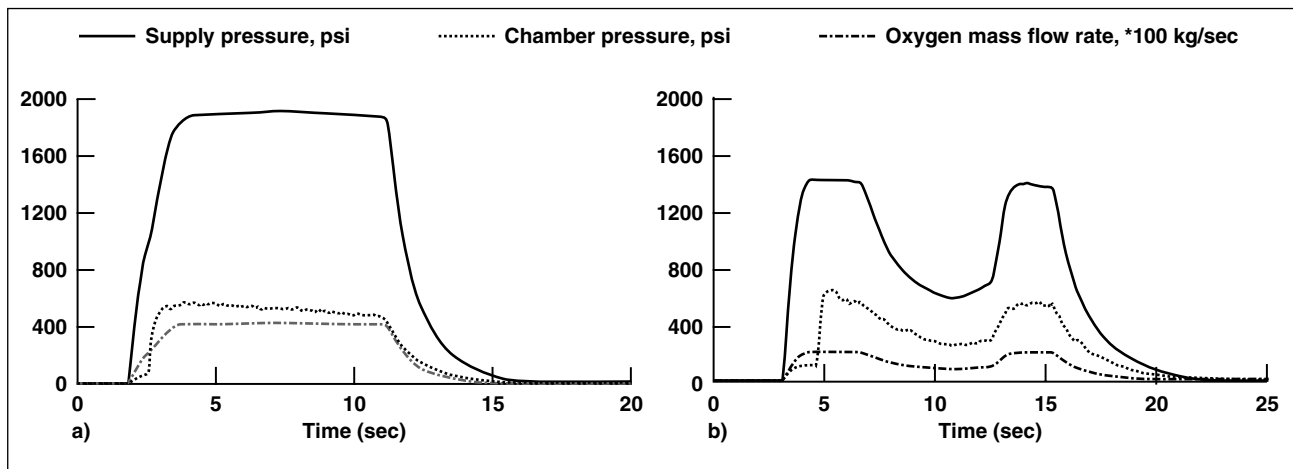


Fig. 2. (a) Results from a typical run; (b) demonstration of throttling.

systems. The burning rates were found to be consistent with the rates measured at Stanford and demonstrate that large-scale hybrid rocket systems using paraffin waxes are feasible and would be thrust-competitive with conventional systems. Also, the ability to throttle the mass flow (figure 2(b)) as well as to stop and restart the same fuel grain have been demonstrated.

The continued development of hybrid combustion systems utilizing these new high-regression rate fuels will be supported by follow-on research to quantify and understand the three-phase flow

mechanisms that govern the combustion processes. To this end, a rectangular cross-section combustion chamber has been designed that includes optical access through the side and top walls. This will allow visualization of the process and the use of laser instrumentation to investigate the phenomena involved with the mixing and burning of paraffin and oxygen.

Point of Contact: G. Zilliac
(650) 604-3904
Gregory.G.Zilliac@nasa.gov

Mars Rotorcraft Scout

Larry A. Young

A new approach to the robotic exploration of Mars is being studied at Ames: the use of small, ultralightweight, autonomous, rotary-wing aerial platforms (figure 1). Missions based on robotic rotorcraft could be excellent candidates for the NASA Mars Scout program.

Many of the most interesting geological features on Mars lie in terrain that is essentially unreachable by rovers and other current landing systems. Examples

include the headwaters of the newly discovered small Martian gullies and the layered cliff faces along the walls of Valles Marineris. Yet, in situ exploration of these features is critical to the understanding of their formation and of the role of water in Mars' present and past climate. A vertical-lift planetary aerial vehicle (a Mars rotorcraft) would have the flexibility to takeoff nearby, transit to, then hover over and examine such high priority science targets. Unlike fixed-wing aircraft concepts, a Mars

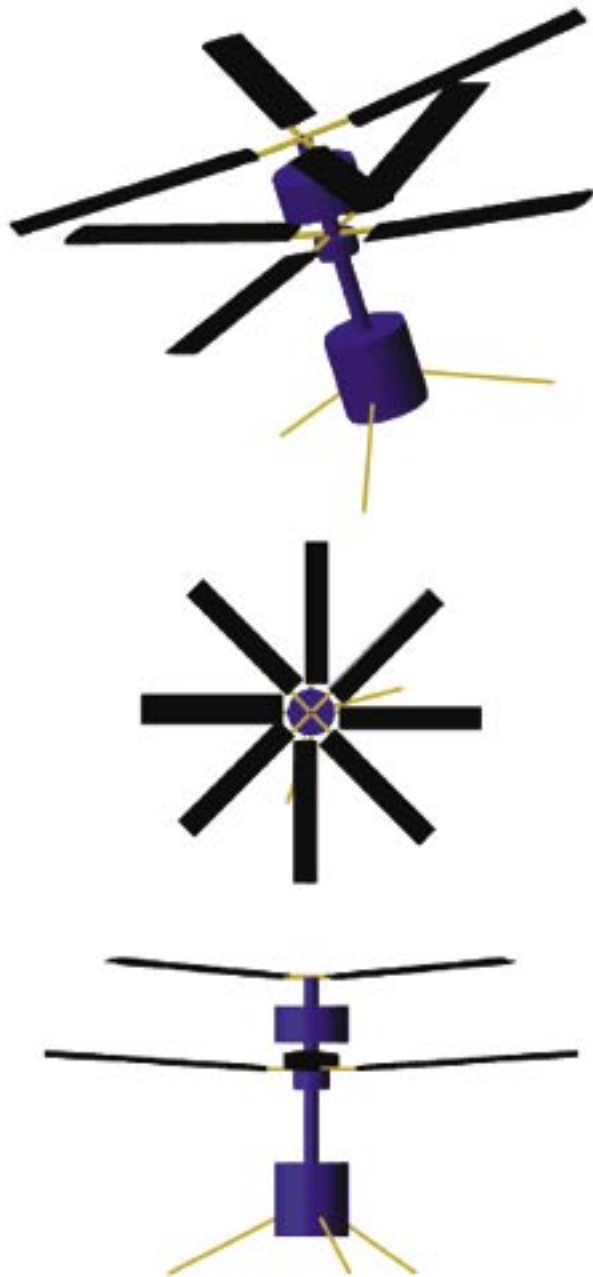


Fig. 1. A Rotary-Wing Mars Scout.

rotorcraft scout offers the opportunity to perform multiple flights by recharging, or refueling, at the lander. The rotorcraft would image and obtain spectral data for geological sites, and acquire samples from distances of up to 10 kilometers or more from the lander. The small samples would then be returned to the lander for in-depth analysis.

The feasibility of vertical flight in the Martian atmosphere has been established by design studies by Ames Research Center and by independent analyses performed by several university teams. Work on the Mars rotorcraft concept is transitioning from preliminary system analysis to proof-of-concept test article design and fabrication, to assessment and fundamental experimental investigations of the unique aerodynamics of these vehicles. In particular, an isolated rotor experimental model—subject to design constraints consistent with flight in the Martian atmosphere—has been designed and fabricated and is currently undergoing pre-test preparation for hover testing in an Ames environmental chamber. Complementary comprehensive rotorcraft aeromechanics analyses and computational fluid dynamics (CFD) studies are being performed to aid in the development of this unique aerial vehicle (figures 2(a)-(c)). Work is also under way to examine autonomous system technology and other critical enabling technologies for vertical-lift planetary aerial vehicles.

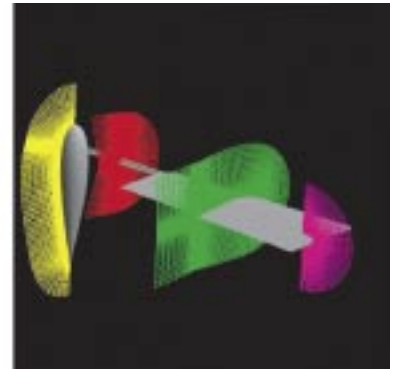


Fig. 2. (a) Experiment; (b) comprehensive rotor analysis; (c) Navier-Stokes CFD.

Point of Contact: L. Young, Code ARA
(650) 604-4022
Larry.A.Young@nasa.gov

PIONEER TECHNOLOGY INNOVATION

Pegasus5 Prepares Overset CFD Grids

Stuart Rogers

The goal of this work is to dramatically reduce the cycle time and the user expertise required to perform computational fluid dynamic (CFD) analysis for complex-geometry configurations. The Pegasus5 software code is a key piece of the series of tools used for CFD analysis using structured overset grids. It is responsible for connecting all of the randomly overset volume grids and preparing them for the flow solver. The previous version of the Pegasus code (version 4) required extensive input from an expert user.

In 1998, as part of the NASA/Boeing Advanced Subsonics Technology (AST) Program, a major milestone was met by reducing the CFD cycle time for a complete aircraft in a high-lift configuration from 1 year to less than 50 days. Of the 48 days that were required to simulate the flow over a Boeing 777-200 aircraft in a landing configuration, 32 days were used to perform the “oversetting” preprocessing of the CFD meshes, utilizing the Pegasus4 code. This program also initiated an effort to develop

Pegasus5, a completely new and improved version of this oversetting code. The approach was to utilize new algorithms which would eliminate the copious amount of input and the highly trained user expertise required by Pegasus4.

Significant improvements to the Pegasus5 software have been made during the past year, including several algorithm improvements, bug-fixes, and parallelization. A coarse-grained parallelization of the code was implemented utilizing the Message-Passing Interface (MPI) standard. This resulted in a speed-up of up to a factor of 14 when using 16 processors on a Silicon Graphics Inc. (SGI) Origin computer. The Pegasus5 software was tested this

year to process the original meshes used for the Boeing 777-200 high-lift configuration. A completed grid-system was processed in only 3 working days, which is an order of magnitude speed-up over the 32 working days required in 1998. The two figures show the complexity of the 777 geometry. Figure 1 shows a planform view of the configuration, figure 2 shows a close-up of part of the high-lift flap system.

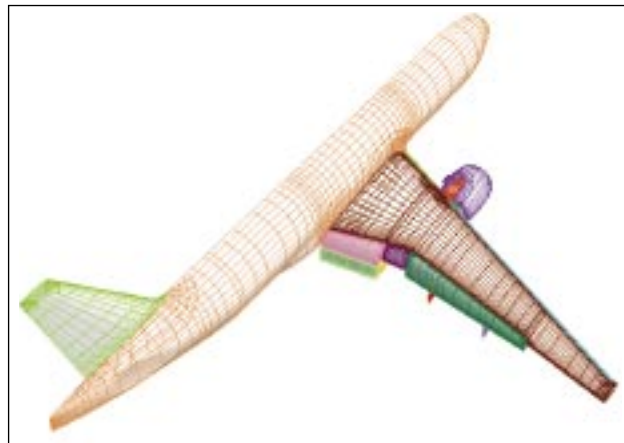


Fig. 1. Surface grids of the Boeing 777-200 high-lift configuration.

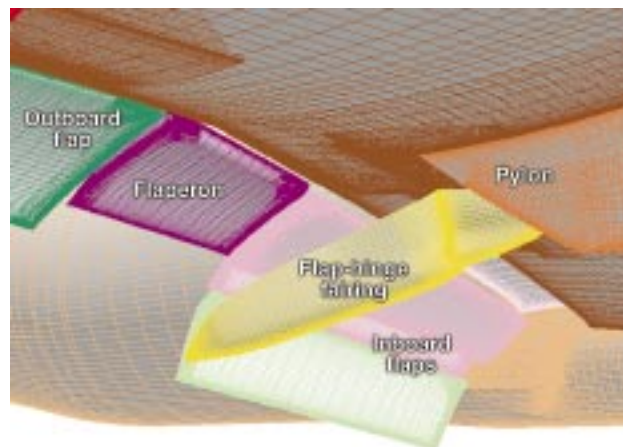


Fig. 2. Surface grids of part of Boeing 777-200 high-lift flap systems.

OVERFLOW flow computations were run on an SGI Origin O2K system with this new grid system, and the results were nearly identical to those computed with the Pegasus4-generated grids. This indicates that the same accuracy can be obtained in significantly less time. Improved turn-around time of the flow solver was also obtained using 128 processors of an SGI Origin system, which required only 24 hours; the previous effort required 48 hours of running on a Cray C90 in 1998.

This speed-up in CFD cycle time and the reduction in user expertise requirements will significantly reduce the cost of applying viscous CFD methods

to complex design and analysis problems. The first public beta release of Pegasus5 was announced at the beginning of this year. Copies of the software have been disseminated to over 90 different NASA, DoD, and industry users so far.

Point of Contact: S. Rogers
(650) 604-4481
Stuart.E.Rogers@nasa.gov

The Information Power Grid (IPG) Project

Arsi Vaziri, William E. Johnston

The Information Power Grid (IPG) is NASA's implementation of a compute and data Grid—an emerging infrastructure that provides seamless and

uniform access to NASA's geographically dispersed computational, data storage, networking, instruments, and software assets (figure 1).

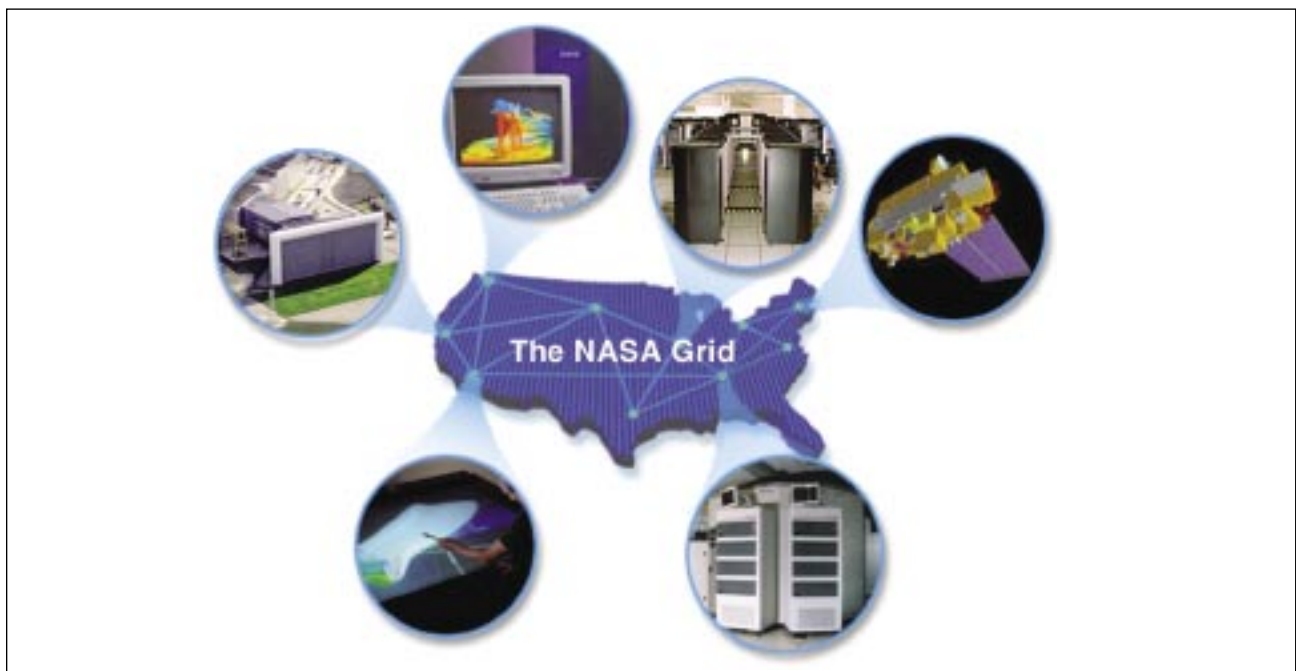


Fig. 1. NASA's distributed enterprise: people, computing, data, and instrument resources are integrated using computing and data grids.

IPG is NASA's high-performance computational grid. Computational grids are persistent networked environments that integrate geographically distributed supercomputers, large databases, and high-end instruments. These resources are managed by diverse organizations in widespread locations, and shared by researchers from many different institutions.

Future directions include new services that will allow users to approach the Grid with a computing or data management problem, and to dynamically "assemble," manage, and use all of the required resources by building a "virtual system" to solve their problem. This will enable the routine use of applications and application portals that require the use of many different distributed computing and data resources to solve a single problem. This view of the IPG provides a radically different use of computing in NASA's science and engineering, through integration of diverse and geographically distributed resources into the users desktop.

IPG is a multi-Center NASA effort and is being developed in collaboration with universities and other government agencies. Grid Services such as security, authentication, resource management, data management, resource discovery, and communication are provided by using the Globus Toolkit. Globus is a community-developed, open-source set of middleware software and libraries that support Grids and Grid applications.

Over the past 3 years, IPG has made significant progress in building and operating a state-of-the-art production Grid for NASA users (see www.ipg.nasa.gov). During FY01, a large-scale computer system (512-processor SGI Origin 2000) was integrated into the IPG resource pool. This addition provided a new level of computing power

to NASA applications running on IPG. IPG's basic Grid services and their operational support are in place at four NASA Centers: Ames Research Center, Glenn Research Center, Langley Research Center, and the Jet Propulsion Laboratory.

In addition to computing and storage resources, IPG also provides mechanisms for the integration and control of remote, high data-rate instruments using Grid services. A remote instrument connected to the Grid as a resource can be made accessible to a user who may access, control, and collect data and store/access data on IPG storage resources.

During FY01, two remote instruments were demonstrated. The Ames DARWIN/DREAM wind-tunnel instrumentation system used IPG services and resources in order to: (1) provide the instrumentation facility access to large-scale computing and data systems; (2) provide a standardized set of highly capable resource access and management services that do not have to be developed by the application developers; and (3) provide wider access to instrumentation data and analysis systems through a widely deployed IPG.

Using the TeleScience for Advanced Tomography facilities at the University of California, San Diego, it was demonstrated that NASA researchers, using remote and non-NASA facilities, can use NASA IPG services and resources to both store and analyze data that are obtained at the remote instrumentation facilities.

See www.ipg.nasa.gov for more information.

Point of Contact: A. Vaziri/W. E. Johnston
650/604-4523/4365

Arsi.Vaziri@nasa.gov/Wayne.E.Johnson@nasa.gov

Programming Paradigms for Adaptive Applications on SGI Origin

Rupak Biswas

Adaptive applications have computational workloads and communication patterns that change unpredictably at runtime, requiring dynamic load balancing to achieve scalable performance on parallel machines. An efficient parallel implementation of such adaptive applications is therefore a challenging task. However, architectural convergence and software tools have made it possible for different programming paradigms to be supported on the same platform. Our objectives were to compare the performance of and the programming effort required for two classes of adaptive problems under three parallel programming paradigms on an SGI Origin2000 system, a machine that supports all three models efficiently.

The first adaptive application was a dynamic remeshing problem on an unstructured grid. It represents a powerful and efficient technique in the numerical modeling of physical phenomena on complex irregular domains. The application consists of three main modules: local mesh adapter, dynamic load balancer, and numerical flow solver. The second application was the classic N-body problem that arises in many areas of science and engineering such as astrophysics, molecular dynamics, and computer graphics. Having specified the initial positions and velocities of N interacting bodies, the problem is to find their positions after a given period of time. The solution algorithm consists of three distinct phases: tree building to represent the distribution of the bodies, calculation of the force interactions between individual bodies, and updating each body's position and velocity based on the computed forces.

At present, the three leading parallel programming paradigms are explicit message passing, one-sided communication using symmetric private address spaces, and cache-coherent shared address space

(CC-SAS). The message-passing paradigm is the most popular, and it is commonly implemented by using the Message Passing Interface (MPI) library. Communication is performed by means of send-receive pairs, so processes on both sides are explicitly involved. The SHMEM (Shared Memory) library is similar to MPI but uses symmetric address spaces for the individual processes. Thus, any process can specify remote data by using their local name and the process identifier. CC-SAS, on the other hand, assumes a global shared address space, leverages hardware cache-coherency features, and accesses remote data implicitly by means of ordinary loads and stores. We chose the SGI Origin2000 machine as the common platform to compare and contrast these three programming models. The Origin is a scalable, hardware-supported cache-coherent non-uniform memory access system with an aggressive communication architecture. It therefore automatically supports the CC-SAS paradigm. The MPI and the SHMEM models are built-in software but leverage the machine's shared address space and the efficient communication features.

For the dynamic remeshing problem, we simulated flow over an airfoil and geometrically refined regions corresponding to the locations of the stagnation point and the shocks. The original mesh contained 59,000 (59K) triangles, and grew to approximately 156K, 441K, 1 million (1M), and 1.3M triangles through four levels of refinement. In this rapidly adapting flow simulation, local mesh refinement and the ensuing load balancer were invoked after 10 iterations of the numerical solver. Performance results are presented in table 1. Each of the three modules in this application had distinct performance characteristics. None of the programming paradigms was a clear winner. MPI and SHMEM outperformed CC-SAS during the adaptation phase; however, CC-SAS reduced programming com-

Table 1. Performance of the dynamic remeshing problem

Program- ming Paradigm	Lines Of Code	Time (seconds)											
		156K triangles			441K triangles			1M triangles			1.3M triangles		
		16p	32p	64p	16p	32p	64p	16p	32p	64p	16p	32p	64p
MPI	16,015	0.50	0.42	0.57	1.05	0.73	0.75	2.80	1.66	1.36	4.02	2.30	1.69
SHMEM	15,585	0.44	0.32	0.39	1.03	0.65	0.73	2.86	1.60	1.39	4.10	2.24	1.83
CC-SAS	8,430	0.47	0.43	0.57	1.09	0.84	0.90	2.60	1.68	1.51	3.52	1.95	1.57

Table 2. Performance of the N-body problem

Program- ming Paradigm	Lines Of Code	Time (seconds)											
		16K bodies			64K bodies			256K bodies			1M bodies		
		16p	32p	64p	16p	32p	64p	16p	32p	64p	16p	32p	64p
MPI	1,371	0.22	0.14	0.12	0.93	0.50	0.35	4.00	2.11	1.21	20.7	9.17	4.64
SHMEM	1,322	0.22	0.14	0.10	0.93	0.51	0.31	4.18	2.08	1.10	19.2	8.87	4.58
CC-SAS	1,065	0.23	0.12	0.08	1.02	0.54	0.31	4.42	2.28	1.22	21.8	12.0	6.69

plexity and did not require data remapping after load balancing. Moreover, the benefits of CC-SAS became evident with larger mesh sizes. For the N-body problem, we also tested four cases: 16K, 64K, 256K, and 1M bodies. These data sets model two neighboring Plummer model galaxies that are about to undergo a merger. Performance results for this application are presented in table 2. Here, MPI and SHMEM significantly outperformed CC-SAS for the largest data set.

Overall results indicate that all three programming paradigms can deliver comparable performance; however, the implementations differ considerably, even though the same basic parallel algorithms were used. CC-SAS provides substantial ease of programming, but currently has portability limitations and suffers from poor spatial locality of distributed-shared data.

Point of Contact: R. Biswas
(650) 604-4411
Rupak.Biswas-1@nasa.gov

Facilitating Human Performance Modeling

Alonso Vera, Roger Remington, Michael Matessa, Michael Freed

A computational modeling tool was demonstrated that automatically constructed a model of complex behavior from libraries of primitive actions and was able to predict the performance of human operators very accurately. One of the difficulties in developing human interfaces to complex systems is anticipating users' responses to the large space of possible system states and design options. Even extended

empirical user testing can fail to uncover serious difficulties. Moreover, current practice fails to make use of the abundance of data and theory that could be applied to evaluate candidate human-system configurations. A promising solution is to develop a computational representation of the user to allow a designer to simulate user responses to a variety of situations and design options. This goal was approached by packaging the abundance of data on

human perceptual, cognitive, and motor phenomena into sets of behavioral primitives or templates that can be incorporated directly into predictive, computational models. Templates reduce the amount of psychological and methodological knowledge required to build models, allowing the modeler to focus on task analysis instead of on low-level psychological theories and modeling methodology.

A tool was developed for automatically constructing long sequences of behavior from a small set of templates that describe primitive actions such as moving a mouse to a target, typing a key, or pressing a mouse button. The computational modeling approach, based on a powerful cognitive task analysis method called CPM-GOMS (Critical Path Method-Goals Operators, Methods, Selection rules), has been successful in making accurate, zero-parameter, a priori predictions of the routine performance of skilled users in a wide range of procedural tasks. This system, Apex, automatically generates streams of behavioral templates that can be visualized with PERT charts, showing the complex interleaving of cognitive, perceptual, and motor resources deployed by skilled users.

Figure 1 shows the close fit between the performance times generated by the model and those generated by human users for a simple human-computer interaction task. The model predicts each mouse click in the task within 100 milliseconds or less. Resource scheduling in Apex automates the difficult task of interleaving the cognitive, perceptual, and motor resources underlying common human-computer interaction task components (e.g., mousing to and clicking on a button). The user interface to Apex displays the PERT chart on command, allowing modelers to visualize a model's

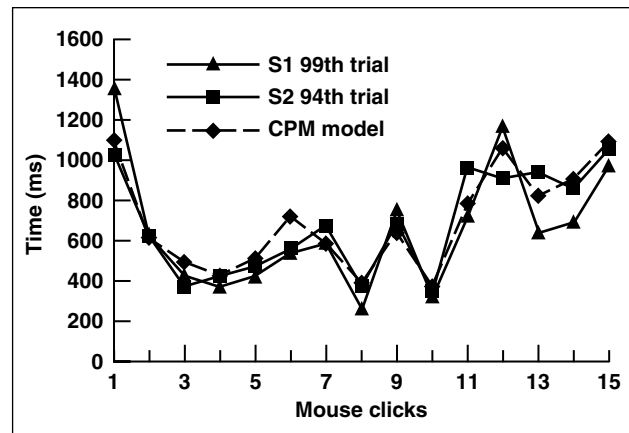


Fig. 1. Sample performance data for two subjects on a human-computer interaction task compared with the predictions generated by the CPM-GOMS model.

complex parallel behavior (figure 2). Because interleaving and visualization are now automated, it is feasible to construct arbitrarily long sequences of behavior. Apex is being developed into a tool that is robust, fast, and usable in the context of predictive modeling for system design with libraries of behavioral templates for common human-computer interaction activities.

Current modeling environments impose barriers to computational human performance models that limit their use to a few special cases. Modeling has been time consuming and error prone, and requires specialized training in cognitive science. In order for computational cognitive modeling to achieve wider use in software design, it is necessary to make model production easier and more valid than it has been in the past. The implementation of a powerful modeling method by researchers at Ames and their collaborators at Carnegie Mellon University marks a significant step toward this goal.

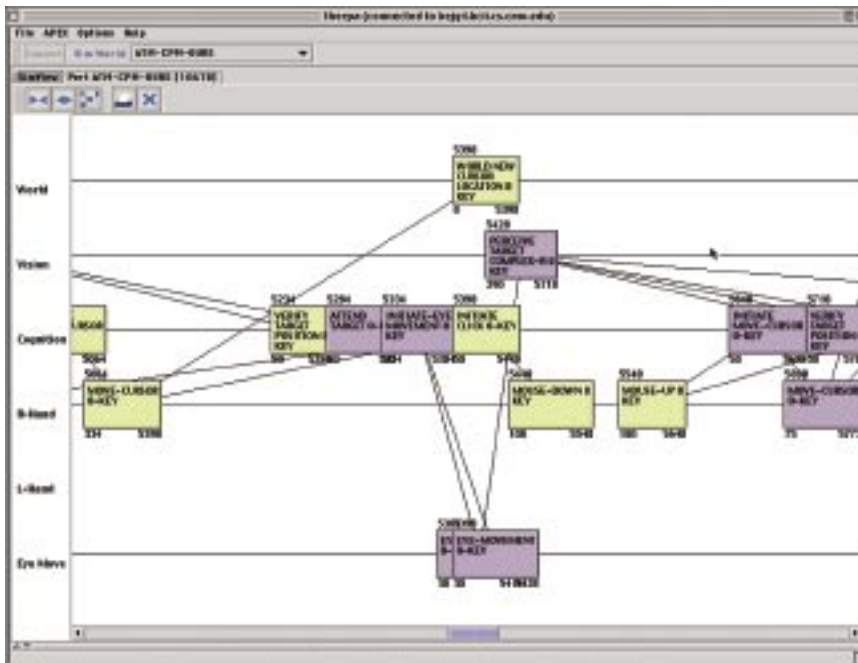


Fig. 2. Behavioral PERT charts automatically generated by the Apex/CPM-GOMS GUI.

Point of Contact: Alonso Vera
(650) 604-6294
Alonso.H.Vera@nasa.gov

Subjective Estimation of Visual Quality

Andrew B. Watson

A standard method for estimating subjective visual quality was developed at Ames Research Center. NASA missions rely extensively on visual communications, from space imagery and remote monitoring of space and aircraft to advanced video communications. In all of these applications, maximizing visual quality, while minimizing weight, power, bandwidth, and cost, is a primary concern. Yet, there have been no standard methods for measuring visual quality. The method developed at Ames is based on the just-noticeable-difference (JND) unit. In psychophysics (the study of the relation between physical stimuli and sensory experience), two physical stimulus intensities that can just be discriminated

are said to be one JND apart. Our method provides a way of measuring the perceptual distance between two stimuli in units of JND.

This method uses a pair-comparison procedure in which a pair of samples are presented to an observer on each trial. The observer selects the one perceived to be greater on the relevant scale (e.g., heavier, brighter, louder). Although simple for an observer to perform, this procedure is inefficient because many comparisons will be uninformative if all samples are compared. In general, samples separated by about 1 JND are the most informative. Thus, a more efficient adaptive method for selecting sample

pairs was developed; it is based on Bayesian estimation of the sensory scale after each trial. It is called Efficient Adaptive Scale Estimation, or EASE (“to make less painful”).

The EASE method was used to measure impairment scales for digital video. Each video was derived from an original source (SRC) with the addition of an artifact produced by a particular form of video compression at a specific bit rate, called a hypothetical reference circuit (HRC). Different amounts of artifact were produced by linear combination of the source and compressed videos. On each pair-comparison trial, the observer selected which of the two sequences appeared to be more impaired. The scale is estimated from the pair-comparison data by using a maximum likelihood method. The value at the top of the scale (with all of the artifact present) is the total number of JNDs separating the original and the compressed video.

Impairment scales for 25 video sequences derived from five SRCs combined with each of five HRCs were measured. EASE was found to be a reliable method for measuring impairment scales and JNDs for processed video sequences. Figure 1 shows the growth of the perceived artifact, in units of JND, as the proportion of artifact is increased from 0 to 1 for one particular video sequence. The black points are a sampled estimate of the impairment scale, and the red curve is a continuous functional estimate. The advantage of JND measurements is that they result in absolute units that are meaningful and unlikely

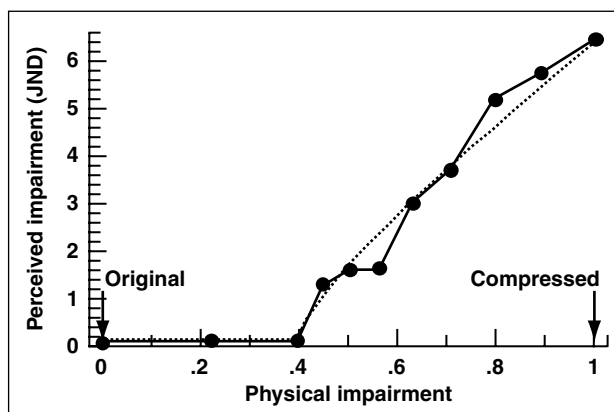


Fig. 1. Perceived impairment as a function of intensity of physical impairment for one video sequence.

to be subject to context effects. JND measurements offer a means of creating calibrated artifact samples and of testing and calibrating video quality models.

This work was performed in close collaboration with the IEEE G-2.1.6 Subcommittee on Video Compression Measurements of the IEEE Broadcast Technology Society so it could be readily adopted as the U.S. standard for measurement of perceived impairment of digital video. The resulting “IEEE P1486/D06, Draft Standard for the Subjective Measurement of Visual Impairments in Digital Video Using a Just Noticeable Difference Scale,” will be balloted in 2002.

Point of Contact: A. Watson
(650) 604-5419
Andrew.B.Watson@nasa.gov

Text Readability Metric Validated for Transparent Text

Albert Ahumada

A text readability metric developed at Ames Research Center was applied to predict the readability of text superimposed on the background in a transparent manner. Both in the cockpit and in the control tower, text readability is an important issue. For many advanced displays, text will be presented on top of complex imagery, such as synthetic scene images or weather maps. In such applications, the text is either additively transparent (e.g., a head-up display that adds light to the external scene), or multiplicatively transparent (e.g., a see-through liquid crystal display that attenuates the light coming through the display). Previous tests of this metric have been restricted to text that overwrote the background.

Text readability was measured for the two types of transparent text (Additive and Multiplicative) at two contrast levels (Low-0.3 and High-0.45) on three background textures (arbitrarily labeled Plain, Wave, and Culture). Five additional contrast levels (0.1, 0.15, 0.2, 0.25, 0.3) were measured for the plain backgrounds. Figure 1 illustrates the observer's task in the validation test. The observer reads a paragraph containing a word (circle, square, or triangle) inserted at random in the text, pressing a button of the corresponding shape when the word is found. The average search time is considered to be indicative of text readability.

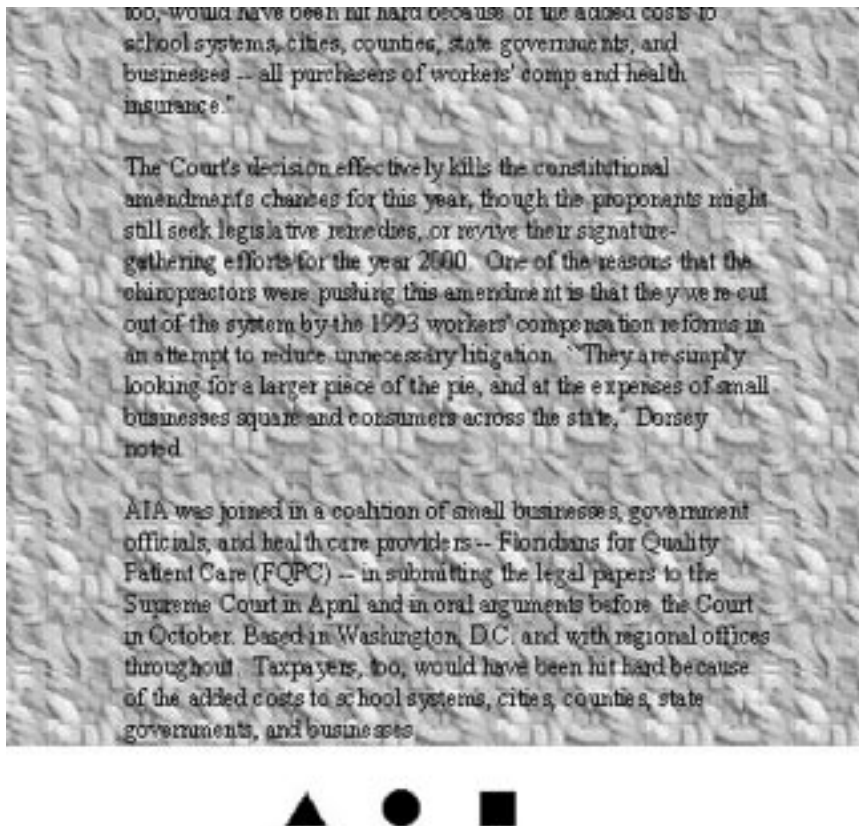


Fig. 1. An example text display with a multiplicative contrast of 1.0 on the culture background; the correct response is to click on the square.

Figure 2 shows the average search times for the different conditions as a function of the text-readability metric scores. The readability metric was found to account well for the difference between the Mul-

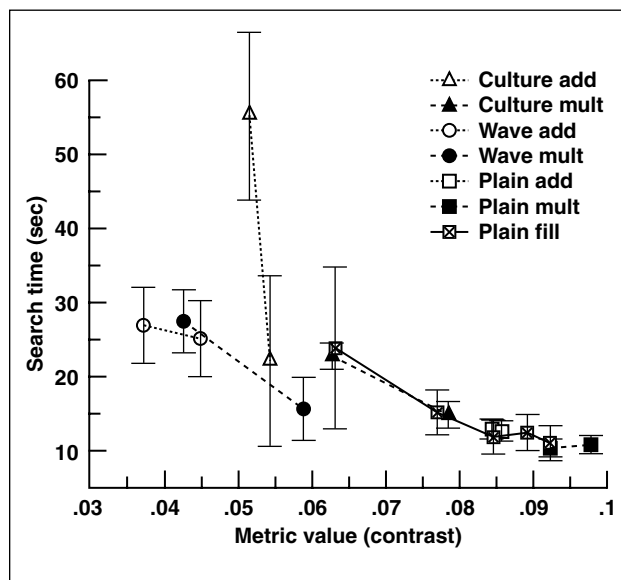


Fig. 2. The relationship between experimentally measured search times and the text readability metric for the experimental conditions.

tiplicative and the Additive conditions; lower effective contrast values were assigned to the Additive conditions. The High Contrast/Culture Texture condition fell along the Plain Texture curve. The Low Contrast/Culture Texture condition appeared to be an extension of that curve, but the metric predicted more masking for the Wave Texture condition than actually produced. The overall rank correlation of the fit is -0.94, where -1 would be a perfect correlation. Although the predictions of the text-readability index were not perfect, it is easy to compute (it depends only on means and variances of pixel luminances) and allows designers to estimate quickly the likely effect of changes in text contrast, mode of presentation, and background imagery on text readability.

Point of Contact: A. Ahumada
 (650) 604-6257
 Albert.J.Ahumada@nasa.gov

Computational Modeling of Hovering Rotors and Wakes

Roger C. Strawn

Large-scale computations have been conducted to numerically simulate the performance of a UH-60A model rotor in hover. These computations were designed with high numerical resolution in order to carefully control numerical effects in the final results. The computations solve the Navier-Stokes equations that govern the aerodynamic flow field around the rotor system. Baseline computations used 10.6 million grid points, and one high-resolution simulation used 64 million points. The 64-million-grid-point solution pushed the limits of today's high-

performance parallel computers. Figure 1 shows computed vorticity contours from this 64-million-grid-point result. All solutions show very good agreement with experimentally measured rotor performance. The computations show that careful attention to numerical details and high-resolution grids can produce hovering-rotor performance results that are very accurate. In addition to providing a wealth of detailed flow-field information, the results show that rotorcraft computational fluid dynamics (CFD) simulations can also provide accurate quantitative performance results as well.

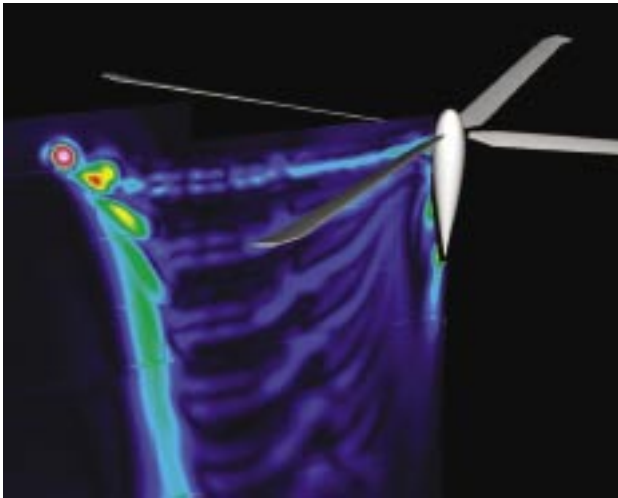


Fig. 1. Computed vorticity contours 45° behind the rotor blade for the 64-million-grid-point solution.

Point of Contact: R. Strawn
(650) 604-4510
rstrawn@mail.arc.nasa.gov

Unsteady Pressure-Sensitive Paint Measurements on an Oscillating Airfoil

Edward T. Schairer, Lawrence A. Hand

Pressure-sensitive paint (PSP) is an optical technique for measuring continuous pressure distributions on aerodynamic surfaces of wind-tunnel models. The technology for making PSP measurements on rigid models in steady flows is well established and has been implemented in large wind tunnels worldwide. In contrast, the technology for making unsteady PSP measurements on a flexible model is still evolving. One such application of particular interest is a helicopter rotor in forward flight. Rotor flows are extremely complex and poorly understood, and traditional methods for measuring pressures on rotors (e.g., using unsteady pressure transducers) are difficult and costly to apply, and they yield woefully inadequate spatial resolution. The high spatial resolution and non-contact nature of PSP make it a potentially valuable tool for understanding rotor aerodynamics.

Over the past several years, a series of experiments at Ames Research Center has addressed the problems of using PSP to measure pressures on helicopter rotors. PSP measurements were made on rigid and flexible rotors in hover in the Ames Anechoic Chamber. In addition, unsteady measurements were made on an oscillating airfoil in the Compressible Dynamic Stall Facility. Although PSP measurements were successfully made in each experiment, one shortcoming the experiments shared was lack of independent verification of the PSP results. The present article summarizes a second oscillating airfoil experiment in which this problem was rectified: in addition to PSP, the model was instrumented with unsteady pressure transducers.

The experiment was conducted in the Compressible Dynamic Stall Facility (figure 1). The model, a

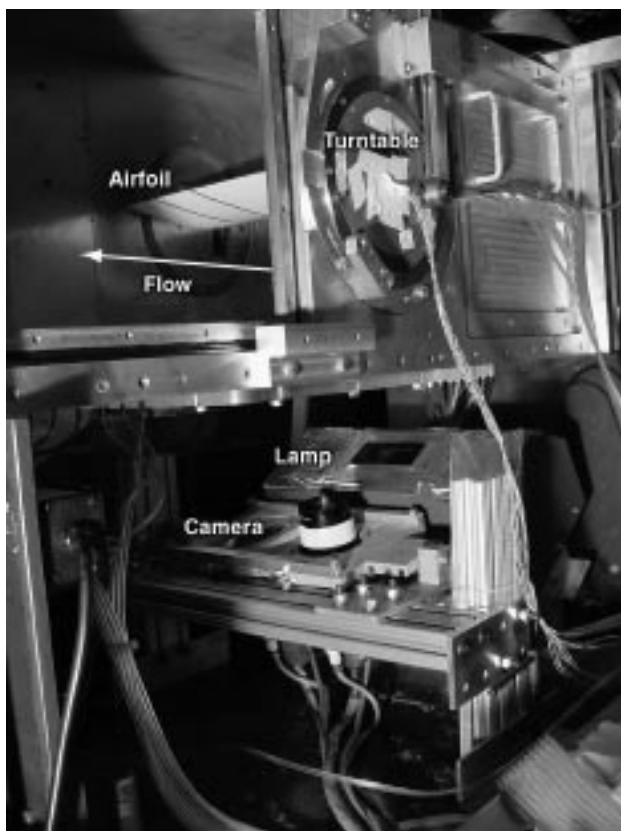


Fig. 1. Test set-up.

6-inch-chord NACA 0012 airfoil, was supported at either end by turntables mounted in the sidewalls of the test section. The turntables and model were driven in simple harmonic motion by a motor on top of the test section. The model oscillated about its quarter chord at an amplitude of $\pm 5^\circ$, mean angle of 0° , and frequencies up to 20 Hertz. The Mach number for all the tests was $M = 0.45$.

The lower surface of the model was painted with pressure paint supplied by Langley Research Center. The model was illuminated through a window in the lower wall of the test section by a xenon flash lamp and was imaged through the same window by a cooled CCD camera fitted with filters to block light from the lamp. The flash lamp could be triggered at pre-selected phase angles, and images were built up over many oscillation cycles. Images were acquired at 20 near-evenly spaced phase angles of a full cycle.

The lower surface of the model was instrumented with eight unsteady pressure transducers located between the leading edge and the quarter chord near the model mid-span. Data were acquired at a rate of 8,000 samples per second and phase-averaged over many cycles.

A PSP sample was calibrated over a range of pressures and temperatures in a calibration chamber. This calibration was used to convert wind-off/wind-on image intensities, measured in the wind tunnel, to pressure distributions. The pressure paint exhibited some temperature sensitivity. To correct for this effect, the temperature of the paint on the model was assumed to equal the local adiabatic recovery temperature.

Wind-off/wind-on image intensities were scaled to force the PSP data to match the pressure measured by one of the transducers ($x/c = 0.25$). Although this compromised the independence of the PSP measurements, it was necessary to account for unexpected variations in average flash-lamp brightness from one image to the next.

PSP data were extracted along a chordwise line near the transducers at each of the 20 phase angles. Figure 2 shows data at three phase angles for the 20-Hz case. Note the enforced agreement between the PSP (solid lines) and pressure-transducer (symbols) data at $x/c = 0.25$. The PSP data track the other transducers reasonably well. The most likely reasons for differences between the PSP and transducer data include imperfect temperature compensation of the PSP and three-dimensional flow effects (the PSP and transducer data were acquired at slightly different span stations). Harmonic analysis of both the PSP and transducer data at all 20 phase angles shows that, upstream of the quarter-chord, the unsteady pressures lagged the model motion.

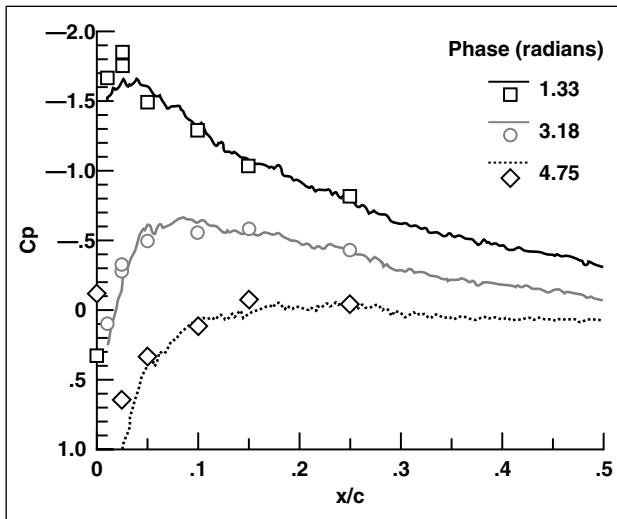


Fig. 2. Comparison of PSP (solid lines) and pressure-transducer (diamonds) data at three phase angles ($f = 20$ Hz, $M = 0.45$).

Point of Contact: E. Schairer
(650) 604-6925
Edward.T.Schairer@nasa.gov

Wind Tunnel Tests to Determine the Air-Wake Characteristics of U.S. Navy Ships

Kurtis R. Long, James T. Heineck

To improve safety during shipboard rotorcraft take-offs and landings, personnel from Ames Research Center and the U.S. Navy have teamed to investigate, understand, and report back to the fleet, the complicated flow patterns associated with ship air-wakes. This long-term effort employs both wind-tunnel and computational fluid dynamics (CFD) techniques to estimate full-scale ship air-wake data for a variety of U.S. Navy ship Program Offices. Five different ship air-wake wind-tunnel efforts were conducted in FY01; these included a project to determine the effects of model fidelity on the air-wake characteristics of a new destroyer, an investigation of the causes of two recent rotor blade/fuselage contact incidents, and a project to collect ship air-wake data using particle image velocimetry (PIV) techniques.

For shipboard air-wake wind-tunnel tests, models were constructed from wood, brass, and plastic. Each ship model represented different levels of

geometric fidelity, quantified by a Characteristic Geometric Fidelity Dimension (CGFD), which represented the size of the largest real-world ship structure modeled accurately in the model. The high-fidelity models (CGFD = 8 inches) included almost all the protuberances, fittings, and mast-mounted emitters of the real ship. Models were operated in various wind-tunnel facilities at Ames Research Center, using various instrumentation to collect the desired air-wake data at multiple vertical-lateral planes spanning the length of each model.

Model fidelity test results indicated that highly detailed models experienced significantly larger (30% of free-stream velocity) deficits in mean downstream velocity ratio, in areas 50-75 feet above the deck and downstream of the mast and yardarms; this difference vanished at eight H-60 helicopter rotor diameters (1 D = 53.6 ft) downstream of the ship's aft deck edge. Elsewhere, there were minimal

(<5%) variations in mean downstream velocity ratio. The high detail models also produced slightly decreased (5 degrees) upflow angle in regions more than 75 feet above the deck, and at heights of 10 to 20 feet above the deck, downstream of the mast and yardarms. The high-detail model slightly increased (3 degrees) the downflow angle elsewhere, but all differences decayed to values less than 3 degrees at 8 D downstream of the deck aft edge. The high-detail model created insignificant (less than 4%) changes in mean spin velocity at all locations investigated.

The PIV effort produced a high quality set of air-wake data that consisted of over 100,000 sets of three-dimensional (3-D) velocity data, acquired in a few hours time. The PIV data were subsequently used to help quantify the ship's air-wake environment for unmanned air vehicle (UAV) operations. The PIV air-wake effort successfully demonstrated that PIV techniques are a practical means for obtaining large quantities of air-wake information in a very short amount of time.

The effort to investigate recent rotor-blade/fuselage contact instances (also known as tunnel strikes)

employed both surface oil visualization and velocity measurements, which showed that the presence of parked aircraft on the starboard side of the ship created different flow patterns than those that occurred for the empty-deck configuration (figure 1). When helicopters were placed at typical starboard side parking locations, a strong longitudinal vortex, which typically hugged the starboard deck edge for the empty deck configuration, was now displaced upward and over the parked helicopters, reattaching to the deck at a location that was more inboard, and therefore closer to the port side landing spots. The results of this effort were forwarded to the deployed ship within 2 weeks of the tunnel-strike incidents; shipboard personnel utilized the information and experienced no further tunnel strikes during the ship's deployment.

These efforts illustrate how existing NASA facilities, expertise, and technology can be used to quickly investigate, analyze, and remedy problems in a variety of nontraditional work areas.

Point of Contact: K. Long/J. T. Heineck
(650) 604-0613/0868
Kurtis.R.Long@nasa.gov
James.T.Heineck@nasa.gov

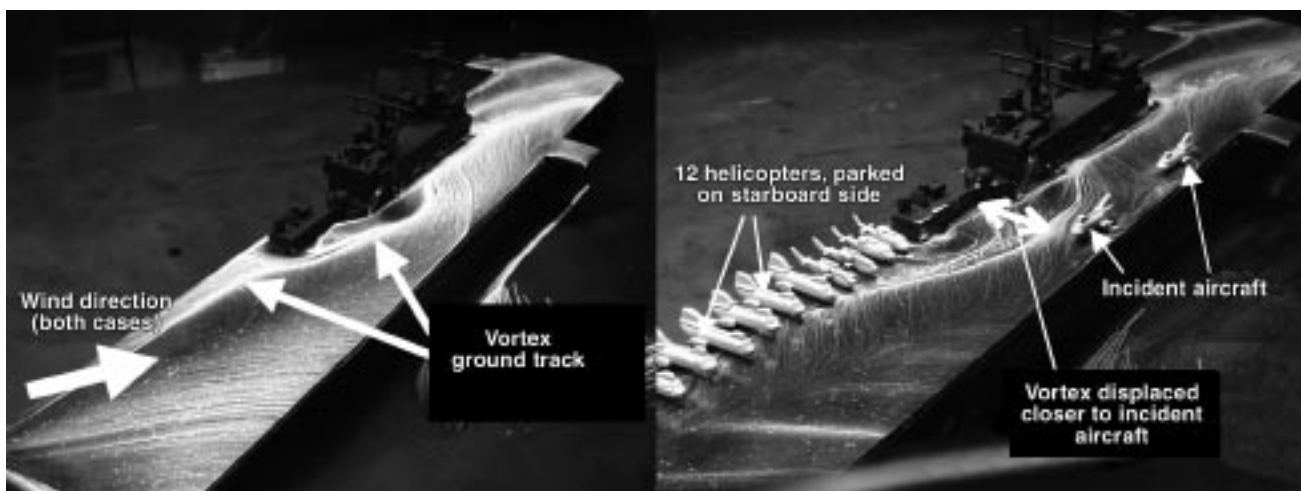


Fig. 1. Surface oil flow visualization: effect of parked helicopters on LHD 1 Class flow patterns.

Semiconducting Nanotube—Electrode Contact Modeling

Toshishige Yamada

Transistors are the heart of present-day electronics. Their miniaturization and integration have resulted in ultralarge-scale integrated circuitry with 10 billion transistors mounted on a tiny 1-centimeter square chip. NASA aircraft are controlled with computers on board and on the ground that are composed of these chips. The transistor performance is determined by intentionally introduced impurities in the channel of the transistor. Following the present miniaturization below 0.1 microns—a thousandth the width of a human hair—the electrons start to see less than a hundred impurity atoms scattered randomly in the channel. To design transistors accurately, the impurity atoms must be positioned in a three-dimensional way with atomic precision, but this is technologically impossible and implies an end of the silicon transistor era. For further progress, Ames researchers needed to reverse the philosophy—from top-down to bottom-up design. The researchers should start from precise atomic structures free from randomness, and build devices using atomically precise blocks, rather than continue with miniaturization. This is the motivation for the Atomic Chain Electronics Project at Ames Research Center.

Carbon nanotubes have a hollow cylinder shape with a diameter of about one billionth of a meter. They are molecules in that all the atoms are located at designated positions without any random fluctuations. All the nanotubes are atomically precise, and this accords with the philosophy of bottom-up design in the Atomic Chain Electronics Project. During the last several years, many experiments have been reported on nanotube devices, but some results cannot be explained at all with conventional theory. In this work, Ames researchers challenged one such mystery and clarified it for the first time.

In 1997, Professor Zettl's group, at the University of California at Berkeley, observed two different current-voltage (I-V) characteristics for a nanotube using a scanning tunneling microscope (STM) tip electrode. In figure 1(a), the current can flow in both bias directions (type-I), but in figure 1(b), it can flow only in one bias direction (type-II). What is surprising is that Zettl's group used exactly the same experimental setup with the same nanotube, and once observed figure 1(a), and at a different time figure 1(b). This has been a mystery for a few years in the science community.

Ames proposed a new theory to explain it in FY01. It is argued that the observed I-V characteristics were a result of the contact properties between the semiconducting nanotube and the metallic STM electrode, and not of the intrinsic nanotube electronic properties. There are two possible contact modes: a vacuum-gap mode (left) and a touching mode (right) as shown in figure 1(c). With a vacuum-gap mode, the current can flow in both bias polarities. When the bias applied to the STM electrode is negative ($V < 0$), the energy band is as shown in figure 1(d), and the electrons can tunnel from the right to the left through an extremely thin vacuum barrier (barrier thickness not to scale). In figure 1(e), $V = 0$ and the electrons cannot flow. In figure 1(f), $V > 0$ and the electrons can tunnel from the left to right. With a touching contact, the current can flow only when $V < 0$ (Schottky forward), where the electrons see little barrier as in figure 1(g). In figure 1(h), $V = 0$ and the electrons cannot flow. In figure 1(i), $V > 0$, but because of the barrier at the nanotube-electrode contact, the electron flow is blocked, resulting in no current (Schottky reverse). Ames researchers performed a quantitative study based on this view, and recovered all the essential features of the experiment successfully.

In electronic applications, all devices must be connected to the electrodes, and then to the lines to carry electronic signals. According to our results, the device characteristics are often changed because of the electrode contact, which is not the case in the silicon transistor technology. This is one of the features of nanoelectronics, indicating that we need to design nanodevices taking into account these electrode effects.

Point of Contact: T. Yamada
(650) 604-4333
yamada@nas.nasa.gov

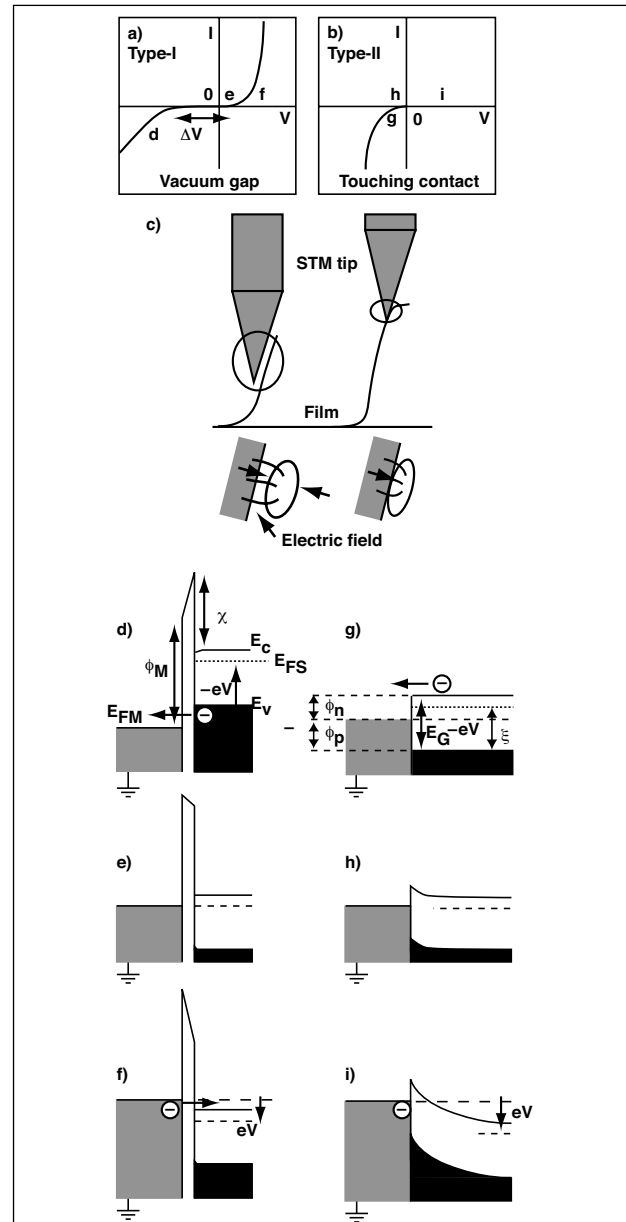


Fig. 1. Nanotube-STM electrode with two different contact modes: (a) type-I and (b) type-II I-V patterns; (c) schematic showing the vacuum gap (left) and touching (right) modes. Parts (d) to (i) are band structures for operation points in the I-V patterns: (d) valence band tunneling ($V < 0$), (e) equilibrium ($V = 0$), (f) conduction-band tunneling ($V > 0$), (g) Schottky forward ($V < 0$), (h) equilibrium ($V = 0$), and (i) Schottky reverse ($V > 0$), where the STM is grounded.

Current Carrying Capacity of Carbon Nanotubes

M. P. Anantram

Carbon nanotubes (CNTs) are molecular wires that are made up of carbon atoms arranged in a hexagonal pattern on the circumference of the wire. Typical diameters of CNTs range from six to tens of angstroms and CNTs can be many microns long. CNTs are considered a primary candidate for molecular electronics because they can electrically be either metals or semiconductors, which are, along with oxides, the building blocks of modern electronics. The primary property of a good metallic wire is high electrical conductivity/conductance at both small and large biases. Typical mechanisms that degrade conductivity involve scattering of electrons that have defects and phonons. This work deals with modeling of the maximum current-carrying capacity of ideal CNT molecular wires, at various applied voltages, in the absence of defects and phonons.

At small applied voltages, electrons are injected only into two modes (also referred to as sub-bands) of the metallic CNT wire. After a critical voltage, which is approximately equal to $\Delta E_{NC}/2e$ (e is the electron charge), electrons can be injected into higher lying modes (see figure 1). Further, ΔE_{NC} and hence the applied voltage at which electrons are injected into the higher lying modes is inversely proportional to the CNT diameter. For example at an applied voltage of 2 volts (V), electrons are injected in 4 and 20 modes in nanotubes with diameters of 15 and 60 angstroms, respectively.

NASA researchers model electron flow through a nanotube connected to ideal contacts without any barriers, using the Landauer-Buttiker approach. In the presence of an applied bias, the potential drops across the nanotube. The potential drop is modeled phenomenologically using a realistic functional. Figure 2 shows the current as a function of the applied bias for nanotubes with diameters that

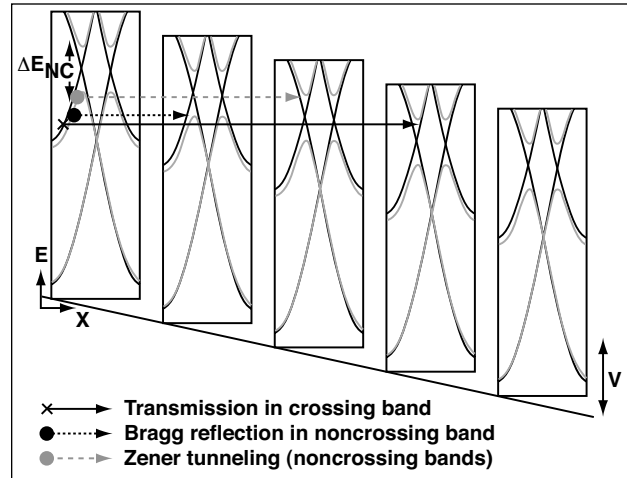


Fig. 1. A semi-classic view of electron flow along a metallic carbon nanotube. The x-axis is position (x) along the wire and the y-axis is energy (E). Each rectangular box represents the energy-versus-wave vector at different spatial locations, in the semi-classic spirit. The black "crossing" and the green lines are called the crossing and noncrossing modes, respectively. An electron injected in the crossing mode (solid circle) is always transmitted to the right for applied voltages smaller than approximately 3 V. In contrast, an electron injected in the noncrossing mode can either be Bragg-reflected (does not carry current) or it can Zener tunnel to the right-hand side (carries current).

vary from 7.5 to 30 angstroms. Researchers find that for small-diameter nanotubes, the current increases linearly with applied bias until about 3 V, and that the increase of current with further increase in applied bias is insignificant. As the diameter increases, the increase of current is small, signifying that the noncrossing modes (green lines of figure 1) do not significantly enhance current with increase in applied voltage. The microscopic reason for this phenomenon is Bragg reflection of electrons incident in the noncrossing modes, which is also explained in figure 1. The solid black lines are the crossing modes and the green lines are the noncrossing modes at an energy $\Delta E_{NC}/2$ away from the band center.

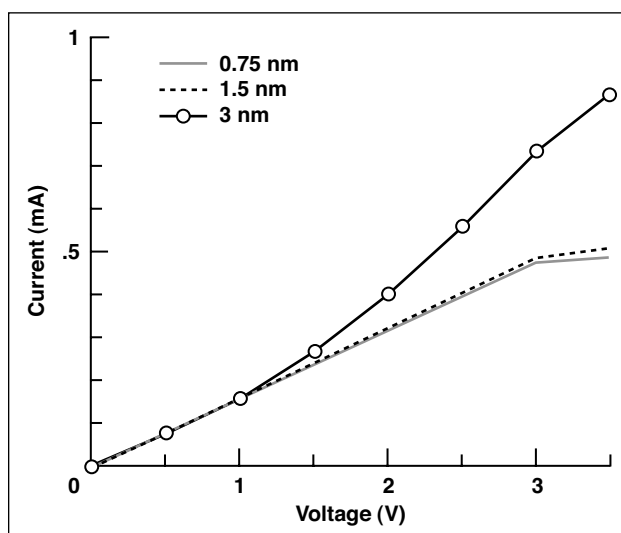


Fig. 2. Current versus applied voltage for three different diameters of carbon nanotubes (shown in the legend).

Figure 1 illustrates that electrons incident in the crossing sub-band can be transmitted to the right. But electrons incident in the noncrossing mode can either be Bragg-reflected at the band edge (dotted line) or can Zener tunnel to the noncrossing mode on the right-hand side (dashed line). The probability

for Zener tunneling depends on the diameter of the nanotube, because the barrier height for Zener tunneling is of the order of ΔE_{NC} . As ΔE_{NC} decreases with increase in the nanotube diameter, the contribution to current owing to Zener tunneling increases with increase in the nanotube diameter. This is the reason for the slow increase in current as the nanotube diameter increases in figure 2, at the larger applied voltages.

Small-diameter metallic single-wall carbon nanotubes carry almost the same current as larger-diameter single-wall carbon nanotubes, even at applied biases where electrons are injected into many modes. The main insight gained in this modeling study is that Bragg reflection of electrons is the primary reason for limited current flow in an ideal case without electron-phonon interaction. Zener tunneling can enhance current flow in the case of large diameter CNT.

Point of Contact: M. P. Anantram
 (650) 604-1852
anant@nas.nasa.gov

Protein Nanotechnology

Jonathan Trent, Andrew McMillan, Chad Paavola

In support of NASA's efforts to make its missions more and more successful, there is a growing need for smaller, stronger, and "smarter" scientific probes that will be compatible with space exploration applications. The necessary breakthroughs in this area may well be achieved in the revolutionary field of nanotechnology. This is technology on the scale of molecules, which holds the promise of creating devices smaller and more efficient than anything currently available. Although a great deal of exciting research is developing around carbon-nanotube-based nanotechnology, investigators at Ames Research Center are also exploring biologically inspired nanotechnology.

The biological "unit," the living cell, may be considered the ultimate nano-scale device. Cells, which are constructed of nano-scale components, are extremely sensitive, highly efficient environmental sensors capable of rapid self-assembly, flawless self-repair, and adaptive self-improvement; not to mention their potential for nearly unlimited self-replication. Ames is focusing on proteins, a major component of all cells, which are capable of self-assembling into highly ordered structures. A protein known as HSP60, currently being studied, spontaneously forms nano-scale ring structures (figure 1(A), end view; 1(B), side view), which can be induced to form chains (figure 1(C)) or filaments (figure 1(D)).

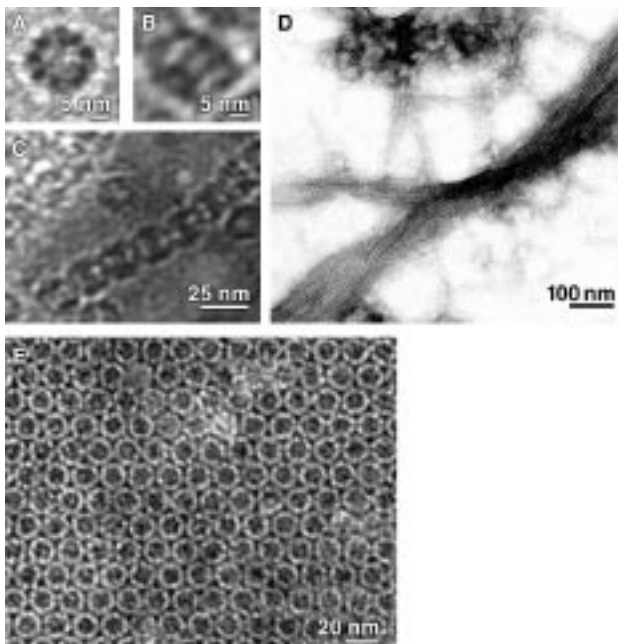


Fig. 1. Protein rings (A) end view, and (B) side view, chains of rings (C), and bundles of chains (D) that can be used in nanotechnology and two-dimensional crystals (E) of mutated rings used for metal array formation.

By using thermostable HSP60s, highly efficient methods have been developed for purifying large quantities of these proteins, and by using the “tools” of molecular biology, their composition and structure-forming capabilities are being currently modified.

Recently, progress has been made in evolving the HSP60 into a structural subunit that can be manipulated in such a way as to make it utilizable in the formation of ordered arrays. Ordered arrays of metals are of interest in the semiconductor engineering community for the fabrication of devices that can be addressed and further assembled into logical circuits. To this end, a portion of the wild-type HSP60 subunit identified as contributing to the formation of filaments, or end-on structures, has been removed at the genetic level. The removal of this region of DNA directs the expression of

a protein incapable of organizing into filaments; however, it possesses the ability to crystallize in two dimensions in a highly ordered hexagonally packed array (figure 1(E)). This ordered array is being used to direct deposition of metals by templating. This process takes advantage of both the propensity of the modified subunit to self-assemble into a highly ordered array and the ability to site-specifically functionalize the protein. Using this approach, specificity for metals can be engineered into the protein that will subsequently localize the metals at defined intervals along the protein and hence into an ordered array (figure 2). A simple removal of the protein leaves the ordered array of metal on the substrate with nanometer scale feature resolution.

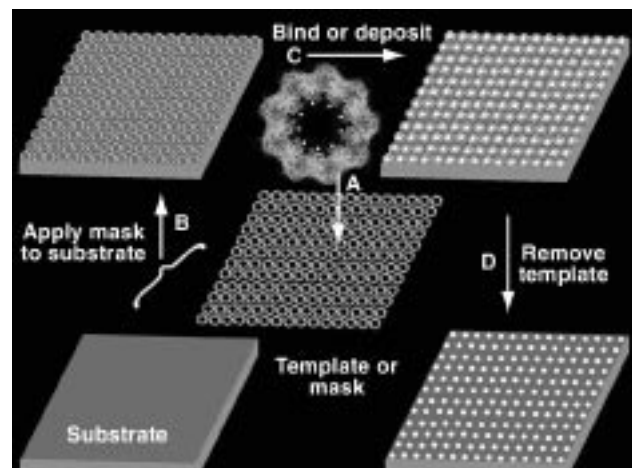


Fig. 2. Mutant forms of HSP60 possess genetically engineered chemical reactivity at specific sites on the rings (A), green dots. These rings are crystallized (A) in two dimensions forming a highly ordered template. The template is applied to the surface of a substrate (B), and metals are bound that specifically attach to defined sites throughout the crystal (C). Finally, the template is removed (D), and the ordered array remains bound to the substrate.

Point of Contact: J. Trent
(650) 604-3686
Jonathan.D.Trent@nasa.gov

Nanostructured Skin Effect: Anisotropic Plasticity of Boron-Nitride Nanotubes

Deepak Srivastava

Nanotubes are sheets of single atomic layers rolled up into tubular or cylindrical structures. Among newly discovered nanoscale or nanostructured materials, nanotubes have been the subject of intense theoretical and experimental investigations because of their unusual strength, stiffness, electronic, chemical, and thermal properties. Carbon nanotubes, which were discovered first, have possible applications in lightweight high-strength composite materials, molecular electronic devices, chemical and gas sensors, gas and energy storage systems, and flat-panel displays. Nanotubes of other materials such as boron-nitride (BN) also have been made; they have similar strength and stiffness but different electrical, chemical, and thermal properties. Whereas initial work just looked at the electronic properties of BN nanotubes, Ames researchers and others have recently started to look at the structural and mechanical properties of BN nanotubes.

Working with researchers from the University of Kentucky and Stanford University, it was found that the strength and stiffness (for strains within the elastic limit) of BN nanotubes are comparable to those of their carbon counterpart. Young's modulus of a single-wall BN nanotube is within 80% of that of similar carbon nanotubes (~1 terapascal). Two significant differences, leading to very different nanomechanical properties of BN nanotubes, were discovered. First B-B and N-N bonds in a BN nanotube are mechanically unstable (bond-frustration effect), and second, each B-N bond is slightly rotated so that the N atom is nearer to the surface than the B atom (bond-rotation effect as shown in figure 1). Based on the first discovery, it was predicted that odd-number ring defects (such as pentagons and heptagons) in a hexagonal lattice of a BN nanotube are unstable, and thus zig-zag nanotubes would

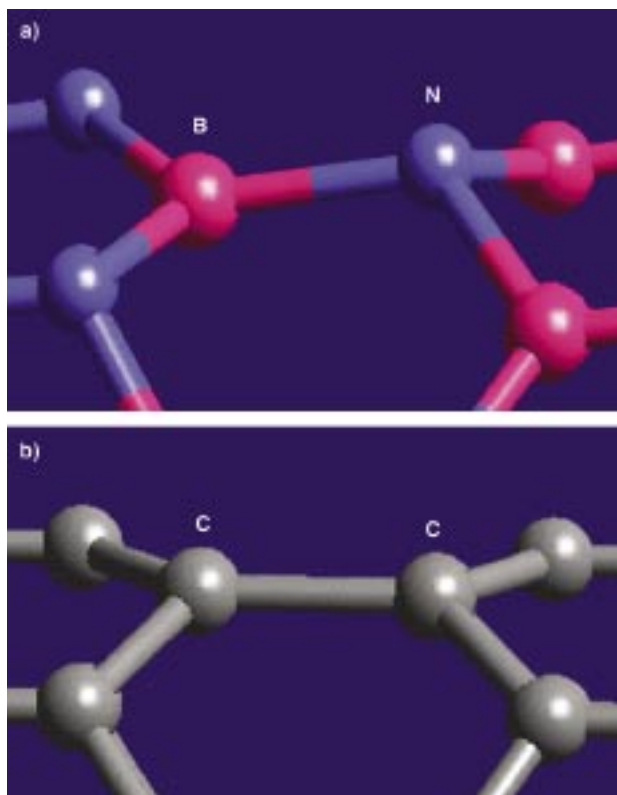


Fig. 1. The rotated B-N bond on a BN nanotube surface is shown in comparison with the non-rotated C-C bond on a carbon nanotube surface.

predominate in the synthesized material. This has been recently verified in experiments done in Europe and Japan.

Based on the second discovery, the bond-rotation effect, it was surmised that BN nanotubes should behave anisotropically when compressed or stretched with large strains. By isotropically compressing BN nanotubes in quantum molecular dynamics simulations, it was found that BN nanotubes plastically buckle in a completely anisotropic manner. For example, in figure 2, a BN nanotube has collapsed

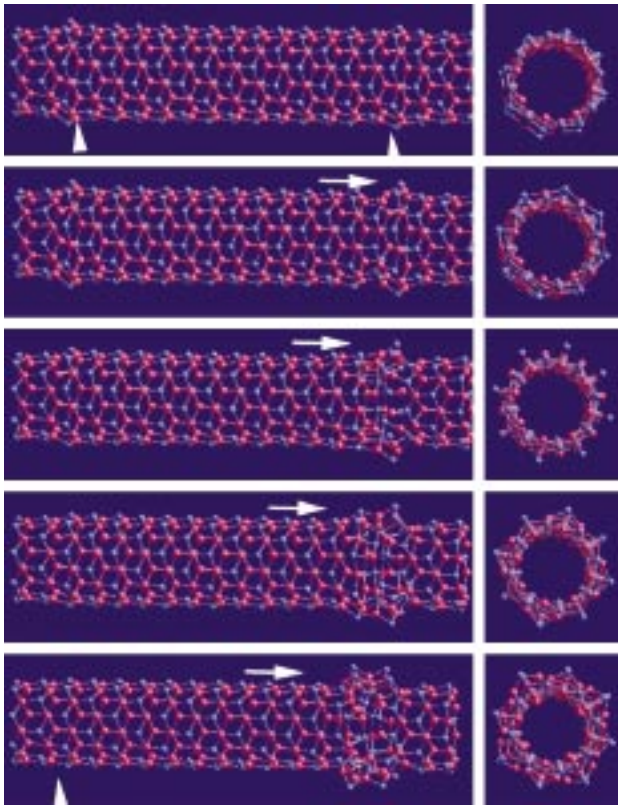


Fig. 2. A quantum molecular dynamics sequence of the anisotropic plastic collapse of a BN nanotube. All the damage has been transferred to one end of the tube that was isotropically compressed at both ends.

only toward one end when isotropically compressed at both ends. The anisotropic plastic collapse in the material is driven by the preferential strain release toward N as the leading edge of a rotated B-N bond in the zigzag nanotube.

These findings show not only that BN nanotubes may be useful as reinforcing fibers in ultralight and strong composite materials, but also that they add a functionality in the sense that BN nanotube composite material will exhibit a nano-structured “skin-effect.” This means that if such a material is exposed to large compressive strains in shock conditions, the axial strain-induced damage will be intrinsically transferred toward the outer “skin” surface of the material while keeping the inner core intact. Practical uses of such a functional or “smart” composite material, if developed, will be in the transportation, aerospace, defense, and armor industries. Under collision-induced shock conditions, in these applications, the coating of such a material may not have time to develop long wavelength instabilities, the excess strain will be released towards the “skin” or surface side, and the inner core will be protected against the damage.

Point of Contact: D. Srivastava
(650) 604-3486
deepak@nas.nasa.gov

Ultrafast Modulation of Coupled Surface-Emitting Lasers

Cun-Zheng Ning, Peter Goorjian

Vertical-cavity surface-emitting lasers (VCSELs) are lasers made of semiconductors such as gallium-arsenide that emit laser light vertically to the semiconductor wafer surface. These are the smallest lasers ever made, smaller than the thickness of a human hair. VCSELs are extremely useful for a number of commercial applications such as data communication and bio-detection. Their small size and intrinsic radiation resistance also make them very attractive for future space missions.

One of the critical parameters that determine the application of VCSELs is the speed at which the light intensity can be easily altered or modulated. There is, however, a fundamental physical limit to such modulation speed when the traditional modulation approach is used. Because of that limit, which is a result of the relatively long electron-hole lifetime in a typical semiconductor, further increases in modulation speed require novel approaches. In the past, Ames researchers have proposed up to a terahertz (THz) (trillion cycles per second) or 10^{12} Hz modulation using a fast-alternating electrical field to heat the electrons in semiconductors. This approach has the potential of achieving a very high speed, but the required terahertz field intensity and the scarce availability of terahertz sources make this approach difficult to implement at the present. As a more realistic alternative, Ames researchers have recently studied the possibility of achieving high-speed modulation through coupling of two or more VCSELs.

The idea works as follows: In a single VCSEL, the modulation speed is dictated by the interaction of the laser field and the electrons in the semiconductor. If two or more VCSELs are put close to each other, inter-laser interaction occurs. As a result, the laser field can predominantly concentrate on one of the two lasers. Since the two lasers are identical and the laser intensity is equally likely to appear in either of the two lasers, the laser intensity spot oscillates between the two. The frequency at which this

oscillation occurs is now determined by the inter-VCSEL coupling, rather than by the coupling between the laser field and electrons. This is why this modulation can avoid the typical speed bottleneck caused by the long electron-hole lifetime.

Ames researchers have implemented this idea in an extensive computer simulation using a computer code developed earlier. The simulation results show that this coupled VCSEL scheme can provide modulation speeds up to 40 gigahertz (billion hertz). Furthermore, the scheme can also be used as a beam switch. As demonstrated in figure 1, the coupled VCSELs can switch a laser beam in two directions separated by about 8 degrees. An additional advantage of the scheme is that both the far-field and the near-field show circular beam shapes, which is a desired property for many applications.

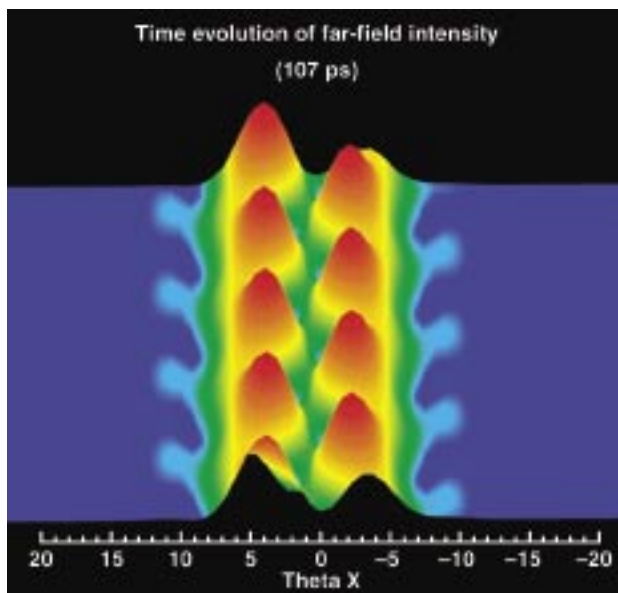


Fig. 1. Time evolution of a cross section of the far-field intensity; the x-axis shows the far-field angle (theta-X).

Point of Contact: Cun-Zheng Ning
(650) 604-3983
cning@nas.nasa.gov

Expanding the Envelope for Shared Memory High-Performance Computing

James Taft

For several years, Ames Research Center has been pursuing the development of the largest shared-memory computing systems in the world. Extensive Ames experience on shared-memory systems consisting of 128, 256, and 512 central processing units (CPUs) has shown that mission-critical production applications can be ported to, and optimized for, these types of systems years faster than cluster-based alternatives. Furthermore, these applications typically sustain higher percentages of the peak performance of the systems as well.

In the past year the NASA push to extend the size of shared-memory systems has culminated in the development of a 1,024 CPU Origin 3000 shared-memory High-Performance Computing (HPC) system (figure 1). This effort was a joint development between Ames and Silicon Graphics, Inc. (SGI). The SGI team focused its efforts on hardware and system software issues; the Ames work was focused on application porting and on extending NASA-developed scalable parallelization methods. A secondary task was to develop and refine the administrative software and tools needed to establish a practical production-quality system for a diverse base of users.

The porting effort relied heavily on the utilization of the Ames-developed Multi-Level Parallel (MLP) approach to shared-memory parallelism, a greatly simplified and highly scalable alternative to the classic message-based MPI technique. This technique, coupled to the shared-memory architecture, has allowed all MLP converted production codes to scale to levels never before achieved. The result of this latest effort has been the successful 1,024 CPU port of mission critical applications in computational fluid dynamics (OVERFLOW-MLP), climate



Fig. 1. The NASA Ames 1,024 CPU Origin 3000 system (Chapman).

modeling (FVCCM3-MLP), and earth science data assimilation (DAS-MLP) representing over 500,000 lines of code. All conversion and optimization was completed in less than 1 year.

One of the major effects of the NASA – SGI effort has been the accelerated development of large shared-memory systems not present in any vendor's product plan. NASA's leadership in this area has had significant benefit to the HPC community as a whole, as test-bed systems originally developed at Ames have been produced by SGI and sold into other HPC sites.

The Ames strategic acceleration of shared-memory HPC systems has been highly successful and has fundamentally changed the way HPC is done at NASA. The OVERFLOW-MLP code executes problems at nearly 40 times the best performance on the recently retired 16 CPU Cray C90 system. The DAS system from the Data Assimilation office executes production calculations 10 times faster than ever before on any system, and with just 9 months work. The FVCCM3 climate model executes almost 15 times faster.

During this effort Ames has actively encouraged all vendors to expand the envelope of shared-memory computing, and is actively working to establish memoranda of understanding with the major players to fully test this alternative to the clustered-computing approach. All vendors have expressed interest, and work is under way to examine the possible next steps in this pursuit.

Point of Contact: J. Taft
(650) 604-0704
jtaft@nas.nasa.gov

Using Electromyography to Predict Head Motion for Virtual Reality Applications

Yair Barniv

The objective of this research is to use neck and shoulder electromyograms (EMGs) to predict head movements in immersive virtual environments (VEs) in order to minimize the time lags in updating the visual scene that can cause disorientation and simulation sickness. Visual update delays are a critical technical obstacle to implementing head-mounted displays in a wide variety of applications—from training simulations and mission rehearsal to teleoperation and telemedicine. These applications require a perceptually veridical mapping between actual head position and virtual spatial position in the synthetic environment. Figure 1 shows an example of a subject attempting to superimpose virtual and real objects where the virtual visual environment appears to “swim” around when head movements are translated slowly into visual updates. These latencies are mostly a result of delays in sensing head motion with inertial sensors (accelerometers and rate gyros). EMG signals from muscles precede force exertion and, therefore, limb or head accelerations by about 30 milliseconds. We expect to gain a comparable reduction in head



Fig. 1. A subject attempting to superimpose virtual and real objects.

position update time by using EMG in the VE stabilization loop instead of or in addition to inertial sensors. We evaluated the pattern of EMG activities in the approximately 30 muscles involved in head motion with a set of up to 32 electrodes placed around the neck (as shown in figure 2) rather than attempting to isolate the effect of each muscle separately. A solution of this many-to-six (32 EMG signals to



Fig. 2. The placement of electrodes on neck of subject is used for registering neck muscle EMG activity.

six inertial linear and angular accelerations) real-time pattern-recognition problem could reduce or eliminate the latencies encountered in current VE applications, making this technology more feasible, especially for see-through applications. In support of this goal, we established an EMG laboratory where data from both EMG and inertial sensors were collected to predict head movements in virtual environments and to minimize update delays. Data from five human subjects have been collected thus far. Data analysis supported the prediction that EMG signals precede inertial measurements by 20 to 30 milliseconds. As an initial step, we have developed a neural network pattern-recognition algorithm that accepts current inertial data and predicts future angular velocity for a single angular velocity component.

Point of Contact: Yair Barniv
(650) 604-5451
Yair.Barniv-1@nasa.gov

A Real-Time System for Unobtrusive Gaze Tracking

Jeffrey B. Mulligan

An efficient method was demonstrated for estimating operator gaze (a product of eye and head position) in real time without constraining the operators' head movements or requiring them to wear uncomfortable equipment. Gaze-tracking is an important approach for unobtrusive performance monitoring in assessing the functional utility of complex display configurations, such as those used to display air traffic. Unfortunately, accurate gaze measurement usually requires either rigid positioning of the operator's head to allow a fixed camera to acquire a highly magnified image of the eye; or the use of a head-mounted camera system so that the eye image will not be lost when the operator makes small head movements. The latter approach is able to produce good data for someone seated naturally at a work-

station but suffers from several drawbacks. In order to prevent slippage (and the consequent loss of calibration), the head mount must be mounted on the head so tightly that it is uncomfortable for extended use. There is always some obstruction of the field of view and it is not clear whether the operator's behavior will be completely natural when a bulky apparatus is attached to the head.

For these reasons, we have been developing a system that employs a steerable camera that can follow the movements of a user's head while maintaining a magnified image of one eye. To accomplish this, it was necessary to address the problem of keeping the eye's image centered within the image in real time to aid with steering. In the past, we had assumed

that measurements of pupil position would be processed off-line to determine gaze. The current system uses a pair of wide-field cameras and an illumination method first developed at the IBM Almaden Research Center to allow real-time localization of the pupils. The two cameras form a stereo pair that should allow recovery of the three-dimensional locations of the eyes, at least in principle. This allows, in turn, computation of the required steering control parameters (figure 1).

It had been assumed that all of these calculations would require careful spatial calibration of the cameras. However, a camera-control method was developed that eliminates the need for precise cali-

bration of the camera geometry. This was possible because it was unnecessary to recover the full three-dimensional position of the eye; it was sufficient to send only the pan and tilt parameters to the camera control unit. Although the functional relationships among the measurements and required settings could be determined, given complete knowledge of the camera geometry, they would be sensitive to small errors in measurement of the camera positions and orientations. Thus, a method that required no knowledge of these parameters was needed. A small laser pointer was mounted on the body of the steerable camera. It was aimed along the camera's line of sight and shone upon a screen placed at various positions in the volume of space within

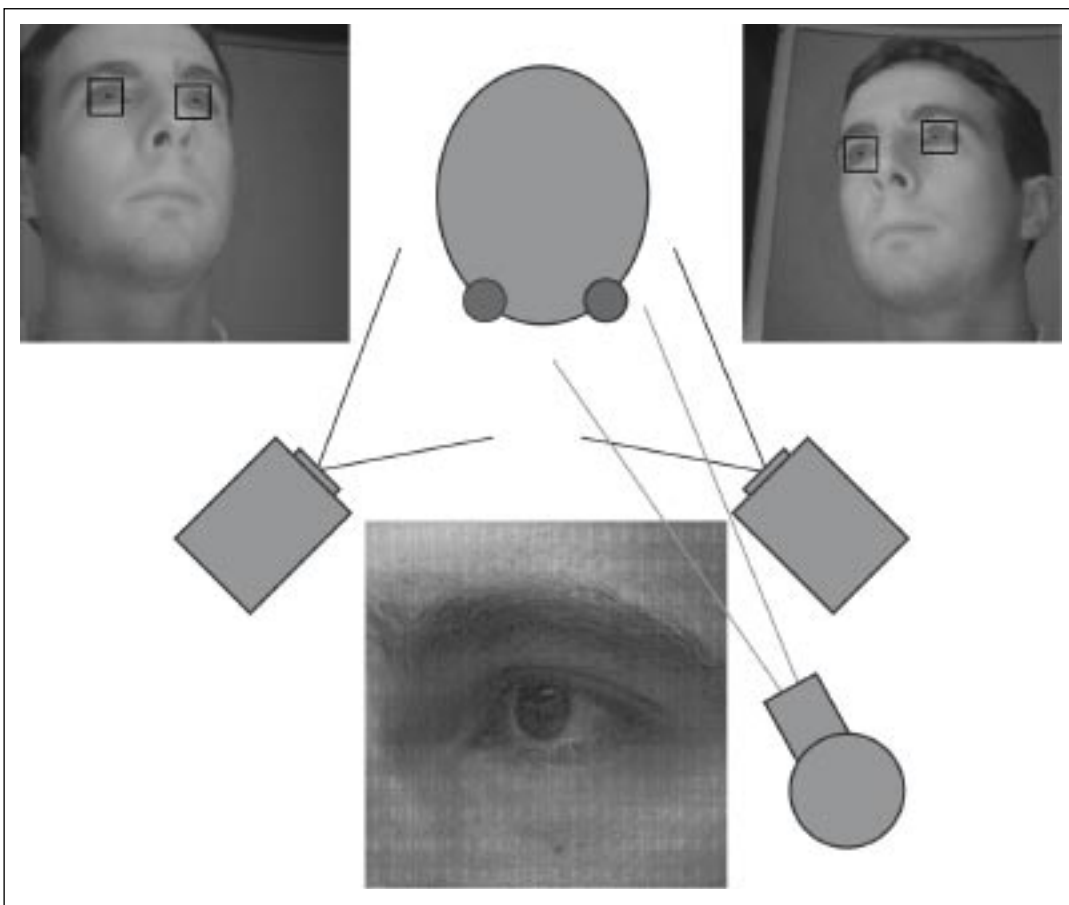


Fig. 1. Schematic of apparatus with representative images: at the center of the figure, the subject's head and the three cameras are shown as seen from above. To the left and right are shown example images from the right and left wide-field face cameras. The pupil locations determined from the face camera images are used to control a narrow-field eye camera; the image from this camera (bottom) is used for gaze tracking.

which the user's head would be tracked. The wide-field cameras image the entire space and can easily detect the small spot made by the laser beam. The pan and tilt positions corresponding to many positions of the spot within each of the wide-field images were obtained to generate a table of values relating pan and tilt settings to the corresponding measurements for the wide-field cameras. A variety of methods were used to generate pan and tilt settings for arbitrary measurement values based on this training set, and it was found that a simple quadratic function was sufficient to produce pan and tilt values accurate to within one or two pixels.

This preliminary work employed a commercial pan-tilt camera designed for teleconferencing applications. Since the mechanism was too slow to follow the fastest natural head movements, work is under way to replace this component with a miniature camera whose line of sight is steered by a pair of galvanometer mirrors capable of much higher speeds.

Point of Contact: J. Mulligan
(650) 604-3745
Jeffrey.B.Mulligan@nasa.gov

Kinesthetic Compensation for Rotational Misalignment of Cameras Used for Teleoperation

Stephen R. Ellis, Bernard D. Adelstein, Robert B. Welch

Kinesthetic feedback was shown to significantly improve the accuracy of teleoperations subject to rotational misalignments between the image source and the operator, even without explicit training. Rotational misalignments are often encountered in teleoperations and telerobotics when a remote image sensor (usually a camera) is oriented so that the resulting display coordinates are rotated with respect to the coordinates in which the user is operating. In the past, users have had to learn to compensate for this misalignment through practice, camera adjustment, or the use of multiple camera images. A new compensation technique is proposed in which the hand not used for control is utilized to provide a kinesthetic cue to the camera orientation. This cue greatly reduces the difficulty operators have had in compensating for control-display misalignment. The cueing hand, which is positioned to copy the attitude of the viewing camera, provides a kinesthetic reference for the movement of the other hand, which controls the teleoperated system. This enables users to make control movements relative

to their kinesthetic sense of the orientation of their own (cueing) hand.

Experimental testing with single-axis rotations was conducted to demonstrate the feasibility of this technique. Operators were required to make small (~2-3-centimeter) radial hand movements controlling a computer-displayed cursor under conditions of rotational misalignment with and without kinesthetic cues. Performance was measured by the length of the movement path normalized to the path length each operator was able to achieve without misalignment. Even without explicit training, this kinesthetic cue reduced control inaccuracy associated with some rotational misalignments by as much as 64% (figure 1). Although the kinesthetic cue clearly improved the accuracy of large movements, its benefit for small movements was particularly important, for these are more typical in the control of NASA robot manipulators, such as the Orbiter Remote Manipulation System. Extension of the technique to multi-axis rotations is currently under way.

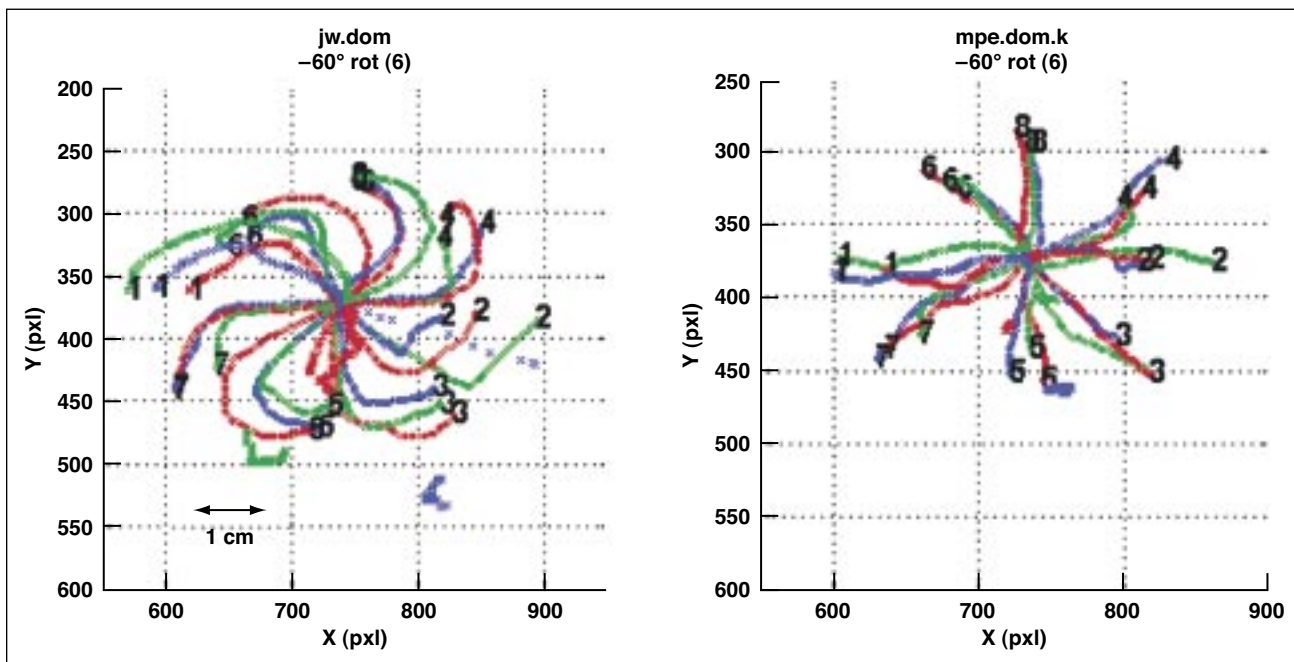


Fig. 1. Sample data from two subjects showing movement paths from a central starting point to eight radially located targets. Each colored path represents a separate movement. The left panel shows the typical curved movement path produced as a user tries to compensate for a misaligned virtual camera. The right panel shows that the curved compensation is largely eliminated by the kinesthetic cue.

Point of Contact: S. Ellis
(650) 604-6147
Stephen.R.Ellis@nasa.gov

S p a c e S c i e n c e

E n t e r p r i s e





Overview

Scientists in NASA's Space Science Enterprise seek to answer fundamental questions about the origin and evolution of life and celestial objects (planets, planetary systems, stars, galaxies, etc.) in the universe. These questions are central to both the new NASA vision for the future: "To improve life here, To extend life to there, To find life beyond," and the new NASA mission: "To understand and protect our home planet, To explore the Universe and search for life, To inspire the next generation of explorers ... as only NASA can," as articulated by NASA Administrator Sean O'Keefe.

Research at Ames Research Center (ARC) implements NASA and Space Science Enterprise goals through five elements dealing with Astrophysics, Planetary Systems, Exobiology, Space Technology, and Advanced Computer Science Applications. Since a unifying theme for these elements is the origin and evolution of stars, planets, and life, the total research effort is a major thrust of the Space Science Enterprise's Astrobiology program. Astrophysics research addresses Enterprise goals and objectives that deal with understanding how the structure in the Universe emerged, the dynamical evolution of galaxies and stars, and the exchange of matter and energy among stars and the interstellar medium. Planetary Systems research addresses Enterprise goals and objectives that deal with understanding star formation, the evolution and distribution of volatile and organic material, the origin and distribution of planetary systems, rings, and primitive bodies, and planetary atmosphere evolution. Exobiology research addresses Enterprise goals and objectives that deal with understanding the origin, evolution, and distribution of life by conducting research on the cosmic history of biogenic compounds, prebiotic evolution, the early evolution of life, computational astrobiology, and extreme environments in which living organisms can exist.

Lake Licancabur, the highest lake on Earth, which is located at the summit of Licancabur volcano (6,017 meters) at the boundary of Chile and Bolivia.

Space Technology efforts address Enterprise goals and objectives that deal with the development of advanced technologies to enable future astrophysics missions, as well as robotic and human Solar System exploration missions. Finally, Advanced Computer Science Applications address Enterprise goals and objectives that deal with optimizing solar system exploration missions and their science return.

Ames is recognized as a world leader in Astrobiology, the study of life in the universe and the chemical and physical forces and adaptations that influence life's origin, evolution, and destiny. In pursuing our primary mission in Astrobiology, Ames performs pioneering basic research and technology development to further fundamental knowledge about the origin, evolution, and distribution of life within the context of cosmic processes. For example, research and technology development are currently conducted to:

- Study the mechanisms of the origin, evolution, and distribution of life in the universe;
- Determine the abundance and distribution of the biogenic compounds that are conducive to the origin of life;
- Identify locations on bodies within our solar system where conditions conducive to life exist or have existed;
- Explore the other bodies (planets, comets, asteroids) of our solar system;
- Locate planets and planet-forming regions around other stars;
- Study extrasolar matter such as interstellar gas and dust.

A s t r o p h y s i c s

As NASA's lead in airborne astronomy, scientists at ARC pioneered the field of astrophysics. Study topics range from star forming regions and processes to interstellar photochemistry to protoplanetary disks. Understanding cosmic processes—the evolution of the universe itself—is a vital part of the Origins initiative.

Ames' astronomers and astrophysicists utilize a wide variety of methods. Ground-based telescopes

such as the Keck and Mount Lemmon Observatories are regularly employed for observations of celestial objects and processes. Development continues on the Stratospheric Observatory for Infrared Astronomy (SOFIA), an infrared telescope to be carried aboard a Boeing 747 aircraft specially modified for the task. Space-based observations are also made through instruments such as the Hubble Space Telescope (HST) and other observatories and missions. Computer modeling and laboratory analogs of chemical processes enhance the observational astronomy performed, as discussed in the accomplishments in astrophysics which follow:

- Successful modeling of the observed color in icy planetary satellites using mixtures of ice and complex organic materials which sheds light on prebiotic organic chemical processes;
- Development of a cryogenic multiplexer for far infrared photoconductor detectors operating at moderate backgrounds for instruments for a new generation of large telescopes such as SOFIA;
- Provided support for the concept that Deuterium enrichment in meteorites indicates that organic species made in the ISM can survive the transition from a dense cloud through infall onto a planetary surface.

P l a n e t a r y S y s t e m s

Scientists in the Space Science Enterprise are interested in how and where in the universe planets form, and the geophysical, geochemical, and atmospheric processes that have occurred over the lifetime of a planet. Further, understanding the dynamics between planetary processes and the origin and evolution of life will help us understand the distribution of life in the universe. A wide variety of accomplishments in planetary systems are highlighted here:

- Development of new models for clouds in brown dwarf atmospheres which produce spectra that are a better fit with observations and account for effects of sedimentation of cloud particles, essentially rainfall;
- Successful modeling of the thermal properties of dust grains on several solar system comets which

has led to a better understanding of the thermal processing, radial transport, and structure of protoplanetary accretion disks;

- Determination that the Jovian atmosphere is statically stable to a depth corresponding to about 20 bars pressure with implications for tidal energy dissipation, banded structure, and mode of transport of internal heat flux.

Exobiology

Ames' Exobiology program is a key element of NASA's Astrobiology Initiative and Ames serves as NASA's lead center in exobiology. The research in exobiology ranges from studying the mechanisms of the origin of living systems, to the processes governing the evolution of life, and to the distribution of life on other planets. When coupled with Ames' pioneering research on the dynamics of galaxies, molecular gases and clouds, planetary systems, and the solar system, our study of life is facilitated by understanding the cosmic environment within which life originates and evolves.

Molecules of exobiological significance are ubiquitous in the universe. It is important to understand the sources and interactions of these building blocks and how living systems emerge from prebiotic molecular chaos. This section of the report highlights a wide variety of accomplishments in exobiology:

- Determination that modern descendants of ancient microbial mats can be used to study differences in aerobic versus anaerobic communities which can in turn be used to determine if the biosphere passed through an earlier stage where its photosynthetic populations depended upon nonbiological sources for reducing power;
- Analysis of the suite of organic compounds in the well preserved Tagish Lake meteorite that demonstrates the presence of distinct organic synthetic processes in primitive meteorites and implies that there may have been multiple, separate evolutionary pathways for organic matter;
- Development of interactive computational tools for biologists to build regulatory models using microarray data to measure gene activity in terms of RNA expression levels in an organism.

Space Technology

To support the Space Science Enterprise in conducting future space science and exploration missions, Ames scientists and engineers develop and validate technologies and instruments, develop calculation-based and modeling algorithms, and refine analytical methods. An accomplishment in space technology follows:

- Testing both near-infrared and mid-infrared candidate detector arrays for NGST in simulated on-orbit radiation environments and then feeding the information back into the manufacturing process in order to minimize radiation damage.

Advanced Computer Science Applications

Ames scientists provide leadership in Information Sciences for NASA by conducting world-class computational sciences research, developing and demonstrating innovative technologies, and transferring these new capabilities for utilization in support of Space Science Enterprise missions. Emphasis is placed on enabling a new era of autonomous spacecraft and autonomous robotic exploration and on extending human capacity through novel utilization of human/computer interactions and data analysis. Highlighted in this section are accomplishments in advanced computer science applications:

- Demonstration in the K9 planetary exploration rover prototype of execution of a command sequence to autonomously carry out a number of science exploration activities including determining if spectrometer data indicated presence of carbonates and collecting high resolution images of a prioritized target;
- Release of a new version of ScienceOrganizer, a specialized knowledge management tool designed to enhance the information storage, organization, and access capabilities of distributed NASA science teams;
- Release of version 2.0 of software tools that provide high capability development and debugging tools that support model-based autonomy projects and can be used throughout the spacecraft design process.

Organic Solids Color the Icy Bodies in the Outer Solar System

Dale P. Cruikshank, Bishun N. Khare

Many of the objects in the outer parts of the solar system (at Jupiter and beyond) have surfaces (and interiors) composed largely of ordinary water ice, which can be readily identified by remote-sensing observations. These bodies include the large satellites of the giant planets, Jupiter through Neptune, the rings of Saturn, the comets, Pluto-Charon, and the objects that populate the Kuiper disk and the Oort cloud. None of these bodies can be sampled directly at the present time, and we rely upon remote sensing to learn about their compositions and history of formation. The techniques of near-infrared spectroscopy, accomplished with large telescopes or by planetary probes, reveal the presence of water ice by showing characteristic absorption bands in the spectral region 1–5 micrometers (μm).

Whereas pure water ice is highly reflective of the sunlight incident on solar-system bodies, and is neutral in color, all of the ice-rich objects have distinct color, and many are nearly black. The coloration of the ice in the short wavelength region, 0.2–1.0 μm , has been especially difficult to model quantitatively, because minerals, logical and naturally occurring contaminating materials, do not have the appropriate optical properties.

The observed color in icy planetary satellites has been modeled by using mixtures of ice and complex organic materials. The organic material is synthesized in the laboratory in experiments that approximate the conditions of formation of similar material in various environments in space, usually by irradiating a mixture of simple gases (methane and nitrogen) or ices (water plus methanol, carbon dioxide, etc.) with ultraviolet light and charged particles from a plasma. The resulting brown-colored substance is termed “tholin,” and is structurally

similar to some of the carbon-rich material found in carbonaceous meteorites. It is also similar in its optical properties to the organic-rich aerosol haze in the atmosphere of Saturn’s satellite Titan (see figure 1).



Fig. 1. Tholin, this orange-brown material produced by exposing a mixture of nitrogen and methane gases to ultraviolet light and charged particles from a plasma discharge, has optical properties similar to those of Saturn’s satellite, Rhea. Modeling studies of the spectra of Rhea and other icy bodies in the outer solar system suggest that tiny quantities of complex organic material of this kind occur as a contaminant on their surfaces. In addition, studies indicate that organic matter may arise from meteoric infall of interplanetary dust, or it may be produced in situ in the ice, by the influence of energetic particles in the space environment.

Specifically, the spectra of Saturn's icy satellites Rhea and Iapetus have been modeled, as well as the Uranus satellite Titania and the moon of Neptune called Triton, by incorporating small amounts (<1%) of various organic solid materials in the surface ices. All of these objects are key to understanding the origin of their respective satellite systems, the nature and time scale of geological activity on them, and the space environments in which they have evolved. The occurrence of complex

organic materials in the surface ices of these bodies, spread throughout the planetary system, tells us that the products of prebiotic organic chemical processes occur in diverse environments far beyond Earth, and they have existed from the beginnings of the solar system to the present.

Point of Contact: D. Cruikshank
(650) 604-4244
Dale.P.Cruikshank@nasa.gov

A Cryogenic Multiplexer for Far-infrared Astronomy

Jessie L. Dotson, Edwin Erickson, Chris Mason

The instruments for a new generation of large far-infrared (FIR) telescopes, such as the Stratospheric Observatory for Infrared Astronomy (SOFIA), will require detector arrays with small enough pixels (picture elements) to exploit the improved angular resolution and a sufficient number of pixels to take advantage of the large fields of view. In order to make the step to arrays with more pixels, suitable multiplexing amplifiers, or multiplexers, must be developed. With this need in mind, Ames Research Center collaborated with personnel from University of Arizona and Raytheon Infrared Center for Excellence to develop the SBRC 190, a cryogenic multiplexer for FIR photoconductor detectors operating at moderate backgrounds.

The circuit is based on the 32-channel CRC 696 CMOS device used on the cryogenic Space Infrared Telescope Facility (SIRTF). For applications such as those encountered on SOFIA or Herschel (the FIR and submillimeter space observatory), the new device permits higher backgrounds, a wider range of backgrounds, faster sampling, and synchronization of sampling with chopping. Major design differences relative to the CRC 696 that have been incorporated in the SBRC 190 include: an AC coupled, capacitive feedback transimpedance unit cell to

minimize input offset effects, thereby enabling low detector biases; selectable feedback capacitors to enable operation over a wide range of backgrounds; and clamp and sample and hold output circuits to improve sampling efficiency, which is a concern at the high readout rates required.

An end-to-end system suitable for testing the multiplexers in conditions similar to their eventual applications has been developed. This includes a photoconductor detector array, test dewar, driving electronics, and the required software. The photoconductor array is composed of 2 rows of 24 Ge:Sb detectors mounted in integrating cavities. Incoming radiation is coupled to the cavities by light-collecting cones. The liquid helium test dewar has room for the necessary optics and can achieve a range of operating temperatures from 2.0 kelvin (K) to 4.2 K. The driving electronics provide the bias voltages and clock signals required to drive the multiplexers. The electronics also contain 16 analog-to-digital converters to process the signals coming out of the multiplexers. Software to control the driving electronics, to receive the results, and to write them into a Flexible Image Transport System (FITS) file has been developed. Software to analyze the obtained data has also been developed.

Testing is currently under way. Initial results imply that the multiplexers are suitable for use in FIR instruments, but additional tests are necessary to fully examine their operation at faster rates and with novel readout strategies.

Point of Contact: J. Dotson
(650) 604-2041
Jessie.L.Dotson@nasa.gov

Scientific Requirements of the NGST Mid-IR Instrument

Thomas Greene

The Next-Generation Space Telescope (NGST), which will be the successor of the Hubble Space Telescope, is scheduled for launch in 2008. NGST will make unprecedented discoveries in the realms of galaxy formation, cosmology, stellar populations, star formation, and planetary systems. NGST is currently in the conceptual design phase of development, and Ames Research Center has been involved in defining the scientific instrumentation it will need to conduct its observations. NGST will have three instruments: a near-infrared (NIR) camera (NIRCAM), a NIR spectrometer (NIRSPEC), and a mid-infrared instrument (MIRI).

MIRI will be the only NGST instrument built in a joint NASA/European Space Agency (ESA) collaboration. It must function as both a wide-field camera and a moderately high resolution spectrograph over the wavelength range 5–28 microns (about 10–40 times longer than visible to the human eye). Ames personnel have contributed to planning its scientific observations, developing its infrared detectors, and determining its scientific requirements.

The Mid-IR Steering Committee (MISC) was formed in FY01 to determine the detailed scientific requirements of MIRI and oversee its conceptual design. This international scientific committee included Ames representation. The MISC evaluated the MIRI scientific objectives and studied the instrument concept presented by the consortium of ESA states that will participate in MIRI development (the United

Kingdom, France, Germany, Italy, and the Netherlands). The scientific objectives were translated into requirements for the instrument that were consistent with the MIRI instrument concept.

MIRI will consist of three optical subsystems, all employing reflective optics. A common set of fore optics will relay images from the NGST telescope focal plane to the MIRI camera and spectrograph subsystems. The fore optics will also provide a common focus mechanism, while the camera and spectrograph subsystems each have their own dedicated mirrors, field masks, filters, and detectors. The camera module images a field of 1.7 arc-minutes by 1.7 arc-minutes onto a 1024 x 1024 pixel detector. It includes a selection of filters and a coronagraphic mask that will allow suppressing the light of bright objects so that fainter ones close to them may be seen. This device will be used for searching for planets around nearby stars.

The spectrograph channel will take the light from every point in a small field (4 arc-seconds by 4 arc-seconds) and disperse it into a spectrum. The first element is an integral field unit that relays and realigns the small field into an image onto slits that are followed by optics and diffraction gratings that disperse the light. A multielement camera then images the resultant spectra onto a dedicated infrared detector that is at least 1024 x 1024 pixels in size (preferably larger).

The MIRI subsystems will be built by ESA contractors and will be delivered to NASA after they are integrated and tested. The Jet Propulsion Laboratory will integrate this assembly with U.S. infrared detectors and will test the entire instrument before delivering it to Goddard Space Flight Center for

integration with the other NGST instruments. A new international mid-infrared science team will provide scientific oversight for these activities.

Point of Contact: T. Greene
(650) 604-5520
Thomas.P.Greene@nasa.gov

An Interstellar Rosetta Stone: A Database of the Infrared Spectra of Polycyclic Aromatic Hydrocarbons (PAHs)

Douglas M. Hudgins, Louis J. Allamandola

In recent years, a host of observations at infrared wavelengths has revealed the unmistakable fingerprint of polycyclic aromatic hydrocarbons (PAHs) in the spectra of objects at all stages of the life cycle of matter in the interstellar medium (ISM). Moreover, analyses of meteorites and interplanetary dust particles have demonstrated that PAHs are also commonplace within our own solar system. Enormous molecules by interstellar standards, PAHs are composed of varying arrays of fused hexagonal rings of carbon atoms. Not only do these species hold tremendous potential as probes of the ISM, they also represent the single largest reservoir of prebiotic organic carbon in developing planetary systems. Unfortunately, only rarely do scientists have the luxury of directly analyzing samples of extraterrestrial materials. Instead, they must rely heavily on spectroscopic data from remote sensing platforms such as NASA's Infrared Telescope Facility (IRTF), and the upcoming Stratospheric Observatory for Infrared Astronomy (SOFIA) and Space Infrared Telescope Facility (SIRTF) missions for clues to the nature of these materials. The complete interpretation of these data, in turn, requires a thorough knowledge of the spectroscopic properties of PAHs—information obtainable only through appropriate laboratory studies. Toward this end, researchers in the Astrochemistry Laboratory at Ames Research Center have been actively engaged in a systematic study of the infrared spectroscopic prop-

erties of PAHs under conditions that mimic those of interstellar space. The long-range goal of this work has been to compile a comprehensive infrared spectral database and to apply those data to model the observed interstellar spectra.

The diverse physical and chemical conditions in different astronomical objects give rise to variations in the native PAH population. These variations are reflected by (often subtle) differences in the observed infrared spectrum of the objects. By carefully modeling interstellar spectra using the spectra of a wide variety of PAHs representing a broad cross-section of sizes, structures, and stabilities, scientists can determine which PAH structures are favored in a particular region. The power of this process is illustrated in Figure 1, which shows a comparison of the infrared spectrum of a star-forming region to a model spectrum generated by adding the spectra of species drawn from the database. In such a region, the interstellar material is bathed in the harsh, ionizing radiation of the adjacent hot, young O- and B-type stars. The composition of the mixture that provides the best fit to the Orion spectrum is quite revealing about the nature of the PAH population there. Sixty-three percent of the PAHs in the model mixture have highly stable, "condensed" structures (that is, the most compact arrangement of the hexagonal rings). Also, 70% of the model mixture is contributed by PAHs in their

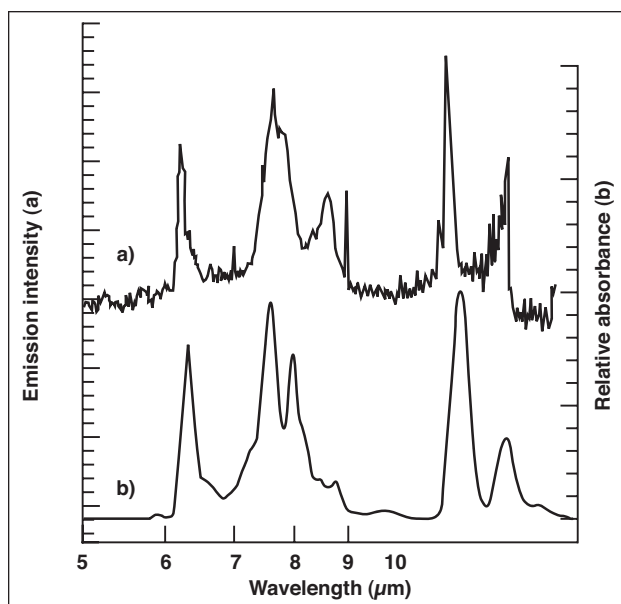


Fig. 1. Comparison of a typical ISM infrared emission spectrum with the composite absorption spectrum generated by adding the individual spectra of 11 PAHs. (Figure adapted from Peeters et al., *Astron. Astrophys.*, 2002, in press).

ionized forms. The PAH population reflected in the model spectrum is entirely consistent with what one would expect given the nature of this object. The molecules found in this region are those that have survived the fierce radiation from the nearby hot stars. Lesser stable components of the population have long since been “weeded out,” and a substantial fraction of the population has been ionized by the harsh ultraviolet radiation from the nearby cluster of hot stars. Thus, it is entirely reasonable that the model PAH mixture reflects a disproportionately large contribution from the hardest species and from ionized species.

To date the infrared spectra of more than 100 neutral, cationic, and anionic PAH species ranging in

size from $C_{10}H_8$ to $C_{48}H_{20}$ have been measured, and much of the wide acceptance and utility that the PAH model enjoys today rests upon these data. The species currently represented in the dataset include: the most thermodynamically stable PAHs through coronene, $C_{24}H_{12}$; species from the fluoranthene family, aromatic hydrocarbons which incorporate a five-membered ring in their carbon skeleton; a variety of large PAHs (“LPAHs”) having between 36 and 50 carbon atoms; and a variety of “aza-PAHs,” polycyclic aromatic compounds with a nitrogen atom incorporated into their carbon skeleton. This is the most extensive compilation of astrophysically relevant spectral data on PAHs available. Most of these spectra are available in the peer-reviewed chemical literature, and an extensive review of the astrophysical implications of this work is being prepared for publication in the astronomical literature. Much of the data are also available to the astronomical community on the Web at <http://www.astrochemistry.org/pahdata/index.html>.

Today, scientists around the world are incorporating these data into comprehensive new astrophysical models—models far more sophisticated and physically realistic than the crude illustrative example given previously. Those models use the measured absorption data to calculate PAH emission spectra as a function of such astrophysical parameters as radiation field intensity, charge balance, extinction, and density. Models such as this hold the key to unlocking the potential of PAHs as probes of the ISM, and it is through the availability of this database that this goal will be realized.

Point of Contact: D. Hudgins
(650) 604-4216
Douglas.P.Hudgins@nasa.gov

The SOFIA Water-Vapor Monitor Nears Completion

Thomas L. Roellig, Robert Cooper, Brian Shiroyama, Regina Flores, Lunming Yuen, Allan Meyer

The Stratospheric Observatory for Infrared Astronomy (SOFIA), a 3-meter class telescope mounted in a Boeing 747 aircraft, is being developed for NASA by a consortium consisting of the University Space Research Association, Raytheon E-Systems, and United Airlines. This new facility will be a replacement for the retired Kuiper Airborne Observatory that used to fly out of Moffett Field. As part of this development, Ames Research Center is providing an instrument that will measure the integrated amount of water vapor seen along the telescope line of sight. Because the presence of water vapor strongly affects the astronomical infrared signals detected, such a water-vapor monitor (WVM) is critical for proper calibration of the observed emission. The design and engineering model development of the WVM is now complete and the hardware to be used in the flight unit has been fabricated and is now being tested. Because the SOFIA observatory will be certified under Federal Aviation Administration (FAA) Part 25, extensive analysis and testing is needed, much more extensive than was required for earlier Ames airborne observatories that flew under an FAA research aircraft certification.

The SOFIA WVM measures the water-vapor content of the atmosphere integrated along the line of sight at a 40° elevation angle by making radiometric measurements of the center and wings of the 183.3-gigahertz (GHz) rotational line of water. These measurements are then converted to the integrated water vapor along the telescope line of sight. The monitor hardware consists of three physically distinct subsystems:

1) The radiometer head assembly, which contains an antenna that views the sky, a calibrated reference target, a radio-frequency (RF) switch, a mixer, a local oscillator, and an intermediate-frequency (IF) amplifier. All of these components are mounted together and are attached to the inner surface of the

aircraft fuselage, so that the antenna can observe the sky through a microwave-transparent window. The radiometer and antenna were ordered from a commercial vendor and have been rebuilt and modified at Ames to include an internal reference calibrator and meet FAA Part 25 requirements.

2) The IF converter box assembly, which consists of IF filters, IF power splitters, RF amplifiers, RF power meters, analog amplifiers, analog-to-digital (A/D) converters, and an RS-232 serial interface driver. These electronics are mounted in a cabinet just under the radiometer head and are connected to both the radiometer head and a dedicated WVM computer (CPU). All of the flight electronics boards have been fabricated and have been shown through testing to meet their requirements. A small microprocessor that handles the lowest-level data collection and timing has been programmed in assembly language to collect and add the radiometer data and communicate with the software residing in the WVM CPU.

3) A dedicated WVM CPU that converts the radiometer measurements to measured microns of precipitable water and communicates with the rest of the SOFIA Mission and Communications Control System (MCCS). A nonflight version of this computer hardware has been procured for laboratory testing and development of the flight software is near completion, with approximately 95% of the software coded and unit tested. Proper command and data communications between the WVM and the SOFIA MCCS have been demonstrated using an MCCS simulator that was developed by the SOFIA development team.

Point of Contact: T. Roellig
(650) 604-6426
Thomas.L.Roellig@nasa.gov

Using Deuterium to Trace the Links Between Interstellar Chemistry and the Organics that Seeded the Early Earth

Scott A. Sandford, Louis J. Allamandola, Max P. Bernstein, Jason P. Dworkin

This research investigates the importance of interstellar chemistry in the origin and early evolution of life. The interstellar medium (ISM) mediates gas-phase, gas-grain, and solid-state chemical processing that produce a variety of new molecules. Because new stellar and planetary systems are produced in dense molecular clouds in the ISM, these molecules may have become incorporated into—and aided in the formation of—the early biosphere on Earth. Many of these organic compounds are relatively complex and of potential prebiotic importance. For example, this research shows that the ultraviolet (UV) irradiation of ices condensed onto grains in dense molecular clouds should produce quinones, amphiphiles, and amino acids—all compounds crucial for life.

These important compounds are irrelevant to the origin of life if they cannot survive the transition from the general dense cloud through the stellar/planet formation stage to subsequent infall onto a planetary surface. The best evidence that interstellar organics survive this process is the presence of complex organics enriched in deuterium (D) in primitive me-

teorites. The presence of excess D is generally taken to indicate an interstellar chemical heritage, because it has long been known that interstellar gas-phase ion-molecule chemistry produces D-enriched products. In the past year the various chemical processes that can make or alter organics in the ISM (figure 1) were examined. All of these processes should yield products enriched in D, with each process producing a unique “signature” with regard to the extent and molecular distribution of the excess D.

This work strengthens the interpretation that D enrichments in meteorites indicate the presence of organic species made in the ISM and provides a fundamental framework for the investigation of the nature of the links between interstellar chemistry, the organics in meteorites, and the origin of life on Earth, and by extension, planets in other stellar systems.

Point of Contact: S. Sandford
(650) 604-6849
Scott.A.Sandford@nasa.gov

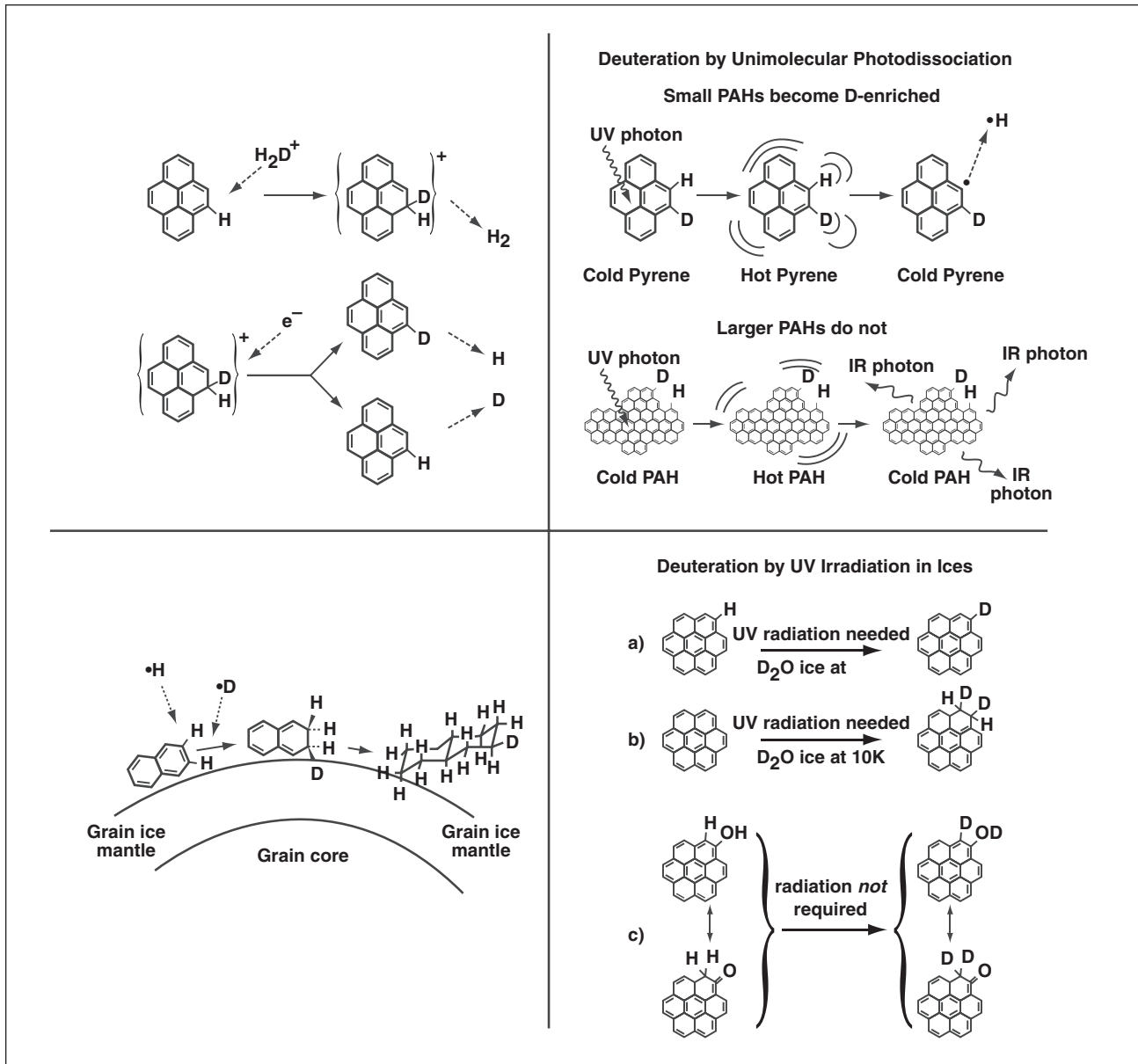


Fig. 1. Examples of how interstellar processing by ion-molecule reactions, gas-grain surface reactions, unimolecular photodissociation, and solid-state ice irradiation can result in D enrichment of the products. Each process leaves a unique signature in the placement of excess D. Polycyclic aromatic hydrocarbons (PAHs) are used to illustrate each process.

EMERG Greenhouse One: Simulations of Remote and Ancient Earth Environments at Ames

Brad M. Bebout

The Ames Microbial Ecology/Biogeochemistry Research Laboratory, in combination with the Early Microbial Ecosystems Research Group (EMERG), has completed a greenhouse simulation facility designed to enable the maintenance and manipulation of microbial mat communities. Microbial mat communities are extant representatives of the oldest forms of life on Earth. Two major experiments, a salinity manipulation and a sulfate manipulation, have now been conducted. These experiments have demonstrated that the facility is capable of maintaining these complex communities of microorganisms for periods of more than a year, while enabling experimental manipulations and the collection of high-quality data. The experimental apparatus notably enables the collection of measurements of the distribution of important chemical and biological parameters within the communities on the microscale (submillimeter).

The salinity manipulation, in which the salinity of half of the experimental microbial mats was raised by a factor of about 30%, provided the important result that the community composition of the major photosynthetic population in the mats (cyanobacteria), as revealed using molecular biological methods, is essentially identical to that of field-collected popula-

tions. Increased salinity reproduced cyanobacterial community changes that are also observed with increases in salinity in the natural environment. The importance of this result is a validation of the methods being used to conduct manipulations.

The sulfate manipulation, in which the sulfate concentrations of half of the experimental mats were reduced by a factor of nearly 1000, recreates conditions that were important early in Earth's history but are not presently found in the natural environment. This manipulation has produced numerous fundamental changes in the microbial mats, including changes in sulfate reduction, oxygen distribution within the mat, and photosynthetic efficiency. In addition, changes in important biomarker gases were observed between the treatments, including higher rates of methane and dimethyl sulfide production in mats incubated at lower sulfate concentrations. These results will be important in evaluating the strategy of looking at biomarker gases in the atmospheres of extrasolar planets.

Point of Contact: B. Bebout
(650) 604-3227
Brad.M.Bebout@nasa.gov

A Terrestrial Analog for the Martian Meteorite ALH84001

David Blake, Allan H. Treiman, Hans E.F. Amundsen, Ted Bunch

Carbonate minerals present in the ancient Mars meteorite ALH84001 may hold clues to the processing and fate of volatiles and the potential for primitive life on early Mars. However, because

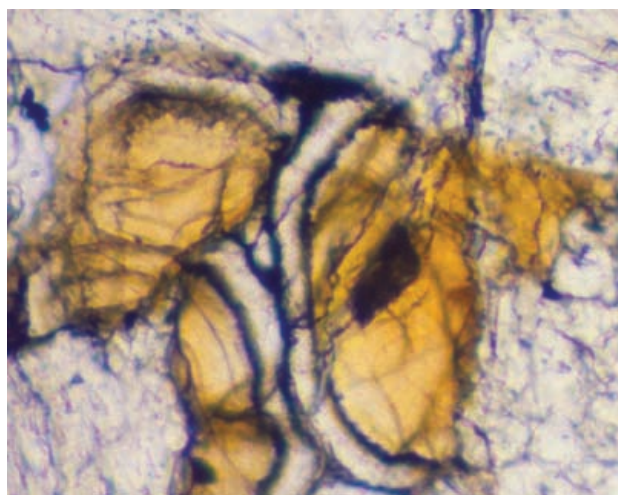
ALH84001 is separated from its surrounding rocks, the context of its formation and processing is unknown and the origin of the carbonate globules has, therefore, been controversial—scenarios range

from groundwater deposition through high-temperature shock metamorphism. In terrestrial field geology, such rocks are called “float” when they are found removed from their original setting. The ALH84001 meteorite is an extreme example of “float,” having been separated from its source locality (Mars) by hundreds of millions of miles.

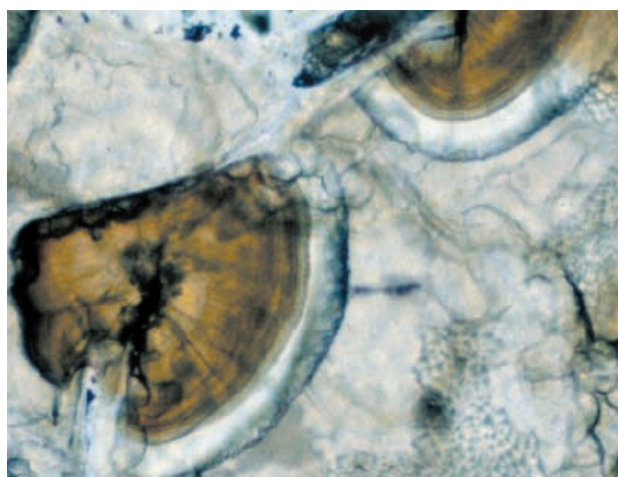
One way to investigate the origin of rocks whose context to the surrounding strata has been lost is to find and study analogous rocks where field relationships can be obtained. Igneous rocks from volcanoes on northern Spitsbergen (Svalbard, Norway) contain carbonate globules strikingly similar to the globules in ALH84001 (see figure 1). Field and laboratory data suggest that the Spitzbergen carbonates formed as a result of late-stage hydrothermal (i.e., hot springs) activity. The ALH84001 carbonates probably formed in a similar environment.

Xenoliths (rock fragments dislodged and entrained in rising magma) comprise up to 20% of the exposed volumes of basalt from several volcanoes on Spitsbergen. The mantle xenoliths within the basalt include rock types similar to ALH84001. Globules of carbonate minerals occur in the xenoliths and their host lavas along cracks, in vesicles, and as replacements of olivine. Typical carbonate globules in the Spitsbergen rocks are ellipsoids cored by ankerite, siderite, and magnesite (ASM), carbonate minerals also present in ALH84001.

Results suggest that the ASM carbonates were deposited in situ, in restricted areas, in the volcanic centers by hydrothermal fluids. The ASM carbonate globules from the Spitsbergen volcanoes are similar to the carbonate globules in ALH84001, having similar sizes, shapes, chemical compositions, general patterns of chemical zoning, and host rock compositions. These similarities suggest that the Spitsbergen and ALH84001 carbonate masses formed in comparable geological environments.



(a)



(b)

Fig. 1. Optical microscope views of carbonate globules from Mars and Earth. Semicircular globules, ~200-micron (μ m) diameter, have cores of ankerite and siderite carbonates (brown, Fe- and Ca-rich), and rims of magnesite (clear, Mg-rich). (a) Mars. Meteorite ALH84001. Black layers are magnetite-rich (originally were siderite, Fe-rich carbonate). Globules surrounded by orthopyroxene and feldspathic glass. (b) Earth. Spitsbergen xenolith, sequence of carbonate minerals similar to ALH84001 globule above. Globules surrounded by olivine, orthopyroxene, clay, and silica; globules cut by clay-filled veinlets.

The current focus of Mars exploration is on water and ancient environments where life may have prospered, including hydrothermal systems. The

ALH84001 carbonates are critical to this search, almost by default, because they are our only direct clues about ancient Martian aqueous environments and geochemistry. Further study of the Spitsbergen rocks will help clarify the formation conditions for the carbonates, provide a sound terrestrial basis for interpreting the carbonates in ALH84001, and aid in

planning geological and geochemical studies of the Martian highlands.

Point of Contact: D. Blake

(650) 604-4816

David.F.Blake@nasa.gov

Microbial Mats and the Origins of Photosynthesis

David J. DesMarais, Dan Albert, Brad M. Bebout, Mykell Discipulo, Tori M. Hoehler, Kendra Turk

The Early Microbial Ecosystems Research Group (EMERG) at Ames Research Center is defining the structure and function of microbial biofilm (mat) communities. Recent observations of aerobic and anaerobic processes within these communities offer clues about our earliest origins and about the nature of Earth's ancient atmosphere. Such studies contribute directly to NASA missions that seek to chart the distribution of habitable planets and biospheres beyond Earth.

When our biosphere developed photosynthesis, probably in microbial mats, it tapped an energy resource that was orders of magnitude larger than the energy available from oxidation-reduction reactions associated with weathering and hydrothermal activity. The onset of oxygenic photosynthesis most probably increased global organic productivity by more than two orders of magnitude. This productivity materialized principally because oxygenic photosynthetic bacteria can capture hydrogen for organic biosynthesis by cleaving the water molecule. This virtually unlimited supply of reduced hydrogen forever freed life from its sole dependence upon abiotic sources of reducing power such as hydrothermal emanations and weathering. Communities sustained by oxygenic photosynthesis thrived wherever supplies of sunlight, moisture, and nutrients were sufficient. The microfossil record of cyanobacteria is evident for more than 2.5 billion years, and their ancient stromatolitic reefs rival

modern reefs in size. Vast sedimentary deposits of organic carbon, reduced sulfide, and ferric iron on continental platforms and margins are among the most prominent and enduring legacies of billions of years of oxygenic photosynthetic activity. The biosphere passed through an earlier stage where even its photosynthetic populations depended exclusively upon nonbiological sources of reducing power from hydrothermal emanations and rock weathering. Can we recognize such a stage? In order to chart the development of oxygenic photosynthesis as well as its impact upon the atmosphere and ancient sediments, it is important to learn how to discriminate between the fossil remains of aerobic versus anaerobic populations.

The Ames team examined modern descendants of these ancient mats in subtidal and intertidal marine environments at Guerrero Negro, BCS, Mexico, specifically those dominated by *Microcoleus* (subtidal) and *Lyngbya* (intertidal to supratidal) cyanobacteria. Differences in the aerobic versus anaerobic communities were observed that indeed might be preserved in the sedimentary record. We examined the exchange of oxygen (O₂) and dissolved inorganic carbon (DIC) between mats and the overlying water, during diel (24-hour) cycles. *Microcoleus* mats assimilated near-equal amounts of DIC during the day as they released at night, but *Lyngbya* mats typically showed net uptake of DIC over the diel cycle. Patterns of O₂ daytime release and nighttime

uptake mirrored these DIC trends in both mat types. Nighttime DIC effluxes from *Microcoleus* mats were equivalent in the presence versus absence of O₂, whereas nighttime DIC effluxes from *Lyngbya* mats dropped markedly in the absence of O₂. Thus, aerobic diagenesis was more important in *Lyngbya* mats than in *Microcoleus* mats, perhaps because trapped O₂ bubbles persist only in *Lyngbya* mats at night, and thus sustain populations of aerobes. In both mat types, effluxes of hydrogen gas (H₂),

methane (CH₄), and short-chain fatty acids were much greater at night in the absence of O₂, emphasizing the importance of fermentation reactions. Differences observed between *Microcoleus* versus *Lyngbya* mats forecast differences in their microbiota and in their patterns of gene expression.

Point of Contact: D. DesMarais
(650) 604-3220
David.J.DesMarais@nasa.gov

Large-Magnitude Biological Input of Hydrogen to the Archaean Atmosphere

Tori M. Hoehler, Brad M. Bebout, David J. DesMarais

Earth's earliest biosphere is often thought to have depended primarily on chemicals vented from deep underground (as in volcanoes or hydrothermal vents) as its primary source of energy. Before long, however, life "learned" how to use solar radiation (light) as the primary energy source. Because light provides a much more abundant supply of energy, the new photosynthetic biosphere had the potential to be more productive than the earlier biosphere by as much as two or three orders of magnitude. Accordingly, the capacity of life to alter the chemistry of our planet's surface must have increased by a similar magnitude. The Early Microbial Ecosystems Research Group (EMERG) at Ames Research Center is studying modern relatives of Earth's ancient photosynthetic biosphere in order to understand the possible biological impacts on planetary chemistry during the early stages of our history.

Recent studies have focused on the production of hydrogen gas, H₂, by modern microbial mats (analogs for ancient photosynthetic communities). During photosynthesis, microbial mats break water, H₂O, into its component elements of hydrogen and oxygen. Ordinarily, the H₂ is used to turn carbon dioxide from the atmosphere into sugar-like materials—which are subsequently used to synthesize

the complex organic molecules that comprise living organisms. However, when microbial mats are exposed to a simulated Archaean (early Earth) atmosphere that is very low in oxygen, they instead release much of this hydrogen to the environment. Without this mechanism, the primary source of H₂ to the Archaean atmosphere would have been geothermal venting (e.g., volcanic emissions); the present research suggests that the biological release of hydrogen may have exceeded the geological one by 100 to 10,000 times.

Such a profound addition of hydrogen to the Archaean environment could have had important implications for both biology and chemistry on a global scale. Hydrogen is widely utilized as a food source by many of the organisms thought to have comprised the early biosphere. The numbers and global distribution of such organisms could have been greatly enhanced by an atmosphere containing significant quantities of H₂. Each of the particular chemistries mediated by these organisms could thereby have a proportionately larger impact on the local or global environment than in the absence of a photosynthetic H₂ flux. In addition, H₂ itself can have an important impact on atmosphere and ocean chemistry. Hydrogen is "light" enough to escape to

space, and in the process, carries electrons with it. The removal of electrons from our planet in this fashion would facilitate the oxidation of our oceans and atmosphere from an initially reducing or neutral condition to the highly oxidized and oxygenated state that permits the existence of multicelled life forms—including us!

Point of Contact: T. Hoehler
(650) 604-1355
Tori.M.Hoehler@nasa.gov

Analysis of the Tagish Lake Meteorite

Sandra Pizzarello, Yongsong Huang, Luann Becker, Robert J. Poreda, Ronald A. Nieman, George W. Cooper, Michael Williams

Carbonaceous meteorites provide an important record of organic compounds that were synthesized very early in the solar system and delivered to the planets. Because a goal of NASA is to understand the origin and evolution of life, it is desirable to analyze a variety of such meteorites for their organic content.

The Tagish Lake meteorite fell in Canada in 2000 and was kept frozen until analysis. It may provide the most pristine material of its kind. Analyses have shown this carbonaceous meteorite to contain a suite of soluble organic compounds (~100 parts per million) that includes mono- and dicarboxylic acids, dicarboximides, pyridine carboxylic acids, a sulfonic acid, and both aliphatic and aromatic hydrocarbons. Surprisingly, some of the most abundant organic compounds of the well-studied Murchison meteorite were found to be very scarce in Tagish Lake. Amino acids, monocarboxylic acids, and amines are three orders of magnitude less abundant than in Murchison.

The difference between the two meteorites is also qualitative, and very few species were found for each class of Tagish Lake compounds, contrary to Murchison's large isomerism. For example, although there is a series of straight chain carboxylic acids from formic to nonanoic acid, of the many possible branched isomers only isobutyric acid was detected. For amino acids and amines, the list of identified

compounds contains few: glycine, alanine, α -amino iso- and n-butyric, and γ -amino butyric acids; and methyl, ethyl, and isopropyl amines. In addition, only the first two members of each series, e.g., acetic and formic acids, are present above trace levels. Also in contrast to Murchison, the abundance ratio of the first or second member of each series to the third ranges from approximately 10 to 100 (2 to 4 is typical Murchison).

The case of Tagish Lake sulfonic acids (organic sulfur compounds) is an extreme example because they were found to be represented in the meteorite by just methane sulfonic acid (MSA). MSA was found to be several times more abundant in Tagish Lake than in Murchison. Although other members of the series may ultimately be found, it is apparent that the ratio of MSA to the other sulfonic acids would still be much higher in Tagish Lake than in Murchison. In Murchison, sulfonic acids are present as a homologous series that extends to at least 4 carbons. MSA was found to be different from its homologs in having much higher amounts of carbon-13 and the heavier isotopes of sulfur. The present findings in Tagish Lake may be consistent with these isotopic differences.

The finding of just one suite of organic compounds matching those of Murchison and of some (but not all) the carbonaceous phases and compounds seen in

other meteorites demonstrates the presence of distinct organic synthetic processes in primitive meteorites. It also implies that the more complex organic matter of heterogeneous meteorites may result from multiple, separate evolutionary pathways.

Point of Contact: G. Cooper
(650) 604-5968
George.W.Cooper@nasa.gov

Computational Modeling of Regulatory Networks in Cells

Andrew Pohorille, Stephen Bay, Pat Langley, Jeff Shrager

Understanding how an organism regulates its level of gene expression in response to external stimuli is a central problem in molecular biology. Although scientists understand the basic mechanisms through which DNA produces proteins and thus biochemical behavior, they have yet to determine most of the regulatory networks that control the degree to which each gene is expressed. This knowledge is necessary for understanding effects of space environments on cells and explaining interactions of organisms in ecosystems. Faulty cellular regulation is responsible for numerous diseases, of which cancer is the best known example. The BioLingua project, described here, provides interactive computational tools for biologists to build regulatory models using microarray data, which measure gene activity in terms of ribonucleic acid (RNA) expression levels in an organism. When the data are ambiguous, BioLingua relies on biological knowledge in the form of initial models and information about plausible causal relations between gene products.

The approach to discovering regulatory networks is based on linear causal models. In this approach, each variable is represented as a linear function of its direct causes plus an error term. Variables correspond to the expression levels of genes or measurements of external quantities. A regulatory network is represented as a graphical model, in which each variable is a node and causal influences are represented as arrows from the cause to the effect. The structure of the initial model can be obtained from constraints imposed by partial correlations between

experimentally measured values of different variables. For example, a zero partial correlation between two variables means that they are connected through the third variable. A nonzero partial correlation implies that the variables are directly causally connected. The initial model is further refined through a search in the space of models consistent with biological knowledge to ensure that the predicted directions of changes in gene expression (up and down regulation) match those measured in experiments.

The methodology described previously is illustrated in the example of photosynthesis regulation in cyanobacteria, which are ubiquitous organisms in terrestrial, marine, and freshwater ecosystems. More than 25% of the oxygen in the atmosphere is generated by cyanobacteria. The model, shown in figure 1, was generated on the basis of the recent microarray studies. It explains why cyanobacteria exposed to high light conditions bleach, and how this protects

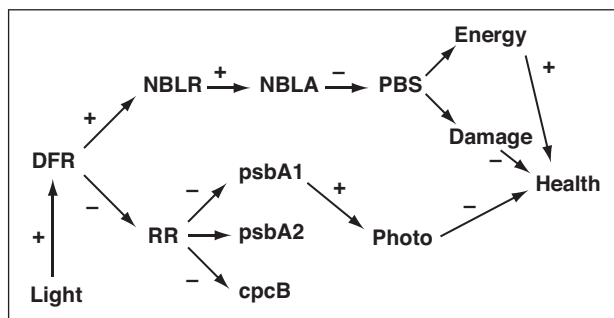


Fig. 1. The proposed regulatory model of photosynthesis in cyanobacteria.

the organism. The model states that changes in light level modulate the expression of a protein *dspA*, which serves as a light sensor. This in turn regulates NBLR and NBLA proteins, which then reduce the number of phycobilisome (PBS) rods that absorb light. The reduction in PBS protects the health of the organism by reducing absorption of light, a process that can be damaging at high levels. The sensor *dspA* impacts health through a second pathway by influencing an unknown response regulator RR, which in turn down regulates expression of the gene products

psbA1, *psbA2*, and *cpcB*, which are all needed to form a functional photosystem. However, only the first protein was found to regulate the level of photosynthetic activity (Photo). High levels of photosynthetic activity would also damage the organism in high light conditions.

Point of contact: A. Pohorille
(650) 604-5759
Andrzej.Pohorille-1@nasa.gov

A High-Performance, Low-Cost Linux Cluster for Genomics

Karl Schweighofer, Rick Graul

In support of genomics research at NASA, the newly formed bioinformatics group (under the title of the NASA Center for Astroinformatics) has developed a Linux-based computer cluster configured with genomics tools. The cluster, also known as a Linux farm, is to serve as a test platform for developing genomics tools, and as an integral component of the newly formed bioinformatics infrastructure to support NASA-specific research and missions. Such an infrastructure is justified because of the large number of scientists whose research employs the direct use of genomic information, and who are currently relying on outside resources to perform their analysis.

The Linux farm, called GRETEL, consists of 10 dual processor Pentium II 400-MHz processors, with an average of approximately 500 megabytes (MB) of memory per node. The network topology employs a single network card in each node, each of which is connected to a local 100-megabit (Mb) switch. Of the 10 nodes, one is configured to be "Mother Superior," and the others act as slaves, although each node has its own disk, operating system, and local copies of important databases. Mother Superior also acts as a Web server and portable batch system (PBS) batch server, and it allows remote

logins for users who wish to have command-line access to tools or to develop their own code. Login access (Secure Shell Protocol (SSH)) and Hypertext Transfer Protocol (HTTP) requests are forwarded by a Linux-based firewall, which insulates the farm network from the Ames Research Center (ARC) outer large-area network (LAN). This is performed by Network Address Translation, which masquerades the nodes so that each one has only a private network address. This allows for a high degree of reliability, because jobs started on the farm will continue even if the outer network experiences an interruption.

Genomics tools are mostly centered around biological sequence analysis algorithms. In a typical analysis, a database of sequences is searched against a query sequence whose function may be unknown. If the search yields a set of "hits" from the database, and if these hits are similar in function, then one can infer the function of the unknown sequence by similarity. This type of search is highly parallel, because the comparison of the query with each sequence in the database is an independent calculation. Thus, an algorithm for splitting up the database and submitting N searches to N nodes is an effective parallelization method for these types of tools.

A benchmark of GRETEL was performed using a common sequence search algorithm known as HMMER, which operates under a parallel virtual machine (PVM). HMMER consists of hidden markov modeling software, and the Pfam database, (a large set of HMMs trained on alignments of known protein domains). These domains may be used to infer the function of a protein, its structure, or whether it is a known drug target, for example. For the present benchmark, a single GPCR sequence was scored against the entire Pfam database of about 3000 HMMs. Figure 1 shows the linearity in the time for job completion with the number of processors. Figure 2 is a photo of the farm. This method of low-cost computing is proving to be a valuable resource for scientists, given the enormous size of datasets associated with the human genome project. The resource is available at <http://genomics.arc.nasa.gov>.

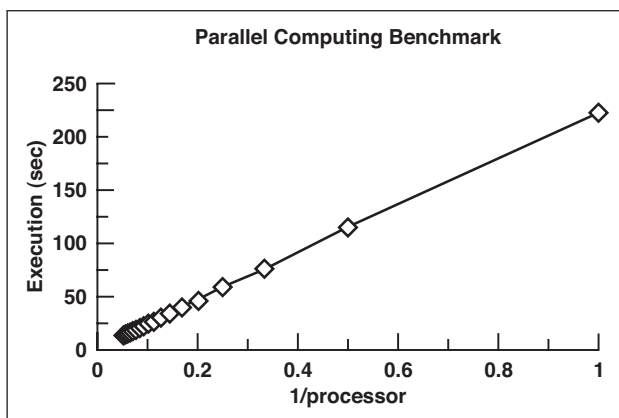


Fig. 1. Time for job completion as a function of the number of processors.



Fig. 2. The Linux farm.

Point of contact: K. Schweighofer
(650) 604-5766
Karl@mail.arc.nasa.gov

Organic Chemistry Leading to Life

Emma Bakes, Alexander Tielens, Charles Bauschlicher, C. P. McKay, Stephen Walch, William J. Borucki, Robert C. Whitten, Bishun Khare, Louis Allamandola, Douglas Hudgins, Sebastien Lebonnois, Hiroshi Imanaka

During FY01, work was done in three primary research areas: (1) the formation of the building blocks of life in space; (2) the formation of macromolecules and the precursors to biology in the Titan haze; and (3) the 30-year-old problem of the unidentified interstellar infrared emission features.

1. Our Solar System was formed from the primordial interstellar medium (or matter) (ISM) when it collapsed to form a disk of gas and dust grains. Everything that composes the solid material in our planetary system originated from primordial interstellar dust, and there is increasing evidence that primordial ISM is intimately related to cometary and meteoritic matter in the Solar System. Amino acids are termed “prebiotic” because they precede the formation of all biological life. Historically, amino acids were thought to reside on Earth only. Recently, however, they have been discovered not only in solid chunks of meteoritic rock from the outer Solar System, but in the material between the stars (the interstellar medium). This finding has profound and far reaching implications for studies of the origins of life. If the molecules that precede life exist between the stars, then life is a potentially universal phenomenon.

The primary goals of the proposed research into the formation of life’s building blocks in space were to (1) predict the chemical pathways and energetics for amino acid synthesis under astrophysically relevant conditions; (2) provide evidence of the survivability of amino acids in the hostile environment of interstellar space; and (3) predict infrared spectra of the relevant species. The results would then be used in an astrochemical model to interpret and analyze astrophysical infrared data from the chemically richest region of our Galaxy, Sagittarius B2, where a pos-

sible detection of glycine, the simplest amino acid, was made. This work has shown that it is possible to make amino acids in interstellar space on solid interstellar dust grains (but not in the gas). The amino acids on these dust grains may then become part of a new solar system when the solid grains collapse to form planets and rocky bodies in the planetary system. In short, it is possible that some of the amino acids found on Earth today originated in the harsh and cold reaches of interstellar space.

2. Research into the formation of macromolecules and biological precursors in Titan’s haze has begun to bridge the gap existing in current models of Titan’s chemistry. It has so far been established that it is possible to form both neutral and cationic, pure, and nitrogenated macromolecules containing up to 10 carbon atoms. Larger molecules are on the way to being analyzed using quantum chemical techniques. This information represents an enormous breakthrough, advocating the ease and energetically favorable formation of macromolecules which can then play a key part in Titan’s thermodynamics, chemistry, and aerosol formation. Laboratory experiments are under way to investigate the chemical scheme discussed above in order to investigate how the starting mixture, temperature, pressure, and molecular complexity alter the final products. Results back up quantum chemical breakthroughs made thus far. The formation of molecular hydrogen by means of aerosol surface catalysis has been investigated and found to play a significant role in the formation and subsequent escape of this molecule from Titan’s atmosphere, solving a longstanding problem in the Titan haze composition. The charging and agglomeration of Titan haze aerosols has been investigated and it can account for daily and (potentially) seasonal variations in the haze albedo.

This occurs through the agglomeration of anionic polycyclic aromatic hydrocarbon (PAH) molecules and highly positively charged aerosols during Titan's daytime and summer phases. It is erroneous to consider a monodisperse aerosol population with one charge—the situation is much more complex and dramatically changes our view of Titan's atmosphere. This is very controversial and will likely cause a storm in the field. The above discoveries may radically change Titan haze conductivity and a new model is currently being formed of the charging of the Titan haze aerosols. This will help revise the results intended to guide the Cassini Huygens probe, which is scheduled to drop into the Titan haze in 2004.

3. Strong infrared (IR) emission features between 3.3 and 12.7 microns are ubiquitous and are the most luminous mid-IR spectral features originating from the ambient ISM. They are valuable diagnostics of the ISM's chemical composition, thermal excitation, and evolution. These features are observed in many astronomical sources at various stages of their evolution, including reflection nebulae, HII regions, young stellar objects, photodissociation regions, postasymptotic giant branch stars, planetary

nebulae, transition objects, novae, the Galactic disk, and even extragalactic sources. These mysterious features are generally attributed to PAH molecules, but the exact identification of the carriers of these IR features with specific molecules has remained elusive, leading to their being termed the “unidentified infrared (UIR) emission features.” This research has made substantial inroads into clarifying the nature of the carriers of the UIR emission. A state-of-the-art model of interstellar IR emission and macromolecular chemistry was constructed. The inclusion of quantum chemistry has taken the prediction of IR emission and the chemical evolution of PAHs to a superior theoretical level, surpassing that of former studies. It has also enabled a logical and systematic search for the UIR emission carriers in a variety of star-forming regions, guided by the fundamental laws of quantum physics. The answer to one of the key questions in astrophysics—What is the nature of the carriers of the UIR emission features?—is within our grasp. We are on the verge of a breakthrough in solving this 30-year-old problem.

Point of Contact: E. Bakes
(650) 604-0787
bakes@shivakali.arc.nasa.gov

Probing Dust Processing Events in Accretion Disk Atmospheres Using Two-Dimensional Radiative Transfer Models

K. Robbins Bell, Diane Wooden, David Harker, Charles Woodward

Progress has been made in observing and modeling temporally variable dust-emission features in young stars surrounded by protoplanetary accretion disks. Multi-epoch mid-infrared spectrophotometry of premain-sequence (PMS) stars, including low-mass PMS T Tauri stars and intermediate-mass PMS Herbig Ae/Be stars, with the Ames High-efficiency Faint Object Grating Spectrometer (HIFOGS) over the 7.5 – 13.5 micron wavelength range has con-

firmed the measurement of variable dust-emission features. The HIFOGS spectrophotometric observations reveal changes in strength in either (1) the 9.7-micron amorphous silicate resonance or (2) the 8.6-micron or 11.25-micron (or both) polycyclic aromatic hydrocarbon (PAH) bands in six PMS stars. Although the dust-emission features change on timescales of months to years, the underlying infrared continua remain constant in flux density.

The interpretation of this variability is that dust in the tenuous regions above the optical disks is being chemically altered through exposure to stellar radiation. These processing events appear to be occurring at disk radii comparable to or larger than Earth's orbit of 1 astronomical unit (AU) and may provide clues to the dynamics of the active planet-forming region below the disk photosphere.

Two-dimensional (2-D) radiative transfer models have been developed and are being used to model these time-variable spectra. These new models allow synthesis of spectral energy distributions of complex disk geometries that include inner gaps and

disk swelling caused by local opacity effects such as those expected from vertical structure models. The 2-D radiative transfer models are being used to interpret data from broad-wavelength spectral energy distributions derived from ground-based photometry and HIFOGS time-variable spectroscopy, as well as from the Infrared Space Observatory (ISO) Short Wavelength Spectrometer (SWS) 6–45 micron spectra.

Point of Contact: K. Bell
(650) 604-0788
Katherine.R.Bell@nasa.gov

The Kepler Mission: A Photometric Mission to Determine the Frequency of Earth-Size Planets in the Habitability Zone of Solar-Like Stars

William J. Borucki, David G. Koch

The Kepler Mission is a Discovery-class space mission designed to detect and characterize Earth-size planets around solar-like stars. The sizes of the planets are determined from the decrease in a star's light that occurs during planetary transits; the orbital period is determined from the repeatability of the transits. The orbital radius and the nearness of the planet to the habitability zone are estimated from ancillary measurements of the stellar mass and brightness. Such measurements determine the spacing of planets, their distribution of size with orbital distance, and their variation with stellar type and multiplicity. Because thousands of stars must be continually monitored to detect the transits, extensive information can be obtained about the star's rotation rates and activity cycles. Observations of p-mode oscillations also provides information on age and metallicity of the parent stars.

These goals are accomplished by continuously and simultaneously monitoring a single field of 100,000 solar-like stars for evidence of brightness changes caused by transits of Earth-size or larger planets. To obtain the high precision needed to find planets as small as Earth and Venus, a wide field-of-view, 0.95-m-aperture Schmidt telescope with an array of charge-coupled device (CCD) detectors at its focal plane must be located outside Earth's atmosphere. Both Solar Maximum Mission (SMM) and Solar and Heliospheric Observatory (SOHO) observations of the low-level variability of the Sun (~1:100,000) on the timescales of a transit (4 to 16 hours), and our laboratory measurements of the photometric precision of charge-coupled devices (1:100,000) show that the detection of planets as small as Earth is practical. If most solar-like stars have terrestrial-size planets in their habitable zone, then several

hundred planetary systems should be detected. Many additional planets should be detected that have shorter orbital periods. Planets as small as Mars or even Mercury could be found if they have orbital periods of a week or less. Based on previously obtained Doppler velocity data, approximately 1,000 giant inner planets should be discovered from their reflected light.

The Kepler Mission was selected on 21 December 2001 for a launch opportunity and is expected to be launched into a heliocentric orbit in 2007. A 4-year mission is planned with the capability of operating for an additional 2 years. The additional 2 years would nearly double the number of detections of planets in the habitable zone of G-dwarf stars like our Sun.

The spacecraft and instrument will be built by Ball Aerospace Technology Corp. (BATC), of Boulder, Colorado. BATC has built most of the optical instruments used in the Hubble Space Telescope and is the industrial partner for the Deep Impact Discovery Mission. The Space Telescope Science Institute

(STScI) is a partner on the Kepler Mission. Mission data will be calibrated and archived, and acoustic-mode data will be used to determine the age and composition of the brighter stars. A frame subtraction technique will be used to remove the effects of dim background stars.

The Smithsonian Astrophysical Observatory will perform ground-based spectroscopy on the 225,000 stars in the Cygnus star field that Kepler will view. These data will be used to select the target stars by culling out evolved stars that are too large to show planetary transits. Candidate planets will be examined and false positives, caused by the presence of white dwarf companions, will be removed.

The Lawrence Hall of Science and the SETI Institute are leading the education and outreach programs to bring the Kepler discoveries into classrooms and to the attention of the general public.

Point of Contact: W. Borucki
(650) 604-6492
William.J.Borucki@nasa.gov

Effect of Negative Ions on the Conductivity of Titan's Lower Atmosphere

William J. Borucki, E. L. Bakes, Robert C. Whitten

Borucki and colleagues previously (1984) calculated the electrical conductivity and electrical charge on aerosols in Titan's atmosphere resulting from their ionization by galactic cosmic rays and by electron precipitation from Saturn's magnetosphere. Based on these calculations, an experiment was designed to fly on the entry probe of the Cassini Mission to measure Titan's conductivity. The calculations showed that Titan's lower atmosphere must be substantially more conducting than the atmospheres of Earth and Venus because of the high concentration of free electrons. The prediction of a high conduc-

tivity is based on the lack of electrophillic species which could form negative ions with low mobility and thereby reduce the number of free electrons. At that time, no molecular species capable of forming negative ions in concentrations sufficient to perturb the atmospheric conductivity were identified. Recently, the formation of polycyclic aromatic hydrocarbons (PAH) has been investigated using quantum mechanical methods. The calculations indicate that these molecules will be highly electrophillic and are likely to be present in the atmosphere at mixing ratios of the order of one part per

10 million. Revision of the atmospheric model is under way to account for the presence of the negative ions formed from the PAHs and to predict their effect on Titan's atmospheric conductivity.

Point of Contact: W. Borucki
(650) 604-6492
William.J.Borucki@nasa.gov

The Vulcan Photometer: A Dedicated Photometer for Extrasolar Planet Searches

William J. Borucki, Douglas A. Caldwell, David G. Koch, Jon Jenkins

A small dedicated photometer for use in detecting extrasolar planets has been constructed and tested at Mt. Hamilton, California. It simultaneously monitors 3,000 stars brighter than 12th magnitude within each star field in the galactic plane. Observations are conducted all night every clear night of the year. A single field is monitored at a cadence of eight images per hour for a period of about 3 months. When the data are folded and phased in order to discover low-amplitude transits, the relative precision of 1-hour samples is about 1 part per 1,000. This precision is sufficient for finding Jovian-size planets orbiting solar-like stars, which have signal amplitudes from 5 to 50 parts per 1,000, depending on the sizes of the planet and star.

Nearly 100 variable stars are found in each star field in each of the two star fields observed. About 50 of these are eclipsing binary stars, some with

amplitudes of only a few percent. Three of these showed transits signatures like those expected from planetary companions. These stars were then observed with high-precision spectroscopy at other observatories to determine the mass of the secondary object. The spectra indicate that two candidates are nearly identical stars in binary pairs in grazing orbits. Spectroscopic observations showed the third object to be a high-mass-ratio single-lined binary with a stellar companion similar in size to a Jovian planet. Detection of the extrasolar planet orbiting the star HD209458 produced an easily recognized signal proving that the photometer has the necessary relative precision to find planetary companions.

Point of Contact: W. Borucki
(650) 604-6492
William.J.Borucki@nasa.gov

Extrasolar Planet Detector for the South Pole

Douglas A. Caldwell, Robert L. Showen, Kevin R. Martin, William J. Borucki, Zoran Ninkov

Recent discoveries of a wide variety of planetary systems highlight the need for statistical information on the numbers and properties of extrasolar planets in order to understand planetary formation and evolution. Transit photometry (observing a planet pass in front of its star) can reveal a wealth of infor-

mation for ~10% of those planets with orbital periods of 1 week or less. Observations of the transit of the extrasolar planet HD 209458b have resulted in the first unambiguous determination of the mass and density of an extrasolar planet, as well as the first detection of the atmosphere of such a planet. The

goal of this work is to extend the transit photometry being done at Ames Research Center (ARC) by developing a photometer for use at the South Pole.

Reliable detection of a transiting extrasolar planet requires observations of at least three transits in order to confirm the periodic nature of the signal. Therefore, the detection rate depends strongly on the duration and phase coverage of the observations. In the ideal case of continuous observation, three transits could be seen in three times the longest period to be detected (~ 7 days). The closest that one can get to continuous observation on Earth is during the long winter nights at the poles. The South Pole is the one of choice because of its permanent station, favorable weather, and excellent astronomical conditions. The three-transit detection rate at the South Pole is three times better than that of a mid-latitude site, even with time lost because of bad weather—historically estimated at 50%. That is, the detection rate for 1 month of observation at the South Pole is equivalent to that for 3 months of observation at mid-latitudes. The poles have the added advantage of constant elevations for the stars being monitored, thereby eliminating the large nightly flux changes as the stars rise and set.

A prototype photometer for use at the South Pole has been constructed and tested at ARC. It is based on the Ames Vulcan photometer, which has been in operation at the Lick Observatory (Mt. Hamilton, Calif.) for several years. The prototype, “Vulcan-South,” was designed with the goal of understanding the operating environment at the

South Pole. In particular, the system must be able to operate largely unattended in the extreme cold and blowing snow. The prototype was designed to be as close as possible to a fully capable transit detection system, including a science-grade charge-coupled device (CCD) camera, full-motion mount, and wide field-of-view optics. The mount and camera-frame were designed to work at -45° Celsius (-45° C) (the late-summer temperature at the Pole), using low-thermal-expansion material and dry lubrication. A heating and insulation system was designed to keep the CCD and mount electronics within operating specifications, as well as to protect moving parts from blowing ice crystals. The photometer was instrumented to monitor temperatures throughout. Subsystems were tested in a cold-chamber during the design and construction phase.

The Vulcan-South photometer was deployed to Antarctica in the austral summer of 2001. The system was installed on the roof of the astronomy building approximately 1 kilometer from the geographic South Pole and operated for 5 days. The heating and insulation system worked as designed, keeping the CCD camera, optical, and mechanical systems between -5° C and -15° C, with ambient near -35° C. Based on the results of deployment, and using automation developed for the Vulcan project, the design of a winter-over photometer for the South Pole has been completed.

Point of Contact: D. Caldwell
(650) 604-3119
dcaldwell@mail.arc.nasa.gov

Circumstellar Carbonaceous Dust

Jean E. Chiar, Alexander G.G.M. Tielens

Aromatic (chain-like) hydrocarbon material is present in both circumstellar and interstellar environments. Its presence is evidenced by either emission or absorption features, depending on the excitation

conditions, at wavelengths corresponding to the fundamental vibrational frequencies of carbon-carbon and carbon-hydrogen bonds. An infrared absorption feature has been detected at 6.2 microns

(μm) directed toward several objects that sample large pathlengths of diffuse interstellar medium dust. It was originally proposed that the aromatic materials were thus residing in the diffuse interstellar medium, and were not related to the objects themselves.

However, our study shows that the 6.2- μm absorption feature is actually circumstellar in nature and is produced by the WC-type Wolf Rayet stars being used to probe the diffuse interstellar medium along their line of sight. These results have implications for dust nucleation in the hostile environment around these hot stars, a topic that has only recently been theoretically explored. Since the circumstellar visual extinction toward these objects is minimal (about 1 magnitude), these dust grains have to be rather large (about 1 μm) and point toward dense clumps as the sites of dust formation.

Late-type WC stars, massive hot stars with fast dense stellar winds, are undergoing extensive mass

loss and show the products of helium burning at the surface. Since their circumstellar material is carbon-rich and hydrogen poor, we attribute the absorption feature at 6.2 μm in their spectra to circumstellar amorphous carbon dust.

The 6.2- μm absorption feature is also detected toward the enigmatic cocoon stars in the Galactic Center Quintuplet Cluster. Thus, as a corollary, our results support a previous suggestion that these sources are themselves late-type WC stars. This absorption feature is not detected in the diffuse interstellar medium toward lines of sight that sample only interstellar dust, with no possible contribution from the circumstellar dust of dusty late-type WC Wolf-Rayet stars.

Point of Contact: J. Chiar
(650) 604-0324
chiar@misty.arc.nasa.gov

Organics and Ices Toward the Galactic Center

Jean E. Chiar, Andrew J. Adamson, Yvonne J. Pendleton, Douglas C. B. Whittet

High-quality, spatially resolved spectra were obtained with the mid-infrared spectrometer CGS4, on the United Kingdom Infrared Telescope, in order to disentangle absorption components owing to dense cloud material and diffuse interstellar medium dust along the line of sight toward the galactic center. It was found that both absorption components vary significantly across the small 2-parallax-second (2-parsec) field studied, implying small-scale inhomogeneity in both the (foreground) diffuse interstellar medium and the dense molecular clouds. Figure 1 shows that the data are uniquely suited to defining the profiles of the dense cloud water-ice feature and the diffuse interstellar medium

3.4-micron (μm) aliphatic (chain-like) hydrocarbon feature, compared with previous studies which relied on fitting local continua over a small wavelength range. A new diffuse interstellar medium (ISM) absorption feature at 3.3 μm is revealed. The central wavelength is indicative of polycyclic aromatic hydrocarbons (PAHs); however, its width is broader than that of the well-studied PAH emission features and the absorption feature seen toward the Galactic Center Quintuplet sources to the north. The difference in profile could be a result of differences in temperature or carrier(s) or both, which are present in these regions.

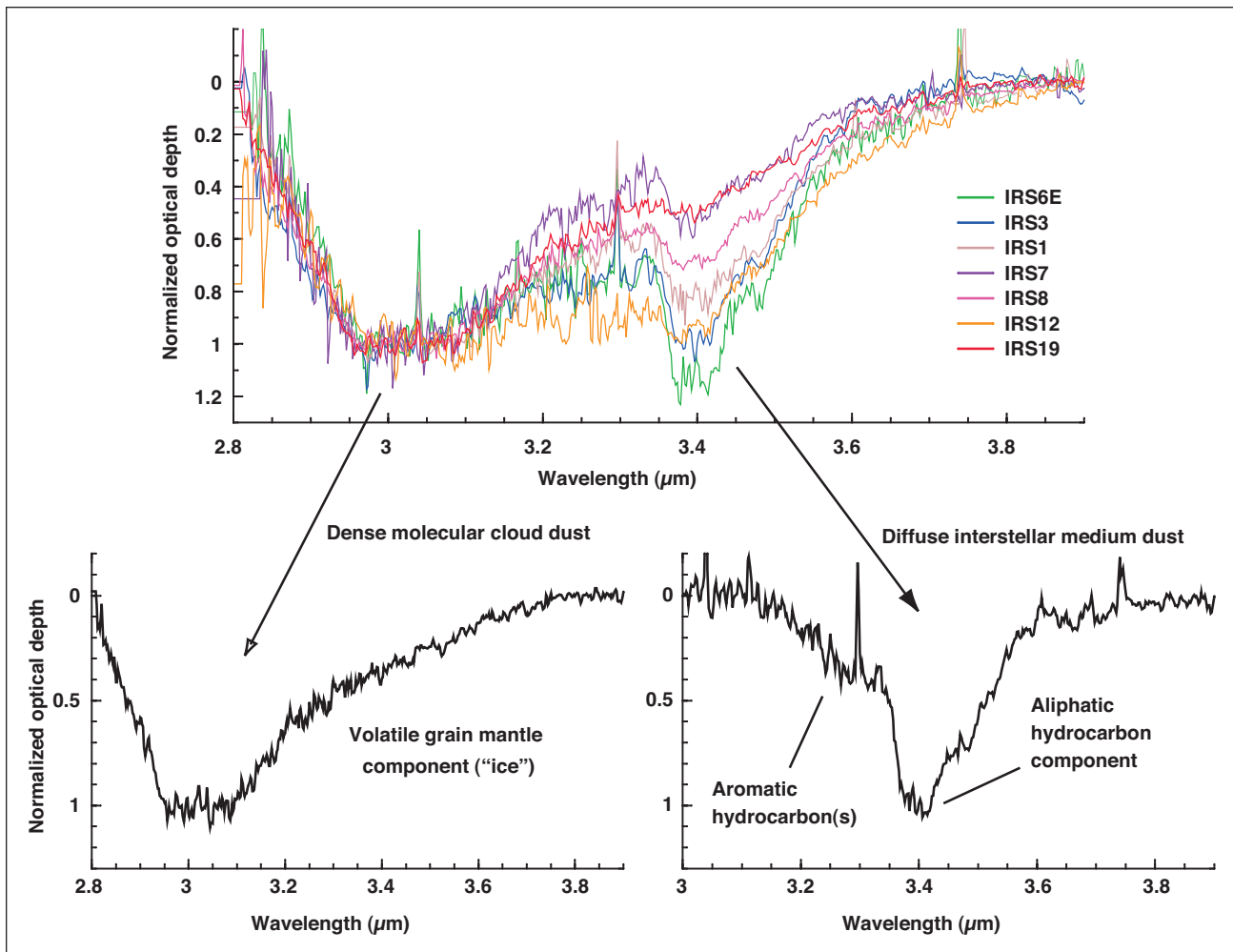


Fig. 1. The spectroscopic signatures of key ice and organic dust components along the galactic center line of sight. Ice and hydrocarbon absorption vary independently of each other.

Point of Contact: J. Chiar
(650) 604-0324
chiar@misty.arc.nasa.gov

Artificial Intelligence Techniques for Large-Scale Surveys of Space Science Data

Paul R. Gazis, Aaron Barnes, Clark Glymour

Many problems in space physics require large-scale surveys of extensive data sets to identify and classify qualitative features such as shocks, discontinuities, energetic particle enhancements, or specific types of spectra. Such surveys can be difficult to accomplish using conventional programming techniques, and the manpower requirements associated with direct physical examination of the relevant data sets can be prohibitive. Artificial intelligence (AI) techniques provide a potential solution to many of the problems associated with large-scale surveys. AI is a mature technology for which the relevant techniques are well-documented and understood; as yet, however, the space science community has made little use of AI techniques.

Investigators of the Space Science Division at the Ames Research Center, in collaboration with Carnegie Mellon University, have been examining a broad range of different AI techniques to evaluate their effectiveness for large-scale surveys of space science data. These techniques include traditional expert

systems, statistical methods, and different neural network-based approaches. Unsupervised classification using self-organizing maps (SOMs) has proved particularly productive. A suite of tools have been developed, tested, and applied to a wide range of problems that involve one-dimensional pattern recognition, such as the classification of visual and infrared spectra and the identification of events in time series of stellar occultation or solar wind plasma and interplanetary magnetic field (IMF) data. These tools have already produced valuable results in surveys of interplanetary shocks observed by the Voyager 1 and 2 and Pioneer 10 and 11 spacecraft. These tools should be useful immediately for many problems involving large-scale surveys of extended data sets that would be difficult or impossible to perform using any other means.

Point of Contact: P. Gazis
(650) 604-5704
pgazis@mail.arc.nasa.gov

Origin of the Thermal Inertia Continents on Mars

Robert M. Haberle

The surface of Mars can be classified into two major “continents” which are distinguished by the ability of their surface material to respond to solar heating. Low-thermal-inertia continents respond rapidly to solar heating and experience significant daily variations in surface temperature. High-thermal-inertia continents respond less rapidly to solar heating and experience much more subdued temperature swings. These different behaviors result from the nature of the surface materials composing these continents. The low-thermal-inertia continents contain fine

sandy materials (poor thermal conductors) and the high-thermal-inertia regions consist of hard consolidated rocky materials (good thermal conductors). These continents have fairly well-defined boundaries and occupy vast regions of the planet. The question is how did they come about?

The answer appears to be related to the planet’s global scale wind systems, which in turn are strongly controlled by topography. The low-thermal-inertia continents represent accumulations of

fine particles, which settle out of the atmosphere. In these regions, winds are relatively calm, and once the dust settles to the surface it tends to stay there. On the other hand, the high-thermal-inertia regions are subject to strong winds, which scour the surface clean and expose the underlying bedrock.

This hypothesis was tested with the Ames Research Center Mars General Circulation Model (GCM). The GCM predicts Martian wind systems using state-of-the-art numerical methods. These winds were then used to estimate how much dust could be lifted annually from the surface, a quantity called the “deflation potential.” The spatial distribution of the deflation potential was examined for a variety of orbital configurations because Mars’ orbital properties are known to oscillate considerably on time scales ranging from tens of thousands of years to millions of years. In particular, the planet’s obliquity (the angle between its spin axis and orbit

plane) may have varied anywhere from almost 0° to as high as 60° during the past 20 or 30 million years or so. Such changes were found to have a profound effect on the planet’s climate system. Yet, surprisingly, the regions of low thermal inertia never experienced significant deflation events regardless of the planet’s orbital configuration. Figure 1 shows a typical spatial pattern of the deflation potential as simulated by the GCM. Also shown is the present day distribution of thermal inertia; the correlation is remarkable.

If surface winds never get strong enough to erode away the fine material in the low-thermal-inertia regions, then it implies that these “continents” are old, much older than previously thought. In fact, these accumulations must have begun very early in the planet’s history—3.5 billion years ago—when its topography stabilized to near its present elevation. This notion can be easily tested with future

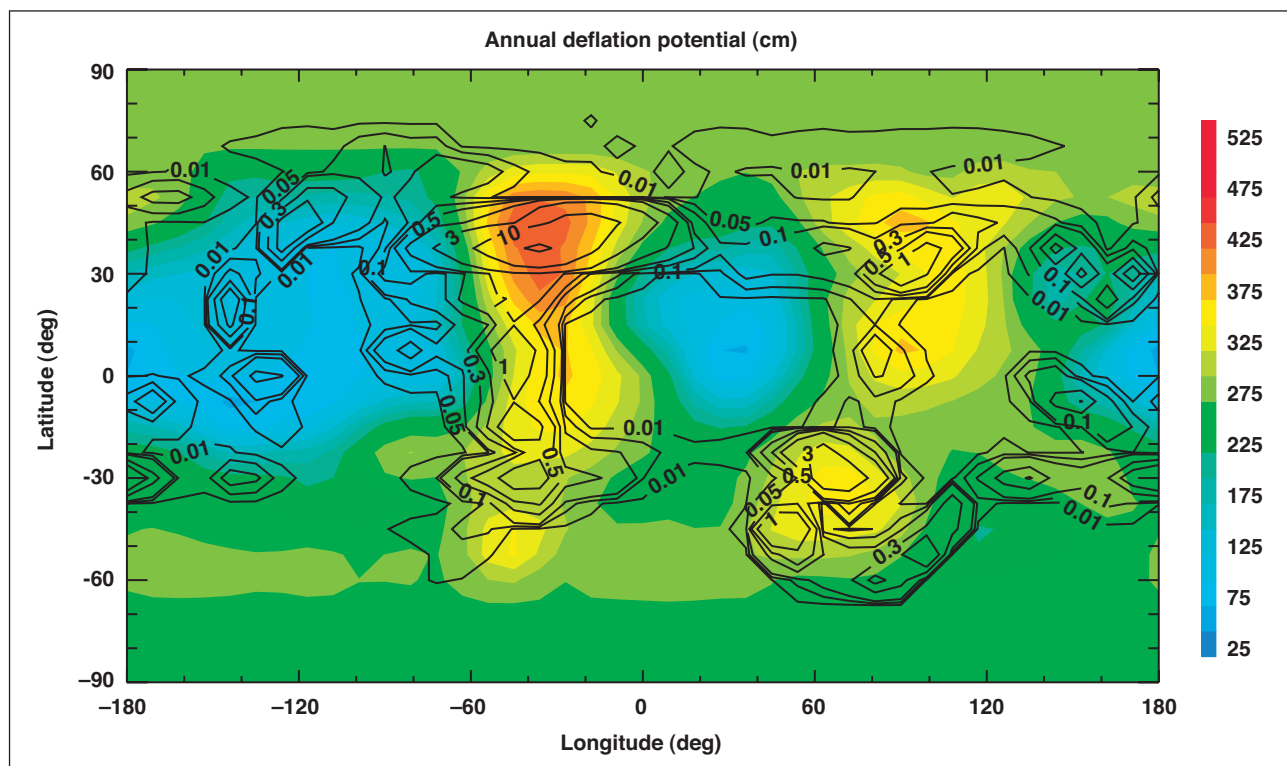


Fig. 1. Color shading indicates thermal inertia in Système International (SI) units. Scale bar is on the right. Black contours represent GCM prediction of the deflation potential in centimeters. Note the high positive correlation between the deflation potential and thermal inertia.

landers or sample-return missions. If correct, it means there is a readily accessible climate record that dates back to very early in the planet's history.

Point of Contact: R. Haberle
(650) 604-5491
Robert.M.Haberle@nasa.gov

The Center for Star Formation Studies

D. Hollenbach, K. R. Bell

The Center for Star Formation Studies, a consortium of scientists from the Space Science Division at Ames Research Center (ARC) and the astronomy departments of the University of California at Berkeley and Santa Cruz, conducts a coordinated program of theoretical research on star and planet formation. The Center, under the directorship of D. Hollenbach (NASA Ames), supports postdoctoral fellows, senior visitors, and students, meets regularly at ARC to exchange ideas and to present informal seminars on current research, hosts visits of outside scientists, and conducts a weeklong workshop on selected aspects of star and planet formation each summer.

In July 2001 the Center held an international workshop entitled "Star Formation in the Galactic Context" on the University of California at Santa Cruz campus. The weeklong workshop had approximately 130 attendees, and included an invited talk by D. Hollenbach on "Neutral Phases of the Interstellar Medium: Is Star Formation Self-Regulated by the Ultraviolet Field in a Galaxy?"

One focus of the ARC portion of the research work in the Center in 2001 was on the study of the thermal balance, chemistry, dynamics, and spectra of disks of gas and dust orbiting young stars. These disks, called protoplanetary disks, are the birthplaces of planets; they originally consist primarily of molecular hydrogen gas, small amounts of other gaseous species such as carbon monoxide, and a small admixture of dust particles. A number of processes heat the gas and dust in these disks, including radiation from the central star, radiation from a

nearby luminous star, and the gravitational energy released as the gas and dust spirals toward the star. Previous researchers have focused on the heating of the dust and on the infrared spectrum of the dust; ARC researchers focused on the gas and on the infrared and millimeter-wavelength emission from the gas. Comparison of data from NASA missions (see below) with these models provides constraints on the distribution of gas and dust and on the likelihood and duration of planet formation. In addition, the heating in the outer regions of the disks can be sufficient to drive evaporation of the outer disk regions in times that are short compared with the times required for planet formation, and thus can thwart or modify planet formation in the outer parts of the disk. These models were used to explain the smaller size and lack of hydrogen in Uranus and Neptune compared with Saturn and Jupiter.

Another focus of the ARC portion of the Center research in 2001 involved a study of dust particles in the optically thin dust layer at the surfaces of these protoplanetary disks. Only a very thin layer of dust particles is directly exposed to radiation from the central star; the rest of the disk is heated by the emission of infrared photons from this dust layer. Because dust absorbs stellar radiation efficiently but radiates only inefficiently in the infrared, this dust layer is typically hotter than the underlying disk photosphere and thus may dominate the emission from the entire system at certain wavelengths. In order to use observations to understand processes occurring in the underlying disk, emission from this dusty surface layer must be accounted for. In

addition, these dust particles produce features in the infrared that reveal the mineralogical, chemical, and geometric properties of the disk's grain population, thus providing clues to processes occurring in the disk below.

The theoretical models of the Center have been used to interpret observational data from such NASA facilities as the Infrared Telescope Facility (IRTF), the Infrared Astronomical Observatory (IRAS), the Hubble Space Telescope (HST), and the Infrared Space Observatory (ISO, a European space tele-

scope with NASA collaboration), as well as data from numerous ground-based radio and optical telescopes. In addition, they have been used to determine requirements on future missions such as the Stratospheric Observatory for Infrared Astronomy (SOFIA) and the Space Infrared Telescope Facility (SIRTF).

Point of Contact: D. Hollenbach
(650) 604-4164
David.J.Hollenbach@nasa.gov

Understanding the Cloudy Skies of Brown Dwarfs

Mark Marley, Andrew Ackerman, Richard Freedman

Unlike the conditions in a normal star, the temperatures and pressures inside a brown dwarf are too small to ever ignite its nuclear furnace. Hence as it ages, a brown dwarf cools by radiating its primordial energy away to space. During this process a number of important species condense and form clouds within the object's visible atmosphere. First iron, then silicates, and later water form thick clouds. With over 200 brown dwarfs now known, an understanding of these clouds is critical to modeling brown dwarf atmospheres and interpreting their spectra. An innovative collaboration between space and atmospheric scientists at Ames Research Center has focused on understanding these unusual clouds in the atmospheres of brown dwarfs. The lessons gained from modeling cloudy brown dwarf atmospheres will also be directly applicable to the first observations of extrasolar giant planets, which are expected to also have cloudy atmospheres.

Whether for a planet's or a brown dwarf's atmosphere, an atmospheric model predicts the variation in temperature and chemical composition with height. Coupled with a description of any clouds, this information allows model spectra to be computed and compared with observations. For cloudless

atmospheres, the modeling procedure is relatively straightforward; adding clouds to the modeling mix, however, severely complicates the calculation. Previously, workers studying brown dwarfs have either ignored the effects of clouds completely or included extraordinarily simplistic clouds that did not behave as do real clouds in the Solar System. Both approaches failed to reproduce the characteristics of observed brown dwarfs. Specifically they predict infrared colors for the warmer class of brown dwarfs known as L dwarfs that are either much redder or bluer than is observed to be the case. Secondly the simplistic models cannot reproduce the change in color, from red to blue, as the L types evolve to the cooler T type brown dwarfs.

The new cloud model captures some of the most important physics that governs clouds in Earth's atmosphere. Most importantly the model includes the effects of sedimentation of cloud particles, essentially rainfall. Models that include sedimentation produce physically thinner clouds with larger particles than those postulated by other research groups. Unlike complex terrestrial cloud models, the new brown dwarf model has only a small number of free parameters, one of the most important of

which is a “sedimentation efficiency factor.” Interestingly, efficiency factors of 3 to 5 can reproduce some essential aspects of both deep cumulus clouds on Earth and ammonia clouds in the atmosphere of Jupiter.

When used in brown dwarf atmosphere models, the new cloud formulation produces much better results than previous efforts. The model not only reproduces the red colors of the L dwarfs and the blue colors of the T dwarfs, it also allows, for the first time, a consistent explanation for the transition between these two brown dwarf types. As iron and silicate clouds form progressively deeper in cooling brown dwarfs, they sink from sight. The removal of

silicate and iron grains then allows water and methane atmospheric absorption to pull brown dwarf colors blueward. Previous models that ignored sedimentation produced clouds that were much too thick; thick clouds prevented the color transition from ever occurring in those cases. Interestingly, the same sedimentation efficiency factor that best reproduces some terrestrial and Jovian clouds also best describes “rainfall” in the atmospheres of brown dwarfs.

Point of Contact: *M. Marley*

(650) 604-0805

mmarley@mail.arc.nasa.gov

The Ultraviolet Photodecomposition of Martian Carbonates

Richard C. Quinn, Aaron P. Zent, Christopher P. McKay

The effect of ultraviolet (UV) light on the stability of calcium carbonate (CaCO_3) in a simulated Martian atmosphere was experimentally investigated. Sample cells containing ^{13}C -labeled calcite (most common form of CaCO_3) were irradiated with a xenon arc lamp in 10 millibars (mbar) of simulated Martian atmosphere, and a mass spectrometer was used to monitor the headspace gases for the production of $^{13}\text{CO}_2$ (carbon dioxide). We have seen no evidence of UV-decomposition of CaCO_3 when the calcite sample is exposed to UV light in a simulated Martian atmosphere at 10 mbar. Based on the experimental lower limit of detection, the upper limit of photodecomposition on Mars is 3.5×10^{-8} molecules/photon. However, it is most likely that UV photodecomposition of CaCO_3 does not occur on Mars, because of the high pressure of atmospheric CO_2 . In vacuum, the decomposition of CaCO_3 may occur as a result of the photodetachment and photodissociation of CO_3^- radical defects

generated by UV light. In a CO_2 atmosphere, the decomposition of CaCO_3 is suppressed by the reformation of the UV-generated CO_3^- by adsorbed CO_2 and surface O^- radicals.

In the event that photodecomposition is occurring at rates below 3.5×10^{-8} molecules/photon, the depth to which carbonate is decomposed in the regolith will be limited by the rate at which unreacted material is exposed through wind abrasion and the rate at which mechanical mixing of the regolith can cycle carbonates to the surface. Based on our upper limit of photodecomposition on Mars, the maximum depth of a carbonate-free zone in the regolith would be 10 meters (m). However, assuming that the formation of a carbonate-free zone is limited by the photodecomposition rate, and not by the erosion rate, the actual depth of the zone will depend on the rate and depth of mechanical mixing of the soil. If the mixing zone is less than 10 m deep, the depth of

the carbonate-free zone will equal the depth of the mixing zone. If the mixing zone depth exceeds 10 m, the amount of carbonate moved to the surface will exceed the total load of carbonate that can be removed from the surface over geological time, resulting in a nonzero gradient which will move carbonate back into the upper 10 m of the regolith.

Point of Contact: R. Quinn

(650) 604-6501

rquinn@mail.arc.nasa.gov

Reflectance Spectra of Titan Tholins at Cryogenic Temperatures

T. L. Roush, J. B. Dalton

Compositional interpretation of remotely obtained reflectance spectra of outer Solar System surfaces is achieved by a variety of methods, including matching spectral curves, matching spectral features, quantitative spectral interpretation, and theoretical modeling of spectra. All of these rely on laboratory measurements typically obtained with the sample at ambient temperatures and pressures. However, surface temperatures of objects in the outer Solar System are significantly cooler than ambient laboratory conditions. It has been clearly illustrated that the infrared spectra of silicate materials change as a function of sample temperature, and that these changes can have a significant effect on compositional interpretations.

The optical constants of Titan tholin, a solid residue created by energetic processing of H-, C-, and N-bearing gases, have been used as a coloring agent in compositional models of several outer Solar System surfaces. Because these surfaces are well below room temperature, we have undertaken a laboratory study to measure the reflectance spectra of Titan tholin with the sample at temperatures of approximately 310 kelvin (K), 300 K, 280 K, 270 K, 250 K, 200 K, 150 K, and 100 K. A subset of these spectra is shown in figure 1.

At low temperature, the visual and near-infrared colors of Titan tholin become redder, that is, the reflectance increases more at longer wavelengths

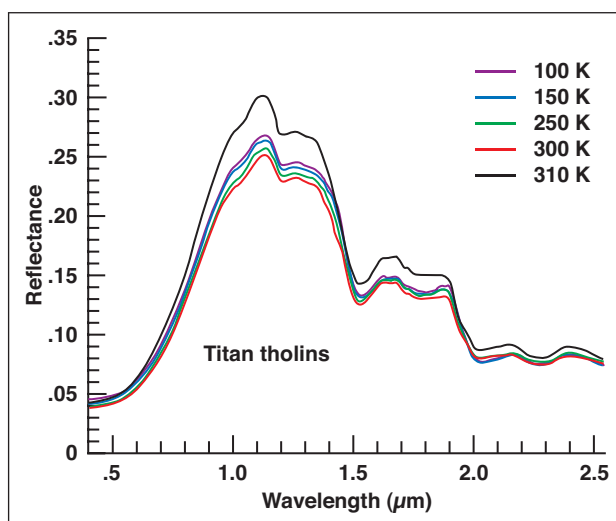


Fig. 1. Measured reflectance spectra of Titan tholins at various temperatures.

(to ~1.3 microns (μm)) than it does at shorter wavelengths, by ~5% as the material cools from 300 K to 100 K.

We estimate the effects of temperature on compositional interpretation as follows. The observed ~5% color change is used as a guide to adjust the Titan tholin optical constants reported by others. The imaginary index of refraction was decreased chiefly in the 0.6–1.3- μm wavelength region corresponding to the most noticeable spectral changes in the reflectance data.

Titan tholin has been used previously in modeling the surface of the Centaur Pholus. These calculations were repeated, and the results are shown in figure 2. Then the original Titan tholin optical constants were replaced with the values altered to account for temperature effects. The results are also shown in figure 2. After comparing the results, it was concluded that unless there is a sudden change at even lower temperatures, the temperature effects will likely have little influence on the compositional interpretation of the Pholus spectrum.

Point of Contact: T. Roush
(650) 604-3526
Ted.L.Roush@nasa.gov

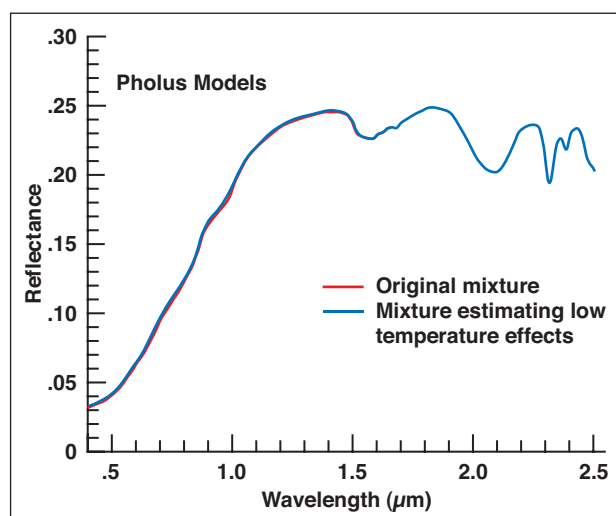


Fig. 2. Estimate of the influence of temperature effects on model spectra of Pholus. The red curve is based on the original model and the blue curve includes the estimated influence of low temperatures on the optical constants of Titan tholin within the same mixture.

New Algorithms for Mining Time Series and Image Databases

Jeffrey D. Scargle

A collection of algorithms for extracting structural information from time series and image data has been developed, based on Bayesian segmentation theory. Once the observational errors in the data have been modeled, the procedure is fully automatic, yielding high-level feature information. The software has been tested on synthetic data of known properties, and applied to the analysis of time-series data from the Compton Gamma-Ray Observatory's Burst and Transient Source Experiment (BATSE) and to two-dimensional positional data from the Palomar Distant Cluster Survey. Application of the

software to spatial power spectrum data on the cosmic background radiation, the solar neutrino flux as a function of time, the detection of planetary transits in various datasets, and to other astrophysical problems is in progress. Extension to cluster analysis in high-dimensional data sets and other data mining contexts is under way.

Point of Contact: J. Scargle
(650) 604-6330
Jeffrey.D.Scargle@nasa.gov

Grain Properties of Solar System Comets

Diane Wooden, David Harker, Charles Woodward

The observation of Solar System comets yields insight into the conditions of the primordial solar nebula before the gas and ices were swept up into cometesimals. Mid-infrared observations provide information on the mineralogical content and size distribution of the dust in comets.

Modeling of the thermal properties of dust grains has been successfully performed on several Solar System comets including comet Hale-Bopp. Since Hale-Bopp was an extraordinarily bright comet, the Ames Hi-efficiency Faint Object Grating Spectrometer (HIFOGS) obtained spectrophotometric data at mid-infrared wavelengths of 7.5–13.5 microns (μm) at epochs pre- and post-perihelion. In addition, far-infrared spectra were obtained at 15–22 μm post-perihelion. Modeling of the dust grains in Hale-Bopp showed that (1) the amorphous dust grains became more porous as the comet approached perihelion; (2) the amount of crystalline dust grains increased with a decrease in heliocentric distance; and (3) the dust grains became less porous as the comet receded from perihelion. The latest observations of short-period comet 19P/Borrelly show that the dust grains from this comet are much larger than those from Hale-Bopp.

Learning about the mineralogical content of comets such as Hale-Bopp yields insight into solar nebula processes. For example, the existence of crystalline silicate in comets suggests that amorphous grains (which all but dominate the interstellar medium, out of which the solar nebula formed) have to be processed at temperatures greater than 1,000 kelvin to form crystalline silicates. Such a processing mechanism implies that either the grains needed (1) to be transported close to the Sun to be heated, crystallized, and then transported out to the comet-forming zones where they formed icy mantles before being incorporated into cometary bodies, or (2) that some process, such as a nebular shock wave resulting from gravitational instabilities in the early protoplanetary disk, heated the amorphous silicate grains to a high enough temperature over a sufficient period of time for the grains to be crystallized.

Constraining the properties of dust grains in comets in conjunction with studies of the chemical makeup of Solar System bodies leads to a better understanding of the thermal processing, radial transport, and structure of protoplanetary accretion disks.

Point of Contact: D. Wooden
(650) 604-5522
Diane.H.Wooden@nasa.gov

Static Stability of Jupiter's Atmosphere

Richard E. Young, Julio A. Magalhães, Alvin Seiff

One of the particular scientific objectives of the Galileo Probe Mission to Jupiter was to determine the static stability of Jupiter's atmosphere. Static stability is defined as the difference between the vertical gradient of temperature in an atmosphere, called the temperature lapse rate, and the adiabatic lapse rate. The adiabatic lapse rate is the rate of change of temperature with height that would occur if temperature

depended on pressure in the same way as it would for an adiabatic compression or expansion of atmospheric gas parcels.

Static stability is one of the most fundamental properties of a planetary atmosphere; it represents the stability of the atmosphere to vertical overturning or mixing. The characteristics of the dynamic meteo

rology of an atmosphere directly depend on how large or small the static stability is. An atmosphere having zero static stability will exhibit large vertical mixing of air parcels, such that, for example, a parcel of air near the surface can easily be carried to high altitudes by winds. On the other hand, if the atmosphere has large static stability, it is quite difficult for an air parcel originally near the surface to be lifted to high altitudes, and therefore that parcel will tend to remain near the surface.

When the Galileo probe, which was managed by Ames Research Center, entered Jupiter's atmosphere on 7 December 1995, instruments onboard measured the temperature and pressure of Jupiter's atmosphere as the probe descended. Although these data have previously been analyzed in efforts to compute the static stability of Jupiter's atmosphere, error sources associated with the pressure sensors, caused by unpredicted thermal excursions in the probe interior, cast serious doubt on the results.

Because the static stability of a planetary atmosphere is such an important factor in the dynamic meteorology of the planet's atmosphere, a method was developed in the past year that avoided completely the errors induced in the probe atmospheric pressure sensors. For a hydrostatic, ideal gas atmosphere, it can be shown that for a probe in equilibrium descent (aerodynamic drag balanced by gravity), the temperature measurements alone can be used to derive the static stability. Unlike the pressure sensors, the Galileo probe atmospheric temperature sensors were unaffected significantly by the thermal excursions that occurred in the probe interior. Thus this method has been applied using only Galileo probe atmospheric temperature data to derive the Jovian atmospheric static stability.

Based on radiative convective models of Jupiter's atmosphere, it was anticipated that the atmosphere was neutrally stable, that is, had zero static stability. However, observed dynamical features in the atmosphere seemed to imply a small positive static stability. The results from the analysis show that the atmosphere to a depth corresponding to about 20 bars pressure generally is statically stable, exhibiting a static stability of the order of 0.2 kelvin per kilometer. The stability varies with pressure, such that over limited altitude regions the stability becomes small, but in general the stability is positive.

The implications of a stable Jovian atmosphere are significant. The tidal energy dissipation which is associated with orbital evolution of the Galilean moons of Jupiter, and in particular the volcanism on the moon Io, depend on the stability of the Jovian atmosphere. The banded structure of Jupiter associated with east-west jet streams requires a stable atmosphere if the winds extend to large depths. Atmospheric wave modes observed to occur at many locations are sensitive functions of the stability. The mode of transport of internal heat flux from the deep interior of Jupiter, that is, convective versus radiative heat transport, depends on whether the atmosphere is neutrally stable or statically stable, as does the latitudinal distribution of the heat flux. For all these reasons the derivation of a positive static stability in Jupiter's atmosphere to at least 20 bars pressure is an important finding.

Point of Contact: R. Young
(650) 604-5521
Richard.E.Young@nasa.gov

Carbon Dioxide Cycling and the Climate of Early Earth

Kevin Zahnle, Norm Sleep

The continental cycle of silicate weathering and metamorphism dynamically buffers atmospheric carbon dioxide (CO₂) and climate on geological time scales. In this cycle, silicate rocks and atmospheric CO₂ react with the aid of water to form, ultimately, silica and carbonate rocks. The cycle is balanced by the metamorphic branch of the rock cycle, in which carbonate rocks are cooked under pressure to release carbon dioxide gas back into the atmosphere. The carbonate cycle acts as a negative feedback loop that limits climate change on time scales of a 100 million years. Carbon dioxide is an important greenhouse gas. When the climate is warm, CO₂ and silicate rocks react more quickly. Meanwhile the continental rock cycle produces metamorphic carbon dioxide gas from old carbonates at a more-or-less constant rate. Thus the net CO₂ in the air decreases, and so the climate is cooled. On the other hand, when the climate is cold, the reaction between CO₂ and silicate rocks slows down, CO₂ builds up in the atmosphere, and the climate warms. Because the reaction rate between CO₂ and silicates is exponentially sensitive to temperature, the negative feedback is strong, and the climate stays temperate.

Over still longer time scales—billions of years—two other factors become important. The first is that the Sun evolves. When the Earth was young, the Sun was only about 70% as luminous as it is today. Because Earth's orbit is not thought to have changed much since Earth was fully accreted some 4.4 billion years ago, early Earth presents a puzzle: geological evidence suggests that Earth has usually been warm enough to have had liquid water oceans, with temperatures and hydrologic cycles not grossly different from those today. Yet the early Sun was so faint that, without a significantly stronger greenhouse than today, the Earth should have been encased in ice. The traditional view has been that the continental weathering cycle described above keeps pace with the evolving Sun to keep climate clem-

ent. Atmospheric CO₂ levels would have been 100-1,000 times higher than they are today. However, geological evidence, albeit scant, indicates that there was not nearly this much CO₂ during the Archean Eon ca. 2.5-3.8 billion years ago.

The second important difference on billion-year time scales is that the fluxing of carbon dioxide into and out of the mantle becomes important. In the mantle branch of the cycle, CO₂ is outgassed at mid-ocean ridge axes where mantle rocks well up to the surface, while subduction of cold carbonatized oceanic basalt and pelagic sediments return CO₂ to the mantle. This too is a negative feedback loop, because the amount of basalt carbonatization depends on CO₂ in seawater and therefore on CO₂ in the air. However this feedback cycle does not depend on the climate. The mantle cycle would have kept atmospheric and oceanic CO₂ reservoirs at levels where the climate was cold before ca. 2 billion years ago unless another greenhouse gas was important. At times when life was present on Earth, an attractive candidate greenhouse gas was methane, which the biota produced in vast amounts and which makes a very effective greenhouse gas. But before life arose, Earth was likely to have been on average quite cold.

The earliest Earth, the time before 3.8 billion years ago called the Hadean, is contemporaneous with the heavy impact bombardment of the Moon. Earth was subject to many and frequent impacts by large asteroids or comets. Chemical reaction of CO₂ with voluminous impact ejecta and its eventual subduction imply very low levels of atmospheric CO₂ and small crustal carbonate reservoirs in the Hadean. Despite its name, the Hadean climate would have been freezing unless tempered by other greenhouse gases.

Point of Contact: K. Zahnle
(650) 604-0840
Kevin.J.Zahnle@nasa.gov

The Martian Regolith and Climate

Aaron P. Zent, Richard C. Quinn

Our objectives in FY01 were to elucidate the role of the Martian regolith in controlling and recording the history of the Martian climate. During FY01, we addressed the question of whether water vapor finds a substantial diurnal reservoir in the Martian regolith. Data from observations vary as to whether or not the atmospheric column abundance of H₂O varies as a function of time of day. Some observations, chiefly from ground-based telescopes and Russian spacecraft, indicate a tremendous variation over the course of a day. Other observations, specifically those from Pathfinder and the Viking Orbiters, are most easily interpreted to indicate no diurnal variations in H₂O column abundance. Computer models of the atmosphere are unable to predict diurnal variations in atmospheric H₂O abundance. The simplest way to force substantial exchange is to posit that the Martian surface is locally covered with a highly adsorbing clay. These clays have larger adsorptive capacity than ordinary silicates, because they have interlayer sites that are available for adsorption.

In order to force computer models to predict strong diurnal H₂O exchange, the clays must equilibrate with the surrounding pore gases rapidly. However, the equilibration process is temperature dependent, and it is not clear that clays can play a role in exchanging a substantial fraction of the atmospheric column.

To address this issue, we measured adsorption uptake in sodium-rich clay from Wyoming. In figure 1, we show the results of the uptake experiments. The simplest interpretation of the data is evident in the equilibration time of the two lowest curves. When the soil is held at 211 kelvin (K), the adsorbed population continues to increase throughout the experimental period, up to 50 hours. In contrast, the case where the soil temperature is held at 273 K, and the relative humidity (R_H) is held at 4%, ap-

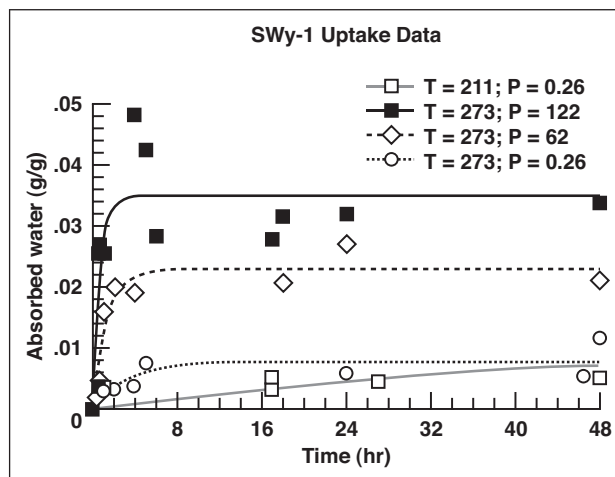


Fig. 1. The uptake of water by Mars-analog clays.

pears to equilibrate over the course of a few hours. Adsorption on Martian clays is not a plausible mechanism by which to account for strong diurnal variations in the H₂O column abundance of the Martian atmosphere.

Also in FY01, we completed a collaborative study of H₂O melting on the Martian surface. The times and locations where the surface pressure and surface temperature meet the minimum requirements for this metastability of liquid water were calculated. These requirements are that the pressure and temperature must be above the triple point of water, but below its boiling point. There are five regions on Mars where these requirements are periodically satisfied: in the near equatorial regions of Amazonis, Arabia, and Elysium, and in the Hellas and Argyre impact basins. Whether liquid water ever forms in these regions depends on the availability of ice and heat, and on the evaporation rate. The latter is poorly understood for low pressure CO₂ environments.

Point of Contact: A. Zent
(650) 604-5517
Aaron.P.Zent@nasa.gov

SPACE TECHNOLOGY

Focal-Plane Detector Array Development for Astronomy in Space

Mark E. McKelvey, Kimberly A. Ennico, Roy R. Johnson, Robert E. McMurray, Jr., Craig R. McCreight

A team at Ames Research Center is evaluating the suitability of a number of detector and readout-device technologies for space-infrared (IR) astronomy applications. This program aims to foster development of focal plane array (FPA) detector technology that will allow reliable background-limited infrared astronomy from future Space Science/Origins missions such as the Next Generation Space Telescope (NGST). Microelectronics advances to provide low-noise, low-power device operation in the space radiation environment are keys to the success of this program.

Evaluations at Ames of state-of-the-art Impurity Band Conduction (IBC) focal plane detector arrays are continuing for applications in the mid-infrared (5-30-micron (μm)) wavelength range. IBC detectors rely on a thin, highly doped IR-active layer to provide high quantum efficiency from a small detector volume, minimizing the ionization cross section for cosmic ray events. A high-purity blocking layer prevents excessive dark current, despite the high doping levels in the IR-active layer. IBC arrays also exhibit wider spectral response than alternative photoconductor (PC) architectures, without many of the performance anomalies associated with PC devices. IBC architectures are well suited to modern epitaxial fabrication methods, and the technology has progressed to the point where large-format hybrid FPAs sensitive to IR wavelengths as long as 28 μm can be reliably produced.

Work in FY01 was concentrated on helping advance the state of the art of large-format mid-IR IBC detector arrays to the megapixel class, working with Raytheon Infrared Operations to extend the successful CRC-744 device used in the Infrared

Array Camera (IRAC) on the Space InfraRed Telescope Facility (SIRTF). The new SB226 readout utilizes the simplified unit cell architecture and sampling techniques developed for the IRAC (figure 1). Evaluations at Ames of SB226 lot samples and a complete hybrid verified modest improvement over IRAC-level performance in a device which increases format by a factor of 16.

The Ames test laboratory's role in the NGST includes testing both near-infrared (1-5 μm) and mid-infrared (5-28 μm) candidate detector arrays in simulated on-orbit radiation environments, using the 76-inch Crocker Cyclotron on the campus of the University of California at Davis (UCD) to provide a high-energy proton beam for device testing. Previous radiation tests conducted at UCD by Ames personnel over the last several years have shown a marked difference in radiation-damage susceptibility between similar arrays from different manufacturers. This damage is manifested as dose-dependent activation of dark current that is of crucial importance to the NGST science mission. The results of the Ames tests are fed directly back into the manufacturing process in order to help advance the state of the art. The test group will continue to play an important role in the definition and execution of the NGST detector development program.

Other recent efforts involve continuing hardware and software upgrades to the suite of test instrumentation maintained in our detector laboratory. Recent upgrades have allowed easier manipulation of the data files collected from these large-format detector arrays. Further experimentation and optimization of both hybrid focal-plane-arrays and elemental electronic devices will continue in the next year, with

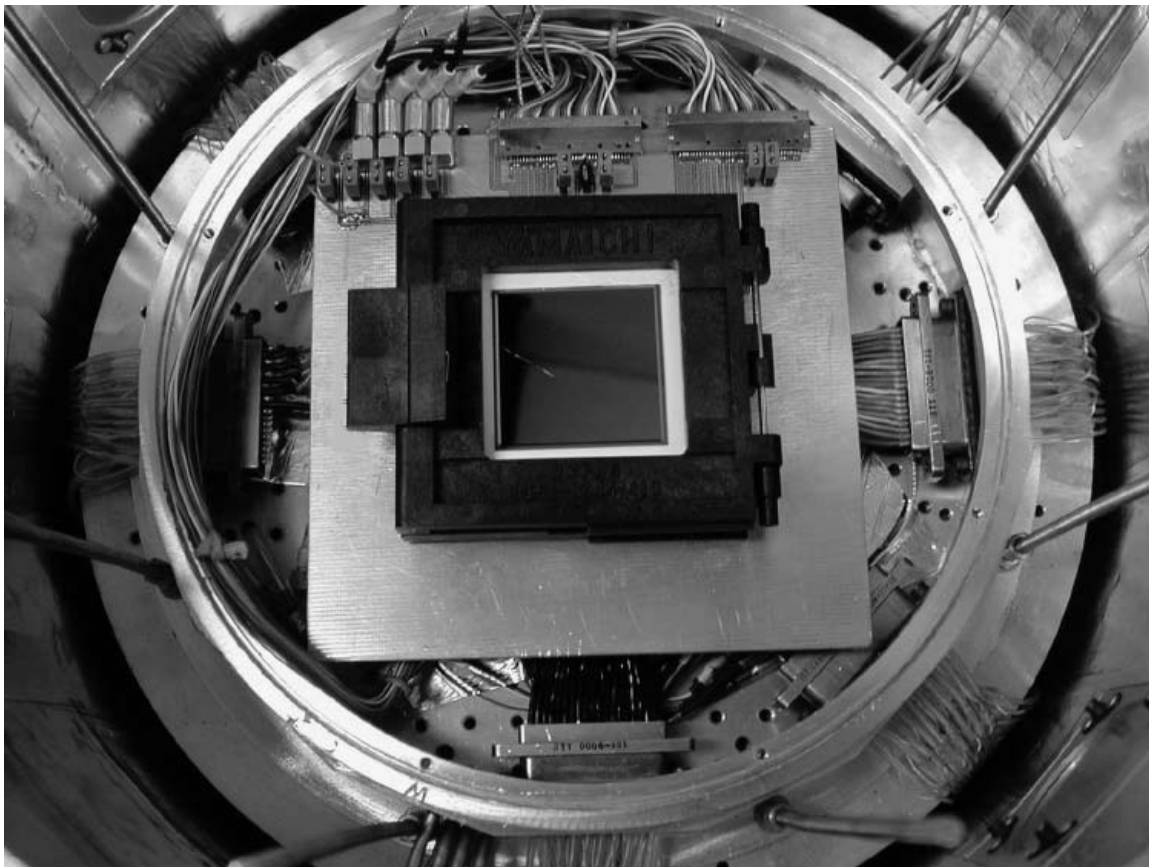


Fig. 1. 1024 x 1024 Si:As SB-226 detector array in low-background test Dewar.

close interaction with user and manufacturing communities. Our work on maturing IBC technology and improved readouts will continue, along with other sensor technologies in our ongoing efforts to enhance overall IR focal plane performance in NASA space- and ground-based applications.

Point of Contact: M. McKelvey
(650) 604-3196
Mark.E.McKelvey@nasa.gov

A Lightweight, High-Efficiency Pulse Tube Cryocooler for Spaceflight Applications

Louis J. Salerno, Peter Kittel, Ali Kashani, Ben Helvensteijn

Zero boil-off (ZBO) cryogen storage using cryocoolers and passive insulation technologies has received significant attention by NASA over the past few years. Conventional passive cryogenic storage systems can have sufficient heat input to cause the loss of about 1% of the cryogen per month from boil-off. In planning missions with storage times greater than 1 year, the resultant growth in tank size and mass to achieve lifetime requirements can make the cost of the mission prohibitive. The longer the mission duration, the more important this becomes. To be affordable, long-term exploration missions require lower tank capacity and longer storage times. This dictates that boil-off be either eliminated or significantly reduced.

Zero boil-off cryogen storage using (1) cryocoolers to either directly cool the cryogen with a circulation loop or reliquefy boil-off vapor, and (2) improved passive insulation technologies will enable long-term exploration missions by allowing designers to optimize tankage without the need for excess cryogen storage. Studies of ZBO have been ongoing in the United States for several years; however, to successfully implement ZBO in a flight configuration, low-mass, high-efficiency cryogenic coolers must be available. As the result of a joint development program between NASA and the Department of Defense (DoD), a lightweight, high-efficiency pulse tube cooler was recently delivered to the Ames Research Center by TRW (figure 1). This cooler was designed for ZBO storage of liquid oxygen or liquid methane. The design operating point of the cooler is 10 watts at 95 kelvin (K) with a rejection temperature of 300 K; the goal is a 10-year operating lifetime. The cooler has a mass of less than 4.0 kilograms, and an efficiency of 13 watts input per watt of cooling. This is nearly 1.5 times the efficiency of previous cooler designs, and approximately one-third the mass. The pulse tube is built by TRW, and



Fig. 1. High-efficiency, pulse tube cooler.

the compressor is built by Hymatic Engineering, in the United Kingdom. TRW integrates the compressor with the pulse tube and performs final testing of the assembly.

NASA's near-term plans call for the Glenn Research Center (GRC) and the Marshall Space Flight Center (MSFC) to integrate the cooler into a ZBO test bed at MSFC for further testing, as preparation for a possible flight-like test in the future, using components sized to simulate an actual flight scenario, including tank, radiator, attachment straps, and mixers. The cooler could be used directly in liquid oxygen (LOx) or liquid methane ZBO systems.

The cooler has been integrated into a cryostat for performance testing at both 280 K and 300 K rejection temperatures. Preliminary results operating the cooler at a rejection temperature of 300 K have shown that the cooler maintains 95 K with 10 watts applied to the cold block.

Point of Contact: L. Salerno
(650) 604-3189
Louis.J.Salerno@nasa.gov

K9 Planetary Exploration Rover Prototype

Maria Bualat

The K9 rover, a planetary exploration rover prototype, is a testbed and demonstration platform for autonomy and robotic technologies primarily targeted at Mars rover missions (for example, 2007/2009). The K9 rover (shown in figure 1) is a six-wheel rocker-bogie chassis outfitted with electronics



Fig. 1. K9 rover.

and instruments appropriate for supporting research relevant to remote science exploration and autonomous operations. This includes high-resolution color imagers and a five-degree-of-freedom arm for in situ instrument placement.

In the fall of 2001, the K9 team presented its accomplishments for FY01. The team also presented the design for the new outdoor test facility at Moffett Field adjacent to Gate 17 at Ames Research Center. The presentation was followed by a demonstration of conditional execution, onboard science understanding, and obstacle avoidance in the rover test yard.

In the demonstration, a contingent command sequence was executed by the onboard executive to autonomously carry out numerous science exploration activities. The rover successfully carried out commands to image the environment, detect rock and layered objects, and select spectrometer targets. In addition, the rover determined whether spectrometer data indicated the presence of carbonates, and evaluated the science value of targets, collecting the high-resolution image of the highest ranked target. The second phase of the demonstration involved autonomously driving to a goal location four meters away while avoiding obstacles.

Point of Contact: M. Bualat
(605) 604-4036
Maria.G.Bualat@nasa.gov

NASA IVHM Technology Experiment for X-Vehicles (NITEX) Propulsion IVHM Technology Experiment (PITEX)

Howard Cannon

The NASA Integrated Vehicle Health Management (IVHM) Technology Experiment for X-Vehicles/Propulsion IVHM Technology Experiment (NITEX/PITEX) team at Ames Research Center has been partnering with Kennedy Space Center (KSC) and Glenn Research Center (GRC) to develop an intelligent automated diagnostic system for vehicle propulsion systems using the Ames-developed Livingstone inference engine. Original development began with NITEX, which was funded through the Future X program at Marshall Space Flight Center (MSFC), and focused on the X34 main propulsion system (MPS). The current project, the PITEX, funded under the Space Launch Initiative (SLI) program at MSFC, is continuing to develop and improve the diagnostic system using the X34 simulation platform. PITEX is a key element of an IVHM risk reduction project led by the Northrop Grumman Corporation. In FY01, the NITEX/PITEX team made numerous advances in terms of architecture, modeling, diagnostic support software, and ground processing.

In NITEX, the team developed a comprehensive architecture that obtained vital information from the flight computer, processed the information with an onboard computer, and then downlinked the information for ground processing. On the ground, facilities were put in place for storing and archiving the information, displaying diagnostic information to ground operations personnel through a graphical user interface, and retrieving data for postflight data analysis. Under PITEX, advancements were made in understanding how this type of diagnostic system for propulsion might fit into a system-wide IVHM architecture for reusable launch vehicles.

The team has built what is perhaps one of the larger and more comprehensive Livingstone diagnostic models to date. In NITEX, the liquid oxygen

(LOX) feed system of the MPS was developed.

Under PITEX, the rocket propellant feed system was added, increasing the size of the model by more than 50 percent. The model is noteworthy in that it pushes the limits of Livingstone into the realm of a semicontinuous versus discrete application domain. It should also be noted that the model is the end result of a huge effort in knowledge acquisition. Much had to be learned about propulsion before it could be represented succinctly in model form.

The NITEX/PITEX team developed most of the software modules required to fly the experiment. Monitors were developed to convert continuous signals into discrete events. Under PITEX, the monitors have been improved to be robust to large amounts of noise. This is particularly challenging given that the monitors in some cases are required to generate events based on the derivative of a signal. Also a real-time interface (RTI) module was developed that translates the events from the monitors into Livingstone model variable settings. The RTI also includes a policy that orders the events temporally before feeding them into Livingstone, makes decisions concerning when to request diagnoses from Livingstone, and decides when to downlink the results to the ground. The RTI developed under NITEX/PITEX is robust to events being received out of order from the monitors, and handles concurrent transitions while maximizing the amount that can be diagnosed during these periods.

In addition to these core software components for the flight code, placeholders were developed for simulating telemetry inputs and telemetry downlink. For NITEX, 13 failure scenarios and 1 nominal scenario were simulated with a ROCETS model at GRC to generate simulated telemetry. The flight software read in this telemetry in approximately real time, and generated the correct diagnosis in each case.

In PITEX, the software was ported to flight-like computer hardware for testing and analysis. It was demonstrated that the system utilized only a small fraction of the available computational resources during all the scenarios.

Point of Contact: H. Cannon
(650) 604-4606
Howard.N.Cannon@nasa.gov

A Collaborative Web Facility for Mars Data Analysis

Glenn Deardorff

Marsoweb (<http://marsoweb.nas.nasa.gov>) is a Web facility that provides an intuitive, interactive interface to Mars geophysical data collected by Mars orbiters. Its goal is to enable online data discovery by planetary scientists. A recent usage report of Marsoweb indicates access by over 20,000 distinct users from government, academia, and Mars enthusiasts from the general public. The original impetus of Marsoweb was to help facilitate the landing-site selection process for Mars rover missions; its current emphasis is the Mars Explorer Rover twin missions of 2003 (MER 2003).

The MER 2003 portion of Marsoweb serves as a comprehensive “one-stop shop” for the landing-site community in several ways: in addition to announcements and memoranda to this community, it houses an archive of landing-site workshop presentations, information about the candidate landing sites, and landing-site characteristics imposed by lander and rover constraints.

A centerpiece of the MER 2003 Web site is a Java-based interactive data map display, which allows users to graphically peruse a variety of data maps pertinent to landing-site selection. Data from the current Mars Global Surveyor (MGS) and earlier Viking missions are used, and include elevation data from the MGS Mars Orbiter Laser Altimeter (MOLA), MGS thermal emission spectrometer (TES) data (which can be used to infer “rockiness” of regions), geology and mineralogy maps, etc., as

well as visible surface imagery. This zoomable, pan-able map interface also displays the locations and parameters of the candidate landing sites.

Some of the data maps in this interface are interactive insofar as users can scroll the mouse over the maps to see the location coordinates and data values of the map pixels (e.g., elevations on the MOLA maps). For MOLA, geology, and visible image maps, three-dimensional (3-D) Virtual Reality Modeling Language (VRML) scenes can also be downloaded. These VRMLs allow Web users to explore regions in 3-D, and use regional data maps mapped onto 3-D terrains composed from digital terrain models (figure 1).

Another prominent component of the MER 2003 Web site is an archive of ultra-high-resolution images (up to 3 meters/pixel) from the current MGS Mars Observer Camera (MOC), specifically taken of the candidate landing sites. This archive of MOC images can be graphically navigated with regional maps; users can zoom into their regions of interest, and peruse the MOC image outlines in the region maps to launch Web pages for each of the MOC images. These MOC image Web pages contain various MOC image display and download options, “context images” showing the MOC image location in a regional context, and a Java-based suite of online image processing tools (such as contrast enhancement).

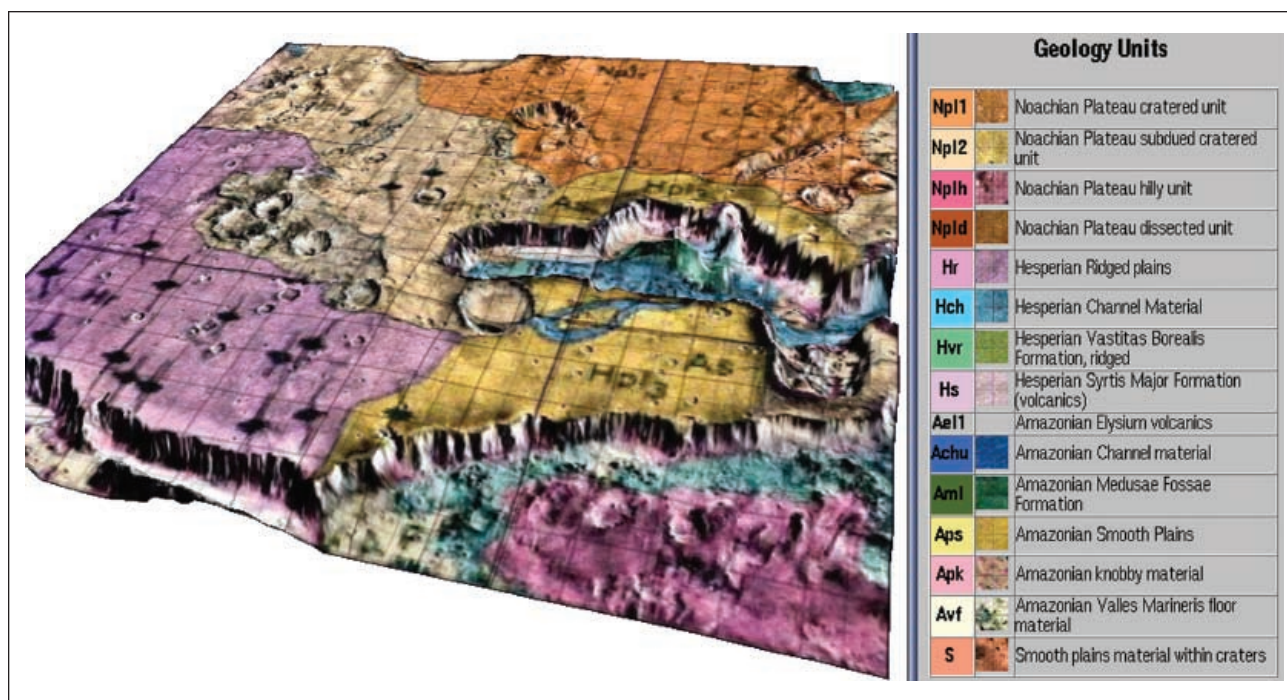


Fig. 1. A 3-D VRML scene of Viking terrain data is texture mapped with a geology map in the Melas Chasma region. This tool is a component of the MER 2003 landing-site selection resources.

Marsoweb facilitates dissemination of information from planetary scientists; it provides a “value-added service” for special products produced by landing-site community members. As an example, a set of detailed, high-resolution composite maps utilizing various data was made by the Jet Propulsion Laboratory (JPL) scientists for the prime landing sites; these were deployed on the MER 2003 Web site as interactive image maps, such that users can use them to easily launch the full-resolution MOC images displayed in miniature on these maps.

In addition to landing-site selection for rover missions, Marsoweb serves as an interactive archive of global data for general Mars research. These archives allow users to query the data maps in the same fashion as the MER 2003 data map interface (mouse scrolling displays location and data values), and also provide for profile creation from user-drawn cross-sections in the data maps (e.g., elevation profiles can be created from lines drawn in the MOLA elevation maps). These profiles can be mouse queried for location and data as well (figure 2).

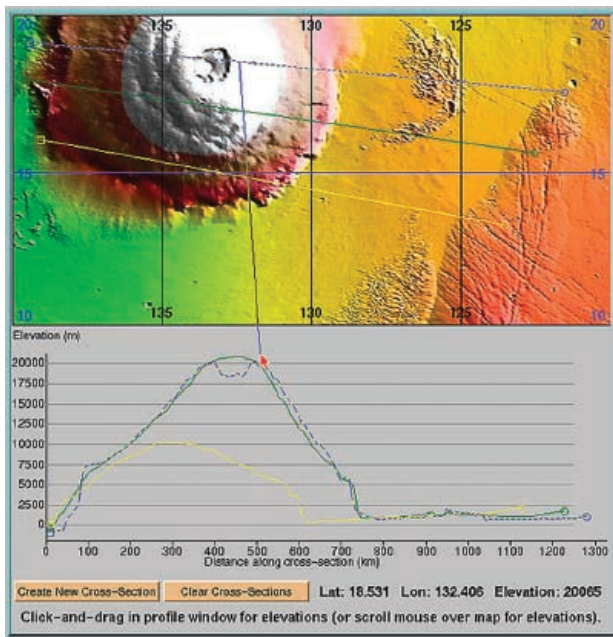


Fig. 2. The interactive global data archive supports user profile creation and querying of data. Shown here are MOLA data in the Olympus Mons region.

Point of Contact: G. Deardorff
(650) 604-3169
gdeardorff@nas.nasa.gov

A Planner-Based Software Agent for Data Management

Keith P. Golden

Managing the terabytes of data gathered by satellites and other sensors is one of NASA's greatest challenges. Anticipated "sensor webs" will collect huge quantities of heterogeneous data from Earth-orbiting satellites and in-situ sensors and process the data to detect and track short-term phenomena such as storms, fires, and volcanic eruptions, as well as intermediate and long-term trends, such as global climate change and the health of crops. Past approaches for processing and tracking data will not scale to handle such quantity and diversity of data-processing tasks with the fast response times needed to respond to short-term events.

IMAGEbot is a software agent for automating data management tasks. The goals of IMAGEbot are twofold: first, to address the scaling problem men-

tioned previously by providing a *goal-oriented* interface to scientists and other customers of data. Instead of writing a program or script to perform a given set of data-processing operations, the user provides a *semantic description* of desired data products, such as "Change in Net Primary Productivity for Montana between 2001 and 2002." Additionally, users can specify *syntactic* restrictions on data, such as file format, resolution, projection, and color scheme for a false-color image. Given this *data goal*, and knowledge about the data sources and data-processing programs that are available, the system determines the sequence of operations needed to obtain and process the requested data. Secondly, IMAGEbot will help future users find relevant data products by recording searchable semantic descriptions of all

data products generated, and help users assess the appropriateness of the data by recording information about the “pedigree” and quality of the data.

To achieve these goals, in FY01 the team developed a *constraint-based planner* that accepts data product requests and synthesizes parallel *data-flow* programs that will output the requested data. The planner uses descriptions of available data-processing commands and data inputs to reason about how the data can be manipulated by the commands to produce the desired output.

This study uses the Terrestrial Observation and Prediction System (TOPS) to apply IMAGEbot to the problem of *Biospheric NowCasting*, real-time ecosystem modeling from Earth science data. TOPS is a modular system, comprising a collection of filters and scientific models for processing satellite and weather-station data and generating secondary data products such as estimates of soil moisture and plant growth. TOPS can incorporate a variety

of alternative data sources and models, which the IMAGEbot planner can exploit by dynamically adjusting to the availability of data and trying multiple alternate inputs, filters, and models in an effort to provide the best possible output.

IMAGEbot is unique among planner-based approaches to data processing in the detail with which it represents and reasons about data contents and data-processing operations. Data can be described at multiple levels of granularity, from a very high level to the level of individual bytes or pixels. Likewise, the planner can reason about high-level operations, such as running ecological models, as well as pixel-level image-processing procedures. This expressiveness is the key to reasoning about how data are transformed by arbitrary sequences of operations.

Point of Contact: K. Golden
(650) 604-3585
Keith.P.Golden@nasa.gov

PathExplorer: A Runtime Verification Tool

Klaus Havelund, Grigore Rosu

The success of most technological experiments, including spacecraft and rover technology, depends heavily on the correctness of software. It is widely accepted that future spacecraft will become highly autonomous, making decisions without communication from the ground, so the required software is becoming significantly more complex, increasing the risk of mission failures. Ames researchers have developed a tool, PathExplorer (PAX), which is a program monitoring tool that can detect faults in software in a scalable way, and is, therefore, applicable to very large systems, possibly written using several different programming languages. The technique consists of monitoring program executions and verifying that the generated execution traces satisfy certain properties. The fundamental

idea consists of instrumenting the program with instructions that emit events to an observer during execution of the program. The observer examines the event stream, event by event, and performs various flaw-detecting analyses. PathExplorer implements two kinds of monitoring: specification-based monitoring and algorithm-based monitoring.

Specification-based monitoring consists of monitoring the execution of a program, represented by a sequence of events, by validating the events against a requirements specification. The specification is written in a formal language based on temporal logic, a special branch of mathematical logic that is suitable for expressing properties about reactive systems that interact with the environment.

For example, a requirement can be “Whenever the TEMPERATURE becomes HIGH the ALARM goes on within 20 seconds.” A typical requirement specification for a system has many such assertions. When a property is violated, a warning can be issued to the user. Alternatively, the violation can be used to steer the system under observation into a safe state. The advantage of using temporal logic to monitor program executions is that it relieves humans from performing a detailed analysis of program executions to see whether the program behaves correctly.

Algorithm-based monitoring, like specification-based monitoring, watches the execution of a program emitting events. Rather than matching against user-defined specifications, algorithm-based monitoring uses certain general algorithms for detecting particular kinds of error conditions. Examples are algorithms for detection of deadlock and data-race potentials in concurrent programs. These algorithms are interesting because the actual deadlocks and

data-races do not have to occur in the execution trace in order to be identified as a potential problem. An arbitrary execution trace normally suffices to identify problems. For example, a cyclic relationship between the locks in a concurrent program (process P takes lock L1 and then L2, while process Q takes L2 and then L1, that is, in reverse order) is a potential deadlock. A data race can occur if several processes access a shared structure, at least one process modifies the structure, and there is no mechanism for preventing simultaneous access. Such situations can also be detected. In 2001, the PAX was applied successfully to a 35,000-line C++ program controlling a rover, detecting a deadlock situation that had been otherwise undetected during testing, and confirming the potential of a data race.

Point of Contact: K. Havelund
(650) 604-3366
havelund@mail.arc.nasa.gov

Clickworkers Project

Bob Kanefsky

The Clickworkers project was a pilot study to see whether massive science data analysis can be accomplished by distributing the work to large numbers of volunteers, each working for a few minutes at a time on an ordinary Web browser. The study tested the ability of pooled efforts to accomplish time-consuming but scientifically useful tasks. The study was designed to answer the following questions: (1) Are people interested in volunteering their free time on routine scientific work, and (2) Does the public have the training and motivation to produce accurate results in a scientifically important task? An experiment such as this can determine whether people are willing to produce the required quantity and able to produce the required quality.

The project set up a Web site at <http://clickworkers.arc.nasa.gov> that offered the public the tasks of surveying and classifying craters on Mars. The Web site went online in November 2000 and was quietly advertised on a moderately popular Web site and in a Usenet newsgroup. Volunteers were given a choice of two tasks: click around the rim of each crater (thus specifying its latitude, longitude, and diameter), or classify the age of one crater as “fresh,” “degraded,” or “ghost.” The site covered the U.S. Geological Survey (USGS) Mars Digital Image Mosaic (version 1) from 30°N to 30°S at 64 and 256 pixels per degree, divided into overlapping 256 x 256 regions.

The original intent was to create a small-scale demonstration of the kind of response a popular Mars mission such as Pathfinder would get if it solicited help from the public in systematically extracting science from its images. However, within a month or two, with no further attempt at advertising, the project began gaining attention from the news media, and soon thousands of volunteers were marking hundreds of thousands of craters. As of mid-August 2001, over two million crater-marking entries and about 280,000 crater classification entries had been submitted by as many as 49,000 individuals (see figure 1).

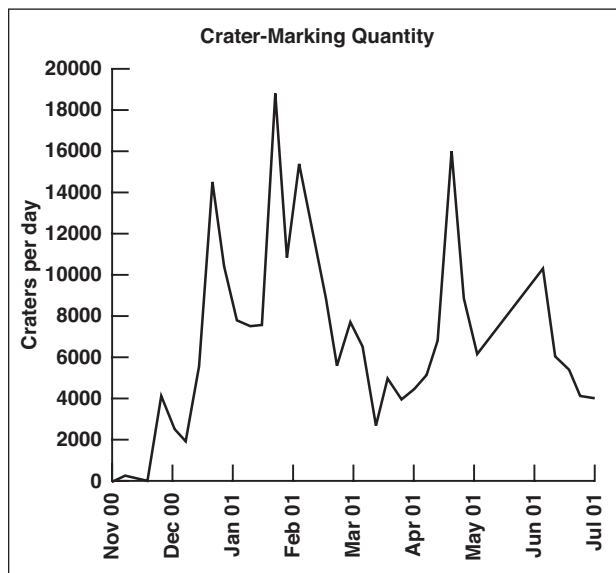


Fig. 1. Clickworkers crater-marking entries, by month.

A comparison of 20 randomly chosen Martian locations in Margaritifer Terra that were marked by a crater expert and also marked by a large number of clickworkers showed that the consensus of the volunteers is virtually indistinguishable from the opinion of the expert (see figures 2(a) and 2(b)).

In addition, it is possible to make some extrapolations about how many clickworkers a mission could recruit, assuming the media made no direct

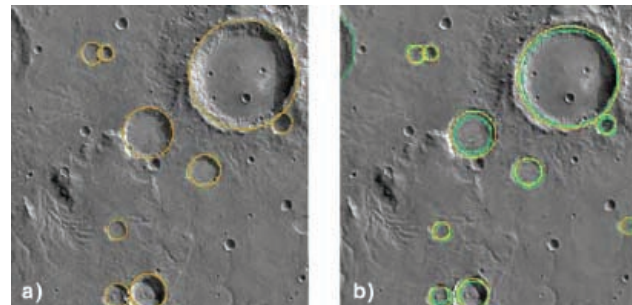


Fig. 2. Four small regions of the Mars Digital Image Mosaic, all randomly chosen from within Margaritifer Terra, were marked by a crater expert, (orange circles, Figure 2(a)) and by a large number of volunteer clickworkers (yellow circles, Figure 2(b)). Note that the orange and yellow circles match each other very closely. The yellow circles are the consensus of 200 clickworkers. The only difference is that the clickworker consensus is systematically smaller (closer to the inside lip of the rim) by a tiny amount.

mention of the opportunity. The number of clickworkers recruited directly from the banner ad on the Mars Atlas site was 2500 in seven months, with a click-through ratio of 1.9%. Of those, only 84 contributed any work, amounting to 5400 craters total (with five individuals accounting for half the work). To the extent that this information can be extrapolated, it suggests that a major Mars mission could get data-analysis work equivalent to marking 10,000 to 100,000 craters for every million page views—perhaps more, because of the motivation of participating in an active mission. For scale, the unsuccessful Mars Polar Lander mission attracted 16 million page views (200 million hits), whereas Mars Pathfinder attracted 1.2 billion hits. This suggests that either mission could have recruited a planet's worth of volunteers.

Point of Contact: B. Kanefsky
(650) 604-3514
kanef@ptolemy.arc.nasa.gov

ScienceOrganizer

Richard Keller

ScienceOrganizer is a specialized knowledge management tool designed to enhance the information storage, organization, and access capabilities of distributed NASA science teams. ScienceOrganizer provides a common electronic repository in which science team members can store and share project information. Team members access the system through an intuitive Web-based interface (see figure 1) that enables them to upload, download, and organize project information—including data, documents, images, and scientific records associated with laboratory and field experiments. Information in ScienceOrganizer is “threaded,” or interlinked, to enable users to locate, track, and organize inter-related pieces of scientific data. Linkages capture important semantic relationships among information resources in the repository, and these relationships assist users in navigating through the information related to their projects.

ScienceOrganizer serves as an information repository/ digital library for distributed scientific project teams, combining the functionality of a database, a document-sharing system, a Web-like hypermedia information space; and a semantic net. ScienceOrganizer enables storage and retrieval of heterogeneous project information: images, datasets, documents, and various types of scientific records describing people (e.g., science team members), places (e.g., laboratories, field sites), and things (e.g., equipment, samples). ScienceOrganizer supports cross-linkage among stored items to enable rapid access to interrelated information.

ScienceOrganizer has users affiliated with the NASA Astrobiology Institute, the Ames Exobiology Branch, and other institutions. A major new version of ScienceOrganizer was released in FY01 to more than 50 registered users at the ScienceOrganizer

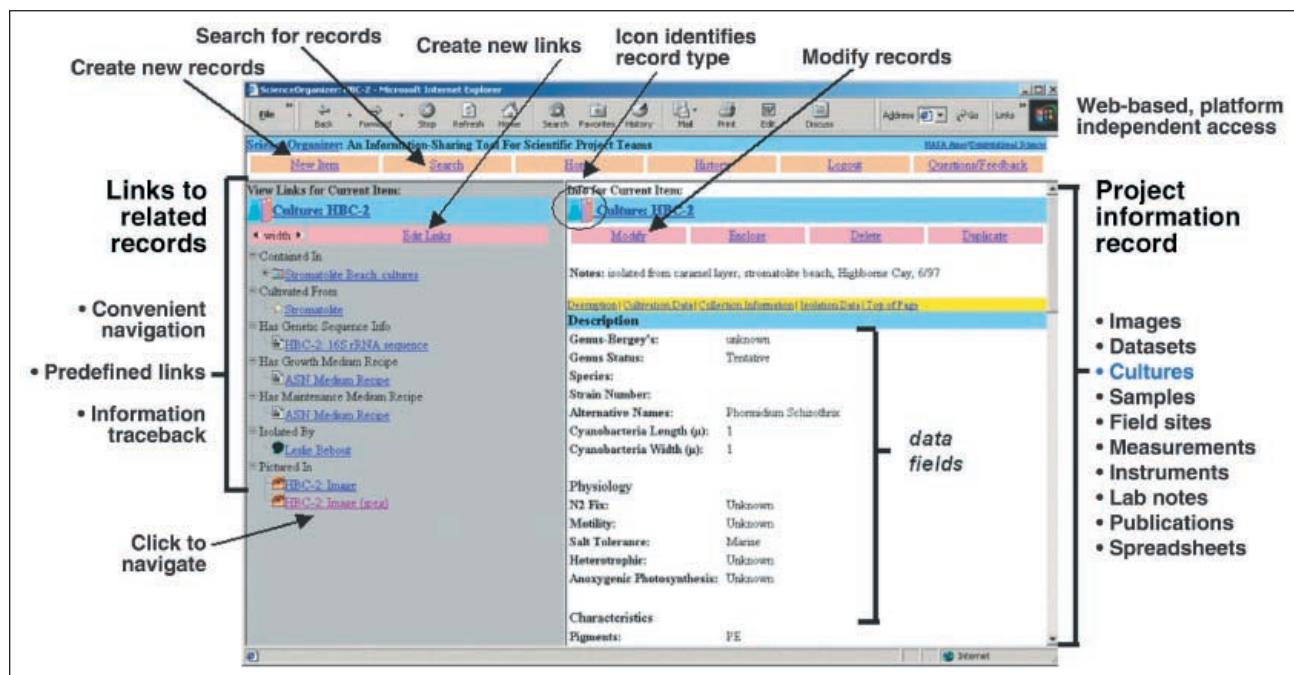


Fig. 1. ScienceOrganizer user interface.

Web site (<http://sciencedesk.arc.nasa.gov/organizer>). This version incorporates numerous usability enhancements to the user interface and other system functionality, a facility to automatically infer relationships among items in the repository based on preestablished inference rules, and access controls to restrict read and write access to items in the repository based on membership in groups or projects. In addition, this version of ScienceOrganizer permits

users to organize files or documents that are not physically stored on the ScienceOrganizer server, but are stored remotely on a network-accessible Hypertext Transfer Protocol (HTTP) server.

Point of Contact: R. Keller
(650) 604-3388
Richard.M.Keller@nasa.gov

Livingstone Qualitative Modeling Development Software Tools

Mark Shirley

The goal of the Model-Based Programming Skunkworks task is to create high-capability development and debugging tools that support model-based autonomy projects, beginning with the Ames-developed inference engine Livingstone. These tools are intended for subsystem teams to use throughout the spacecraft design process.

Livingstone accepts a model of the components of a complex system such as a spacecraft or chemical plant and infers from them the overall behavior of the system. Livingstone notes the commands that are being given to the system and the observations that are available. From this, Livingstone is able to monitor the operation of the system, diagnose its current state, determine if sensors are giving impossible readings, recommend actions to put the system into a desired state even in the face of failures, and so on.

Because Livingstone reasons about explicit models of the system it is interacting with, rather than following a program or rules, a Livingstone-based controller is highly capable, flexible, and easy to maintain. Livingstone also accounts for all available

information and observations, drawing conclusions that reach across a complex system in a way that would be difficult for a traditional software system or time-consuming for a human operator.

In FY01, the Livingstone and Skunkworks projects released version 2.0 of their qualitative modeling development software tools. In addition to the Livingstone qualitative model reasoning engine, the Skunkworks support tools include the Skunkworks command line “wrapper” around the Livingstone engine, the Candidate Manager (which allows the user to select from possibly several fault diagnoses), the History Table (which allows the user to view all qualitative model variable values at the current time and at previous time slices that have been saved by Livingstone), and Stanley (which allows the user to view model variable values mapped to a graphical representation of the hardware schematic that corresponds to the qualitative model created by the user with Stanley).

The Skunkworks team understands that model-based methods are an increasingly important part of the rapid deployment of such software. The team is committed to providing support to improve the

current methodology in order that it may become a well-defined software engineering process that may be used by teams outside of NASA research laboratories.

Point of Contact: M. Shirley
(605) 604-3389
Mark.H.Shirley@nasa.gov

Quantum Optimization Algorithms

Vadim Smelyanskiy, Dogan Timucin

Quantum computing is a revolutionary paradigm that offers fundamentally new perspectives toward developing efficient algorithms for solving classically intractable problems. The focus of this research in FY01 was to determine the computational complexity of quantum optimization algorithms (relative to their classical counterparts), aiming to provide justification for further research into quantum computing algorithms and their physical implementations.

Many of the computationally difficult optimization problems belong to the NP-complete class: their solution typically takes a prohibitively long time (e.g., exponential in the problem size) on classical computers, thus rendering them essentially intractable. On the other hand, relying on the unique principles of superposition and entanglement, a quantum computer can simultaneously explore an exponentially large number of computational pathways. By clever algorithm design, these pathways can be made to interfere in a fashion that produces the desired solution in a much shorter time (e.g., polynomial in the problem size), thus providing a drastic speedup over classical computers. The central outstanding research question, then, is whether such ingenious quantum algorithms with a superior computational complexity do indeed exist.

The approach to quantum algorithm design in this research was based on the recently proposed idea of continuous adiabatic quantum evolution of a physical system in its instantaneous ground state. Here, the optimization problem is encoded into the system via a suitably chosen energy (or cost) function, and

the solution is extracted by measuring the quantum state of the system after adiabatic evolution with a composite Hamiltonian $H(t)$ for a suitable time period T . This adiabatic quantum algorithm (AQA) was recently simulated on a classical computer for several NP-complete problems using large numbers of randomly generated problem instances believed to be computationally difficult for classical algorithms. Results of these simulations suggested a quadratic complexity for AQA, and the purpose of this study was to reconcile this highly intriguing discovery with the widely held (contradictory) belief in computer science that $P \neq NP$.

For this work, AQA was applied to the set-partition problem (SPP)—one of the core NP-complete problems of theoretical computer science with many practical applications: partition a set of n positive numbers into two disjoint subsets whose partial sums are as nearly equal to each other as possible. (Because problems in the NP-complete class are known to be reducible to each other in polynomial time, it is sufficient to study the complexity of AQA for only one of them.) Now, the complexity of the algorithm is determined by establishing the functional dependence of the run-time T on the problem size n such that a high probability of the correct solution is guaranteed (i.e., the system stays in its ground state throughout its evolution) for all problem instances. The analytical criterion for this was found to be $T \ll V/(g_{\min})^2$, where V is the matrix element of the operator $dH(t)/dt$ between the adiabatic ground state and the first excited state, and g_{\min} is the minimum gap separating the energies of these states for $\tau \in (0, T)$. The calculation of these

parameters for SPP led to a run time that scales as $T \sim 2^n/n$, which was substantiated by our extensive numerical simulations of AQA for SPP (shown in figure 1). Closer investigation revealed that the

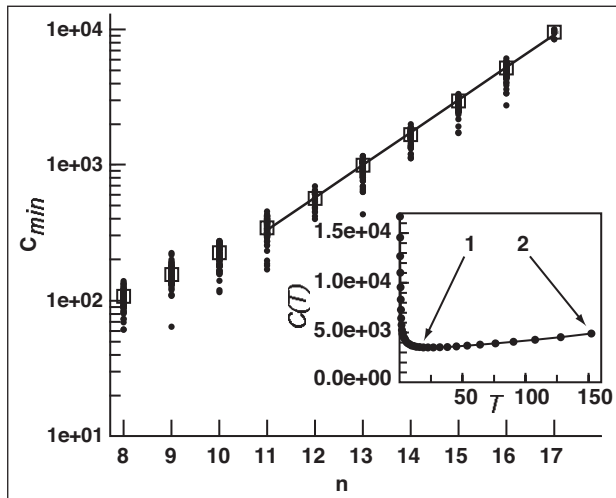


Fig. 1. Logarithmic plot of algorithmic complexity C_{min} vs. problem size n for randomly generated instances of SPP with 25-bit precision numbers. Vertical sets of points indicate results of different trials (≈ 100 trials for each n , 10 trials for $n = 17$); rectangles indicate the median value for each set. A linear fit to the logarithmic plot of median values for $11 \leq n \leq 17$ gives $C_{min} \approx 2^{0.8n}$. (The result is very similar if all the data points are used for the fit.) Inset: plot of complexity $C(T)$ vs. run-time T for $n = 15$. Points 1 and 2 indicate run-times that achieve ground-state populations of 0.15 and 0.70, respectively.

main reason for the poor performance of AQA is related to the ultrametric structure of the SPP cost-function values: configurations that are close in cost (energy) are separated by large Hamming distances (spin flips), and transitions between adjacent states via quantum-mechanical tunneling are, therefore, exponentially slow. Incidentally, this insight also points the way for future improvement of AQA for NP-complete problems.

Current understanding, therefore, is that the reported polynomial complexity of AQA is not the rule, but the exception: AQA appears to be an excellent quantum heuristic that can vastly outperform classical heuristics such as simulated annealing in certain problem instances, but cannot, in general, solve all NP-complete problem instances within a polynomial time bound.

Point of Contact: D. Timucin
(605) 604-1262
Dogan.A.Timucin@nasa.gov

Human-Centered Computing for the Mars Exploration Rover 2003 Mission

Jay Trimble

The Mars Exploration Rover (MER) Human Centered Computing (HCC) and Human Factors (HF) Program is working with the Jet Propulsion Laboratory (JPL) MER Mission System and Science Teams to develop tools and operational procedures to reduce the chances of operational errors during surface operations for the twin rovers, scheduled to land in 2004.

In 2001, the Ames Team interviewed MER Team members, and observed as the rover operations and science teams performed field tests to simulate the MER Mars Surface operation. The team produced a Phase 1 report covering issues and recommendations for specification and communication of science intent across multiple shifts during surface

operations. The team also specified target naming conventions for the mission.

The team produced a design for the MERBoard Collaborative Workspace, a tool to assist the mission teams with data display, capture, annotation, and distribution. The tool is designed to enhance the collaborative process that the team engages in as observations and activities for the rovers are planned. The MERBoard design has been accepted for inclusion as a mission system enhancement.

The MER operations team will be located in a Mission Support Area (MSA) at JPL. The MSA must support two rover operations teams and must be optimized to support the kind of collaboration and work practice that the science and engineering teams will engage in. Ames is working with the JPL team to develop facility layouts and designs for the MSA based on the observed work practice from rover field tests, as well as requirements and design inputs from team members.

The MER daily tactical command process design is built around the assumption that the team will work on Mars time. As the Mars day is roughly 24.7 hours this means that team members working on Mars time will have to shift their hours by approximately 40 minutes each day, and through the nights. There has been concern about the human

factors issues associated with working this proposed schedule. The MER Team requested that the Ames HCC/HF Team report on the causes and effects of fatigue and stress during Mars Pathfinder operations and on how the associated human factors issues may have affected operations. This report was delivered to the MER Team in FY01 and was used to assist in the development of staffing and shift plans for Mars Surface Operations.

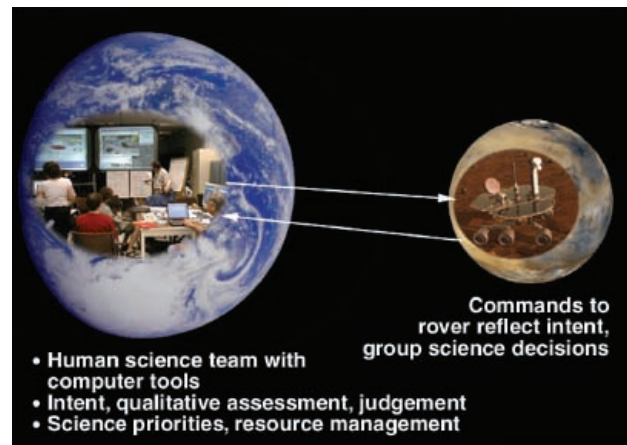


Fig. 1. Scientists and engineers on Earth communicate each day with the rovers on Mars.

Point of Contact: J. Trimble
(650) 604-6060
Jay.P.Trimble@nasa.gov

Autofilter: Generation of Trusted State Estimation Code from Mathematical Models

Jonathan Whittle

A critical component of any NASA mission is the guidance, navigation, and control software, and a key part is the software for estimating the vehicle's current state—its position, velocity, attitude, etc. The goal of Autofilter is to automate the process of developing state-estimation software by allowing

an engineer to express the software as a high-level mathematical specification that is then used to generate highly documented, certified code. In January 2001, Autofilter was successfully demonstrated at Ames (at that time it was called Amphion/NAV).

The Autofilter specification language consists of a mathematical description of the state-estimation problem. Autofilter is primarily geared toward problems that can be solved by the use of Kalman filters. Therefore the description is in terms of the physical model of the vehicle dynamics, the measurement model relating the observations to the states being estimated, and an architectural description of the Kalman filter (e.g., a single Kalman filter, Kalman filters running in parallel, nested Kalman filters). Unlike commercially available code generators, the relationship between specification and generated code is not one to one, but can be as high as 30 lines of code generated for each line of specification. This leverage factor comes from the fact that Autofilter has built in a wide range of knowledge about the domain, in the form of equational solvers, symbolic evaluators, approximations, linearizations, and code templates. In addition, Autofilter can generate multiple alternative programs for the same specification—for example, it can generate a linearized or an extended Kalman filter algorithm.

Autofilter's domain knowledge is organized into code-generation schemas. Each schema is a “program with holes” representing an uninstantiated

program fragment along with uninstantiated documentation for that fragment. If the applicability constraints for a schema are satisfied, the schema is instantiated with problem-specific details. The application of multiple schemas results in pseudo-code (i.e., language-independent code) with documentation based on the current problem. This pseudo-code can then be translated (along with appropriate optimizations) into C or Matlab code. Much of the architecture of Autofilter is built upon the existing Autobayes system, which was also developed at Ames.

Autofilter is currently being validated by application to real examples in the domain of Kalman filter-based state estimation. Two case studies are currently under way: an example from automated spacecraft docking, and an example based on Deep Space One Attitude Determination software.

Point of Contact: J. Whittle
(650) 604-3589
jonathw@ptolemy.arc.nasa.gov

Designing Collectives for Distributed Control

David Wolpert, Kagan Tumer

There are many information-processing problems that can only be solved by the joint action of large communities of computational agents, each running a sophisticated machine-learning algorithm where those algorithms are not subject to centralized, global control. Examples are routing of air traffic, control of swarms of spacecraft, routing of packets across the Internet, and communication between the multiple processors in a modern computer. The emerging science of “Collective Intelligence” is concerned with the design of multi-agent systems where there is a well-specified global objective

function that needs to be optimized through the collective action of the agents. We focus on the case where agents are “selfish” in that they act to try to optimize their own utilities, without explicit regard to cooperation with other agents.

This work recently considered the problem of designing (perhaps massively distributed) collectives of computational agents to maximize a provided “world” utility function. For such cases the central design issue is how to initialize/update the payoff utility functions of the individual agents

so as to induce the behavior of the entire collective to produce good values of the world utility. In such a system, as the individual agents work toward maximizing their individual payoff functions, their collective action works toward achieving the overall global objective.

Traditional “team-game” approaches to this problem simply assign to each agent the world utility as its payoff utility function. However, this strategy scales poorly in large systems, because the agents have a hard time discerning the effect of their own action on their utilities. In other words, their “signal” (the effect of their actions on their utility) is swamped by the “noise” of the system (the effect of other agents’ actions on their utility). In previous work collective intelligence-derived payoff utility functions proved superior to team-game utilities.

In FY01 researchers at Ames Research Center extended these results using a novel mathematical framework. They reviewed the derivation under that

new framework of the general class of payoff utility functions that are both easy for the individual agents to try to maximize, and have the property that if good values of these payoff functions are achieved, a high value of world utility is ensured. These are the “Aristocrat Utility” and a new variant of the “Wonderful Life Utility” that were introduced in previous work.

This project demonstrated experimentally that using these new utility functions can result in significantly improved performance over that of previously investigated collective intelligence-derived payoff utilities, over and above those previous utilities’ superiority to the conventional team-game utilities on a wide array of applications.

Point of Contact: K. Tumer
(650) 604-4940
Kagan.Tumer-1@nasa.gov

Biological and Physical Research Enterprise





Overview

The Fundamental Biology Lead Center Program Office, located at Ames Research Center (ARC), stated in the FY01 Strategic Plan that, "...the Program Office leads the Agency's efforts in fundamental biological research and relevant technology development, and supports activities conducted on the ground and in space." Thus, the activities related in this R&T Report address gravity's effects on various systems. Questions asked include:

- Through what mechanisms gravity is sensed, transduced, and responded to by biological systems at all levels of complexity
- How do biological systems integrate these gravity-related signals to respond and adapt to microgravity and the other characteristics of the space environment
- What are the fundamental biological mechanisms underlying physiological changes in humans caused by the spaceflight environment
- What are the effects of the space environment on biological processes that have an impact on space exploration
- What role has gravity played in shaping life on Earth

One reported research effort addresses activities at the subcellular level, and looks at protein subunits called Tropomodulins. These are of interest because the proteins are eventually responsible for muscle activity, which, like bone, is degraded under microgravity conditions. Other research at the subcellular level addresses cellular machinery required for radiation resistance through genetics. Radiation damage is a well known hazard of long-term spaceflight in high radiation flux. Yet another report relates how using the tools of genetics and creating transgenes in frogs addresses what happens in the gravity sen-

Biological Visualization, Imaging, and Simulation (BioVIS) Technical Center with the Virtual Glovebox.

sor system and the ability to adapt to altered gravity environments.

Bone loss in space has stimulated interest in the similar earth condition—osteoporosis, which is prevalent in older populations. Research of bone loss at the whole animal level is reported which implicates high salt diets as increasing the risk for osteoporosis. The biological process of bone formation itself has been found to be controlled by osteoblasts. Both *in vitro* and *in vivo* models were developed to investigate the molecular responses of osteoblasts to mechanical forces. Methodologies for investigation of mechanical forces used exposure to hypergravity, utilizing the Life Sciences Division's acceleration facilities.

The acceleration facilities were also utilized to obtain insights into maturation of mammalian systems while comparing the similarities with microgravity. Studies were reported with rodents to determine adaptation of physiological responses under altered gravity conditions, e.g., circadian rhythms and deep body temperature.

Bone density measurements, using computed tomography scanners, are the prime method of determining if bone formation is occurring properly. Technology development is reported which enhances the X-ray spectrum along with new and better methods for calibration of such equipment.

Simultaneously, technology development addressed miniaturization and automation of biological, analytical, and research processing, along with research efforts in bioinformatics, advanced bioimaging, and data processing. Specifically, this report relates progress on a microfluidic disc capable of automated microgravity environment assays and optical detection supporting natural and induced fluorescence. A fully automated cell culture habitat and

associated characterization of flow field velocities encountered by cellular systems in such a habitat functioning under microgravity conditions is reported. In the area of bioimaging, simulation software is reported that allows surgical procedure training on soft tissue for astronauts under microgravity conditions, including haptic feedback which will allow the user to “feel” what they are doing.

In planning future exploration beyond our planet, the physical aspects of actually living under microgravity conditions for prolonged periods was investigated. Research is reported which addresses incineration flue gas cleanup that allows use of carbon dioxide in plant growth systems along with extended in situ resource utilization of various other gases.

Though the International Space Station (ISS) will not be fully outfitted for several years, research on ISS has already begun and was supported by ARC. The Passive Dosimeter System developed by the ISS Biological Research Project, in coordination with the Hungarian Space Office, was used by a German researcher conducting experiments in the Human Research Facility. This piece of equipment is a follow-on to similar equipment flown by the Hungarians on the Mir Space Station. Simultaneous to sending hardware to ISS, ARC continued to utilize the Shuttle mid-deck for rodent experiments, and supported an experiment with the Commercial Space Center Bioserve (University of Colorado, Boulder) and the pharmaceutical company Amgen. The drug under study may provide answers to osteoporosis prevention and even act as a countermeasure for the treatment of similar effects on bones experienced by humans under microgravity conditions. This first full duration mission with mice may also pave the way to further flights with this rodent that has become a powerful research tool as transgenics.

Flow Field Measurements in a Cell Specimen Chamber

Stephen Walker, Michael Wilder

To support long-duration life science experiments on the International Space Station (ISS), cell culture units must be developed that provide the required life support environment while remaining compatible with the ISS infrastructure. The typical cell culture unit includes multiple cell specimen chambers (CSCs) in a closed loop system that provides fluids to the CSCs. An environment for controlled cell growth experiments is maintained within the individual CSCs, which are intended to accommodate diverse cell specimen types. Many of the functional requirements for cell growth experiments (e.g., feeding and gas management) depend on the fluid flow field within the CSC. A design goal of the cell culture unit is to match all environmental conditions, other than gravity, independent of whether the hardware is in microgravity (mg), normal earth gravity, or up to 2-g on the ISS centrifuge. As a first step in achieving this goal, Ames Research Center is conducting a series of investigations to establish a baseline database on the velocities and accelerations that cells currently encounter during ground-based testing in traditional Erlenmeyer flasks. In addition, the CSCs are also being tested and modeled to ensure that the fluid flow conditions found in 1-g can be replicated from microgravity up to 2-g while still supporting successful cell growth experiments. The techniques that are being used to achieve these goals include flow visualization, particle image velocimetry (PIV), and computational fluid dynamics (CFD).

To characterize laboratory cell culture conditions in current ground-based testing, PIV is being used to determine the flow field velocities and accelerations in the Erlenmeyer flasks on orbital shakers. PIV is a measurement technique that can determine instantaneous three-dimensional velocity fields in a plane.

These measured velocity fields are numerically differenced to determine the acceleration fields within a measurement plane. The data will be compared to PIV measurements in the CSCs to ensure that the flow field characteristics in the CSCs are within the bounds determined for laboratory (Erlenmeyer flask) experiments. Figure 1 shows an example of PIV results from a test using an Erlenmeyer flask on an orbital shaker. In Figure 1, the in-plane velocity data are shown as vectors, and the colored contour plot shows the magnitude of temporal accelerations calculated in the moving reference frame of the orbital shaker. Spatial accelerations, the elements of the 9-component fluid velocity shear tensor, have also been calculated using the PIV data.

Flow visualization using the injection of dye has been used to gain a global perspective of the characteristics of the CSC flow field. Using a spectrometer during flow visualization testing also yielded quantitative measurements of the mixing and flushing characteristics of the CSC flow field. Figure 2 shows a visualization of the flow field within the basic 10 milliliter (internal volume) CSC, with steady flow on both inlets. Each inlet/outlet pair established a re-circulating flow region, as indicated in Figure 2. As can be seen by the isolation of the red and blue marked streams, little mixing occurred between the two streams. Flow visualization was vital to the development of the current design of the CSC, which included the addition of magnetic stir bars to create an optimum flow field for successful cell growth experiments.

Using CFD, a detailed simulation is being developed to predict the flow field within the CSC for a wide variety of flow conditions, including

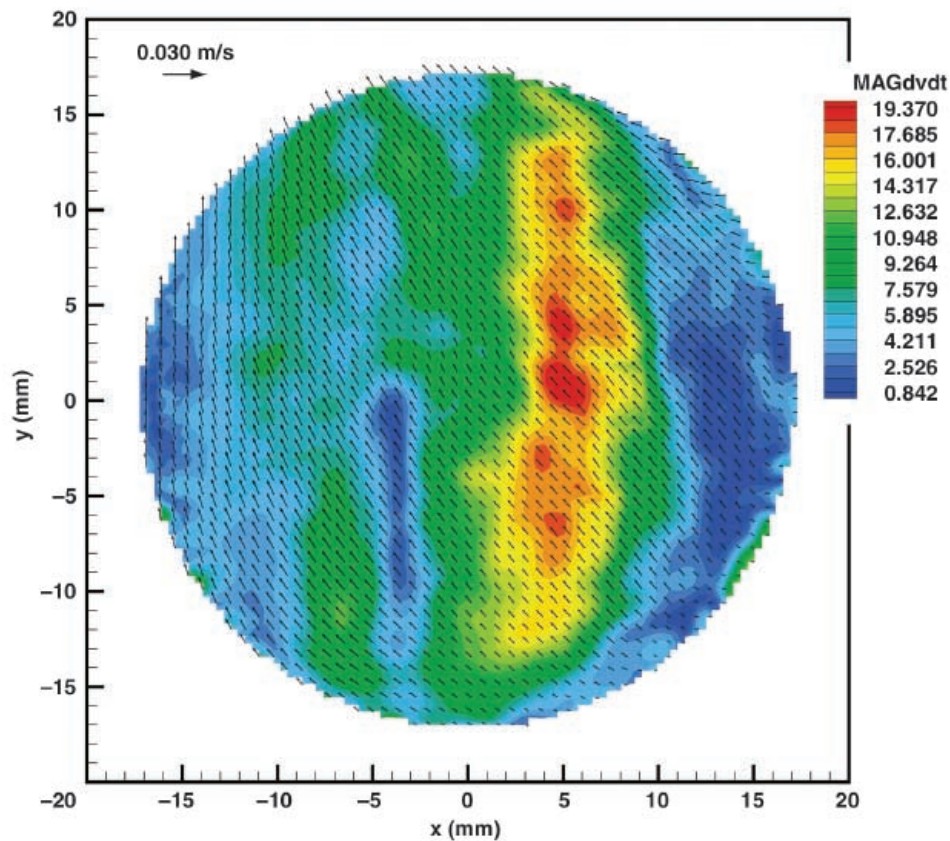


Fig. 1. Typical PIV data in an Erlenmeyer flask. Vectors indicate in-plane velocities and color contours indicate temporal accelerations in the y-direction.

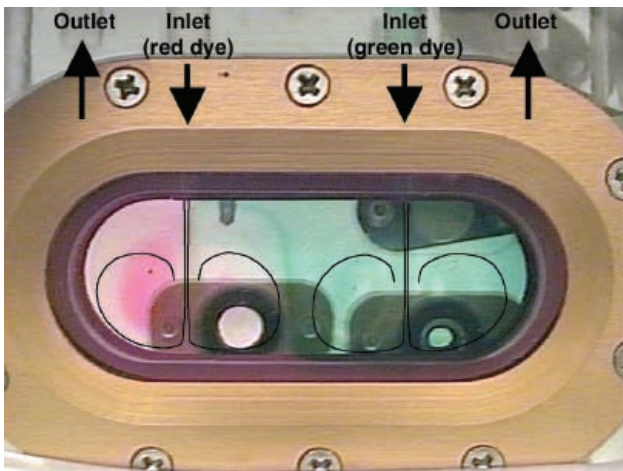


Fig. 2. Flow visualization in a 10 ml Cell Specimen Chamber.

microgravity environments. Results from all these measurements and analyses of the CSC flow environment will be used to optimize the final design of the CSC. Furthermore, based on flow field parameters such as those derived from these first-of-their-kind measurements, researchers performing cell growth experiments in the CSC will have a greater understanding of the flow field dynamics that the cells encounter. This additional knowledge will accelerate progress in the understanding of the cell growth life cycle.

Point of Contact: S. Walker
(650) 604-6720
Stephen.M.Walker@nasa.gov

International Space Station Module Noise Control

Nathan J. Burnside, Paul T. Soderman

To ensure an acceptable working and living environment for the astronauts within the International Space Station (ISS), it is critical that the acoustical noise generated by ISS science modules be held to a minimum. Because the ISS comprises reverberant, confined spaces that contain a variety of self-contained life support systems and science experiments that often house motors, cooling fans, compressors, and other equipment, the potential for excess noise is quite high. Using its extensive expertise in measuring and controlling acoustical emissions, Ames undertook a project to assess a candidate science module and to develop design guidelines for future systems.

In FY01, Ames personnel tested a generic 12-panel unit designed to house and cool a variety of biological or physical experiments. Figure 1 shows the module mounted in the anechoic chamber in preparation for free-field acoustic measurements. Sound spectra were acquired using the hemispherical sound field survey apparatus visible in the left corner of the photo. The primary noise source was a cooling fan, and the resultant noise field exceeded

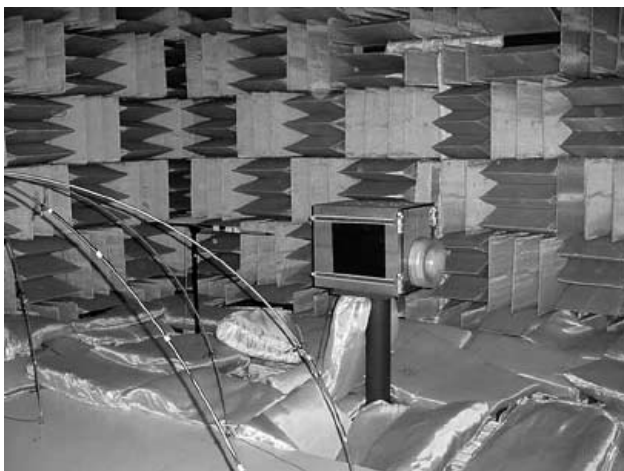


Fig. 1. Test module in anechoic chamber.

the accepted standards. Analysis of the data showed that the principal mechanism for sound energy escaping the module was through the air-exhaust stream. However, a significant amount of the noise was also transmitted through the structure. A duct muffler was designed to isolate the exhaust noise from the surrounding area. Figure 2 shows the resulting octave-band levels with the muffler installed compared to the space station express rack limits. At many frequencies, the noise was well below the acceptable level. However, at other frequencies the noise still exceeded the specified limits. Recommendations for reducing the structure-borne noise were developed and communicated to the sponsor. Furthermore, it was also apparent that the flow characteristics of the fan were not properly matched to the module being cooled. Mismatched components can create excess flow losses within the unit or fan, resulting in excess noise and reduced cooling effectiveness. Guidelines for properly integrating bio-habitat components were developed.

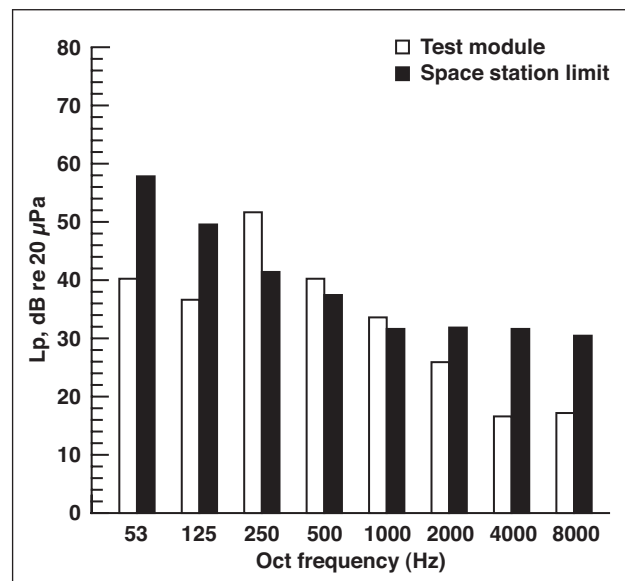


Fig. 2. Measured noise radiation and limits.

In summary, expertise in fluid dynamics and acoustics coupled with acoustic-measurement capability has been adapted for the development of low-noise ISS experiment modules. Similarly, ongoing work within the group includes the adaptation of advanced fluid-dynamics instrumentation to support the analysis and design of cell culture units for use on the ISS.

Point of Contact: P. Soderman
(650) 604-6675
Paul.T.Soderman@nasa.gov

SPRING: A Surgical Simulator Adapted to Astronaut Training for Space Life Sciences Research

Richard D. Boyle, Jeffery D. Smith

The benefits of computer-based surgical simulation have been widely recognized as broadening surgical training through scenario production and simulations of anatomical variations, pathologies, and operating environment conditions, all without actual risk to patients. However, independent efforts at combining the clinical knowledge of the surgeon and the engineering technology of the computer scientist results in many variations on a working and usable simulation system. SPRING was thus developed by Stanford University's National Biocomputation Center to provide a surgical simulation framework of shared code for use in generating working simulators at an effective level of understanding for the general public. In close collaboration with Ames Research Center (ARC), researchers have developed a real-time surgical simulation system generalized to work with numerous scientific applications. The SPRING software has also been adapted to astronaut training applications in areas of space life sciences research.

The system itself is written in C++ and is cross-platform to run on Unix and Windows platforms. As a program, it is an evolving framework for a general simulator with an emphasis on real-time performance. During its production, a number of applications have been developed to ensure that the system is usable and useful to the computer-based simulation community. For example, SPRING has the capability to use haptic devices that allow users to "feel" what they are doing in the computer simulation. In addition, the software is based on multi-user interfaces so that different computers and display systems can be linked together through the

Internet. This feature allows the simulation to be run from several different locations. Furthermore, it performs soft-tissue modeling, some limited rigid-body dynamics, and suture modeling. These are manipulated by a library of virtual tools created to interact with the tissue of interest, such as scalpels and scissors. Finally, a number of extra components, such as voice input/output, real-time texture-mapped video input, stereo and head-mounted display support, and replicated display facilities have been added to make the program expedient.

Today, astronauts have begun using the International Space Station as a permanent laboratory to address fundamental questions of the influence of microgravity on living organisms. Many of these biological experiments will require astronauts to perform complex tasks, under highly controlled conditions and within strict time constraints. Providing state-of-the-art training to astronauts for these research tasks will be of the utmost importance, maximizing the quality and quantity of data returned from these ground-breaking biology experiments in space. NASA has adapted the core capabilities of the SPRING software system to the realm of astronaut training. Scientists at ARC have developed virtual environment technologies to assist astronauts in training and performing biological procedures within the Space Station Glovebox through development of the Virtual Glovebox. By integrating advanced hardware and real-time simulation, computer vision and parallelization technologies gained in part from SPRING software, researchers can now provide a realistic immersive environment in the Virtual Glovebox (see Fig. 1).



Fig. 1. SPRING software running in the NASA Virtual Glovebox. The SPRING surgical simulator code is cross-platform and runs on Unix (Sun Solaris, SGI Irix, and Linux) and Windows (98, NT, 2000) platforms. It is written in C++ and uses OpenGL for graphics; GLUT, GLUI, and MUI for user interface; and supports parallel processing using the pthreads facility of POSIX. It allows for the relatively easy introduction of patient-specific anatomy and supports many common file formats: SMF, Wavefront OBJ, VRML, Mesh, and Cyberware formats. It performs soft-tissue modeling, some limited rigid-body dynamics, and suture modeling. The simulator interfaces to many different interaction devices and provides for multi-user, multi-instrument collaboration over the Internet in latency-dependent or latency-moderated modes. Many surgical and non-surgical virtual tools have been created and their interactions with tissue have been implemented. Collision detection is provided through an enhanced bounding-sphere algorithm. In addition, extra features such as voice input/output, real-time texture-mapped video input, stereo and head-mounted display support, and replicated display facilities are implemented. The SPRING simulator shown here is running an astronaut training application in the NASA Virtual Glovebox

This technology not only demonstrates NASA's collaborations with educational institutions that benefit the medical community, but also gives astronauts the option to practice conducting experiments in a simulated, real-time microgravity environment while still on Earth.

Point of Contact: R. Boyle
(650) 604-1099
Richard.D.Boyle@nasa.gov

Skeletal Unloading in a Salt-Sensitive Hypertension Model

Sara B. Arnaud

Genetic differences in the calcium metabolism of a small animal model for salt-sensitive human hypertension may influence the response of the bone to skeletal unloading. Dr. Thierry-Palmer (Morehouse School of Medicine, Atlanta, GA) has established differences in vitamin D status and in calcium excretion in the urine of Dahl salt-sensitive and salt-resistant hypertensive rats that appear to be gender specific. The nutritional status of vitamin D is lower in female rats with salt-sensitive hypertension than in the salt-resistant strain. Salt-sensitive females also lose more calcium in the urine when fed high salt diets than salt-resistant females. This combination of abnormalities places the Dahl salt-sensitive female fed a high salt diet at increased risk for osteoporosis and possibly osteopenia following skeletal unloading.

Before the dynamic unloading experiments, basal studies of the long bones of salt-sensitive and salt-resistant female rats fed normal diets did not reveal any differences in the mineral content or strength. Mineral content was determined by the weight of bone ash after incineration for 18 hours. Breaking strength was evaluated by the peak torque measured at torsional failure by internal rotation of the femurs with an instrument developed at NASA for testing the bones of small animals (R. Whalen and T. Cleek). After 4 weeks of skeletal unloading, femurs of salt-sensitive juvenile females fed low normal salt diets (0.3%) showed greater decreases in mineral content than salt-resistant rats. The difference was less clear in rats fed high salt diets

(2%) during exposure to a spaceflight model (Fig. 1). The decrease in femoral strength, based on our torsion test, was similar in all 4 groups (Fig. 2). The discrepancy in measures of bone composition and structure was unexpected. The salt-resistant strain of Sprague-Dawley rats were better able to maintain bone mineral content than the salt-sensitive strain. Impaired vitamin D nutrition and calcium wasting in salt-sensitive animals appears to make them more vulnerable to the osteopenia induced by simulated weightlessness.

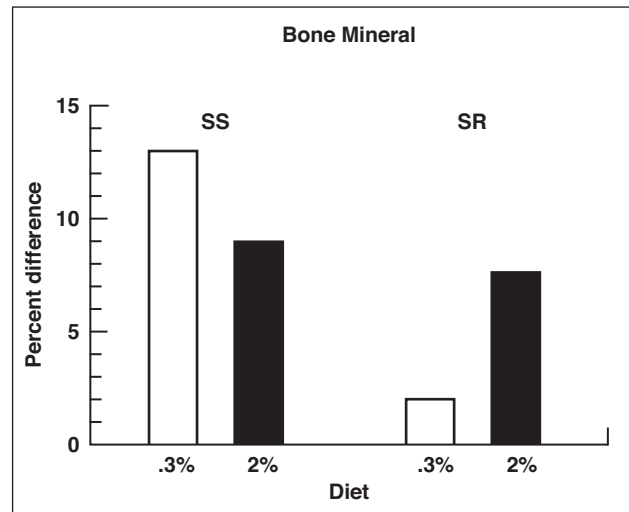


Fig. 1. Average percent differences in mineral content of femurs from juvenile female Dahl salt-sensitive (SS) and salt-resistant (SR) rats fed normal (0.3%) or high (2%) salt diets after four weeks unloading compared to loaded bones. Differences between unloaded and loaded bone measurements were significant at $p < 0.05$ level except for the mineral content in SR at both levels of dietary salt.

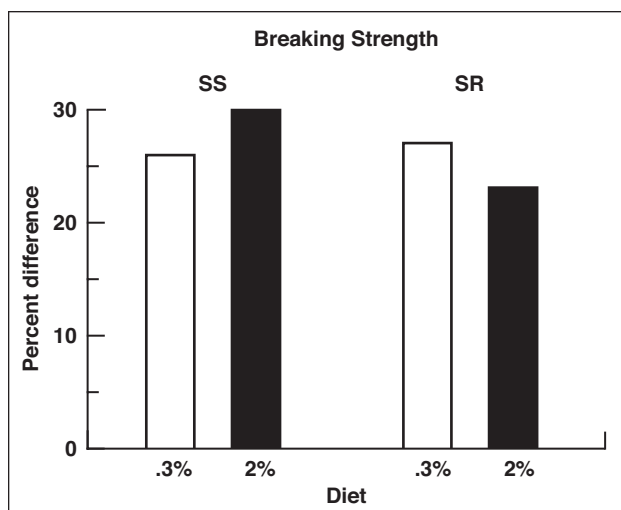


Fig. 2. Average percent differences in breaking strength of femurs from Dahl rats as described in Figure 1. The differences ($p < 0.05$) between unloaded and loaded bones were similar in all groups.

Point of Contact: S. Arnaud
(650) 604-6561
Sara.B.Arnaud@nasa.gov

Computed Tomography X-ray Beam Spectrum Estimation

Robert Whalen, Tammy Cleek, Miki Matsubara

The objective of this research project is to perfect a method for estimating the effective X-ray beam spectrum of a clinical computed tomography (CT) scanner. Ames previously patented an image processing technology that corrects an artifact of X-ray imaging known as “X-ray beam hardening.” By correcting beam hardening errors, more accurate and precise measurements of bone density throughout the interior volume of a bone are obtained. The patented error-correction technique requires that the effective beam spectrum that took the image to be corrected is known.

The X-ray source of all clinical X-ray scanners produces X-rays with a “spectrum” of photon energies, and not all X-ray sources are alike. Two spectra with slightly different shapes will produce two slightly different images of the same object. X-ray attenuation is a function of (X-ray) photon energy; lower energy photons are absorbed preferentially. The X-ray attenuation properties of a specific material

depend primarily on its physical density and chemical composition; materials with higher density and higher atomic number will attenuate X-rays more. A good example of a highly attenuating material is lead; conversely, X-rays pass right through air with little attenuation.

In order to estimate the effective beam spectrum of a CT scanner, a phantom was constructed (shown in Fig. 1), composed of five materials machined into steps of different thickness. The five materials—aluminum, teflon, polyvinyl chloride, polymethylmethacrylate, and high density polyethylene— bracket the X-ray absorption characteristics of living tissue with aluminum closest to bone tissue, and polyethylene closest to fat or bone marrow. Each of the five materials has a known physical density, known chemical composition, and therefore, known X-ray attenuation as a function of photon energy.

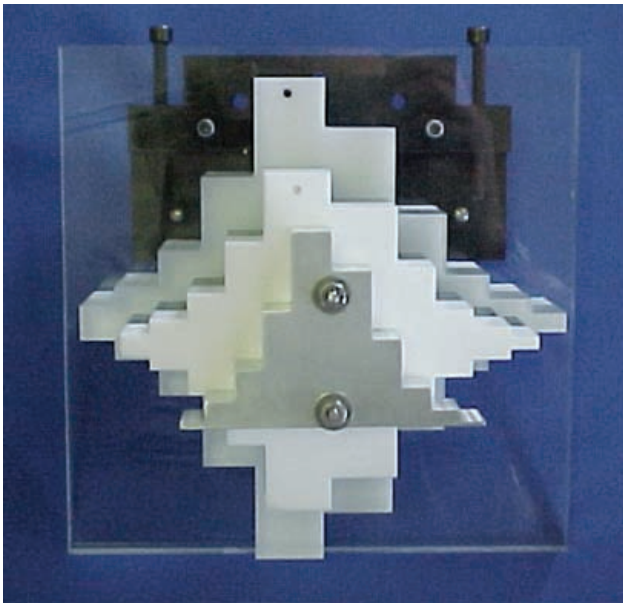


Fig. 1. Precision-machined computed tomography X-ray beam spectrum estimation phantom constructed of five materials with known X-ray attenuation properties.

The beam estimation phantom shown in Fig. 1 is mounted on the end of a CT scanner table and scanned in helical mode at three standard peak voltage settings: 80, 120 or 140 Kilo electron Volts peak (KeVp). Cross-sectional images of each of the five materials are processed to obtain the amount of X-ray attenuation caused by the beam passing through each step of each material. These attenuations, and the respective material and step thicknesses, form the experimental data set. Because the X-ray attenuation function of each of the materials is known, the X-ray attenuation through any thickness of material can also be computed analytically for any beam spectrum shape. An optimization algorithm

estimates the “best-fit” beam spectrum by iteratively altering the beam spectrum shape until the X-ray attenuation values for all materials and thicknesses, computed analytically, match the experimental data set with a minimum of error. Results for the three standard CT peak voltage settings are shown in Fig. 2.

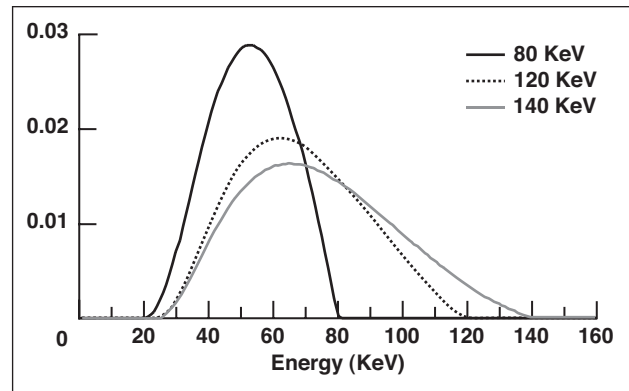


Fig. 2. Best-fit estimated effective beam spectra for 80, 120 and 140 KeV obtained from the GE CTi HiSpeed Advantage Clinical Computed Tomography scanner housed at the Stanford University Hospital (KeV: Kilo electron Volts).

In the last year, the entire procedure including scanning and image processing has been reduced from hours to minutes. The next step is the addition of more materials to the phantom in order to increase further the accuracy of measuring bone density.

Point of Contact: R. Whalen
(650) 604-3280
Robert.Whalen@nasa.gov

Accurate Measurement of Bone Density with Quantitative Computed Tomography

Robert Whalen, Tammy Cleek, Miki Matsubara, Gary Beaupré, Chye Yan

The objective of this research is to determine the accuracy and precision of measuring bone density with a new quantitative computed tomography technology. In this study, a phantom of known configuration and material composition was designed at Ames Research Center (ARC) and fabricated by QRM GmbH in Germany. This company also manufactures the European Spine Phantom, considered a “gold-standard” for cross-calibration of bone densitometry machines and imaging modalities. The phantom is composed of two materials, a water-equivalent compound and hydroxyapatite, mixed together in precise proportions. The water-equivalent material is an epoxy matrix with additives to give the composite the computed tomography (CT) imaging properties of water, the major component of human soft tissue. The other material, hydroxyapatite, is the mineral component of bone tissue.

The bone density phantom was scanned at 80, 120 and 140 Kilo electron Volts peak (KeVp) with the GE CT/i HiSpeed Advantage scanner with a beam hardening ring (polyvinyl chloride or teflon) in the image field. Figure 1(a) is a CT image of the phantom alone, and Fig. 1(b) is an image with the beam hardening ring in place. The phantom was designed to have the approximate physical size and range in bone density as a human calcaneus (heel bone), but not designed to resemble its shape. In the CT image shown in Fig. 1(a), the outer thick ring is composed of water-equivalent material, the inner 50.0 millimeter (mm) diameter, 2.0 mm thick ring is composed of 800 milligrams/cc (mg/cc) hydroxyapatite in a water-equivalent matrix. Inside the ring are five smaller solid cylinders of various mixtures of water-equivalent material and hydroxyapatite. The remaining material inside the ring is composed

of 200 mg/cc hydroxyapatite in the water-equivalent matrix. A high X-ray attenuating material (either polyvinyl chloride or teflon) was slipped over the phantom and the combination imaged with CT (see Fig. 1(b)). The purpose of the beam hardening ring was to alter the reconstructed image by introducing non-axisymmetric beam hardening as shown in the color-coded image in Fig. 1(c). In an error-free image, materials with the same composition should have the same CT number (color). Variations in color in the image indicate image artifacts caused by beam hardening.

All images were corrected using the new quantitative computed tomography beam hardening correction technology. Unlike other QCT methods, the technology does not use bone calibration standards placed in the image field. Instead, the method uses an estimate of the effective X-ray beam spectrum that produced the image in order to correct the image. Obtaining an estimate of the effective beam spectrum is the subject of another article in this report. Another important difference is the manner in which results are calculated. Since the bone density phantom is constructed of a combination of only two materials, the algorithm computes the volume fraction of hydroxyapatite and water-equivalent matrix in each voxel. The color-coded corrected image is shown in Fig. 1(d).

The error in computed volume fraction of hydroxyapatite was relatively insensitive to beam hardening ring material, hydroxyapatite concentration, and scan voltage setting (80, 120 and 140 KeVp). Therefore, the relative error in measuring hydroxyapatite volume fraction was higher for the lower concentrations. The improvement in accuracy following correction is shown in Figs. 2(a) and 2(b). Figure 2(a)

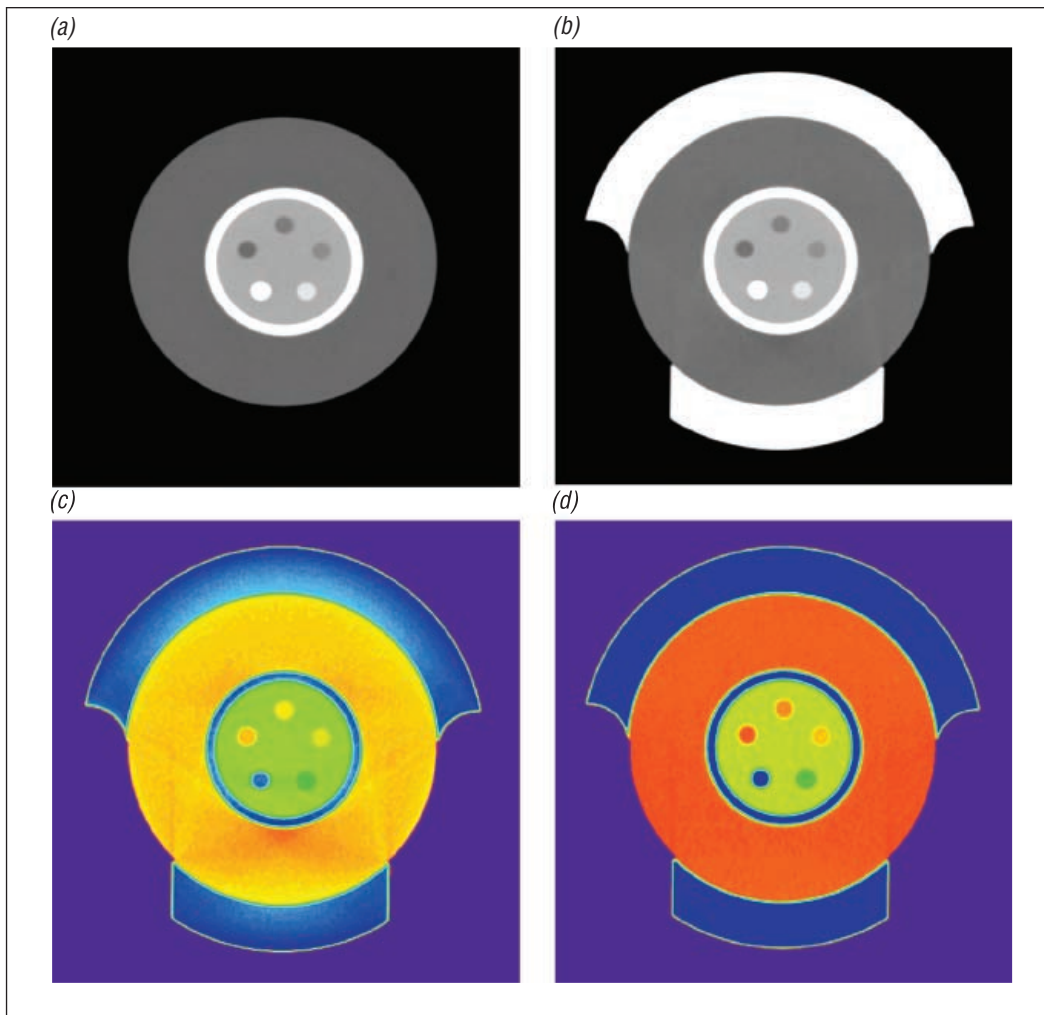


Fig. 1(a)-1(d). Computed tomography (CT) images of a bone density phantom with and without an outer beam hardening ring. (a) CT image of the bone density phantom (QRM GmbH, Germany) composed of mixtures of water-equivalent matrix and hydroxyapatite. Five inner solid cylinders: 0, 50, 100, 400 and 800 mg/cc hydroxyapatite; inner ring: 800 mg/cc hydroxyapatite. (b) CT image of the phantom with an outer beam hardening ring. (c) Uncorrected color-coded CT image showing significant errors in CT number. (d) Beam-hardening-corrected image. Each material composition now has a single color dependent on the X-ray attenuation characteristics of the material. Colors range from orange (low attenuation water-equivalent) to deep blue (800 mg/cc hydroxyapatite in the phantom and the beam hardening ring).

plots uncorrected values for the CT number for each volume fraction (concentration) of hydroxyapatite for each of the three scan voltage settings. Note that the CT number depends on the voltage setting and whether the phantom was scanned alone or with one of the beam hardening rings. Once the image

is corrected (Fig. 2(b)), the scanning conditions no longer affect the results. In addition, the measured value is close to the “true” value. It is believed that these results can be improved upon by refining the estimate of the effective X-ray beam spectrum. This is a current research task.

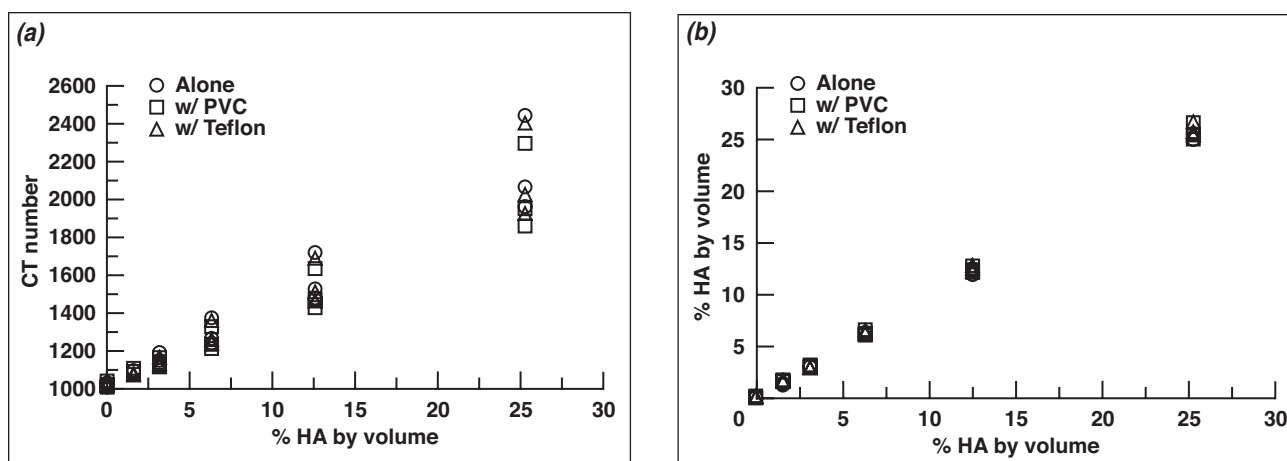


Fig. 2(a)-2(b). Plots of accuracy in measuring hydroxyapatite (HA) volume fraction (concentration) with uncorrected 2(a) and corrected 2(b) images for the following scan conditions: without a beam hardening ring (alone); with polyvinyl chloride (PVC) ring; and with a teflon ring. Each condition was scanned at 80, 120 and 140 KeVp. 2(a) The CT number for each volume fraction of hydroxyapatite is highly dependent on the scan condition. 2(b) The measured volume fraction is close to the "true" value and highly independent of the scan conditions.

Point of Contact: R. Whalen

(650) 604-3280

Robert.Whalen@nasa.gov

Mechanical and Gravitational Loading of Osteoblasts

Nancy D. Searby, Ruth K. Globus

Mechanical forces, generated by gravity, weight-bearing, and muscle contraction, play a key role in the genesis and maintenance of skeletal structures. Astronauts exposed to prolonged spaceflight suffer from bone loss, which has been shown in growing rats to result from reduced bone formation by osteoblasts. It is not understood at a molecular level how mechanical forces regulate cells, although some signals are transmitted along a network of proteins that extend from the proteinaceous matrix residing outside the cell (extracellular matrix) via cell membrane receptors (integrins) to intracellular polymeric arrays (cytoskeleton). The long-term goal of the research program is to understand at a molecular level how mechanical forces, such as those generated by weight bearing and gravity, regulate osteoblasts. The specific research objectives are to (1) establish

and characterize both *in vitro* and *in vivo* models for determining the effects of gravity and mechanical strain on osteoblasts; (2) identify components in the extracellular matrix/integrin/cytoskeleton network which are crucial for the proliferation, differentiation, and survival of osteoblasts; (3) determine specific cellular responses to changes in mechanical load; and (4) identify molecular mechanisms that mediate cellular responses to mechanical loads.

Two approaches were employed to establish useful *in vitro* models for investigating the molecular responses of osteoblasts to mechanical forces. One approach involves determining the response of cultured osteoblasts to a mechanical stimulus that mimics the forces generated during weight-bearing. To this end, a novel loading apparatus was used

to apply physiologic levels of mechanical strain by deforming the growth substrate of live cultured osteoblasts during real-time confocal microscope imaging (see Fig. 1). Experiments investigating cell shape changes resulting from application and release of a single step uniaxial tensile load revealed that osteoblast shape, known to influence gene expression, changed slowly upon application of loading, but quickly upon release of loading. A second way to evaluate the responses of osteoblasts to mechanical forces is to expose cells to hypergravity by centrifugation. Using the Ames

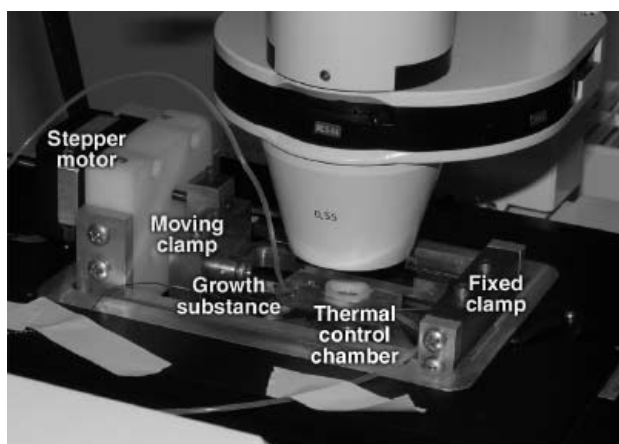


Fig. 1. Loading system.

Research Center One Foot Diameter Centrifuge (see Fig. 2), experimental studies investigated whether hypergravity induces osteoblast cytoskeleton and overall shape changes, and whether the paracrine signaling factor prostaglandin E2 (PGE₂) increases as observed with other types of mechanical stimulation. Centrifugation of cultured osteoblasts led to increased PGE₂ production, minor morphological changes in the microtubule network architecture, and reduced microtubule network height. Additional experimental studies determined that the responses depended on the maturity of the osteoblasts, the orientation of the gravity vector, the magnitude of the hypergravity stimulus, and the duration of hypergravity exposure.

To evaluate the physiologic role of integrins in response to mechanical loads *in vivo*, studies were performed using transgenic mice exposed to altered weight bearing (hind-limb unloading). These transgenic mice were genetically engineered to express a dominant negative form of the beta 1 integrin subunit in osteoblasts. It was found that as the transgenic mice age, the animal's body mass and bone size and mass is greater than in wild-type controls.



(a)



(b)

Fig. 2. One-foot diameter centrifuge. (a) Centrifuge with adjacent control incubator. (b) Close-up of centrifuge rotor.

Thus, signals from the beta 1 integrin within osteoblasts appear to influence overall metabolism. Furthermore, hindlimb unloading caused deficits in bone mass both in transgenic and wild-type mice, suggesting that the skeletal effects of disuse are not affected by a disruption of beta 1 integrin signaling in osteoblasts.

Point of Contact: N. Searby
(650) 604-6794
Nancy.D.Searby@nasa.gov

Molecular and Cellular Characterization of a Mitotic Checkpoint Gene during Zebrafish Development: Implications for the Responses to Space Radiation and Human Breast Cancer

Gregory Conway

A major goal of the NASA mission is understanding biological responses to the space environment. Space imposes two conditions quite different from terrestrial life: lack of gravity and increased radiation exposure. The Conway laboratory, in collaboration with another laboratory (also at Ames Research Center), has discovered a gene that monitors radiation damage in cells and ultimately allows damaged cells to repair themselves. The human gene has also been found by others to be amplified in aggressive breast tumors. Thus this research not only addresses a critical NASA mission, but also has important implications for human health here on Earth.

The zebrafish is used as a model organism (Fig. 1) in the laboratory. The zebrafish possesses most of the major organ systems and tissue types found in humans. The development of the zebrafish is almost identical to human development, with the advantageous exception that a single cell develops into a complete fish in only two days. The precocious development, clear transparent embryos, prodigious reproductive capacity (each female lays 300 eggs per day), transgenic capabilities, and gene knockout



Fig. 1. The adult zebrafish is approximately one inch long and found at most pet stores. In the background is a male, and in the foreground a female.

technologies make this organism an ideal system for developmental studies. Also, the entire zebrafish genome is being sequenced and all the genes of the zebrafish will be known by October 2002.

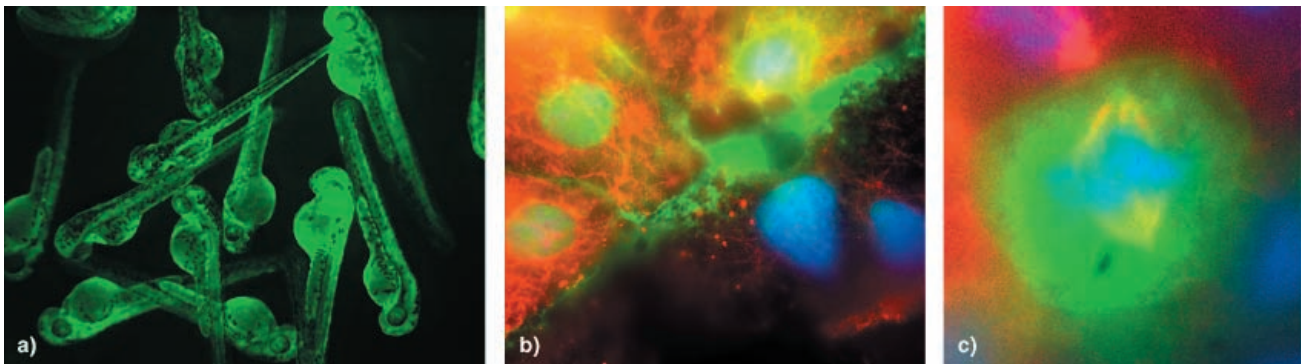
A general strategy used in the laboratory is to knockout a gene in the zebrafish by injecting a specific gene inactivator (called a morpholino). Embryos are then examined for any developmental defects. If development is affected, it can be con-

firmed that the defect is caused by specific gene inactivation by replacing the gene in morpholino-treated embryos and looking for developmental rescue. This “knockout-replacement” strategy is a powerful technique, since the rescuing gene can be modified prior to injection so that functionally important parts of the gene can be identified. Portions of the gene can be deleted (called a splice and dice experiment), regions thought to be important changed (called a wreck and check), or portions of other genes fused with the gene of interest (called a cut and paste experiment). Also, the replacement gene can be fused or joined to a gene that encodes a green fluorescent protein (GFP). This fused gene combination will produce a chimeric protein with one end that fluoresces. By viewing embryos and cells with fluorescence, the location of the gene of interest can be determined in the whole animal (Fig. 2(a)), at the level of individual cells (Fig. 2(b)), or even at the subcellular level (Fig. 2(c)).

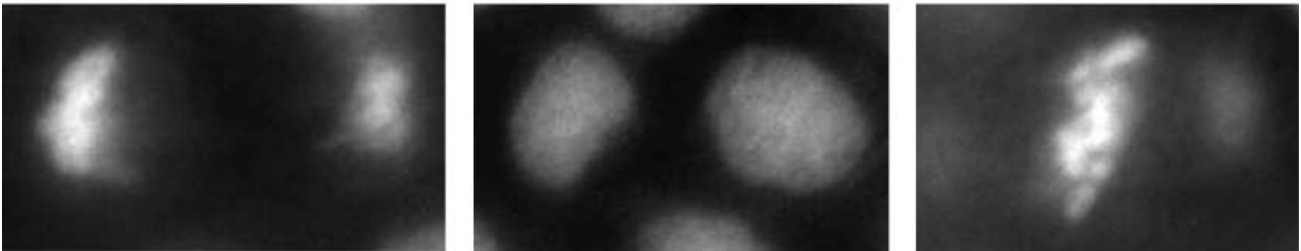
Using molecular techniques, a gene (G12) has been identified that is robustly activated during early development. Using the knockout-replacement strategy described above, it was found that the G12 gene is required for the cells of embryos to accurately progress through mitosis (cell division). In the absence of this gene, chromosomes often fail to separate and segregate to daughter cells, a defect called nondisjunction. When this happens, mitosis continues leading to dumbbell shaped cells with two nuclei connected by a thin bridge (Fig. 2(d)). When G12 is replaced, aberrant mitosis is not observed. Nondisjunction is a hallmark of DNA damage, and in normal cells when DNA damage occurs, mitosis is arrested by a specific group of proteins called checkpoint proteins. During mitotic arrest damage is corrected and mitosis then resumes, or if the DNA damage is too severe the cells undergo a self-destruction/death program called apoptosis. Dumb-

bell shaped cells are normally never observed in cells with intact checkpoints. Injection of the G12 gene fused to GFP indicates that this gene is localized to the cellular machinery (the mitotic spindle) that separates chromosomes (Fig. 2(c)). This localization agrees with the defects that are seen when it is inactivated. It makes sense that a component of the chromosomal separating machinery would lead to aberrant chromosomal separation when inactivated.

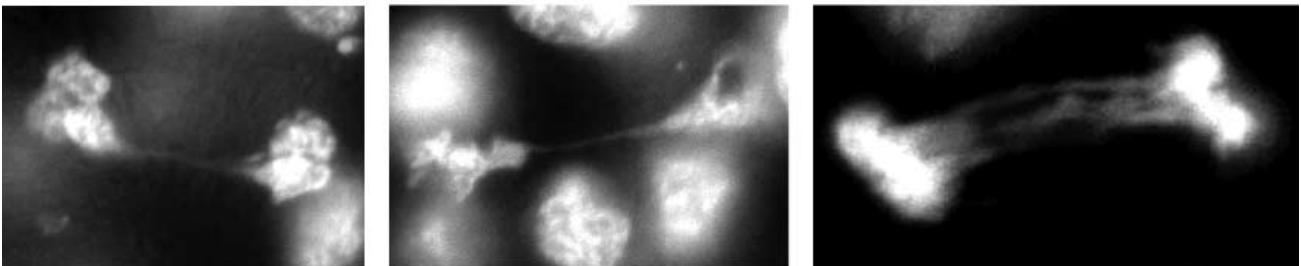
Many checkpoint genes are found to be duplicated in human tumors. At first it would seem paradoxical that a gene whose function is to insure faithful cell duplication would be amplified in tumors. However, it has been found that when genes like this are amplified, the amplified copies are usually not functional and often act as oligomers with themselves. Amplified “bad copies” inactivate the good genes when they associate with one another. G12 acts as a dimer and we hypothesize that the amplified copies found in aggressive breast tumors are inactive. This hypothesis will be investigated with clinician colleagues using tumors removed from human patients. It will be interesting to see if the number of copies of this gene correlate with tumor aggressiveness and metastatic potential and to see if amplified copies contain inactivating mutations. Amplification of this abnormal gene would allow cell division even in the presence of chromosomal abnormalities, creating further damage and mutation leading to especially deadly cancer. This gene is a potential drug target for breast cancer therapies. With regard to the NASA mission, the importance of this gene in the cellular and organismal response to radiation is obvious. Understanding the cellular machinery required for radiation resistance will lead to countermeasures that enable long-term space-flight in high radiation flux. This project is an excellent example of NASA mission-relevant research benefiting human life on Earth.



Normal cell division



Cell division in the absence of G12



d)

Fig. 2. The G12 protein expressed as a fluorescent fusion product with a green fluorescent protein (GFP) is indicated by the green color. The distribution of G12 can be viewed in the whole animal a), at the level of individual cells b), or at the subcellular level c). In figure c), the G12 protein is indicated by yellow as well as green color. Chromosomes are shown in blue color. Notice in figure C the yellow G12 containing structures in the cell attached to the blue chromosomes in the middle of the cell. These yellow G12 containing structures are spindle poles and will ultimately separate the blue chromosomes to the daughter cells that arise from this dividing cell. In figure d), chromosomes have been stained and appear white. In normal cells, well defined groups of chromosomes or cell nuclei are seen. When G12 is eliminated chromosomes fail to completely separate to daughter cells, and strands of chromosomes can be seen connecting daughter nuclei.

Point of Contact: G. Conway
(650) 604-3595
Gregory.Conway@nasa.gov

Cell Culture Unit Development for the International Space Station

Nancy D. Searby, Donald P. Vandendriesche

The Cell Culture Unit (CCU) is being developed by Payload Systems Inc. (PSI) to support basic research onboard the International Space Station using animal, plant and microbial cells, small swimming aquatic cells, and small tissues. The hardware development effort during FY01 has focused on completion of the first hardware item, the Science Evaluation Unit (SEU), which is used to demonstrate the feasibility of supporting the required science in the hardware. The SEU hardware is built, engineering testing is complete, and science testing is currently in progress. One of the three SEUs in the program was delivered to Ames Research Center (ARC), and it has been used by the ARC consultant to test and validate SEU hardware performance with yeast cells. The SEU is shown in Fig. 1(a), and a schematic of one perfusion loop is shown in Fig. 1(b).

Testing has focused on accommodating a diverse array of candidate cell types, of which each challenges the hardware in a different way. To date

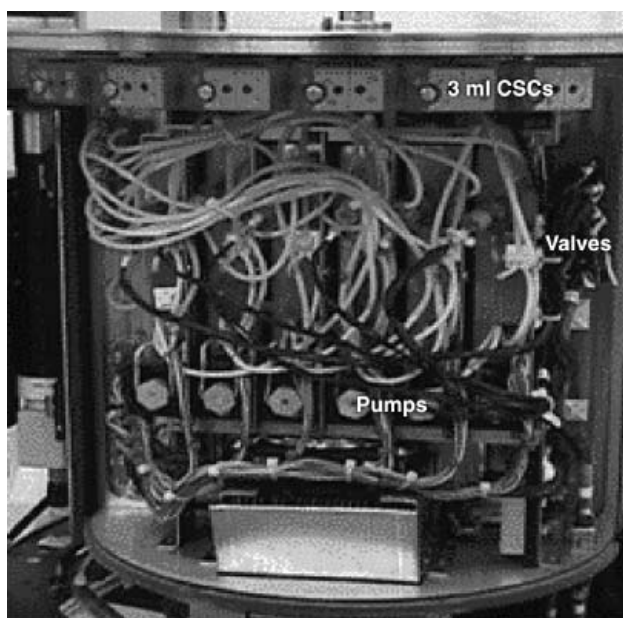


Fig. 1(a). Science Evaluation Unit.

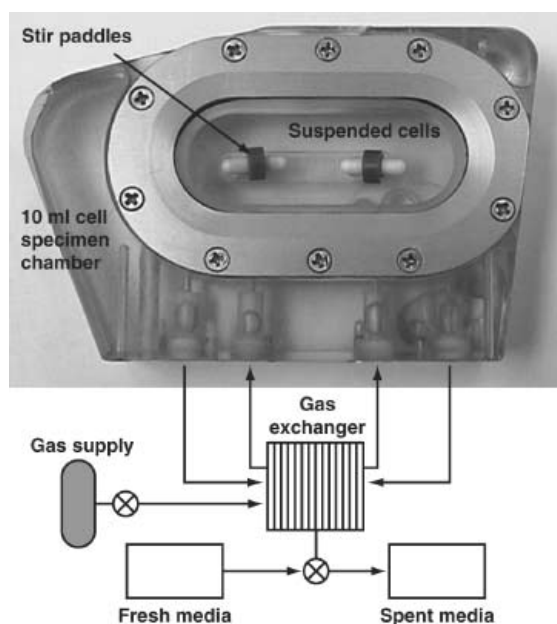


Fig. 1(b). Schematic of Cell Culture Unit Perfusion Loop.

science testing with the SEU at the contractor's facility has included yeast, tobacco BY2, and C2C12 muscle myoblast cells. Success criteria have been established for each cell type and the results of each test in the SEU are compared to standard lab controls that are maintained concurrent with the SEU test. The parameters established as success criteria for yeast are viability, proliferation, suspension, morphology, and genetic stability. Samples of cells and media are taken from the Cell Specimen Chambers (CSC)s in the SEU at predetermined time points and are compared to the shaker flask controls. Tests are also performed to detect for cell escape from the CSC, where the cells are maintained within the SEU, and to measure pH, the partial pressure of oxygen, and the partial pressure of carbon dioxide in the media. The success criteria for yeast were successfully demonstrated in SEU tests performed both at the contractor's facility and at ARC. Figure 1(c) shows a photo of yeast taken using the Video Microscopy System (VMS) in the SEU. Testing has

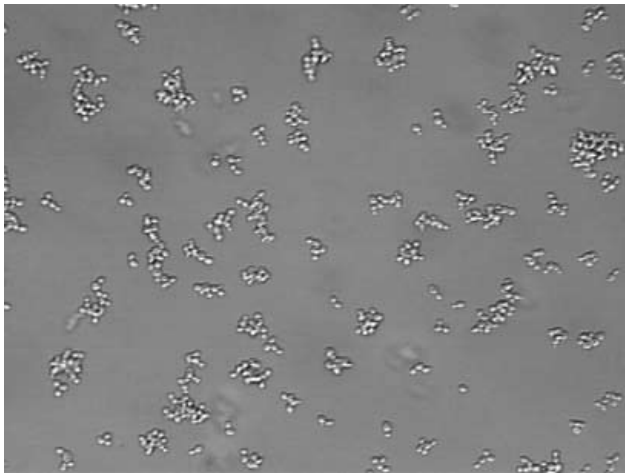


Fig. 1(c). Yeast cell image taken with SEU Video Microscopy System.

progressed well with tobacco BY2 cells and C2C12 muscle monolayer cells in the SEU, and future tests are planned to demonstrate all of the success criteria for each of these cell types.

A collaborative effort is underway between ARC, PSI, and NASA Glenn Research Center (GRC) to optimize the flow environment within the CSC to meet the following complex and even conflicting requirements: to provide uniform gas and nutrient exchange, to maintain cell suspension, and to control hydrodynamic stresses acting on the adherent or suspended cultures. ARC and PSI performed flow visualization studies using primarily the 10 milliliter volume (10 ml) CSC to characterize the nominal flow environment within the CSC, and then this data was used to define flow parameters for the different cell types experiments. ARC is performing Particle Image Velocimetry with both the 10 ml CSC and a laboratory shaker flask to quantify the actual magnitude of the hydrodynamic forces that the cells would be exposed to in these two different environments. The forces generated by the flow field that cells encounter within the CSC will be compared to the shaker flask to ensure that they are within the bounds of typical laboratory experiments. ARC and GRC are using computational fluid dynamics (CFD)

to study the flow environment around the cell in the CSC. Using CFD, a detailed model of the CSC has been developed to predict the flow field within the CSC for a wide variety of flow conditions. CFD can be used to predict the microgravity fluid flow environment in the CSC prior to any microgravity tests. Because the CCU will be placed on a centrifuge onboard the International Space Station, and will be subjected to hypergravity up to twice Earth's gravity (or 2-g), ARC has performed a 2-g single loop, fluid flow visualization test using the ARC Hypergravity Facility for Cell Culture. The data from the 1-g and 2-g flow visualization tests will be used for comparison to validate the CFD model, and to ensure that the flow regimes are adequate at both g-levels.

In parallel with the SEU hardware development and science testing efforts, the flight design has progressed. Figure 2 illustrates the latest flight design concept. Lessons learned as a result of SEU testing are being folded into the flight design. Prototypes of key subsystems of the flight design, including the Video Microscopy System, Automated Sampling

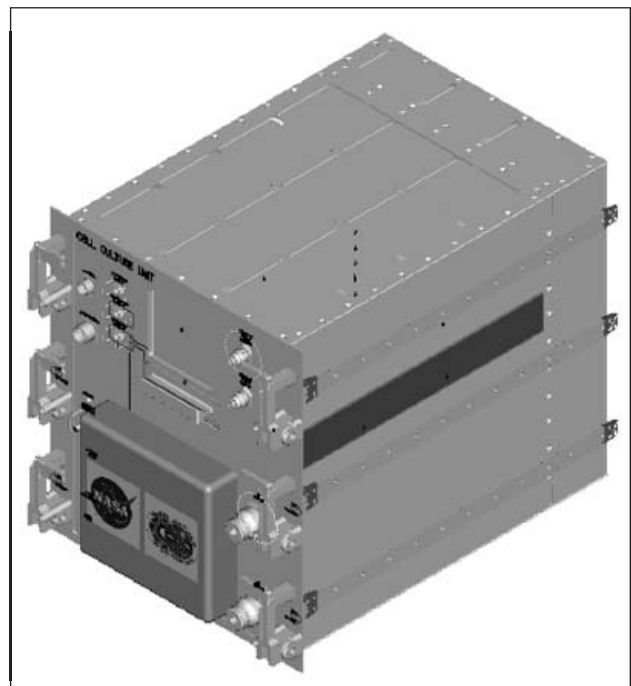


Fig. 2. Cell Culture Unit Flight Design Concept.

Module, and Cell Lighting Module have been designed, built, and tested. The effort for the flight design has focused on packaging of all the components into a standard International Subrack Interface Standards 12 Panel Unit drawer. A thermal model has been built and tested to characterize the thermal environment of the CCU. The actual test data will be used to validate the analytical model used for the flight design. Extensive long term stability testing

has been performed with both the microelectrode and commercial glass electrode pH sensors. Planning is in progress for a critical design review for the flight design in 2003.

Point of Contact: N. Searby
(650) 604-6794
Nancy.D.Searby@nasa.gov

Tissue-Level and Whole Animal Responses to Altered Gravity

Catharine A. Conley

The evolutionary development and cell biology of members of the Tropomodulin (Tmod) family of actin-filament capping proteins is the major focus of this laboratory. The Tmods make up a small well-conserved protein family, the members of which show no significant sequence similarity to other known proteins. Functionally, every member tested of the Tmod family is able to bind at least some tropomyosin isoforms in *in vitro* assays as well as *in vivo*, and displays capping activity at the slow-growing 'pointed' end of pure or coated actin filaments. The Tmods are the only proteins known to display these biochemical functions together, and until recently, were the only proteins known to cap actin filaments at the slow-growing ends. Structurally, the Tmods are divided in two subfamilies, the ~40 kilo Daltons (kD) tropomodulins and the 60-70 kD leiomodins (Lmods). Four 40 kD Tmod isoforms have been found in vertebrates, and all four isoforms are conserved between rats, mice, and humans; to date, some but not all of these isoforms have been identified in birds, amphibians, and fish. Two (of three) additional Lmod isoforms have been identified that are conserved between rats, mice, and humans. Only one Tmod isoform of 40 kD has been found in *Drosophila*, and two in *C. elegans*, while no significant similarity has been shown between any Tmod isoform and plant or fungal proteins, sug-

gesting that this family represents an animal-specific lineage. All family members contain an ~180 amino-acid region thought to be involved in actin capping that makes up the carboxy-terminal half of the 40 kD Tmods and is centrally located in the Lmods, as well as an amino-terminal 50-100 amino acid (aa) region that is involved in binding tropomyosin. Understanding the function of Tmods and Lmods at the cellular and biochemical levels, and deducing their folded structures using both experimental and computational approaches, are areas of active research in the laboratory.

Specific Tmod and Lmod isoforms are expressed in a developmentally-regulated and tissue-specific manner in mammals. The function of some Tmod isoforms appears to be essential *in vivo*, based both on work from other laboratories using transgenic mice, and a close linkage of Tmod1 with a human familial cardiomyopathy. Other Tmod family members are potentially involved in disease states, as well. The Lmod1 isoform, also known as SM-Lmod because it is predominantly expressed specifically in smooth muscle, was originally identified as a potential autoantigen in Graves' disease. I previously demonstrated that this protein is expressed in a subset of extraocular muscle fibers as well as smooth muscle, research that is continuing in the

lab. Some Tmod isoforms display altered expression under conditions of muscle atrophy, an area of interest to NASA due to concerns for astronaut health.

The other major research activity is more directly related to NASA's interest in Astrobiology: microarray analysis is being used to determine the effects of spaceflight, simulated hypergravity, and other mechanical stimulation conditions, on gene expression in two model systems: rat tissues, in collaboration with Affymetrix in Sunnyvale, and *C. elegans*, in collaboration with Stuart Kim at Stanford.

Preliminary results from these studies suggest that fewer than 100 genes display significantly altered expression levels in each system. *C. elegans* treated by centrifugation at 10xG for 4 days displayed statistically significant alterations in the expres-

sion of structural proteins and cell-surface signal receptors, as well as genes of unknown function. By comparing centrifugation with other types of mechanical stimulation, we expect to identify components of mechanosensory pathways, including possibly 'weight-detector' systems. In the future, the opportunity to perform spaceflight experiments with *C. elegans* is anticipated, which could provide additional insight into these responses. Because centrifugation of *C. elegans* is a common laboratory procedure, this research has the potential for rather broad relevance.

Point of Contact: C. Conley
(650) 604-0234
Catharine.A.Conley@nasa.gov

Insertional Mutagenesis Screen for Otic and Other Genes in *Xenopus Tropicalis*

Marcela Torrejon, Sigrid Reinsch

Sensitivity to gravity is essential for spatial orientation. Consequently, the gravity receptor system is one of the phylogenetically oldest sensory systems, and the special adaptations that enhance sensitivity to gravity are highly conserved. The vestibular apparatus of humans and other vertebrates is combined with the auditory apparatus. Since the sensory epithelia of both vestibular and auditory structures of all vertebrates share a common basic tissue architecture of hair cells and supporting cells, genes that are identified that have a role in generating these structures in one vertebrate are relevant to studies of human sensory epithelial defects.

A transgenic approach is used in the frog, *Xenopus tropicalis*, to identify genes expressed during vestibular/auditory and neural development. A transgenic animal is one that is engineered to carry a for-

eign gene, or "transgene," as part of its own genetic material. These animals are very useful for discovering new genes and for determining or confirming the function of genes. The transgene that is being used is a jellyfish gene called "green fluorescent protein" (GFP). Cells that express GFP are green under fluorescent light. The GFP gene is randomly inserted into the *Xenopus* sperm chromosomes in a test tube. When the sperm are united with the egg, the resulting embryos now have the transgene. The GFP gene can be inserted anywhere in the sperm DNA; where it is inserted determines the organ in which it is expressed. In some cases the GFP transgene will insert in a gene that is active during ear development. When this happens, the tadpoles (frog embryos) will have green ears that allow easy identification of these animals. The normal function of the gene into which the GFP transgene is inserted may be disrupted causing abnormal (mutant) ear

development. This is called insertional mutagenesis. Such mutants will help us understand the normal function of the genes during ear development.

Using these mutant frogs, we will clone and identify the mutated genes (and subsequently the normal genes). The GFP transgene sequence not only creates a tag for visual screening of mutant animals, but also creates a tag for cloning the mutated otic gene. This tagging process is referred to as a gene-trap.

Stable GFP-expressing lines carrying transgenes expressed in the otic regions and other tissues are being generated. To date we have identified and are characterizing animals with insertions in genes expressed in ear, kidney, central nervous system,

eye, muscle and epithelia. Figure 1 shows a typical transgenic tadpole with GFP expression in the developing nervous system. Once transgenic tadpoles are identified, these founders are pooled, raised to adulthood, and outbred to establish the lines.

Results of these investigations will provide essential knowledge of specific genes involved in development as well as mutant lines that can be used for future studies of the specific function of the genes identified through this screen. These studies will lead to a better understanding of the molecular mechanisms involved in vestibular and auditory development and function, and could lead to the identification of genes that are clinically significant in diseases affecting the vestibular and auditory apparatus in humans.

Collaborators on this project include Elba Serano (New Mexico State University, Las Cruces), Richard Boyle (Ames Research Center), Robert Grainger (University of Virginia), and Enrique Amaya (Wellcome/CRC Cambridge University).

Point of Contact: S. Reinsch
(650) 604-3093
Sigrid.Reinsch@nasa.gov

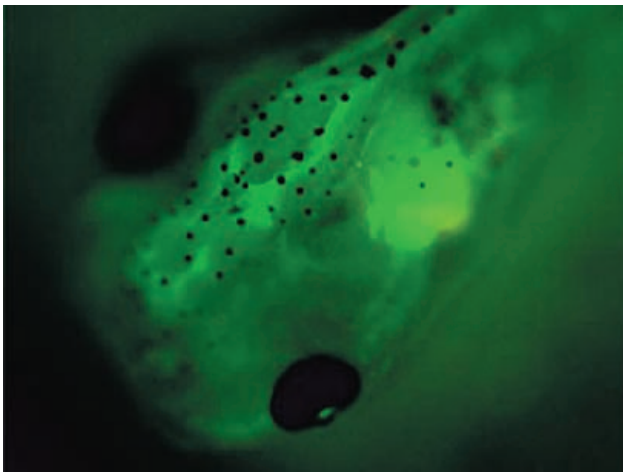


Fig. 1. A typical transgenic tadpole with green fluorescent protein (GFP) expression in the developing nervous system.

Toward the First Mammalian Birth in Space: Insights Derived from Hypergravity

April E. Ronca, Lisa A. Baer, Charles E. Wade

The objective of this research is to advance the understanding of how the universal mammalian processes of pregnancy, birth, and offspring development are influenced by gravity. In mammals, nurturance by the mother is of considerable importance to the survival, growth, and development of young mammals. Our laboratory and others have reported that, throughout birth and lactation, characteristic maternal caretaking patterns give rise to important neural and physiological changes that promote healthy infant development and well-being. Maternal care in mammals evolved under the constant force of the Earth's 1-g gravitational field. It is therefore reasonable to predict that the maternal-offspring relationship is modified when gravity is changed. Beginning at birth, rat mothers typically lick and handle their young, retrieve and group them, and crouch over them to provide warmth and sustenance. In the early phases of lactation, mothers retain their pups within the nest, helping to maintain their pups' body temperatures and providing nearly constant access to her nipples. One can envision that, in either hypo- (reduced) or hyper- (increased) gravity, dams may be impeded from adequately maneuvering their pups and maintaining close

proximity to them. Dams may encounter further difficulty removing their pups' amniotic membranes at birth, an action that is essential for clearing the nares and onset of respiratory gas exchange. Retrieving behavior, important for maintaining close proximity between mothers and offspring during nursing, may be of limited effectiveness in the weightless environment of space; pups, once retrieved, may simply float away. Specific maternal processes related to nursing and lactation, e.g., mammary metabolism, are also affected by exposure to altered gravity. Fluctuations in the mother's endocrine status or changes in sensory characteristics of newborns may interfere with the onset and maintenance of maternal care. These considerations raise numerous possibilities for disruptions of maternal-offspring relations during spaceflight and centrifugation.

Research on mammalian reproduction and development in space has progressed slowly. Over the last 20 years, only six spaceflight missions have carried pregnant and lactating rat dams and their litters into low-earth orbit; one of these flights carried pregnant mice (Table 1).

Table 1. Comprehensive list of spaceflight missions carrying mammalian mothers and offspring.

Year	Flight	Dur (days)	Age at Launch [‡]
1982	COSMOS - 1514	4.5	G13
1994	NIH.Rodent (R)1 (STS-66)	11	G9
1995	NIH.R2 (STS-70)	9	G11
1996	NIH.R3 (STS-72)	8	P5, P8, P15
1998	NEUROLAB (STS-90) [†]	16	P8, P15

[‡] G = Gestational age (G1 = sperm positive; G22/23 = term); P = Postnatal age (P0 = day of birth)

[†]Both nursing rat litters and pregnant mice (*Mus musculus*) were flown this mission.

These studies of mammalian pregnancy and prenatal development revealed many commonalities between animals flown in space and those observed on Earth. Pregnant rat dams flown in space during the latter half of gestation for periods ranging from 4.5 to 11 days (Cosmos-1514, NIH.R1, and NIH.R2) gave birth to well-formed, live offspring upon recovery. A study of labor and birth in the NIH.R1 and NIH.R2 dams revealed no effects on the overall duration of parturition or the temporal patterning of individual births; however, flight dams had twice as many labor contractions relative to ground controls. Changes in connexin proteins that form gap junctions within the near term myometrium may underlie the changes in contractile activity. Postnatally, the dams treatment of newborn pups (measured by pup-directed licking, handling, and retrieving) was unchanged. Flight mothers showed evidence of lactation and nursing. Together, these studies show that mammalian pregnancy and prenatal development of offspring can proceed within the microgravity of space.

No mammal has yet been given the opportunity to give birth in space. This is due, in part, to results reported for nursing rat litters flown in space. In contrast to the positive results reported for fetuses developed in space, postnatal mortality and poor growth was observed among the youngest litters flown on the NIH.R3 and Neurolab flights. The losses of the young animals may have been caused by the mother's inability to keep free-floating pups gathered within the nest. The functional coherence of the litter and close proximity of mother and young help foster important maternal behaviors that keep the pups warm and nourished. Together, spaceflight studies of mother rats and their offspring that have been conducted to date reveal much about the abilities and limitations of the maternal-offspring system to adapt to microgravity. Spaceflight during the second half of pregnancy did not disrupt the ability of rat mothers to undergo birth or to care for their young after they were returned to Earth. In contrast, spaceflight beginning at five days of

postnatal age had negative effects on the neonate's survival. This finding raises questions about whether rats can successfully give birth and maintain their young in space.

In recent studies, we have begun to lay the groundwork for space studies on these early developmental phases by studying the behavior of pregnant and lactating rat mothers and their pups in hypergravity. The first goal was to establish a well-grounded experimental paradigm for studying rodent development during centrifugation. To facilitate comparisons with existing flight data, pregnant rats were exposed to centrifugation beginning on G11 of the rats 22-day gestation period, the timetable followed for the NIH.R2 spaceflight experiment. A modest gravity level of 1.5-g was selected which enabled us to maximize neonatal survival while producing detectable hypergravity effects in the neonates. Comparisons were made among hypergravity-exposed (HG), stationary yoked control (SYC), rotational control (RC) and Vivarium (VIV) groups with dams weight-matched across conditions. Following centrifugation onset, HG dams showed an immediate decline in body mass averaging 8-15% less than those of SYC dams. Food intake and water intake (adjusted per 100g dam body mass) were also reduced in HG relative to SYC dams during the first three days of centrifugation but not thereafter. Behavioral activity of the HG and SYC dams encoded from timelapse video (12:1 tape:playback ratio) during centrifugation revealed that HG dams were consistently less active (an average of 25% across the first four days) than SYC dams. Together, the findings indicate that adaptation of pregnant rats to hypergravity is similar to that exhibited by non-reproducing adult animals.

After nine days of centrifugation, late pregnant (G20 and G21) SYC dams reduced their previous levels of activity, but HG dams failed to do so. The increased activity of HG dams during late pregnancy led us to examine specific behaviors of the dams during this period. The amounts of time

spent feeding, drinking, and self-grooming were comparable in the HG and SYC dams, regardless of circadian cycle. In contrast, the late pregnant HG dams spent three times more time engaged in nest-building behavior in preparation for impending birth.

This latter observation suggested that changes in patterns of maternal care might play an important role in neonatal outcome during hypergravity exposure. Next, the hypothesis that maternal reproductive experience determines neonatal outcome following gestation and birth under hypergravity conditions was tested. Primigravid (first pregnancy) and bigravid (second pregnancy) female rats were exposed to 1.5-g centrifugation from G11 through birth and the first postnatal week. On the day of birth, litter sizes were identical across gravity and parity conditions although significantly fewer live neonates were observed among hypergravity-reared litters born to primigravid dams as compared to bigravid dams (82% and 94%, respectively; 1.0-g controls, 99%). Within the hypergravity groups, neonatal mortality was comparable across parity conditions from the first to the seventh postnatal day at which time litter sizes stabilized. These results indicate that prior pregnancy and birth can ameliorate neonatal losses in hypergravity during the first 24 hrs after birth, but not on subsequent days.

In seeking to explain the neonatal losses in hypergravity, postpartum maternal behavior of the HG and SYC dams was compared. Similar to the results of the spaceflight studies, there were no observable changes in the mothers' behavior during birth. The behavior of primigravid HG mothers differed from that of the other conditions in that these dams tended to disrupt nursing bouts and the nesting litter by frequently digging and rearranging the pups. This pattern was highly correlated with neonatal mortality ($R^2 = 0.99$, $N = 4$ litters; $p < 0.02$). The data suggest that during the period around the time of birth, the maternal-offspring system is

particularly sensitive to relatively modest (0.5-g) increments in the Earth's gravitational field. In the present study, we have identified maternal reproductive experience as a major determinant of postpartum survival in hypergravity. The newborn rat is profoundly vulnerable to changes in the Earth's gravitational field, in part through changes in the mother's behavior.

These studies emphasize issues pertinent to mammalian pregnancy and development spanning the gravity continuum from hypo- to hypergravity. Comparisons are summarized in Fig. 1, which illustrates survival rates of prenatal and postnatal rats at 0-g (top), 1.5-g (middle), and 2.0-g (bottom). The 0-g data represent a compilation of 10- to 16-day spaceflights of rats of differing ages (NIH.R1, NIH.R2, NIH.R3 and Neurolab [NL]; see Table 1). The 1.5-g data and 2.0-g data are redrawn from centrifugation studies of developing rats that were 8 to 32 or more days longer in duration.

Where data are available, spaceflight and centrifugation studies of developing rats share common outcomes. Exposure to either hypo- or hypergravity during the second half of pregnancy does not interrupt prenatal development. In contrast, survival of neonates (during the first postnatal week) appears to be compromised under both conditions. In the case of hypergravity, the early postnatal hours are most sensitive; comparable data are not available from spaceflight. Survival of rats greater than one week of age at the time of initial exposure to either spaceflight or centrifugation is excellent. Importantly, these results do not imply that all physiological and behavioral systems of the offspring were intact and properly functioning or that their development was unaffected by exposure to altered gravity. The findings indicate that hypergravity exposure disrupts patterns of nursing in rats, thereby impairing pup survival and well-being. The considerations discussed herein identify an important need for additional detailed and systematic studies of al-

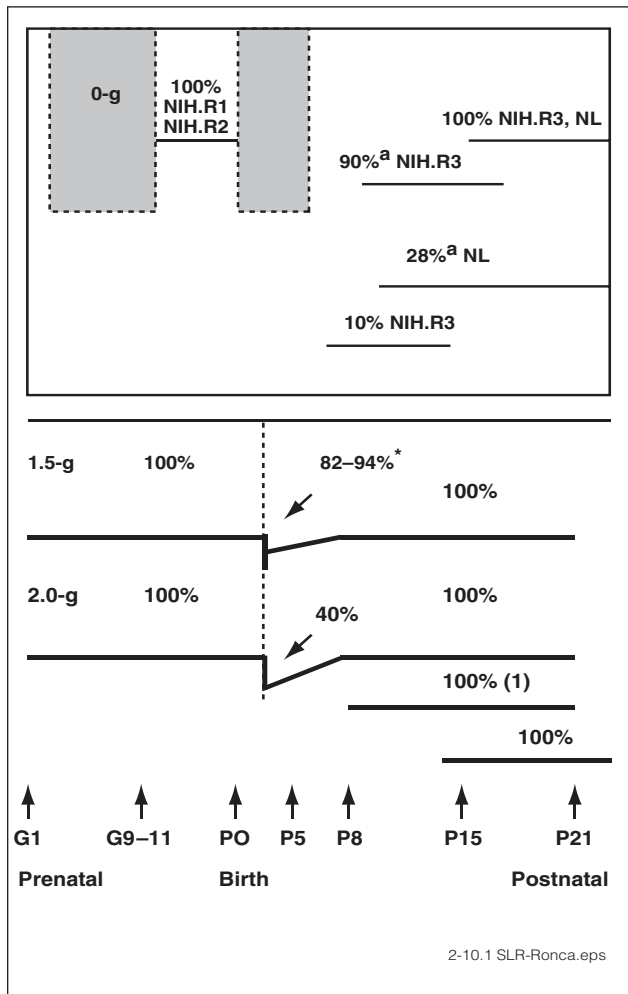


Fig. 1. Summary of spaceflight (upper bars) and centrifugation (lower bars) studies of prenatal and postnatal rats. Values represent offspring survival rates at developmental phases spanning from gestation to weaning. (G = Gestational day; P = Postnatal day). The shaded area depicts the absence of spaceflight data corresponding to early pregnancy and the perinatal period. Rats that were either P8 (NIH.R3) or P9 at launch (NL) were maintained in two different types of flight housing. *The lower survival rate shown corresponds to primigravid dams; the higher survival rate corresponds to bigravid dams.

tered gravity effects on maternal-offspring relations, particularly around the time of birth. The role of maternal factors cannot be underestimated in studies through which we seek to understand formative roles of gravity in reproduction and development. These kinds of studies promise to yield important insights into how gravity shapes the earliest phases of life in mammals.

Point of Contact: A. Ronca
(650) 604-2644
April.E.Ronca@nasa.gov

Chronic Acceleration (Hypergravity) Influences the Circadian System of the Rat

Charles W. DeRoshia, Daniel C. Holley, Margaret M. Moran, Charles E. Wade

This study was conducted to evaluate the adaptation response of rat deep body temperature (DBT) and locomotor activity (LMA) circadian rhythms to acute hypergravity onset and chronic hypergravity exposure. This study was performed on the 24-foot-diameter centrifuge in the Center for Gravitational Biology Research at Ames Research Center, with 24 white rats randomly assigned to stationary control (1.0 G) and 1.5 G and 2.0 G hypergravity groups. DBT and LMA data were recorded digitally by telemetry at 5 minute intervals. Lights were on a 12:12 hour light (45 lux):dark cycle with lights on at 06:00 a.m. Following a three day baseline data collection phase, in which the centrifuge was stationary, the animals were exposed to the chronic centrifuge environment for 14 days.

Figure 1 shows that centrifugation onset resulted in a dramatic acute decrease (hypothermia) in rat DBT (-1.4, -2.4, -3.1 degrees C for the 1.25, 1.5 and 2.0 G groups, respectively), along with visually evident disruption of the rhythmic waveform with reduced rhythm amplitude for several cycles. LMA was suppressed (Figure 1) for the duration of centrifugation (-26.9% (1.25 G), -44.5% (1.5 G), and -63.1% (2.0 G), for days 12-14 relative to the baseline stationary phase. Internal DBT-LMA rhythm phase synchronization was significantly disrupted at hypergravity onset and took 2.6, 3.0, and 4.5 days in the 1.25, 1.5, and 2 G groups, respectively, to return to baseline levels. Certain circadian rhythm metrics (DBT cross correlation, LMA mean and amplitude) did not readapt by day 14 but did stabilize by 8.6 days. This indicates that these rhythm metrics stabilized to new steady state levels. In general, circadian rhythmic amplitude took longer to readapt and stabilize than circadian phase (peak times).

Circadian rhythm splitting was identified as the dissociation of a single circadian rhythm into two statistically significant peaks in the circadian periodicity range of 16-45 hours. Rhythm splitting occurrences increased from 3 of 7 (DBT) and 1 of 7 (LMA) rats at 1.25 G to 6 of 8 (DBT and LMA) rats at 2 G. Circadian rhythm splitting in one rat is illustrated in Figure 2, where periodicity analysis shows that about two days after the onset of hypergravity the DBT rhythm period (24.1 hrs) shortened and then dissociated into two separate rhythm components, which progressively diverged to 34.1 hrs and 19.0 hrs, respectively, then converged and fused into a single circadian rhythm. The LMA rhythm (Fig. 2) shows a more complex pattern, with progressive period lengthening (free-running rhythms), rhythm splitting, and arrhythmia interspersed.

This study shows (a) hypergravity dose-dependent decreases in both core body temperature and gross locomotor activity, (b) a dose-dependent relationship between hypergravity level and duration of readaptation and stabilization, and (c) the first to show circadian rhythm splitting induced by hypergravity exposure. Circadian rhythmicity in the rat is profoundly disrupted by exposure to hypergravity. This may be the consequence of circadian phase shifts induced by hypergravity onset, emotional fear in response to the unanticipated environmental changes, or attenuation of light/dark cycle entrainment. The results of this study have implications for humans exposed to gravitational load transitions in the space microgravity environment, since the potential induction of hypothermia and circadian rhythm disruption may have significant deleterious effects upon cognitive performance and sleep quality in space.

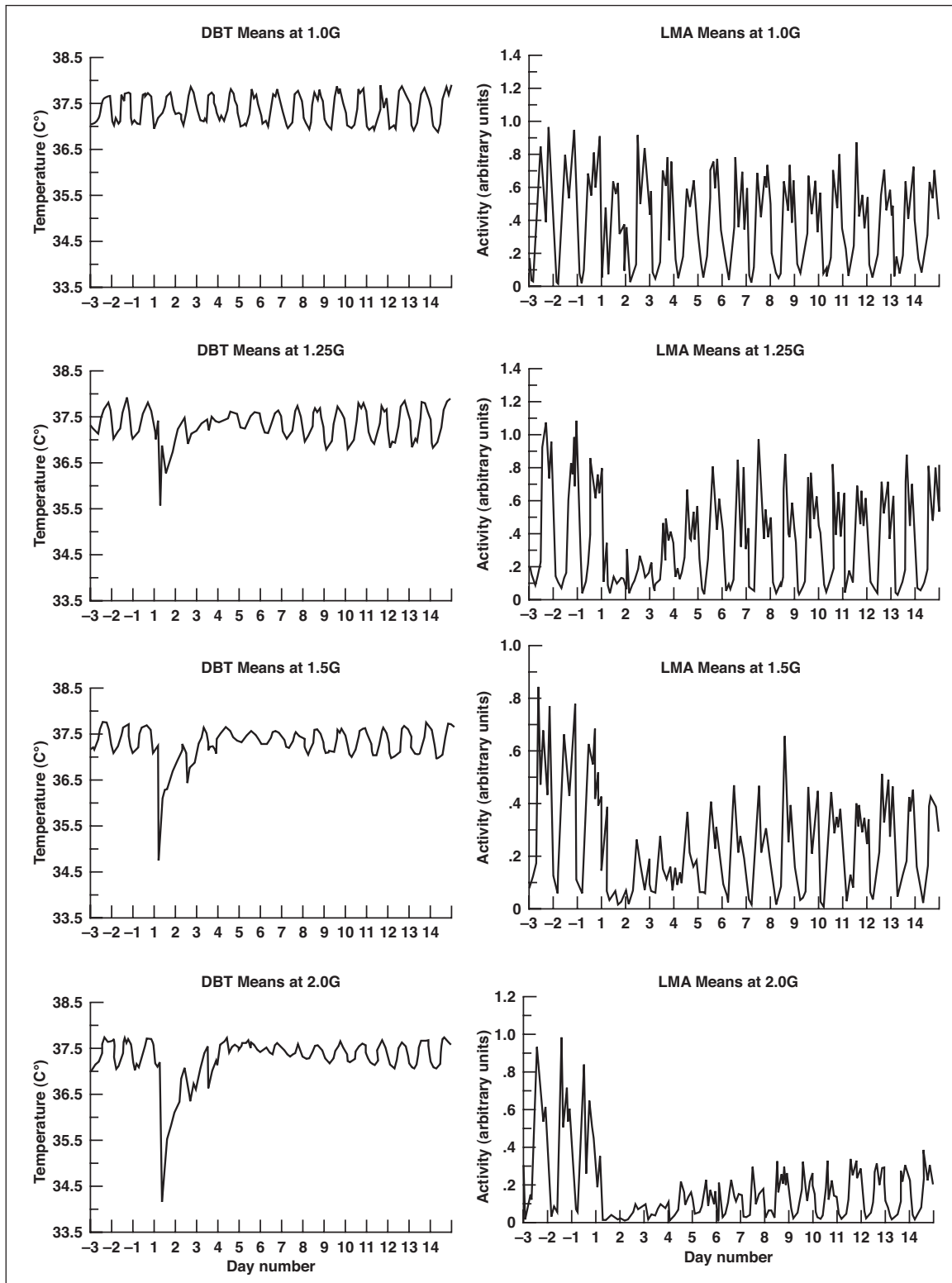


Fig. 1. Deep body temperature (DBT) and locomotor activity (LMA) circadian rhythms (30 min means) in white rats (means across 7-8 animals) during stationary baseline (days -3 to -1) and hypergravity (days +1 to +14).

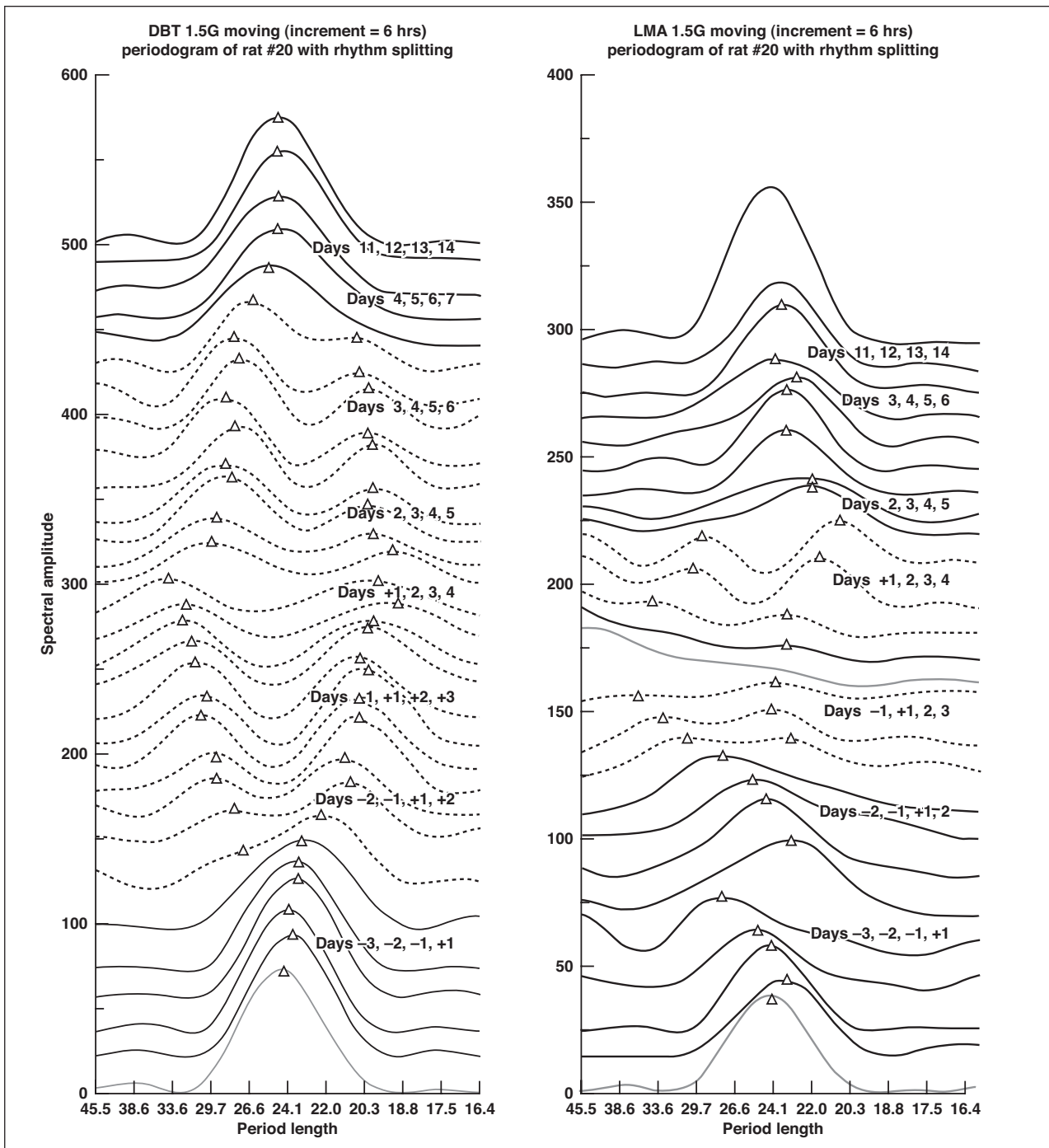


Fig. 2. Moving periodograms for DBT and LMA circadian rhythms during stationary baseline (days -3 to -1) and hypergravity (days +1 to +14), showing the splitting of the circadian rhythm into two components (marked by triangles) in rat #20 at 1.5 G. Periodogram spectra were computed on 4-day data sets incremented at 6-hr intervals.

Point of Contact: C. DeRoshia
(650) 604-5456
Charles.W.DeRoshia@nasa.gov

Atmospheric Resources for Exploration of MARS

John Finn, Dave Affleck, Lila Mulloth

The atmosphere of Mars has many of the ingredients needed to support human exploration missions. It can be “mined” and processed to produce oxygen and buffer gas for breathing (used to dilute oxygen). With lightweight hydrogen transported from Earth, or using water found in local deposits as a hydrogen source, storable methane rocket fuel can also be produced. The use of local materials, called ISRU (for *in situ* resource utilization), is an essential strategy for a long-term human presence on Mars from the standpoints of self-sufficiency, safety, and cost. It is a key cost-reduction element of NASA’s Strategic Plan.

The atmosphere of Mars is roughly 95% carbon dioxide, 3% nitrogen, and 2% argon. There are also trace amounts of other gases. Carbon dioxide is the resource for oxygen, and also provides the carbon that can be used in methane production. The production of these gases will likely dominate any early Mars manufacturing plant because of the quantity of materials needed to return samples or humans to orbit or to Earth. However, it is important to recognize that buffer gas also represents a considerable launch mass, estimated on the order of two to three tons for a human mission (mainly due to airlock activity). With the proper selection of gas acquisition and processing technology, a more optimal ISRU plant can be designed that will provide all these resources with minimal mass and power consumption.

For example, carbon dioxide must be acquired from the Mars atmosphere, and purified and pressurized in order to be useful in a propellant production plant. Buffer gas is a potential by-product of the purification process. Ames Research Center developed a process whereby the small amount of nitrogen and argon present in the atmosphere is efficiently separated from the carbon dioxide during an adsorption

compression process (see fig. 1). Carbon dioxide adsorbs in the first bed, while nitrogen and argon pass through and are collected in a separate adsorption bed. When the first bed is heated, carbon dioxide is driven off at elevated pressure. Similarly, the nitrogen and argon are driven off at pressure when the second bed is heated. Such temperature-swing adsorption compression and separation processes are highly efficient and are expected to work well on the cold Martian surface. Being virtually solid-state, they do not suffer the wear and reliability problems associated with operating mechanical pumps in that hostile environment.

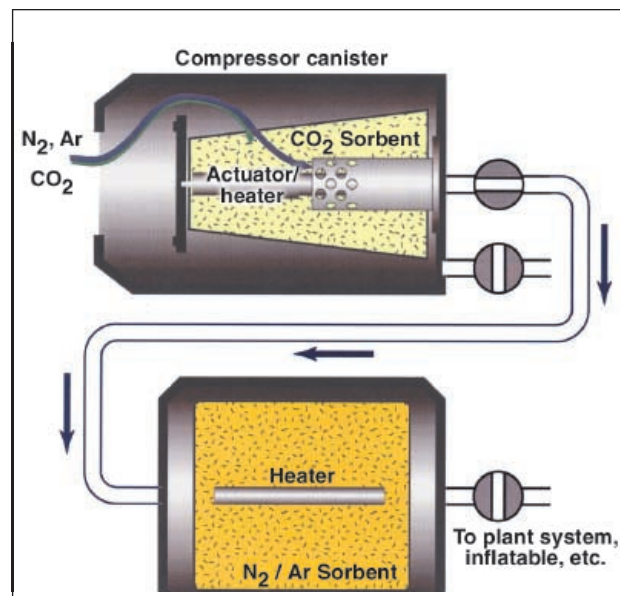


Fig. 1. Flow diagram of an adsorption-based CO₂ compression and N₂-Ar separation device for the Mars atmosphere.

Point of Contact: J. Finn
(605) 604-1028
jfinn@mail.arc.nasa.gov

Rotating-Disk Analytical System (R-DAS)

Michael Flynn, Bruce Borchers

One of the main limitations in increasing the scientific return from fundamental biology and life sciences experiments onboard the International Space Station (ISS) is the inability to conduct a variety of biological and analytical assays in flight. The Rotating-Disk Analytical System (R-DAS) is an automated analytical/cell culture laboratory that has been developed as a biotech and chemical analytical instrument for use on ISS and other spaceflight platforms. R-DAS uses a microfluidics rotating disk and predetermined spinning profiles to accomplish complex fluid management tasks. Analysis is accomplished through the use of a custom optical imaging system. The instrument can conduct a wide range of protocols in orbit with onboard 1-g and micro-g controls without the need for the ISS centrifuge.

The system has a variety of unique design features such as automated microgravity environment assays and optical detection schemes which support natural and induced fluorescence. It is capable of conducting calorimetric, spectral, and image analysis and will provide in-flight 1-g control studies without the need for the ISS centrifuge. It uses sealed and disposable sample disks which are pre-configured with all necessary reagents. The use of centrifugal force to control fluid flow minimizes acceleration velocities and shear forces, and creates an environment which is insensitive to two-phase microgravity flow restrictions, thereby simplifying sample preparation and introduction procedures.

The system is designed to fit into a double mid-deck locker (1/4 Space Station rack). It is designed to remain on orbit with only the disks being transported back and forth to orbit. A disk storage/holding system will be provided in order to allow for multiple disks processing. Operational protocols can be written on CD disks and experimental results can be re-written on the CD disks.

Ames Research Center has recently completed a rapid system prototype development effort that has resulted in the development of the prototype R-DAS system. The prototype is shown in figure 1. This system is fully automated and uses a single microfluidic disk (single assay) with six parallel flow paths. The disk is shown in figure 2. A fluorescent microscope is incorporated into the design in order to image samples and to provide complete image analysis. The system is portable, having dimensions of only 8 in. x 20 in. x 20 in. The prototype was completed on January 1, 2002, and is currently being validated against standard laboratory protocols. In order to provide a first demonstration assay, a unique microfluidic disk was fabricated using the Molecular Probes Live/Dead stain assay. Live/Dead Bacterial Viability Kit stains are based



Fig. 1. R-DAS Instrument.



Fig. 2. R-DAS Microfluidic Disk.

on the use of SYTO 9 green fluorescent nucleic acid stain and the propidium iodide red-fluorescent stain. Live/Dead kits are also available for animal cells and yeast assays, both of which will work in the existing R-DAS disk system.

Initial test results from the prototype system Live/Dead assay are encouraging. In addition, the system design is such that R-DAS is readily adaptable to a variety of other assays/disks being evaluated. With further development, R-DAS promises to usher in previously unavailable biological laboratory analysis capability onboard ISS and other future space-flight platforms.

Point of Contact: M. Flynn
(650) 604-1163
Michael.Flynn-1@nasa.gov

Clean Incineration for Space Missions

John W. Fisher, Suresh Pisharody

One of the research objectives at Ames Research Center (ARC) is the development of solid waste processing technologies for long duration exploration missions. A major part of this research effort entails the recovery of resources from life support wastes, such as the recovery of carbon dioxide and water from waste biomass via incineration. Carbon dioxide and water can be used as part of a regenerative life support system to grow plants for food. One of the central problems associated with incineration is the production of undesirable or toxic byproducts of combustion. ARC has developed an incineration flue gas cleanup system that allows use of the carbon dioxide in a plant growth system, and allows release of the remainder of the clean flue gas back to the crew cabin.

As space missions increase in duration, there will be an increased need to transition from life support systems using stored life support materials to life support systems using recycled life support materials. For instance, for short duration missions food can be stored; however, for missions lasting several years, food will need to be provided from a number of possible sources. One viable source is a plant growth chamber. Growing food in space will require recycling waste materials for the raw materials necessary for plant growth: carbon dioxide, water, and nutrients. Incineration offers a method of converting waste materials such as inedible biomass (the part of a plant that can not be eaten) back into carbon dioxide, water, and nutrients (ash).

The process of combustion of biomass in an incinerator operates in a way similar to the combustion of wood in a fireplace—the biomass is almost completely oxidized to gaseous carbon dioxide and water vapor, and only a small residue of inorganic substances (ash) is left. Even in the best of combustors, however, some unoxidized material remains, and toxic byproducts and/or contaminants such as nitrogen and sulfur oxides are formed.

In recent years, research at ARC has focused on developing methods to eliminate the undesirable combustion byproducts. One approach has been to use reductive catalytic systems to convert the nitrogen and sulfur oxides to nitrogen and elemental sulfur, innocuous materials at room temperature. Oxidative catalysts can then oxidize the remaining hydrocarbon contaminants to very low levels. In collaboration with outside university and corporate organizations, an integrated incineration system has been developed and tested that utilizes a fluidized-bed combustor followed by a catalytic cleanup system. In the past year, this system has demonstrated the ability to burn inedible biomass and produce a very clean exit flue gas. The concentration of contaminants in the gas exiting the incinerator is generally less than a few parts per million. Except for the carbon dioxide, which is toxic to humans at high concentrations, the exit stream from the incinerator is able to meet the Space Maximum Allowable Contaminant (SMAC) standards for clean air in a spacecraft.

A second research effort at ARC is investigating the use of waste material to prepare the flue gas cleanup system. A pyrolytic process converts inedible biomass to char, and the char is then converted to activated carbon. The activated carbon is used to remove contaminants such as nitrogen oxide and sulfur dioxide from the incinerator flue gas by adsorption followed by chemical reaction with the carbon. The contaminants are thus converted to innocuous nitrogen gas and elemental sulfur. In the past year, the process of producing activated carbon from wheat straw has been demonstrated, and the activated carbon produced from wheat straw has been used to reduce the concentration of nitrogen oxides in incinerator flue gas from 300 ppm (parts per million) to less than 1 ppm. This meets the SMAC limits within the crew cabin.

With the development of energy efficient, optimized incineration and flue gas cleanup systems, NASA will have the technology necessary to “close the loop” on carbon. Ultimately, carbon will move within the system from plant to person and/or incinerator and back to the plant without ever becoming a stored waste, achieving a significant milestone in the development of advanced life support systems which approach self-sufficiency.

Point of Contact: J. Fisher
(650) 604-4440
jfisher@mail.arc.nasa.gov

SLO SCIENCE PAYLOADS OPERATIONS

Cooperative Approach to Commercial Biomedical Testing in Space

Beverly Girten

One important way to develop effective strategies and products that may help prevent or attenuate some of the physiological changes that take place in astronauts during spaceflight missions is to complete preclinical tests with potential countermeasures in space. The first Commercial Biomedical Testing Module (CBTM-01) experiment successfully flew on the STS-108 mission on the space shuttle Endeavour in December, 2001. This experiment was a collaborative effort between Amgen Inc., BioServe Space Technologies, Marshall Space Flight Center (MSFC), and Ames Research Center (ARC) (Life Sciences Division), as well as several other organizations that participated in secondary science opportunities. This joint venture marked the first time that flight hardware developed at ARC was used for a commercial-sponsored flight experiment that was manifested through the Office of Space Products Development at MSFC. BioServe is one of the nonprofit NASA-sponsored Commercial Space Centers and is located at the University of Colorado. BioServe coordinated the experiment with the commercial sponsor, Amgen, to study the effects of microgravity on bone loss in mice, and to test a new pharmacological agent to determine how effective the new Amgen product might be as a countermeasure for this type of microgravity-induced change.

The main scientific objective of this payload was to examine the effectiveness of the new Amgen pharmacological agent called osteoprotegerin (OPG) on decreasing bone density loss during spaceflight. The primary bone experiments were led by Principal Investigator, Dr. Paul Kostenuik, from Amgen. Initial results from some of the bone analyses suggest that

OPG was effective as a countermeasure. Additional analyses on bone changes and other parameters are in progress, and more complete information on results from this flight experiment are expected to be submitted for publication in 2002.

This joint effort could serve as an important model for future collaborative efforts involving commercial payload opportunities. The roles for ARC during this payload included provision of the flight and ground hardware, operational support preflight, during flight and post-flight, and crew training. The ARC project and operational support was provided by staff from both NASA and Lockheed Martin. Hardware that was provided included the NASA-developed Animal Enclosure Modules (AEMs) (see figure 1), which have flown over 20 times, as well as some additional ARC hardware to control payload noise level and to help ensure welfare of the

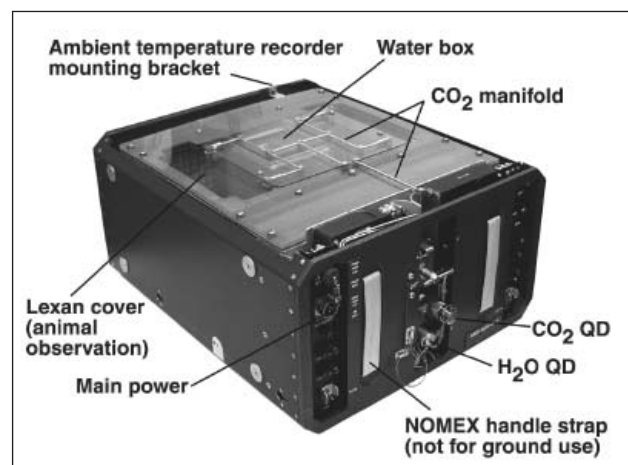


Fig. 1. Animal Enclosure Module (AEM). Hardware provided by Ames Research Center to support the CBTM-01 experiment on STS-108.

experimental animals. This payload was the first full duration mission where mice were flown in space in AEMs, and there were a number of important observations made concerning differences between housing mice versus rats in these modules (figure 2). ARC was a major player in preflight ground-based odor/filter tests (conducted by Monell Chemical



Fig. 2. Expedition 4 crew members in Endeavour middeck with CBTM payload during flight of STS-108.

Senses Center and BioServe) that served to qualify mice to fly in the AEMs for this payload. This activity may pave the way for future “mouse flights.”

This cooperative effort between several different types of organizations demonstrated the mutual benefits resulting for all those participating. As human presence in space continues to expand, missions increase in duration, and the cost of missions remains expensive, the need for more cooperative, collaborative efforts to facilitate discovery and development of effective countermeasures and other space-related biomedical testing will increase.

Point of Contact: B. Girten
(650) 604-0579
Beverly.E.Girten@nasa.gov

SFD SYSTEMS DEVELOPMENT

Passive Dosimeter System

Nina Scheller, Kristofer Vogelsong

The Passive Dosimeter System (PDS) is part of the Space Station Biological Research Project (SSBRP) Laboratory Support Equipment (LSE). Launched in March 2001 aboard STS-102 (ISS Flight 5A.1), the PDS is used for science experiments and measurements on board the International Space Station (ISS). It measures biologically active space radiation doses at any location that can accommodate its small, compact dosimeters (see Figure 1). The PDS combines two different types of dosimeters—a Thermoluminescent Detector (TLD) system and a Plastic Nuclear Track Detector (PNTD) system.



Fig. 1. The Thermoluminescent Detector (TLD) system with the Plastic Nuclear Track Detector (PNTD) system holder wrapped around it.

The TLD system consists of TLD dosimeters to accumulate dose and a Reader to measure that dose on orbit (see Figure 2). The TLDs are placed at various locations within ISS and exposed for specific durations. At the end of the exposure period, the TLD is placed in the Reader, which heats it and measures the cumulative radiation exposure, and records it on a memory card. The heating process also returns



Fig. 2. The Thermoluminescent Detector kit which includes the reader, TLDs, memory cards, power and data cables, and space fuses.

the TLD to an “un-exposed” state ready for another measurement. The Reader can be programmed to automatically read a TLD that has been left inserted into the Reader. This makes possible a continuous recording of exposure during small time increments until the space on the memory cards is exhausted.

TLDs are not 100% sensitive to high linear energy transfer (LET) particles, so it is necessary to use Plastic Nuclear Track Detectors (PNTDs) to determine the energy spectrum of radiation absorbed by the TLDs. The PNTDs are co-located with TLDs during dose accumulation (see Figure 1). The PNTDs are returned to the ground and are processed and analyzed in a laboratory to obtain the LET spectrum. The LET spectrum is then combined with the dose information from the TLDs to determine a corrected total dose, dose equivalent, and average quality factor.

The Hungarian Space Office (HSO) provided the TLDs and Readers under a Memorandum of Agreement with NASA, and Eril Research Inc. provided the PNTDs and data analysis.

Ames Research Center/SSBRP was responsible for integrating the two systems, and for verification, flight planning, and crew training activities. SSBRP was also responsible for the development of kits to house the individual components, for fabrication of power and data cables, and for preparation of software for the host system laptop computer.

The first use of the PDS occurred in the spring and summer of 2001. The TLD system was launched on STS-102 (ISS Flight 5A.1) and the PNTD system was launched on STS-100 (ISS Flight 6A). The PDS was operated in support of the Human

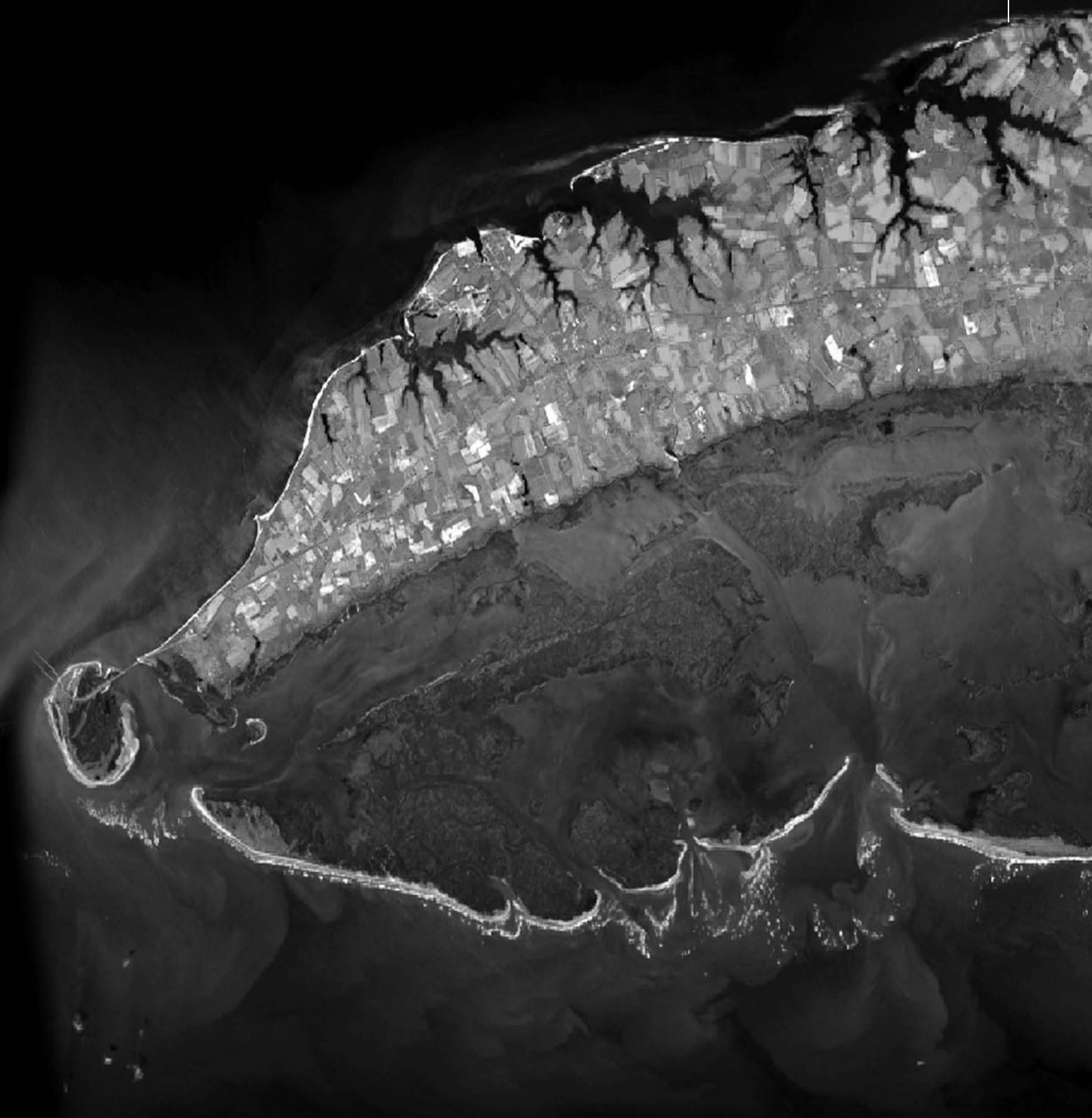
Research Facility DOSMAP experiment during Increments two and three. The PNTDs and memory cards were returned to the ground on STS-105 (ISS Flight 7A.1). Dr. Guenther Reitz was the Principal Investigator for the DOSMAP Experiment.

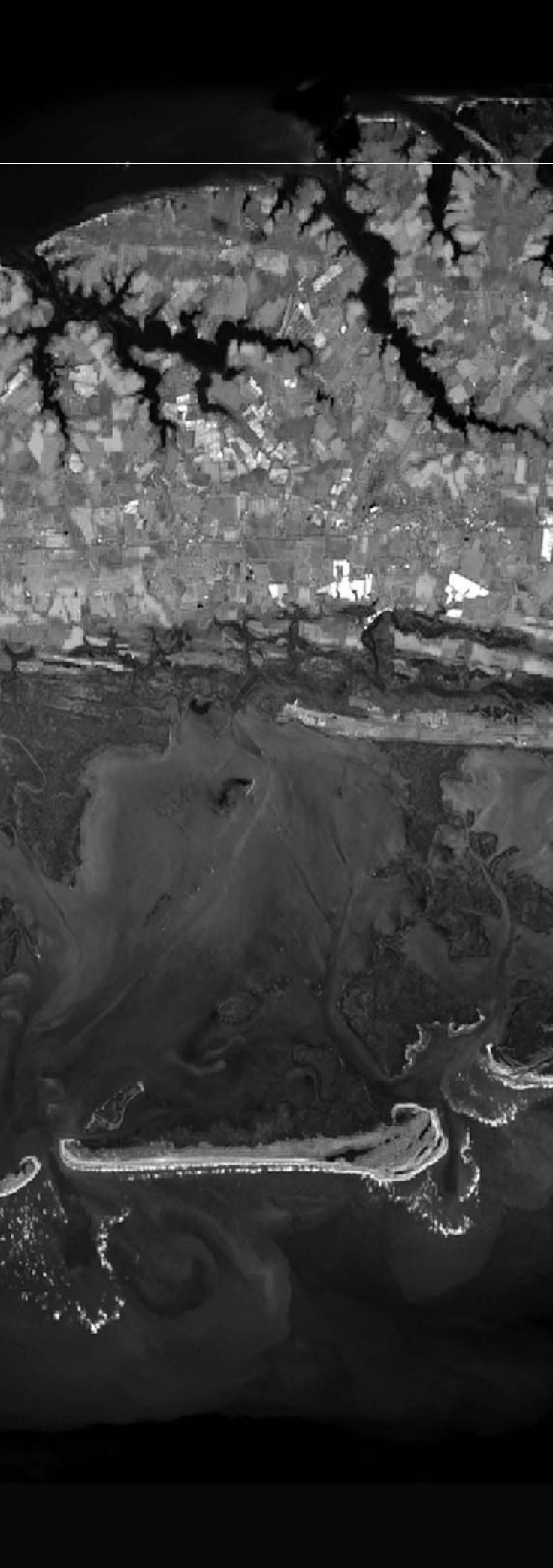
The PDS data was realistic and in-line with expectations based on past Mir Space Station measurements made in similar orbits. The quality of the data, ground-based characterization, and calibration of the instrument has been highly praised by world space radiation experts.

Point of Contact: J. Connolly
(650) 604-6483
James.P.Connolly@nasa.gov

E a r t h S c i e n c e

E n t e r p r i s e





Overview

The natural environment accommodates humanity by providing a rich supply of ecological and physical services that help to preserve our health and well-being, as well as that of many other organisms on Earth. However, as the human population continues to grow in unprecedented ways, the human demands for nature's resources and services continue to escalate and the Earth's life-sustaining systems are taxed and degraded more than ever before. It is critical to understand the natural world, how it is changing both in natural and human-induced ways, and what human society must do to reach a level of sustainability.

NASA's Office of Earth Science (OES) is conducting a study of our living planet at a truly planetary scale. The OES studies the total Earth environment: to understand the state and behavior of the atmosphere, ice, oceans, land, ecosystems, and their interactions; to understand the effects of natural and human-induced near-term changes on the global and regional environment; and to lay the foundation for long-term environmental and climate monitoring and prediction. During FY01, numerous research and technology efforts funded by the OES were accomplished, the results of which address the major goals of the OES Enterprise:

- Observe, understand, and model the Earth system to learn how it is changing, and the consequences for life on Earth.
- Expand and accelerate the realization of economic and societal benefits from Earth Science, information, and technology.
- Develop and adopt advanced technologies to enable mission success and serve national priorities.

MODIS Airborne Simulator (MAS) infrared composite image of the Delmarva Peninsula which is composed of portions of Delaware, Maryland and Virginia. (See the ASF report for a description of the MODIS and MAS instruments (page 176).)

Ames Research Center (ARC) supports the OES by conducting scientific research and by developing technology with the objective of expanding our knowledge of the Earth's atmosphere and ecosystems. Complementary goals are part of NASA's Astrobiology research and technology effort, a program led by ARC. ARC also contributes applied research and outreach to a companion OES objective to apply the scientific knowledge and know-how gained to practical, everyday problems of the public and private sectors by transferring the technology and knowledge to users outside NASA.

Key components of the Earth Science Division's research programs include the study of the physical and chemical processes of biogeochemical cycling; the state and dynamics of terrestrial (and some marine) ecosystems; the chemical and transport processes that determine atmospheric composition, dynamics, and climate; and the physical and biological processes that determine the behavior of the atmosphere on the Earth and other solar system bodies.

Earth scientists at ARC engage in research related to four of the NASA strategic enterprises.

THE EARTH SCIENCE ENTERPRISE

NASA HEADQUARTERS CODE Y

Terrestrial ecology and atmospheric assessments, airborne instrument development, applications, Astrobiology, Information Technology, and Biotechnology

OFFICE OF BIOLOGICAL AND PHYSICAL RESEARCH

NASA HEADQUARTERS CODE U

Application of technology to issues of human health, life beyond the planet of origin

THE AEROSPACE TECHNOLOGY ENTERPRISE

NASA HEADQUARTERS CODE R

Environmental assessments of aircraft operation, unpowered airborne vehicle (UAV) sensor development and science demonstration, space solar power

THE SPACE SCIENCE ENTERPRISE

NASA HEADQUARTERS CODE S

Planetary atmospheres study, Astrobiology

Atmospheric research efforts include the physical mechanisms and chemical interactions that control the concentration and depletion of stratospheric ozone, perturbations in the chemical composition of the atmosphere, and climatic changes resulting from clouds, aerosols, and increasing amounts of greenhouse gases in the Earth's atmosphere. Numerous state-of-the-art instruments are flown successfully each year, and critical data are collected for stratospheric and tropospheric research.

At ARC, scientists and technical personnel design, develop, and perform both remote sensing and in situ experimental measurements. In addition, they perform computer simulations of atmospheric and ecosystems processes to understand exchanges between the biosphere and the atmosphere using both airborne and satellite sensor data. The scientists conceive and develop advanced instrumentation to satisfy the measurement requirements of all supported enterprises, emphasizing both airborne and selected spacecraft sensors. Project managers and project scientists provide science mission management and science leadership for major NASA science programs and other agency science programs. Staff scientists conceive and develop applications programs utilizing proven and developing technology. Additionally, they transfer developed scientific knowledge and technology to commercial and private interests, national and international governmental agencies and ministries, other disciplines, and educational institutions.

The Airborne Sensor Facility (ASF) within the Earth Science Division provides remote-sensing support for OES investigations, and for calibration and validation studies for the Earth Observing System (EOS). It is tasked with maintaining and operating a suite of OES facility sensors that are made available to the science community at large through the

NASA flight request process. The sensors are flown on various NASA, U.S. Department of Energy, and other aircraft, as required.

The ASF does data processing, flight operations, sensor calibration, systems development, and data telemetry. Current activities are centered around the moderate resolution imaging spectrometer (MODIS) and the Advanced Spaceborne Thermal Emission and Reflection Radiometer (ASTER) airborne simulators (the MODIS Airborne Simulator (MAS), and the MODIS ASTER instrument (MASTER)), which are being used to characterize calibration sites and

develop algorithms for the new Terra (EOS AM-1) satellite systems. These data are processed into a calibrated Level-1B product at the ASF, and delivered to the instrument science teams via the EOS Distributed Active Archive Centers (DAACs).

Research results and technology developments are published in the scientific literature. Additionally, many of these results are disseminated to the commercial and educational communities, contributing to a better public understanding of the Earth Science Enterprise within NASA.

The Airborne Sensor Facility - 2001

Jeff Myers, Bruce Coffland, Pat Grant, Ted Hildum, Mike Fitzgerald, Rose Dominguez

The Airborne Sensor Facility (ASF) based at Ames Research Center (ARC), with a field component at Dryden Flight Research Center (DFRC), collects remote-sensing data for the NASA Office of Earth Science (OES). It is charged with operating a suite of facility sensors that support the NASA research community through the flight request process. The services are also made available to other government agencies on a cost-reimbursable basis. These devices are flown on a variety of NASA, U.S. Department of Energy (DOE), and other aircraft.

The primary focus of the group in FY01 was supporting the calibration and validation of the moderate resolution imaging spectrometer (MODIS) and Advanced Spaceborne Thermal Emission and Reflection (ASTER) sensors on the Earth Observing System (EOS) Terra satellite. The ASF operates two sensors, the MODIS Airborne Simulator (MAS) and MODIS ASTER instrument (MASTER), which emulate these instruments. Data from these systems are being used extensively for development and testing of the various algorithms that are used to derive geophysical parameters from the orbital data.

The ASF consists of three main laboratories, which cover a range of functions, from instrument engineering and initial data-collection, through data processing and delivery of a final calibrated product. A short summary of the activities of the three main groups follows.

- **The Sensor Operations and Engineering Laboratory** maintains and operates the sensor hardware of the ASF, conducting data-collection missions worldwide on a variety of aircraft platforms. In FY01, ASF sensors were flown on 180 missions (totaling 605 flight hours) on ER-2 (Figure 1) and DOE B200 aircraft. Data were

collected for a variety of EOS investigations, primarily concentrated on EOS validation and global climate modeling studies.



Fig. 1. The NASA high-altitude ER-2 aircraft.

The MAS instrument was deployed with an ER-2 in support of the Convection and Atmospheric Moisture Experiment (CAMEX). CAMEX is a series of field research investigations sponsored by NASA's Earth Science Enterprise. This was the fourth field campaign in the CAMEX series (CAMEX-4), and it was based out of Jacksonville Naval Air Station, Florida.

CAMEX-4 focused on the study of tropical cyclone (hurricane) development; storm tracking and intensification; and the impact of storm landfall using NASA aircraft and surface remote-sensing instrumentation. The primary aircraft used during CAMEX-4 were the NASA ER-2 and DC-8 research airborne platforms. These instrumented aircraft acquired data over storms and hurricanes as they developed in the Caribbean, Gulf of Mexico, and along the East Coast of the United States (Figure 2). The goal of this study is to understand hurricane structure, dynamics, and motion; such an under-

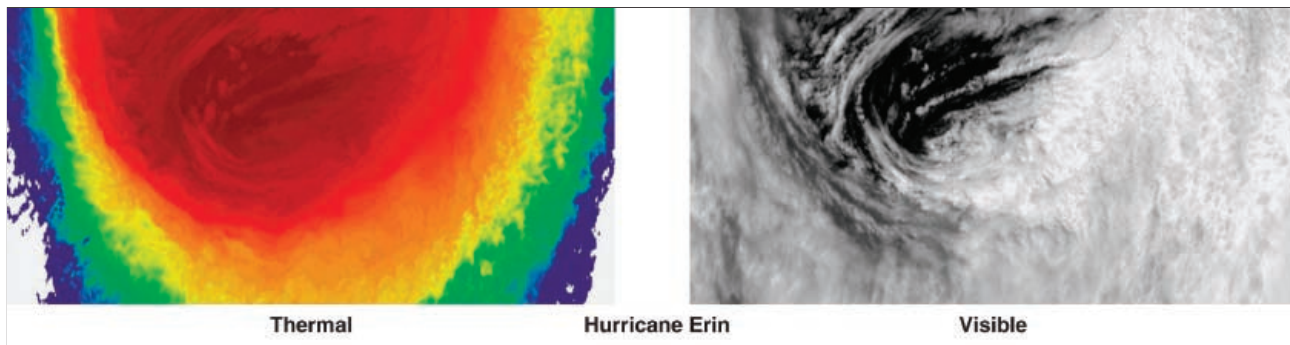


Fig. 2. MAS visible and thermal images of Hurricane Erin (CAMEX-4 deployment).

standing will help hurricane modelers and improve hurricane predictions.

Apart from numerous individual missions flown from DFRC, MAS was also sent aboard an ER-2 to Wallops Island, Virginia, in support of the Chesapeake Lighthouse and Aircraft Measurements for Satellites (CLAMS) campaign. CLAMS scientists are using equipment mounted on the U.S. Coast Guard's Chesapeake lighthouse off the coast of Virginia Beach, Virginia, instruments on six research airplanes, and the orbiting Terra research satellite to enhance their knowledge of how the ocean affects the atmosphere. In addition to MAS data, the ER-2 also acquired data from the Advanced Visible and Infrared Imaging Spectrometer (AVIRIS), data from the Scanning High-Resolution Interferometer Sounder (S-HIS), data from the Airborne Multiangle Imaging Spectroradiometer (AirMISR), and metric camera photography in support of CLAMS.

Measurements from the aircraft instruments and from the long-term CERES Ocean Validation Experiment (COVE) at the lighthouse will be used to improve information from Clouds and the Earth's Radiant Energy System (CERES) and other instruments on NASA's Terra satellite. The major goals of CLAMS are to improve satellite-based estimates of aerosol measurements and to make measurements of ocean characteristics. These data will create a better understanding of how Earth maintains its overall temperature and its energy budget.

The ER-2 was sent to San Antonio, Texas, on a third field deployment with MAS. This deployment supported the University of Wisconsin's Cooperative Institute for Meteorological Satellite Studies (CIMSS). The Institute's primary science objectives were to validate MODIS atmosphere products with underflights of the Terra satellite. The Gulf of Mexico and the Atmospheric Radiation Measurement Cloud and Radiation Testbed (ARM CART) site in Oklahoma were the primary validation sites. Additionally, on this deployment, imagery was acquired over coastal Louisiana for the U.S. Geological Service (USGS) Wetlands Research Center in Louisiana and the Corps of Engineers as part of a wetlands and wildlife habitat ecosystem study.

The MASTER sensor was flown on the DOE Beechcraft B200, collecting data primarily for the U.S. Advanced Spaceborne Thermal Emission and Reflection Radiometer (ASTER) science team and the Environmental Protection Agency (EPA). As in previous years, ASTER team sites included several areas in the Mojave Desert used as Terra calibration targets. The high-resolution MASTER data are being used to characterize the thermal and reflective properties of these areas so that the content of the satellite pixels can be more fully understood. Additionally, MASTER data were collected in support of a U.S. Department of Agriculture (USDA) wildlife refuge study in southern New Mexico. The New Mexico site is also part of the MODIS land-validation program.

MASTER was sent on a one-week deployment to the Pacific Northwest in cooperation with the Department of Civil and Environmental Engineering at the University of Washington. The comprehensive project objectives included validation of ASTER and land satellite (LANDSAT) stream temperature characterizations, a study of the Cedar River watershed, a study of Mount Rainier glaciated area thermal properties, and a study of the urban heat island effects of downtown Seattle.

- **The Data-Processing Laboratory** reduces and calibrates the digital imagery data, provides mission documentation, and distributes hard- and soft-copy products. It also maintains a complete historical archive of the ASF data, which is catalogued in a geographic database. The EOS-related image data are also archived in the NASA Distributed Active Archive Center (DAAC) system. These centers maintain hyperlinks to the ASF MAS and MASTER Web pages, allowing the general public to view imagery for each mission, and to obtain ordering information. One hundred nineteen mission datasets were placed at NASA DAACs this year. These data are calibrated and geo-located (Level-1B) and are in hierarchical data format (HDF).

- **The Calibration Laboratory** provides spectral and radiometric characterization for remote-sensing devices. It maintains a set of integrating spheres and laboratory radiometric standards, as well as both conventional monochromators and a Fourier transform interferometer for spectral measurements. The lab was validated this year in a major experiment supervised by the NASA EOS Calibration Scientist. This included a critical review and a round-robin calibration exercise conducted by the National Institute for Standards and Technology (NIST), Goddard Space Flight Center (GSFC), and the University of Arizona. In addition to performing regular calibrations of the ASF sensors, it also conducted several field validation experiments in conjunction with the Jet Propulsion Laboratory (JPL), ASTER, and Multi-angle Imaging Spectro Radiometer (MISR) science teams.

Refer to the ASF Web page at <http://asapdata.arc.nasa.gov> for further information, including sensor specifications, sample imagery, and online flight documentation.

Point of Contact: J. Myers
(650) 604-3598
jmyers@mail.arc.nasa.gov

Development of a Tactical System for Fire Management and Prediction

James Brass, Steve Wegener, Donald Sullivan, Vince Ambrosia, Bob Higgins, Philip Hammer, Ted Hildum, Roy Vogler

A report by the International Red Cross and Red Crescent Societies states that the United States has one of the higher rates of natural disasters in the world. Studies have shown that between 1992 and 1996, costs of disasters in the United States have averaged \$1 billion per week. Globally, the costs have averaged \$440 billion per year in approximately the same time period. Major episodic events such as these have direct effects on the world's population, as well as on the environment. The National Science and Technology Councils clearly stated that disasters are a growing problem nationally and internationally. It is important to become more aggressive in seeking ways to reduce disaster losses and move toward a more sustainable society and environment. There is a clear need for technology developers and users to define the limitations in current systems, develop improved technologies that provide more timely results than those that exist now, and provide simple access to this technology to save lives, habitat, and monetary resources.

NASA's Earth Science Research Plan explains that natural hazards are inevitable manifestations of Earth processes, but need not be inevitable disasters. NASA has a role in assisting society in reducing loss of life and property damage. Through the development of technologies designed to support NASA's Earth Science program, numerous tools exist that can be effectively developed for understanding, characterizing, and monitoring natural disasters.

Wildfire suppression provides a good paradigm for the information needs, management, and mitigation of natural disasters. Early efforts employing remote-sensing data for forest-fire mapping employed aerial

cameras and infrared line scanners. Those efforts found that the attributes of an ideal system included (1) the detection of fire in its early stages; (2) the ability to prioritize fires, distinguishing between dangerous fires and those of no significance; (3) day and night operation; and (4) the ability to detect fire size and location in relation to ground (topography) and forest resources (vegetation and fuel). All this information must be communicated to fire management personnel quickly and efficiently to meet fire management objectives. Although these requirements were developed 30 years ago, many operational limitations still exist in the optimal system.

Project First Response Experiment (FiRE), designed by NASA's Ames Research Center, the U.S. Forest Service, the State of California, and General Atomics, translated fire management requirements into technology demands and demonstrated remote-sensing capabilities, telemetry, data processing, and communications to the fire management community. During the Project FiRE demonstration, an affordable, simple, and portable system for data downlink and relay was established to accomplish these tasks.

The demonstration flights produced resource and fire-status maps that were sent via satellite communication to NASA Ames Research Center and accessed via the Internet by the user community. The images documented the short-term progression of the actively burning fire in near-real-time (see Figure 1). Fire position and perimeter were determined from the geo-referenced output. Both the dynamic fire perimeters and static vector database were overlaid on the various raster base maps, and hard-copy output was produced. Reports on fire area and perimeter were concurrently produced.

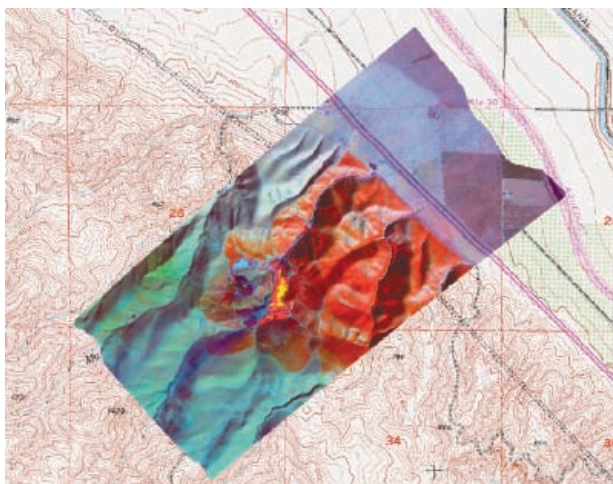


Fig. 1. Example of imagery showing terrain draping.
The project FiRE demonstration documented the potential for analyzing and managing data and mitigating disasters in near-real-time using digital data, data overlay, electronic data transmission, and current communications technology. Datasets transmitted from an aerial platform were mapped and geo-rectified in under 10 minutes. Ancillary information was overlaid with the raster airborne imagery to assist firefighters in allocating resources during the fire. The goal of 15 minutes from “aircraft to map” was accomplished in the flight tests. The precision location and attitude information from the Airborne Infrared Disaster Assessment System (AIRDAS) assisted in reducing the time allocated for geo-correction of the airborne data and increasing precision in the fire product. A new

methodology is currently being incorporated into the data-collection package to better “model” the platform/sensor geometry package to speed geo-correction.

The FiRE demonstration was beneficial to Federal, State, and local resource and disaster agencies responsible for responding to natural disasters, such as wildland fires. Improvements in communications are needed to optimize the complete system, although the technology is currently in place at a low, off-the-shelf price, to effect mitigation efforts under emergency conditions. The agencies and companies involved continue to cooperate in developing various elements of this demonstration, and continue to advance the data collection, remote transmission, geo-correction, and analysis of spatial information.

Collaborators on this project were Phil Riggan, Bob Lickwood, PSW Research Station, U.S. Forest Service; Tom Bobbe, Paul Greenfield, RAC, U.S. Forest Service; Gary Darling, State of California; Los Angeles County, California; California Office of Emergency Services; Sally Buechel, TerraMar Resources, Inc.; and the General Atomics Aeronautical Systems.

Point of Contact: J. Brass
(650) 604-5232
James.A.Brass@nasa.gov

Ecoinformatics: Aerospace Technologies in the Service of Global Health

Byron Wood, Brad Lobitz

Background

In April 2000, NASA’s Chief Scientist held a meeting to determine what activities each NASA Center had in aerospace technologies that might be included in a coordinated NASA program on human health. It was determined that this new program should

be based on the unique capabilities of each NASA Center or organizational code. Each Center was, therefore, requested to provide an overview of its specific capabilities that might be included in an agency-wide program. Based on the material pre-

sented, a decision was made to move forward with the development of a new initiative on Environment and Health.

Environment and Health Initiative

Between January and April 2001, representatives of NASA's Office of the Chief Scientist, Earth Science Enterprise, and Fundamental Space Biology Program developed a preliminary package of materials on the Environment and Health concept. This initiative was based primarily on the application of NASA remote-sensing and Earth science data to studies of human health. In April, NASA Headquarters management reviewed the Environment and Health Initiative package and encouraged the Earth Science Enterprise and Fundamental Space Biology Program to continue existing programs and explore opportunities not addressed in the Environment and Health package.

Ames was encouraged to expand the Center for Health Applications of Aerospace Related Technologies (CHAART) training program and explore new program opportunities based on the Center's capabilities. In a December 2000 workshop at Ames, the idea of a new program, "Ecoinformatics," had been discussed and outlined. This program focuses on integrating Ames' expertise in the human health applications of aerospace-related technologies, fundamental biology, information systems technology, data visualization, and the development of microtechnologies with wireless communications technologies to provide "near-real-time" information on the spatial and temporal patterns of infectious diseases.

Ecoinformatics

The Ecoinformatics concept was developed with collaborators at the National Institutes of Health (NIH). Unlike most previous NASA health-related programs, Ecoinformatics is intended to be driven by user information needs rather than by the availability of NASA (primarily remote-sensing) data. This approach is based on the user community's need to turn large quantities of diverse data into useful information required in research, surveillance, and

intervention. The goal is to understand and forecast the spatial and temporal patterns of infectious disease risk based on modeling the interactions among environmental, epidemiological, entomological, and socio-economic parameters for specific diseases in specific locations. Because data on these parameters are collected by differing methods and at various scales, modeling their spatial and temporal patterns requires the utilization of sophisticated information system, geospatial analysis, and visualization tools. Initial models will be based on the integration and analysis of existing datasets. However, it is anticipated that in the process of developing these initial models, missing data needs will be identified. These will, in turn, provide the parameter and measurement requirements necessary to develop new microtechnologies for remote or in situ data collection. Transmission and integration of these data into forecast models will likewise necessitate the development of improved wireless communications networks. Improved communications are also essential to returning model outputs (i.e., information) to the users who require them.

In December 2001, NASA and the NIH held a retreat at the Asilomar Conference Center, Monterey, California, to outline specific activities on which to initiate an interagency program in Ecoinformatics. Participants included NASA Ames scientists, Program Managers from the National Institute of Allergies and Infectious Diseases (NIAID), and the Center Directors of the NIAID-sponsored International Centers for Infectious Disease Research (ICIDR). Discussions focused on having the ICIDR directors identify and prioritize recommendations for collaborative activities in the application of current aerospace technologies to, or the development of new capabilities for, disease diagnostics, treatment, prevention, and control. From these discussions the following four activities were initiated:

- Development of a prototype in situ/portable device for measuring and communicating physical water quality parameters. This will have immediate use for the collection of field data

necessary to better understand the biology of such water-related diseases as cholera, schisto-somiasis, enterics, and filariasis.

- Development of new information technology and computational approaches to support infectious disease research, surveillance, and control operations. Initially this will focus on the use of “Science Organizer” for data management and communications for the ICIDR malaria project in Kenya.
- Development of data visualization and display tools to integrate health (Hantavirus) and environmental data from the Sevilleta Long-Term Ecological Research site in New Mexico.
- Integration of hand-held PC Global Positioning System/geographic information system (GPS/GIS) and digital imaging hardware and software for collection of site-specific health and environmental field data. Each of the ICIDR teams will be provided with at least one complete system.

Invasions Initiative

A new effort called “Invasions” was initiated. The idea behind Invasions is that many, if not most, disease outbreaks, or introduction of disease vectors or agents, are not anticipated and, when introduced to a new area, they “act” like invading species in terms of their spatial and temporal movement. Another underlying justification is that in addition to developing new recommendations based on workshops, committees, etc., it is time to try to integrate and implement existing agency capabilities. Taking this step should enable assessment of how different agency programs and capabilities can be integrated, what works, what doesn’t work, what the opportunities are, and what the obstacles are to developing an operational system.

The goal of the Invasions Initiative is to develop an operational interagency program in infectious disease research, surveillance, forecasting, and intervention. Several agencies already support programs

that have developed and demonstrated many of these capabilities. Unfortunately, these programs have yet to be combined into a single, integrated program. As a result, there is considerable duplication of effort, “re-invention” of already-demonstrated capabilities, and a failure to address key research and technology needs. One approach to achieve program integration and demonstrate operational capabilities is for key agencies (e.g., the National Science Foundation (NSF), NIH, Centers for Disease Control (CDC), National Oceanic and Atmospheric Administration (NOAA), the Department of Defense (DOD), NASA, etc.) to propose a new initiative in this area. It is proposed that this initiative be led by a single agency or a small group of agencies that have responsibility for and a history of infectious disease research and intervention. The lead agency(s) would be responsible for overall program integration and direction. However, within this structure, individual agencies would be responsible for developing specific program elements. A workshop of agency representatives was organized for September 2001. The goal of the workshop was to agree on a plan to develop an interagency initiative. However, the workshop was canceled because of the events of September 11, and the nature and scope of the interagency program are currently being reviewed in terms of bioterrorism and homeland defense issues.

Collaborators on this project were Durland Fish, Yale University, School of Public Health; Anwar Huq, University of Maryland, Biotechnology Institute; John Beier, Tulane University; Greg Glass, John Hopkins School of Public Health; National Institutes of Health (National Institute of Allergies and Infectious Diseases); Scott Starks, University of Texas, El Paso, PACES; Malaria Research and Training Center, Bamako Mali; and World Bank, Africa (AFTH-2).

Point of Contact: B. Wood
(650) 604-4187
blwood@mail.arc.nasa.gov

Land-Use Effects on Biogeochemistry in the Amazon

Liane Guild, Christopher Potter

In the Amazon, regenerating forests (capoeira) act as potentially important carbon and nutrient sinks during the shifting agriculture fallow period. However, these fallow periods are becoming shorter with the population and economic pressures to maintain cultivation. Shorter fallow periods have decreased the productive capacity of the cropping period. Additionally, droughts associated with El Niño events are becoming more frequent and severe in moist tropical forests. The effects of these droughts on moist tropical forests include potentially large effects on forest metabolism, reproductive biology, tree mortality, biogeochemistry, and forest flammability.

Differences in manipulation practices of crops could have both positive and negative effects on crop vigor. Although burning in shifting cultivation may control for pests and weedy species and resultant ash may provide a pulse of nutrients, the detrimental effects of elemental pool losses associated with burning are considerable. Alternatives to burning include cutting, chopping, and mulching forest and planting with fast-growing leguminous species. This experimental practice (slash and mulch with enrichment), which is under study by the Brazilian Agriculture Agency (EMBRAPA), has shown increased levels of biomass and a reduction in loss of nutrients and organic matter, allowing a shorter fallow period and a longer cropping period. The greater length of the cropping period may affect the soil moisture status of the site and may affect crop vigor, but the effect has yet to be determined. Since the slash-and-mulch practices do not use burning for land preparation, there is no requirement of a dry period. Additionally, the mulch keeps the soil moist for longer periods. These factors allow flexibility in the planting dates, but there is a need to monitor for crop stresses associated with different planting dates, in addition to a longer cropping period.

Research Objective

The objective is to determine the sensitivity of the slash-and-mulch with enrichment sites to soil moisture levels in relation to planting date and cropping duration in contrast to slash-and-burn sites. These objectives entail research occurring over several years of natural rainfall, variations of which will be monitored. To accomplish these objectives, regeneration of forests monitored during the fallow period and crop vigor are measured using ground instrumentation and linking with high-resolution remote-sensing data (i.e., the IKONOS satellite and the land satellite Thematic Mapper (LANDSAT TM)). Also included is monitoring for crop stress of the slash-and-mulch plots planted in different periods of the year and at cropping durations different from traditional slash-and-burn sites.

Fieldwork (August–September 2001, November–December 2001)

Field data were collected during the early dry season (August/September) to coincide with IKONOS overpasses. Data included plant water potential (pressure bomb) every two hours from 6:00 a.m. to 4:00 p.m., plant chlorophyll (Subsystem Positioning Aid Device (SPAD) instrument), reflectance, transmittance, and absorptance radiation (Li-Cor spectroradiometer), and Global Positioning System (GPS) points. EMBRAPA, in collaboration with the University of Bonn, Germany, has an ongoing hydrological study that includes a meteorological station and a soil moisture sampling system in place in the study area. Measurements were taken in fields planted with passion fruit and manioc crops as well as in a capoeira (regenerating forest) site.

Tatiana Sa and Claudio Carvalho of EMBRAPA-Belem, Brazil, collaborated with the authors on this project.

Point of Contact: L. Guild
(650) 604-3915
Liane.S.Guild@nasa.gov

Modeling Terrestrial Ecosystem Processes

Christopher Potter, Liane Guild, Steven Klooster, Vanessa Brooks Genovese, Kelly Decker, David Bubenheim, Hanwant Singh

Carbon Fluxes for the Amazon Basin

Seasonal and interannual controls on net ecosystem production (NEP) have been modeled with integration of high-resolution (8-kilometer) multi-year satellite data to characterize Amazon land surface properties over time. Analysis of temporal and spatial relationships between regional rainfall patterns and satellite observations (for vegetation land cover, fire counts, and smoke aerosol effects) have revealed several important ecological patterns for the Large-Scale Biosphere-Atmosphere Experiment in Amazonia. The ecosystem model (NASA-Carnegie-Ames-Stanford Approach) predicts that undisturbed Amazon forests can be strong net sinks for atmospheric carbon dioxide, particularly during wet (non El Niño) years. However, drought effects during El Niño years can reduce net primary production in forests of the eastern Amazon by 10% to 20%, compared to long-term average estimates of regional productivity.

Modeling Terrestrial Biogenic Sources of Acetone Emission

Acetone is of considerable interest in atmospheric chemistry as a source of HOx radicals and peroxyacetylnitrate (PAN) to the upper troposphere. The potential biogenic sources of acetone include terrestrial plant canopies, oxidation of dead plant material, harvest of cultivated plants, biomass burning, and the oceans. These sources are poorly constrained at present in budgets of atmospheric chemistry. Based on laboratory, field, and satellite observations to date, a first global modeling ap-

proach is derived for estimating monthly emissions of acetone from the terrestrial biosphere to the atmosphere. The modeling approach is driven by observed surface climate and estimates of vegetation leaf-area index (LAI) generated at 0.5-degree spatial resolution from the National Oceanic and Atmospheric Administration (NOAA) satellite advanced very-high-resolution radiometer (AVHRR). Seasonal changes in LAI are estimated using modified moderate resolution imaging spectrometer (MODIS) radiative-transfer algorithms to identify the probable times and locations of crop harvest in cultivated areas and litterfall of newly dead plant material in noncultivated areas. Temperature-dependent emission factors are applied to derive global budgets of acetone fluxes from terrestrial plant canopies, oxidation of dead plant material, and harvest of cultivated plants.

Simulation of Hypersaline Microbial Mats: Modeling Effects of Bacterial Ecosystems on the Atmosphere of Early Earth

A model has been constructed to simulate C, O, and S cycles, and growth of cyanobacteria and sulfur bacteria in a stratified hypersaline mat. The aim was to simulate microbial effects on the atmospheric chemistry of early Earth. Inputs to the mat system include photosynthetically active radiation (PAR), near-infrared radiation (NIR), and temperature. Attenuation of PAR with each layer is modeled, and NIR attenuation depends on the abundance of bacteriochlorophyll a. The bacterial groups whose metabolism and growth are simulated include cya-

nobacteria (CYA), purple sulfur bacteria (PSB), colorless sulfur bacteria (CSB), and sulfur reducing bacteria (SRB). Growth of CYA occurs by either oxygenic or anoxygenic photosynthesis (AP), depending on the available substrate (oxygen (O₂) or hydrogen sulfide (H₂S)). PSB growth occurs by AP using NIR and H₂S or by chemosynthesis (CH), using O₂ and H₂S. Growth of CSB occurs via CH, also using O₂ and H₂S. CSB growth occurs via aerobic CH utilizing sulphur dioxide (SO₂) and creating H₂S in the process. The model consists

of 10 layers (1 millimeter (mm) each), and gains density as biomass increases. Gas exchange occurs between successive layers and with the atmosphere. Claudio Carvalho, EMBRAPA-Belem, Brazil (Amazon carbon fluxes) and Ranga Myneni, Boston University, Boston, MA (acetone emissions) collaborated with the Ames investigators on this project.

Point of Contact: C. Potter
(650) 604-6164
Christopher.S.Potter@nasa.gov

On the Feasibility of Using Support Vector Machines to Automatically Extract Open Water Signatures from POLDER Multiangle Data over Boreal Regions

V. C. Vanderbilt

This research assessed the feasibility of using a support vector machine to identify open water from regions of inundated vegetation and dry (upland) vegetation using single-band multiangle Polarization and Directionality of Earth's Reflectance (POLDER) data acquired over boreal forest regions. Previous work suggested that, when viewed in the solar principal plane, profiles of solar radiance as a function of viewing angle for a fixed wavelength might serve as a means to discern open water quickly and automatically. Classifying solely on the water attribute, support vector learning machines can be trained to discriminate open water automatically, but the accuracy in training competes against the robustness with which the machine may be applied to subsequent data. With the accuracy against robustness optimized, a machine was developed that has an estimated mean probability of misclassifying water of approximately 4% in subsequent data. A conservative bound for the 95% confidence interval for the mean is approximately 32%. The estimates are conservative, because they are independent of the underlying probability distributions of the community types.

The most important result of this research is the portability obtained by training a support vector machine on one dataset and applying it successfully to new regions having different land cover distributions from the training site. These results demonstrate that the method is directly applicable to detecting differing land-cover conditions found on different boreal ecosystems. The analysis results clearly detail the variability in land-cover characteristics among the several boreal areas imaged. By comparison, in the same images classified using traditional methods, some pixels were misclassified because of the presence of more than one class property in the signature or the occurrence of undetermined signatures. For these signatures, the support vectors reduce the possibility of misclassifying data for pixel sizes small enough to be entirely or nearly entirely of one class.

Applicability of the analysis results reported here is not limited to open water. A hierarchical approach can be developed to extend the analysis to classify additional types of both inundated and noninundated vegetation. In this planned analysis, open water will

be masked after it is classified and then additional spectral bands will be added to the multiple-view-angle dataset. If all the spectral and directional bands are used, the probability of uniquely discriminating more classes increases. It is important to emphasize that each spectral band analysis independently classified the multiview-angle dataset as a demonstration of the support vector technique. Using additional spectral and view-angle information would optimize the bidirectional reflectance distribution function (BRDF) spectral signatures for each land-cover type by using the full suite of remotely sensed data.

The following people collaborated with the principle Ames investigator: J. Pierce, Mathematics Department, United States Naval Academy, Annapolis, MD; M. Diaz-Barrios, S. Ustin, S. Tournois, P. J. Zarco Tejada, Department of Land, Air and Water Resources, University of California, Davis; J. Pinzon, NASA Goddard Space Flight Center, Greenbelt, MD; P. Shih, National Chiao Tung University, Taiwan; and G. L. Perry, Silicom Group, Toulouse, France.

Point of Contact: V. Vanderbilt
(650) 604-4254
Vern.C.Vanderbilt@nasa.gov

Oxidative Damage in Nature

Lynn J. Rothschild

Oxidative damage is implicated in a broad range of human health issues, from immune responses to cancer to aging. The presence of oxidants on Earth, Mars, and possibly Europa, and the oxidizing nature of the space radiation regime, hints that oxidative damage is an area of broad astrobiological interest. Recent work done at Ames Research Center on DNA damage and repair in nature suggests that oxidative damage is common, and its effects are not predictable based on current knowledge. In spite of that, surprisingly little is known about oxidative damage in nature.

In FY01, field work was conducted in Yellowstone National Park (6/01 and 9/01) to determine the effects of low levels of the naturally occurring oxidative species, hydrogen peroxide, on DNA synthesis and mitosis. Results showed that in at least two distinct ecosystems, levels of hydrogen

peroxide up to about 1 micromolar (μM) enhanced DNA synthesis and cell division. Work in conjunction with personnel at Arizona State University measured diel changes in catalase and superoxide dismutase, enzymes that detoxify reactive oxygen species. Methods were developed using high-performance liquid chromatography (HPLC) to detect oxidative damage in DNA by determining the ratio of 8-hydroxyguanosine to the nonoxidized form, guanosine.

This work holds promise for other areas of concern to NASA, from the early evolution of life to planetary protection.

Point of Contact: L. Rothschild
(650) 604-6525
Lynn.J.Rothschild@nasa.gov

Past Sea Surface Temperature Derived from Tree Rings

Hector L. D'Antoni, Ante Mlinarevic

The general distribution of the biota in South America is related to the properties and operation of the climate system. The Hadley Cell in the tropical region and the Ferrell cell in midlatitudes control atmospheric circulation. Between both cells the jet stream is formed. The seasonally occurring vortex centered in the South Pole affects climate in the troposphere by introducing anomalies. Precipitation is related to the ocean/atmosphere interface and, in South America, is predominantly dominated by the Atlantic Ocean. The El Niño Southern Oscillation (ENSO) affects these patterns in four regions of South America (Ecuador, Northern Amazonia, Eastern Brazil, and Eastern Argentina) with large increases of precipitation (Ecuador, Argentina), drought (Northern Amazonia), and higher temperatures (Ecuador, eastern Brazil). These changes affect tree growth in these and other regions of South America.

By using dendrochronology data from 25 sites in South America, an artificial intelligence algorithm was trained. With the resulting model, past sea-surface temperatures (SSTs) of the Atlantic and Pacific oceans for the years 1246–1991 were constructed. Atlantic SST appears more stable around 24.5 degrees Celsius (°C). Pacific past SST varies in a much larger range around 21°C and reflects ENSO episodes in the past that are longer than the instrumentally recorded ones.

Point of Contact: H. D'Antoni
(650) 604-5149
Hector.D.Antoni@nasa.gov

Planning and Scheduling of Earth-Observing Satellites

Jennifer Dungan

The implementation of NASA's Earth Observing System strategy over the last decade has resulted in numerous satellites in low Earth orbit. Today, each of these satellites has its own mission control, and science observations from each of the sensors on board are considered independently. This project, headed by Ames' Planning and Scheduling Group in the Computational Sciences (Code IC) Division, is considering a new way of looking at suites of Earth-orbiting (EO) satellites by treating them as a constellation for the purpose of coordinating observations taken by their sensors. The resources required by constellations are expected to increase significantly in the future. This, combined with the drive to reduce costs, the demand for dynamic

science capabilities, and the need to coordinate between satellites, poses a real challenge with respect to how satellite observation operations are planned and conducted. This project is developing an autonomous system for scheduling and rescheduling remote observation requests based on the objective of maximizing the value of the data collected in a dynamic environment.

In FY01, the group developed a model of remote observation tasks and associated constraints, satellite capabilities (instrument, power, memory) and user-defined priorities for a land satellite (LANDSAT)-like satellite. This research provided information on current EO constellations and ways in which

data are used to improve the realism of this model. The model was used with scheduling software developed by Code IC to run several experiments. The experiments were run with various hypothetical sets of user requests and in each experiment, observation times and a satellite were assigned to each user request to satisfy all constraints and assure that the optimal set of priority observations was collected. Future work will investigate the potential for a scheduler aboard a satellite to further optimize the data-collection task.

David Smith, Robert Morris, Jeremy Frank, and Ari Jónsson of Code IC collaborated with the Ames investigator.

Point of Contact: J. Dungan

(650) 604-3618

Jennifer.L.Dungan@nasa.gov

Quantifying Uncertainty About Earth Science Information

Jennifer Dungan

NASA's Earth Observing System (EOS) satellites produce large quantities of images for interpreting the state of the land, ocean, and atmosphere. These images represent reflected or emitted electromagnetic radiation within a spectral region, such as the visible, infrared, or microwave. Models are being used to transform these images of reflected radiation into other biophysical quantities, such as the amount of green vegetation on the land surface, the quantity of aerosol in the atmosphere, or the activity of phytoplankton in surface waters. The models consist of mathematical formulations of physical and biological processes, and they yield information for each picture element, or pixel, in an image. The information can be mapped in a variety of ways to depict geographic patterns. Figure 1 shows an example of such a map, the leaf-area index (LAI) product from March 14, 2001, as derived from moderate resolution imaging spectrometer (MODIS) images.

There are many sources of uncertainty about the results of biophysical models of EOS products. Customarily, biophysical maps are produced with no information on this uncertainty. To improve the ability to interpret and rationally compare maps, uncertainty needs to be quantified. In 2001, Dungan spoke at a conference in Southampton, England, on

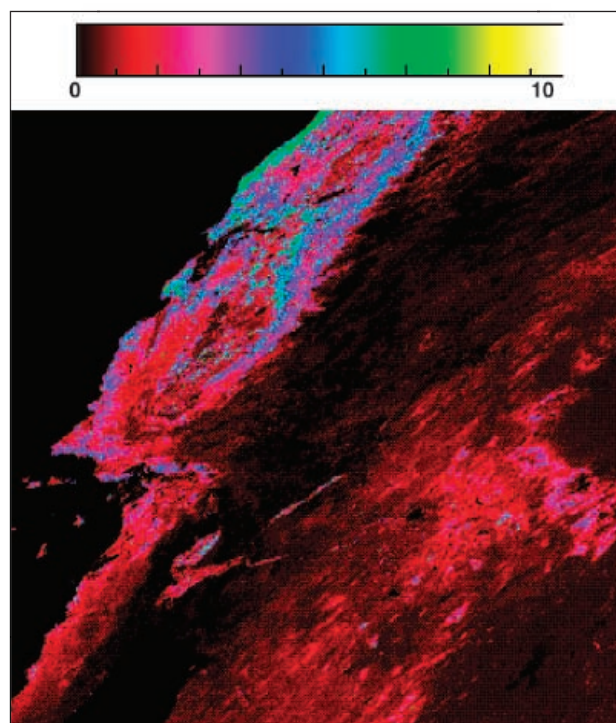


Fig. 1. ARABIC 1. LAI map of parts of California, Nevada, Arizona, and Mexico as produced from a model using MODIS images. LAI is a measure of the area of green leaves per unit ground area.

“Uncertainty in Remote Sensing and Geographic Information Systems.” In an attempt to take a comprehensive view of the problem, a new classification

of uncertainty was advanced that involves uncertainty about model parameters, the structure of models, the area represented by a pixel, the location of the pixel, and finally the prediction uncertainty in the biophysical quantities. This classification can be used as a basis to generate metrics for specific aspects of uncertainty.

Because uncertainty about biophysical quantities varies spatially, it is a challenge to visualize. A map interpreter would like to know where the most reliable values are and whether certain groups of pixels can be classed as features. The simplest approach to this problem is to represent the spread of possible values as a single number, commonly called sigma. Sigma is a limited metric for uncertainty, because the shape of the full probability density function is often nonparametric. Co-investigators at Ames' Advanced Supercomputing Division and

the University of California, Santa Cruz, have created tools to generate pictures of probability density functions (PDFs), functions representing the distribution of probable values at a given pixel. Figure 2 shows one such visual representation showing PDFs across a horizontal and a vertical profile of a map. This work was presented at the Visualization 2001 conference in San Diego, California. Though the work was limited to small synthetic datasets such as those in Figure 2, other work is planned that will use MODIS datasets.

Collaborators on this project were David Kao, Code IN, and Alex Pang, University of California, Santa Cruz.

Point of Contact: J. Dungan
(650) 604-3618
Jennifer.L.Dungan@nasa.gov

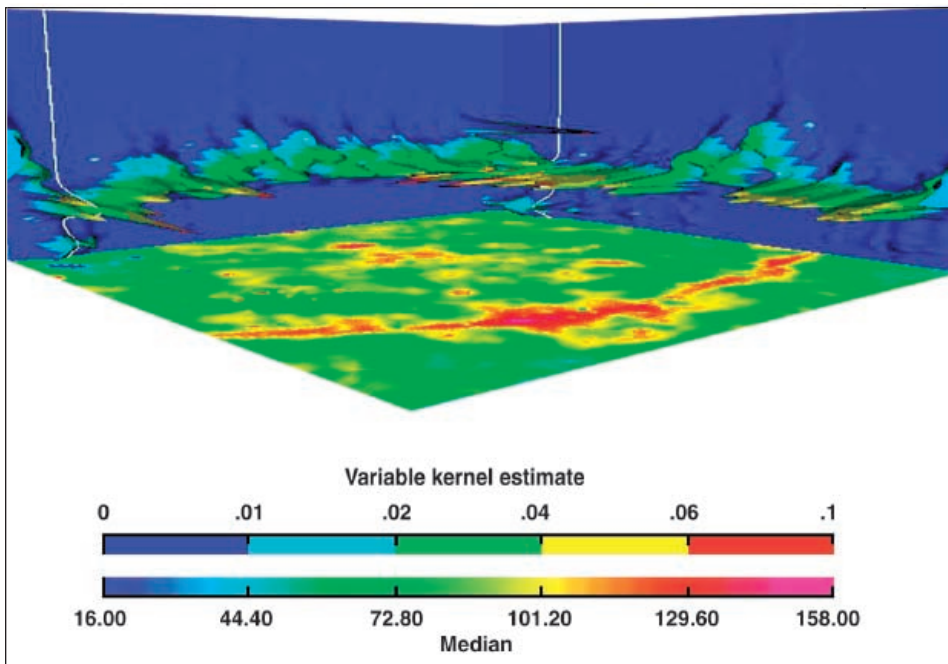


Fig. 2. ARABIC 2. Representation of a synthetic map to illustrate a visualization approach. The bottom plane (associated with the bottom color key) is the median value from the PDF at each pixel. On each "wall" of the figure, the full PDF at each pixel from a straight row or column in the map is shown. The colors on the walls correspond to the top color key, and they represent frequency values.

Space Solar Power—2001

J. W. Skiles

The concept of Earth orbiting satellites collecting solar power in space and transmitting that power to the Earth was first proposed in 1968. Since that time NASA has held a series of meetings and has funded several studies to consider the feasibility of a solar power satellite system. One project being considered is an array of satellites that will collect solar energy, convert the energy into microwave radiation (MWR), and beam the energy to collecting antennas (rectennas) on Earth, where it will be rectified into AC electricity and then fed into the power grid. The benefits of this technology will include reduced dependence on fossil fuels for power generation, reduced pollution from the burning of fossil fuels because there are no waste by-products, and improvements and innovations in space-based construction techniques and robotics.

Microwaves are perhaps the most benign method of sending the energy to Earth, but they have two major drawbacks. The first is the frequency of the beamed radiation. This frequency is planned to be at the 2.45-gigahertz (GHz) level, which is the frequency used by many of the communications satellites now in orbit and the frequency at which most cell phones operate. The second drawback is the size of the microwave receiving stations. These will have to be many kilometers square, and the continental United States alone would need 60 of them.

What is unknown about this technology is the effect of chronic exposure of organisms and ecosystems to beamed MWR. The energy intensity at the rectenna edge is expected to be 0.1 to 1.0 milliwatts per square centimeter (mW/cm^2). There are few reports in the open literature about the effects of MWR on plants or animals. What research that has been done has used frequencies vastly different from the 2.45-GHz planned for space solar power (SSP) and has used exposure intensities and exposure times that do not coincide with the SSP plans.

In order to observe the techniques and technologies used for wireless power transmission (WPT), in May, Skiles traveled to Reunion Island in the Indian Ocean for the WPT 2001 Conference. Reunion is developing a prototype of WPT where electrical power will be broadcast some 700 meters into Grand Bassin, a hiking, camping, and backpacking tourist stop at the bottom of a mountain range. The WPT machinery will be one of the first operational WPT setups in the world using microwaves to send power over a distance.

With the information and observations obtained at the Reunion conference, Skiles, with help from personnel in the Ames Systems Engineering and the Aeronautics and Spaceflight Hardware Development Divisions, assembled a much smaller scale apparatus to beam microwaves at 2.45 GHz and 0.1 to 1.0 mW/cm^2 across numerous test plants growing in a controlled environment in a laboratory. The test species in this instance was alfalfa (*Medicago sativa*, L.). The plants are being grown under continuous MWR at the above intensities. The hypothesis for this study is that there will be no differences between the plants grown under MWR and the control plants shielded from MWR. Variables being tested include gross morphological differences, cellular chemistry, and gas (CO_2) exchange rates.

This project merges botany, plant physiology, electrical engineering, and physics in order to answer questions about how organisms are expected to respond to a constant MWR environment.

Glenn Research Center, NASA Headquarters, Kennedy Space Center, Goddard Space Flight Center, Johnson Space Center, Marshall Space Flight

Center, Jet Propulsion Laboratory, and Langley Research Center collaborated with Ames Research Center on this project.

Point of Contact: J. Skiles
(650) 604-3614
Joseph.W.Skiles@nasa.gov

UAV Remote-Sensing Technology for Agricultural Monitoring

Stanley R. Herwitz, Stephen E. Dunagan, Lee F. Johnson, Robert E. Slye, Donald V. Sullivan, Jian Zheng, Robert Higgins

The Earth Science Division is supporting Clark University and AeroVironment, Inc., of Simi Valley, California, in demonstration of a slow-flying, long-endurance, uninhabited aerial vehicle (UAV) for high-resolution Earth resource imaging. The plan is for NASA's solar-powered UAV Pathfinder-Plus (PF+) to collect imagery over the Kauai Coffee Plantation (KCP), the largest coffee concern in the United States. Two high-spatial resolution imaging payload systems are under development for integration onto PF+: (1) a Hasselblad 555ELD camera body equipped with a Kodak Professional DCS Pro Back (4k x 4k charged coupled device (CCD)) for RGB imaging, and (2) a DuncanTech MS3100 (1k x 1k 3 CCD arrays) for multispectral narrow-band imaging. The payloads will be housed in environmental pods developed by Ames for previous missions of the prototype Pathfinder UAV. Modifications are being performed to comply with PF+ constraints on payload mass, volume, power consumption, and aerodynamic drag.

Three in-flight payload tests using a conventional fixed-wing aircraft were conducted during FY01, two preliminary tests in California and one above KCP. Both camera systems performed nominally. NASA's six-channel Airborne Large Format Imager (ALFI) was flown as a complementary payload primarily to collect imagery with a larger variety of spectral channels and bandwidths. Broadband wireless network connectivity was implemented between aircraft- and ground-based local-area networks for camera operation and image downlink. The

acquired imagery served as a basis for algorithm development in support of the near-real-time image stream. Key developmental elements include identification of optimal spectral bands, ground registration, extraction of spectral information coincident with known fields and subfields (blocks), and results tabulation.

KCP was selected as the test site because of its close proximity to the PF+ host airfield and because of the plantation's large-scale production of coffee ($1.86 \times 10^6 - 2.27 \times 10^6$ kilograms per year (kg/yr)). Mechanical harvesters dislodge coffee cherries at all stages of ripening. Ripe coffee cherries have by far the highest commercial value, commanding \$2–3 more per pound than either under- or over-ripe cherries. Because coffee field ripening is both spatially and temporally dynamic, the challenge for large-scale mechanical operations is to dispatch harvesters to the ripest fields on a given day. The acquired imagery will be downlinked to a payload control station located at KCP for immediate processing and delivery to harvest supervisors. Figure 1 shows the spatial domain of the plantation and the segmentation scheme that will be used to organize and present ripeness index data. In the framework of precision agriculture, the futuristic vision is that an aircraft such as PF+ will serve as a platform for successive-day near-real-time monitoring of coffee-field ripening in localized areas. In the broader picture, platforms such as PF+ can potentially support imaging needs of Earth resource and disaster monitoring.



Fig. 1. Color infrared image of KCP with field segmentation overlay.

The project is consistent with NASA's strategic goal of expanding and accelerating the realization of economic benefits from Earth science technology, and specifically aligns with the Earth Science Enterprise (ESE) Food and Fiber applications theme by furthering the development of remote sensing for agricultural decision-making. In addition, the project supports the ESE's goal of expanding the capability and reducing the cost of Earth observation. The project is sponsored by NASA's UAV Science Demonstrator Program.

Collaborators on this project were John C. Arvesen, Kauai Airborne Sciences; Frank Kidger, Kauai Coffee Plantation; Barry D. Ganapol, University of Arizona; Brian Yamamoto, Kauai Community College; Loren Gautz, University of Hawaii; Glen Witt, New Mexico State University; and Robert Curtin, AeroVironment Inc.

Point of Contact: S. Dunagan
(650) 604-4560
Stephen.E.Dunagan@nasa.gov

Airborne Measurements of Aerosols and Water Vapor in Support of the Chesapeake Lighthouse and Aircraft Measurements for Satellites (CLAMS) Experiment, 2001

Jens Redemann, Beat Schmid, John Livingston, James Eilers, Ric Kolyer, Stephanie Ramirez, Phil Russell

Knowledge of the concentration of atmospheric water vapor and aerosols (solid or liquid particles suspended in air) is crucial for assessing the effect of these constituents on climate. Such information can be determined using sunphotometers, which measure the transmission of the direct solar beam through the Earth's atmosphere in discrete, narrow wavelength bands from the ultraviolet to the near-infrared (IR) part of the solar spectrum. Frequently, suborbital (ground- and aircraft-based) sunphotometer measurements are used to validate aerosol and water-vapor data obtained using space-borne sensors.

One field experiment specifically designed to validate space-borne measurements was the Chesapeake Lighthouse and Aircraft Measurements for Satellites (CLAMS) field campaign, July 10–August 2, 2001. The CLAMS campaign targeted mostly

clear-sky conditions and entailed measurements from the Chesapeake Lighthouse research platform, several land sites, six research aircraft, and the Terra satellite of NASA's Earth Observing System (EOS). CLAMS research goals included validation of satellite-based retrievals of aerosol properties, vertical profiles of radiative fluxes, temperature, and water vapor. As part of the CLAMS experiment, the 14-channel NASA Ames Airborne Tracking Sunphotometer (AATS-14) was operated successfully aboard the University of Washington CV-580 research aircraft during 10 research flights (~45 flight hours total). Suborbital measurements of aerosol optical depth (AOD) and columnar water vapor (CWV) were also carried out at several ground sites and aboard 5 of the 6 airborne platforms using a variety of techniques. Figure 1 shows the AATS-14 installed on the University of Washington research aircraft.

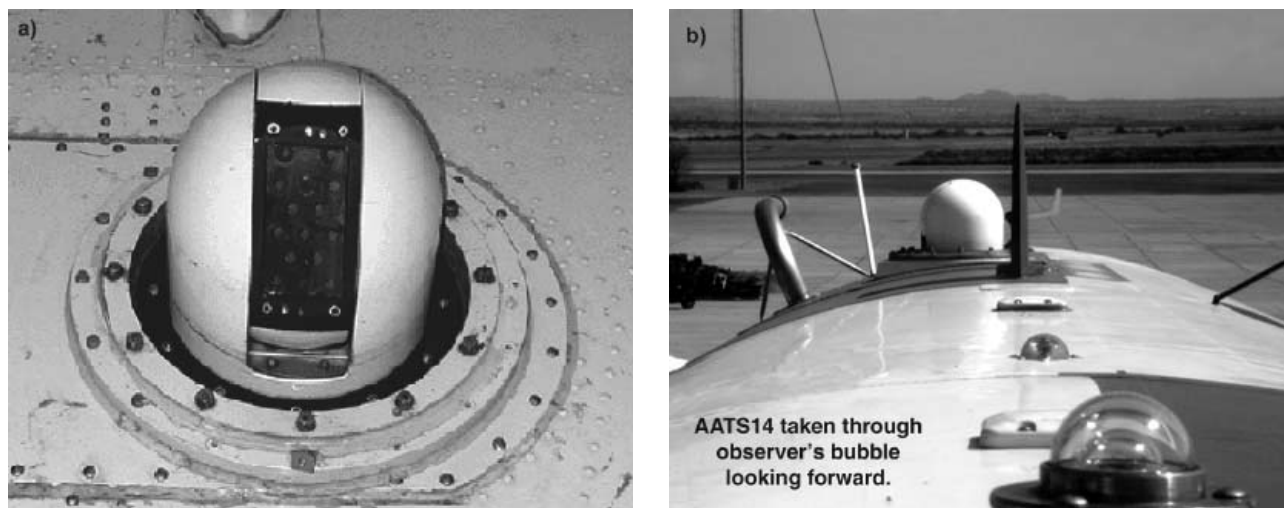


Fig. 1. The AATS-14: (a) close-up filter block of instrument facing the sun, (b) installed on the University of Washington CV-580 aircraft.

The AATS-14 measures the direct solar-beam transmission at 14 discrete wavelengths in the range of 354–1558 nanometers (nm), yielding aerosol optical depth spectra and columnar water vapor. Differentiation of AOD (CWV) with respect to altitude in favorable flight patterns allows the derivation of aerosol extinction (water-vapor density). During coordinated flights of the University of Washington CV-580, the AATS-14 measured full-column aerosol optical depth spectra at exact Terra overpass time on at least 7 occasions. For 5 of these opportunities, AOD in the midvisible part of the solar spectrum was at or below 0.1. During Terra overpass time on July 17, 2001, the AATS-14 measured the largest AOD encountered during the entire experiment (~0.48), including a horizontal gradient

in AOD of more than 0.1 over a distance of ~80 kilometers. Preliminary data can be viewed at <http://snowdog.larc.nasa.gov/ftp/incoming/clams/AATS/index.html>.

The following educational and research institutions collaborated with Ames Research Center on this experiment: University of Washington; University of Sao Paulo; NASA Goddard Space Flight Center; NASA Langley Research Center; Jet Propulsion Laboratory; and University of Maryland, Baltimore County.

Point of Contact: J. Redemann
(805) 658-2637
jredemann@mail.arc.nasa.gov

Airborne Tracking Sunpho-

tometry and Related Studies of Aerosols and Trace Gases

Philip B. Russell, Beat Schmid, Jens Redemann, John Livingston, Robert Bergstrom, James Eilers, Richard Kolyer, Duane Allen, Stephanie Ramirez, Dawn McIntosh

Sunphotometry is the measurement of solar beam transmission through the atmosphere. Such measurements, made for narrow bands of ultraviolet, visible, and infrared radiation, provide valuable information on the properties of aerosols and such trace gases as water vapor and ozone. Atmospheric aerosols (suspensions of particles comprising hazes, smokes, and thin clouds in the troposphere and stratosphere) play important roles in influencing regional and global climates, in determining the chemical composition of the atmosphere, and in modifying transport processes. In all these roles aerosols interact with trace gases through processes such as evaporation and condensation, photochemical reactions, and mutual interactions with the radiation field.

Using a single technique, sunphotometry, to study both aerosols and trace gases is often an advantage in understanding their properties and these interactions. A major objective of the Ames airborne sun-

photometry team is to make unique measurements of aerosols, water vapor, and ozone that address current scientific questions by taking advantage of the three-dimensional mobility of aircraft and other platforms (Figure 1). Another equally important objective is to use those and related measurements together with models in studies that clarify the roles of aerosols and trace gases in radiative transfer, climate change, and the processes that determine atmospheric composition and transport.

In FY01, efforts of the Ames airborne sunphotometry team focused on integrating the AATS-6 and -14 on three aircraft, making many flights in two major field campaigns, and analyzing data from these and previous campaigns. For the Spring 2001 campaign of the Asia-Pacific Aerosol Characterization Experiment (ACE-Asia), the AATS-6 was integrated on the National Science Foundation's

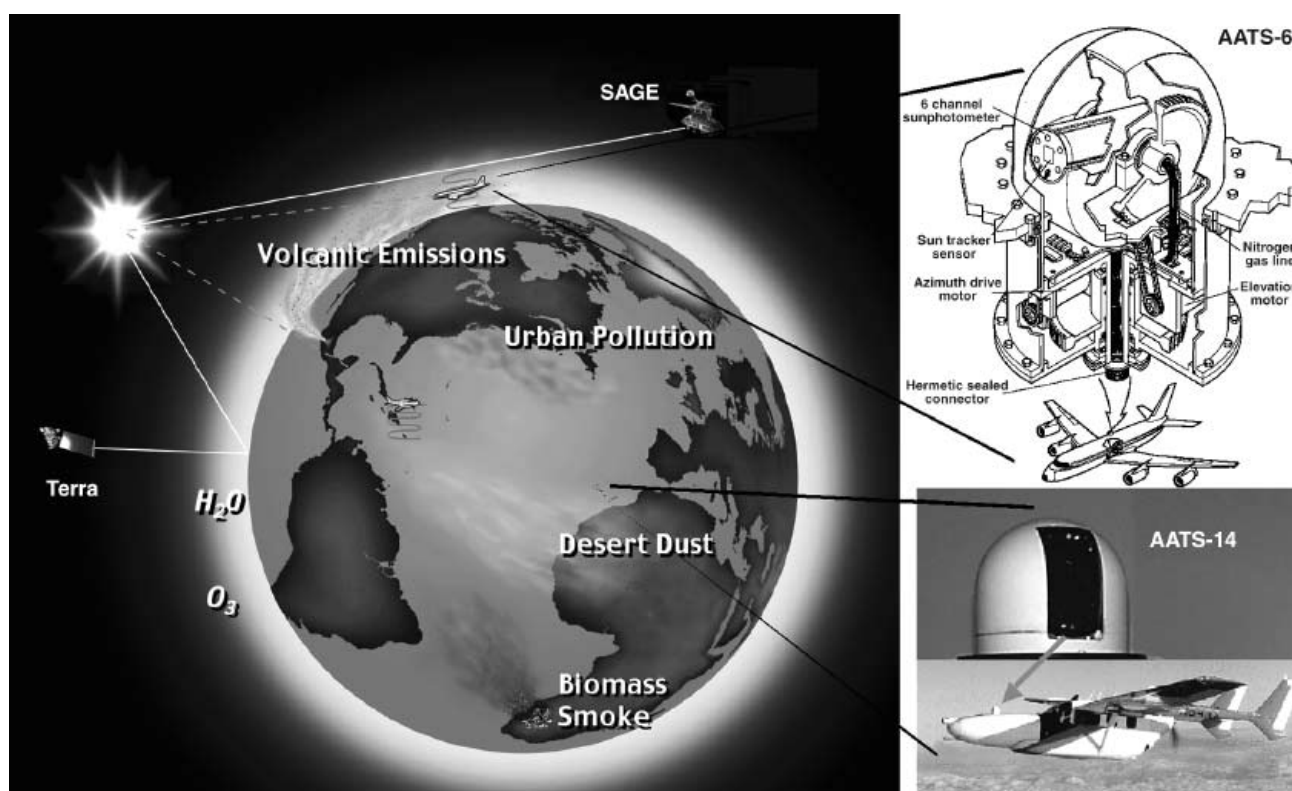


Fig. 1. Illustration of how the 6- and 14-channel Ames Airborne Tracking Sunphotometers (AATS-6 and AATS-14) have been used in a variety of experiments. They have flown on many different aircraft to study the major aerosol types of the globe and the associated water vapor and/or ozone. To help validate and extend satellite retrievals, AATS measurements are often coordinated with satellite overflights. Such coordinated measurements, with both nadir-viewers such as the Earth Observing System (EOS) Terra platform and limb-viewers such as the Stratospheric Aerosol and Gas Experiments (SAGE), also help place the AATS measurements in a larger spatial context. As shown, the AATS-6 and -14 are autotracking instruments that use motors to keep detectors pointed at the sun, independent of aircraft motion. The tracking head of each instrument mounts external to the aircraft skin, both to increase data-taking opportunities relative to in-cabin sunphotometers and to avoid data contamination by cabin-window effects.

C-130 aircraft, and the AATS-14 was integrated on the Twin Otter of the Center for Interdisciplinary Remotely Piloted Aircraft Studies (CIRPAS). For the Summer 2001 Chesapeake Lighthouse and Aircraft Measurements for Satellites (CLAMS) campaign, the AATS-14 was reintegrated on the University of Washington CV-580. The AATS-6 and -14 made 15 and 19 flights, respectively, in ACE-Asia, and the AATS-14 made another 10 flights in CLAMS.

The AATS-14 datasets are being used in continuing studies of several techniques for separating aerosol

and ozone contributions to solar-beam attenuation. The goal of these studies is to provide insights into aerosol/ozone separation for the Stratospheric Aerosol and Gas Experiment (SAGE II and SAGE III) spaceborne sensors, particularly when their measurements extend downward from the stratosphere into the troposphere. Related studies by team members combined SAGE II measurements with those by the Cryogenic Limb Array Etalon Spectrometer (CLAES) to develop maps and histories of stratospheric aerosol properties before and after the Pinatubo volcanic injection to the stratosphere.

Members of the Airborne Sunphotometer-Satellite Group are also active in studies of aerosol and trace-gas properties and effects that do not necessarily use AATS data. In FY01, these other studies produced journal papers on light absorption by carbon and other materials in aerosols, plus comparisons of water-vapor measurements by the AATS-6 and many other techniques in a 1997 experiment at the Department of Energy's Southern Great Plains Site.

The following educational and research institutions collaborated with Ames on this project: Goddard Space Flight Center; Langley Research Center; Jet Propulsion Laboratory; National Oceanic and

Atmospheric Administration (NOAA); California Institute of Technology; Georgia Tech; San Jose State University; State University of New York; University of California at San Diego; University of Illinois; University of Washington; Bremen University; Stockholm University; Tokyo University of Mercantile Marine; UK Meteorological Research Flight, UK Meteorological Office; University of Sao Paulo; and University of Tokyo.

Point of Contact: P. Russell
(650) 604-5404
Philip.B.Russell@nasa.gov

Direct Measurements of Stable Isotope Ratios in Nitrous Oxide in Air

Hansjürg Jost, James R. Podolske

Nitrous oxide (N_2O) is increasing at a rate of about 0.3% per year in the atmosphere. It is an important greenhouse gas and its decay products react with the ozone layer, potentially influencing the future of life on this planet. There is still a large uncertainty in the ground-level sources of N_2O , which are believed to be from biological activity. Isotopic ratios can be used to characterize such sources and help reduce the uncertainties in the source budget and add to our understanding of signatures of life.

Only limited isotopic data of the main sources (tropical soils, temperate soils) is currently available, and almost no isotope ratio data on seasonal and annual variations and changes in anthropogenic sources exist. An instrument with long-term, continuous determination of isotope ratios will contribute tremendously to a better characterization of N_2O sources and understanding of the underlying (physiological) processes.

A prototype instrument is being built to perform in situ, nondestructive measurements of isotope ratios of trace gases in ambient air in real time to allow continuous monitoring. It employs a tunable diode laser and state-of-the-art optical cavities. The cavities are 0.9-meter (m) long and with mirror reflectivities of greater than 99.99%, they have an effective path length of more than 9 kilometers (km). This long optical path allows accurate measurement of the weak spectroscopic features created by the different, rare isotopes of a trace gas.

This technology will lead to a field-deployable instrument.

Todd B. Sauke, SSX, Seti Institute, collaborated with the Ames investigators.

Point of Contact: H. Jost
(650) 604-0697
hjost@mail.arc.nasa.gov

Evolution of an Unmanned Aerial Vehicle Science Mission Capability

Steven S. Wegener

FY01 was a year of significant progress in the development of a capability to conduct airborne science missions from unmanned aerial vehicles (UAVs).

This project supports NASA goals in the Aero-Space Technology (Code R) and Earth Science (Code Y) Enterprises. Code R activities are funded by the Environmental Research Aircraft and Sensor Technology (ERAST) Program. The Code Y activities support the Suborbital Science Program.

The Aero-Space Technology ERAST Program is designed to bring focus to critical technology developments and flight demonstrations that reduce the technical and economic risk of using remotely piloted aircraft as a means to collect scientific data in a timely and cost-effective manner. The Earth Science Division supports ERAST by developing airborne science payloads and flight demonstration missions.

The Earth Science Enterprise (ESE), with the charter to study the Earth systems that drive the environment from the unique vantage point of space, depends on airborne studies to validate space-borne measurement and modeling efforts. UAVs have the potential to make airborne measurements in ways not possible from conventional aircraft, flying long-endurance and dangerous missions. The ESE has created the UAV Science Demonstration Program at the Ames Research Center in an effort to gain operational experience to evaluate the Earth science research and application value of these platforms.

UAVs, as evolving technology, have special needs in order to become viable and productive platforms. The UAV science mission demonstrations, managed by this project, are the only civil UAV appli-

cations being conducted to evolve the operational experience base required to develop the regulatory (airspace management and vehicle certification) framework and market perceptions.

In FY01, the ESE solicited science and application proposals utilizing UAVs as the airborne platform. Eleven high-priority proposals were selected to conduct implementation studies to reduce risk, and revised proposals were requested, reflecting the lessons learned in the implementation study. Final evaluations led to two proposals being selected and awarded. These studies include the "Altus Cumulus Electrification Study (ACES)" science mission to investigate lightning relationships and storm morphology, and the "Coffee Harvest Optimization Using UAV Platforms for the Acquisition of High Spatial Resolution Real-Time Multispectral Imagery" utilizing a solar electric UAV. The Earth Science Enterprise now has added UAVs to the stable of platforms available for airborne science and applications.

Another activity under the evolution of a UAV Science Mission Capability project included the First Response Experiment (FiRE). This effort was designed to put geo-registered multispectral imagery for a UAV in the hands of disaster managers in near-real-time. In September the Altus UAV, carrying the Airborne Infrared Disaster Assessment System (AIRDAS), and a satellite communications system acquired an image of a controlled burn near the El Mirage, California, airport (Figure 1), and placed a JPEG file on the World Wide Web (WWW) within three minutes. A geo-registered GIS image was then developed and placed on the WWW within an additional six minutes (Figure 2). This is the only civilian airborne payload that can provide geo-registered multispectral imagery in near-real-time.



Fig. 1. Altus flying over the controlled burn during demonstration flight at El Mirage, California.

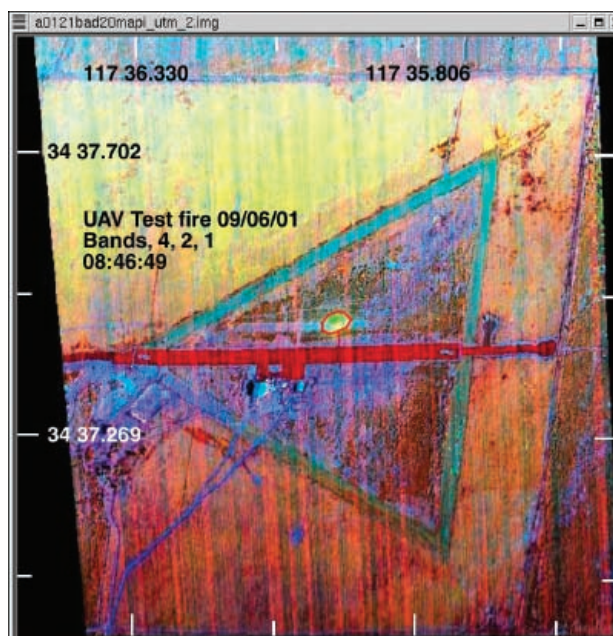


Fig. 2. Three-color image showing AIRDAS quicklook data over General Atomics' test range in El Mirage, California. Controlled burn appears as the bright yellow spot in the center of the image.

Point of Contact: S. Wegener
(650) 604-6274
Steven.S.Wegener@nasa.gov

Fourth Convection and Moisture Experiment (CAMEX 4): 15 August - 26 September 2001

R. Stephen Hipskind, Michael S. Craig

The Convection and Atmospheric Moisture Experiment 4 (CAMEX 4) was a large airborne field campaign sponsored by the Atmospheric Dynamics and Remote Sensing Program in NASA's Earth Science Enterprise. The primary objective of the experiment was to better characterize and understand tropical cyclones to eventually improve the capability to predict their intensification and precipitation amounts. The prediction of tropical cyclones, especially their track and landfall location, has improved dramatically over the last three decades, especially with the

advent of satellite-based surveillance. Still, one of the largest uncertainties is in understanding the mechanisms by which some storms intensify into Category 5 monster hurricanes and some that are predicted to intensify actually fizzle. The other large scientific uncertainty is the amount of precipitation generated by these tropical storms. Some of the largest hurricanes drop relatively light rainfall amounts while other smaller storms may lead to copious precipitation and flooding.

CAMEX 4 assembled an array of platforms and instruments to make measurements from the Earth's surface, space, and everywhere in between (Figure 1). Several research weather radars and a vertical radar wind profiler were set up and operated in the Florida keys. A special radiosonde operation was set up on Andros Island in the Bahamas. The heart of the project was the two NASA aircraft, the DC-8 and ER-2, as well as two National Oceanic and Atmospheric Administration (NOAA) P-3s. NOAA also flew the Gulfstream IV as part of the ongoing operational support of the National Hurricane Center, as did the Air Force 53rd Weather Reconnaissance Wing (the Hurricane Hunters) with their C-130s. NASA also funded the Australian

Aerosonde, an uninhabited aerial vehicle (UAV), to make meteorological measurements in the lowest 1500 meters over the ocean. The NASA aircraft were based at the Naval Air Station in Jacksonville, Florida, and the Aerosonde was based at the Mayport Naval Base just east of Jacksonville.

CAMEX 4 was scheduled to coincide with the climatological period with the most frequent tropical cyclones in the western Atlantic. There was a dearth of tropical storms during the experiment this year, but three tropical storms, two of which were hurricanes, were studied by flying into them. On the last three days of the project, three flight missions were flown into Hurricane Humberto, to study it from its



Fig. 1. A conceptual representation of the teams participating in CAMEX-4 and the relative locations of their bases of operations in the southeastern United States.

genesis as a tropical depression to a tropical storm and finally its intensification into a hurricane. On one of those flight days, six aircraft were stacked from the Air Force C-130s at the low altitude to the ER-2 at the 19-kilometer altitude. These flights returned unprecedented datasets from the storm and should lead to a better understanding of hurricane development. CAMEX 4 also accomplished several flights in support of the Keys Area Microphysics Project (KAMP), which focused on cloud dynamics, microphysics, and quantitative precipitation estimation.

CAMEX 4 was a close collaborative effort between NASA and the NOAA Hurricane Research Division. Unlike the previous CAMEX 3 mission in 1998, more effort was made to coordinate the aircraft flight tracks so that the aircraft were in the same geographical area at the same times. This will greatly enhance the ability to analyze the data from the different platforms. In addition, CAMEX 4 added a

dropsonde capability to the ER-2 aircraft. This is the first time ever that complete soundings have been made from the stratosphere to the surface in the middle of a tropical storm.

CAMEX 4 was composed of 28 Principal Investigators from five NASA Centers, two other government agencies (NOAA and the National Science Foundation (NSF)), and 10 universities. Other collaborators were the Air Force 53rd Weather Reconnaissance Wing, the U.S. Navy at Jacksonville, Mayport, and the Naval Air Station (NAS) Key West.

Robbie Hood, NASA Marshall Space Flight Center, collaborated with the Ames investigators. The Project Staff were Quincy Allison, Steve Gaines, Joe Goosby, Chris Scofield, Betty Symonds, Sue Tolley, and Kent Shiffer.

Point of Contact: S. Hipskind
(650) 604-5076
Roderick.S.Hipskind@nasa.gov

Global Distribution and Sources of Volatile and Nonvolatile Aerosol in the Remote Troposphere

Hanwant B. Singh, W. Viezee, Y. Chen, A. Tabazadeh, R. Pueschel

Airborne measurements of aerosol (condensation nuclei, CN) and selected trace gases made over areas of the North Atlantic Ocean during SASS Ozone and Nitrogen Oxides Experiment (SONEX) (October/November 1997), the south tropical Pacific Ocean during protein-exchange membrane (PEM)-Tropics A (September/October 1996), and PEM-Tropics B (March/April 1999) have been analyzed. The emphasis is on interpreting variations in the number densities of fine (>17 nanometers (nm)) and ultrafine (>8 nm) aerosol in the upper troposphere (8–12 kilometers (km)). These data suggest that large number densities of highly volatile CN (10^4 – 10^5 per cubic centimeter (cm^{-3})) are present in the upper troposphere, particularly over the tropical/subtropical region. CN number densi-

ties in all regions are largest when the atmosphere is devoid of nonvolatile particles. Through marine convection and long-distance horizontal transport, volatile CN originating from the tropical/subtropical regions can frequently affect the abundance of aerosol in the middle and upper troposphere at mid-to-high latitudes. Nonvolatile aerosols behave in a manner similar to tracers of combustion (carbon monoxide (CO)) and photochemical pollution as peroxyacetylnitrate (PAN), implying a continental pollution source from industrial emissions or biomass burning. In the upper troposphere, volatile and nonvolatile aerosol number densities are inversely correlated. Results from an aerosol microphysical model suggest that the coagulation of fine volatile

particles with fewer but larger nonvolatile particles, of principally anthropogenic origin, is one possible explanation for this relationship. In some instances the larger nonvolatile particles may also directly remove precursors (e.g., H_2SO_4) and effectively stop nucleation.

Collaborators on this project were B. Anderson, M. Avery, NASA Langley Research Center; P. Ha-

mill, San Jose State University; H. Fuelberg and J. R. Hannan, Florida State University, Tallahassee.

Point of Contact: H. Singh
(650) 604-6769
Hanwant.B.Singh@nasa.gov

Laboratory Studies of Atmospheric Heterogeneous and Multiphase Chemistry

Laura T. Iraci, Samantha Ashbourn

Interactions between gases and particles occur throughout the Earth's atmosphere, and they have consequences such as the formation of acid rain and the destruction of stratospheric ozone. To understand how these processes occur in the highly complex atmosphere, heterogeneous (gas/surface) interactions in a controlled laboratory setting are studied. By carefully varying parameters such as temperature, relative humidity, and particle composition, it is possible to isolate the response due to changes in each of these conditions in the real atmosphere. Results can then be used in an integrated analysis with field measurements and modeling studies to produce a more complete understanding of the environment and to predict how future changes in temperature or particulates may, in turn, affect the chemistry of the atmosphere.

A recent study was completed of the interaction of methanol with aqueous sulfuric acid solutions that mimic the particles found in the lower stratosphere. The motivation for this work was twofold: the conclusion of coworkers at Ames that a significant methanol sink is needed to balance the global budget, and observation of unexpectedly high levels of methanol in the remote marine atmosphere. In the laboratory, the uptake of methanol in aque-

ous 45–70 wt% H_2SO_4 solutions was measured at temperatures between 197 and 231 kelvin (K). The solubility increases with decreasing temperature and increasing acidity, with an effective Henry's law coefficient ranging from 10^5 to 10^8 moles per liter per atmosphere ($\text{moles liter}^{-1} \text{atm}^{-1}$). This equilibrium uptake of methanol into sulfuric acid aerosol particles in the upper troposphere and lower stratosphere will not appreciably alter gas-phase concentrations of methanol, nor does it provide the "missing sink" in the atmosphere.

In addition to simple dissolution and other equilibrium processes, a reaction between methanol and sulfuric acid at room temperature was observed. Unfortunately, this reaction is too slow to provide a sink for gaseous methanol at the temperatures of the upper troposphere and lower stratosphere. It is also too slow to produce sufficient quantities of soluble reaction products to explain the large amount of unidentified organic material seen in particles of the upper troposphere. These results contradict recent rate coefficients reported by workers at the Jet Propulsion Laboratory.

Another current project investigates the behavior of the halogen species hypobromous acid (HOBr),

hydrobromic acid (HBr), and hydrochloric acid (HCl) at temperatures warmer than those that lead to polar stratospheric cloud formation. The behavior of HOBr under these conditions is important, because it may enable chlorine activation and subsequent ozone destruction in “warm” regions of the atmosphere. A new laboratory facility will allow continued studies of the uptake and reactivity of halogenated and small organic molecules on sulfuric acid solutions that model the global sulfate aerosol

layer. Other areas of interest include the fate of ionic and nonionic solutes upon freezing of cloud droplets, and studies of aqueous phase transformations of oxygenated compounds of biogenic origin.

Point of Contact: L. Iraci

(650) 604-0129

Laura.T.Iraci@nasa.gov

Open-Path Diode Laser Hygrometer Instrument for Tropospheric and Stratospheric Water-Vapor Studies

James R. Podolske

The diode laser hygrometer (DLH), developed by NASA’s Langley and Ames Research Centers, has flown on the NASA DC-8 during several field missions, including subsonic aircraft: contrail and cloud effects special study (SUCCESS), Vortex Ozone Transport Experiment (VOTE), Tropical Ozone Transport Experiment (TOTE), SASS Ozone and Nitrogen Oxides Experiment (SONEX), Pacific Exploratory Mission (PEM) (PEM Tropics A and B), SAGE III Ozone Loss and Validation Experiment (SOLVE), ARM/FIRE Water Vapor Experiment (AFWEX), and the Transport and Chemical Evolution over the Pacific (TRACE-P) campaign of 2001. The optical layout of this sensor consists of the compact laser transceiver mounted to a DC-8 window port and a sheet of retro-reflecting “road sign” material applied to the DC-8 engine enclosure that completes the optical path. This sensor approach has numerous advantages, including compactness, simple installation, fast response time (50 milliseconds (msec)), no wall or inlet effects, and a wide dynamic measurement range (several orders of magnitude).

Using differential absorption detection techniques similar to those described in the literature, gas-phase water ($\text{H}_2\text{O}(\text{v})$) is sensed along a 28.5-meter

external path. For dry conditions (generally altitudes greater than 6 kilometers (km)) the diode laser wavelength is locked onto a strong, isolated line at $7139.1 \text{ per centimeter (cm}^{-1}\text{)}$, while for altitudes typically less than 6 km the laser wavelength is locked onto a weaker line at 7133.9 cm^{-1} . If the laser differential absorption signal is normalized with the laser power signal, the $\text{H}_2\text{O}(\text{v})$ measurement is unaffected by clouds, haze, plumes, etc., thereby enabling high spatial resolution measurements in and around clouds. The $\text{H}_2\text{O}(\text{v})$ mixing ratio is computed by an algorithm from the differential absorption magnitude, ambient pressure and temperature, and coefficients derived from laboratory calibration of the sensor.

During the AFWEX campaign in December 2000, DLH was flown with a suite of in situ and remote-sensing water instruments to assess the level of agreement between the various techniques.

Glenn Diskin and Glen Sachse, Langley Research Center, collaborated on this project.

Point of Contact: J. Podolske

(650) 604-4853

James.R.Podolske@nasa.gov

Thin Cirrus and Horizontal Transport Studies

Henry Selkirk, Leonhard Pfister, Marion Legg, Eric Jensen

This is a three-year program of diagnostic and modeling studies to elucidate two key issues that bear upon understanding the maintenance of water vapor and ozone distributions in the tropical tropopause layer (TTL) between 14 and 19 kilometers (km). The primary issue is the origin and persistence of high-altitude, thin cirrus clouds and their role, either direct or indirect, in controlling the concentrations of water vapor and ozone in the TTL. A second issue is the spatial distribution of quasi-horizontal in-mixing from higher latitudes into the TTL that may affect the vertical structure of ozone in the TTL.

Convective influence analyses are ongoing of airborne differential absorption lidar (DIAL) observations of thin cirrus from NASA missions in the tropical Pacific and Atlantic oceans over the course of the past decade. This analysis will allow determination of whether these thin cirrus layers in the TTL are residuals left over from deep convective events or independent cloud features formed in situ from slow, radiatively forced ascent.

At the completion of the convective influence analysis, simple modeling calculations will be done of the thin cirrus events using the explicit microphysical model developed at Ames Research Center. An attempt will be made to reproduce the gross microphysical characteristics of the observed thin cloud in the context of the thermal history of the air parcels derived from the convective influence analyses.

The investigations of horizontal transport use trajectory analysis techniques to address the spatial variations of ozone in the TTL that may be due to the horizontal transport from higher latitudes, in particular the longitudinal gradient in ozone that has been observed in the equatorial Pacific.

Point of Contact: H. Selkirk
(650) 604-6489
hselkirk@mail.arc.nasa.gov

Transport and Meteorological Analysis

Leonhard Pfister, Henry Selkirk

The objectives of work performed under this overall task are twofold. First, provide meteorological guidance to airborne field missions for NASA's Upper Atmosphere Research Program, NASA's Radiation Sciences Program, and NASA's Global Tropospheric Experiment (GTE). This includes providing, in real time, and archiving extensive meteorological satellite datasets for use by the mission scientist and by the science team. During FY01, significant meteorological mission preparation work was done for the upcoming CRYSTAL-FACE mission, a radiation sciences field program aimed at understanding the radiative and microphysical properties of cirrus

clouds in the Florida region during summer 2002. Among the tools available is providing real-time information on convectively influenced air for mission planning, essentially by a combination of trajectory modeling and satellite imagery. This technique uses this tool to establish which air masses have been recently influenced by convection. It is expected to be used during the upcoming CRYSTAL-FACE mission. For GTE, some preliminary meteorological investigation has been done for the proposed Intercontinental Transport Experiment (INTEX), to be performed in 2004 and 2005.

The second objective is scientific analysis of the data from the airborne field missions. This analysis consists of four basic areas: (1) water vapor and subvisible cirrus clouds in the upper tropical troposphere, (2) water vapor in the winter arctic tropopause region, (3) gravity waves and turbulence, and (4) tropospheric chemistry. The first of these issues is fundamental to the input of water vapor into the stratosphere, which is an important factor in stratospheric gas-phase chemistry and for the formation of polar stratospheric clouds (PSCs). The chemistry on PSCs, in turn, is responsible for much of the ozone loss due to chlorinated hydrocarbons. The second area, water vapor in the arctic upper troposphere and lower stratosphere, is potentially important to the formation of ice clouds that can have similar chemical effects as the PSCs. Gravity waves are important because: (a) they produce turbulence, which can affect vertical mixing of stratospheric trace constituents; (b) they transport momentum upward, which drives important features of the stratospheric circulation such as the tropical quasi-biennial oscillation; and (c) they produce temperature deviations that can produce subvisible cirrus clouds. The fourth area involves investigating the effects of convection on tropospheric chemical trace constituents, including the distribution of boundary layer trace constituents (either naturally or anthropogenically generated) throughout the troposphere by convection.

To deal with the four areas of scientific analysis, some important analysis tools have been developed. The most novel of these is the “convective influence” calculation, whereby calculation is made, using a combination of back trajectories and meteorological satellite data, of the amount and age of recent “convective influence” on an air parcel. This technique has been used in connection with the first area of scientific analysis indicated previously, namely subvisible cirrus clouds in the upper tropical troposphere. Specifically, an assessment was made as to whether subvisible cirrus clouds observed during the 1995–1996 Tropical Ozone Transport

Experiment/Vortex Ozone Transport Experiment (TOTE/VOTE) were produced by local cooling and ice nucleation or were a long-lived outflow from convection. Good correspondence was found between the locations of different types of near-tropopause cirrus and the origins of the air, with smooth laminar cirrus clearly the result of local cooling, and lumpier clouds the apparent outflow of convection. Notably, it appears that some of this convective outflow can last several days, based on calculations. Also noted was the presence of inertia-gravity waves and their characteristics. These waves have a very good correspondence to the sloping cloud shapes, indicating that the cooling associated with these waves is probably responsible for the clouds.

This last result is significant, because it lends support to a hypothesis that is the result of modeling work. This hypothesis suggests that long-period waves produce cirrus clouds, which are then heated and lofted into the stratosphere. As the clouds grow, large particles fall out, dehydrating the air. In effect, this mechanism will move air into the stratosphere and dehydrate it at the same time, possibly resolving a crucial question of how very dry air gets into the lower tropical stratosphere.

The convective influence technique has also yielded insight into some of the results from the Atmospheric Chemistry of Combustion Emission Near the Tropopause (ACCENT) experiment. As a result of this technique, it is possible to trace high values of methyl nitrate in the upper troposphere over the Gulf of Mexico to convection in the eastern Pacific. The significance is that the ability to understand one component (convection) of why air masses have the composition that they do is possible. Developing an understanding of the effect of natural processes (e.g., convection) on air masses is certainly a prerequisite for understanding the effect of human processes (e.g., continental scale air pollution).

With the completion of the SAGE III Ozone Loss and Validation Experiment (SOLVE), some re-

sults on the second area of scientific analysis were obtained, namely water vapor in the winter arctic tropopause region. There are three major conclusions. First, troposphere-to-stratosphere exchange extends into the arctic stratosphere to about 13 kilometers (km), about 3.5 km above the prevailing average tropopause. Second, based on observed water-vapor and temperature histories during early spring, about 20% of air parcels that have ozone values between 300 and 350 parts per billion by volume (ppbv) (in other words, well within the arctic stratosphere) experience ice saturation sometime during a given 10-day period. This is potentially significant, because ice clouds within the lowermost

stratosphere can lead to possible chlorine activation. Third, at the tropopause during a given 10-day period during early spring, 5–10% of parcels experience ice saturation even if their water vapor content is at the prevailing stratospheric value of 5 parts per million by volume (ppmv). This means that the arctic tropopause may act as a major drying mechanism for the upper troposphere during spring, a fact that is important for the Earth's radiation budget.

Point of Contact: L. Pfister
(650) 604-3183
Leonhard.Pfister-1@nasa.gov

Climate Forcing by Clouds and Aerosols: Two Years of Field Studies

Peter Pilewskie, Warren Gore, Larry Pezzolo

Researchers at Ames Research Center (ARC) contributed to four major multiagency field campaigns conducted during FY00 and FY01. These experiments were geared toward improving the understanding of how aerosols and clouds affect global climate through their influence on the radiative energy budget. In the case of atmospheric aerosols, for example, it is considered that their impact may mitigate to some degree the expected warming due to the increasing concentrations of carbon dioxide and other greenhouse gases. The extent to which aerosols may reduce global warming depends on how they absorb and scatter radiation and on the spatial and temporal distribution.

The ARC Radiation Group has measured the spectral distribution of solar radiation from various airborne platforms during the Department of Energy (DOE) Atmospheric Radiation Measurement (ARM) Atmospheric Radiation Measurement Enhanced Shortwave Experiment II (ARESEII) mission in FY00; the Office of Naval Research (ONR)/NASA Puerto Rico Dust Experiment (PRIDE) in FY00; the NASA Southern African Regional Science Initiative (SAFARI) 2000 mission in FY00; and the ONR/National Science Foundation (NSF) Aerosol Characterization Experiment (ACE)-Asia experiment in FY01. During FY01 the group made significant strides in interpreting the data collected from these experiments.

Puerto Rico Dust Experiment (PRIDE)

For the first time the absorption spectrum of Saharan dust aerosol has been derived and its spectral radiative forcing determined. This was achieved by measuring solar spectral radiative flux above and below layers of dust in the atmosphere over the western Atlantic Ocean. The origin of the dust

aerosol can be traced to the Sahara Desert. Thus the influence of Saharan dust is of global scale and the radiometric observations will enable determination of how this dust affects the global energy balance. Figure 1 shows results from PRIDE.

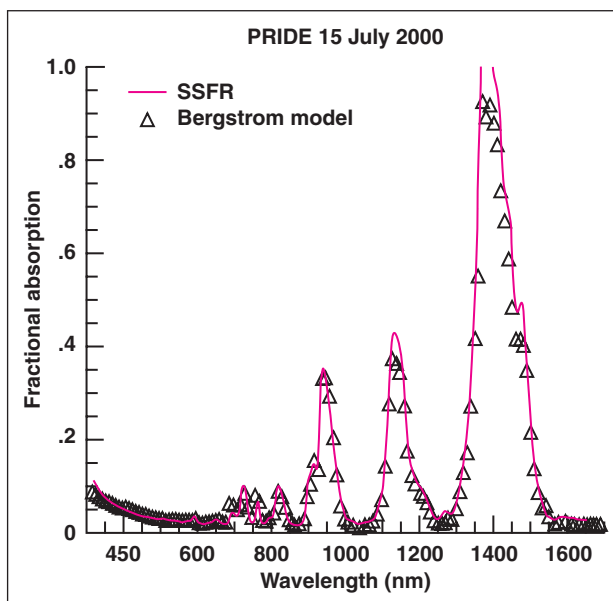


Fig. 1. Measured (blue curve) and modeled (red symbols) fractional dust absorption for a Saharan air layer during the PRIDE flight on July 15, 2000. In the near infrared, water vapor is a strong absorber in several bands; at wavelengths less than 600 nanometers (nm) the absorption is due primarily to dust. The calculation is from a correlated-k distribution model developed by R. Bergstrom and custom designed to match solar spectral flux radiometer (SSFR) spectral range and slit function.

Atmospheric Radiation Measurement Enhanced Shortwave Experiment II (ARESEII)

The ARESEII mission was conducted to determine the amount of solar radiation absorbed by cloud layers. This topic has remained a large source of concern in the radiation science community because

its uncertainty is considered to be the largest in the entire global radiation budget and perhaps four times as large as the expected forcing due to a doubling of carbon dioxide. The Ames Radiation Group has provided the first simultaneous measurements of a complete spectrum of solar radiation reflected from and transmitted through clouds. This enables assessment of the performance of models used to predict the amount of solar radiation absorbed by clouds. One finding is that the most detailed radiative transfer models can quantitatively match the measured cloud absorption over much of the solar spectrum. However, in some bands discrepancies between measurement and model remain and need to be resolved in order to better understand the role of clouds in the climate system. For example, a comparison between measured and modeled cloud irradiance and albedo during ARESEII in Figure 2 shows a discrepancy between measured and modeled upwelling irradiance as high as 5% in the mid-visible. However, this may be due to errors in the

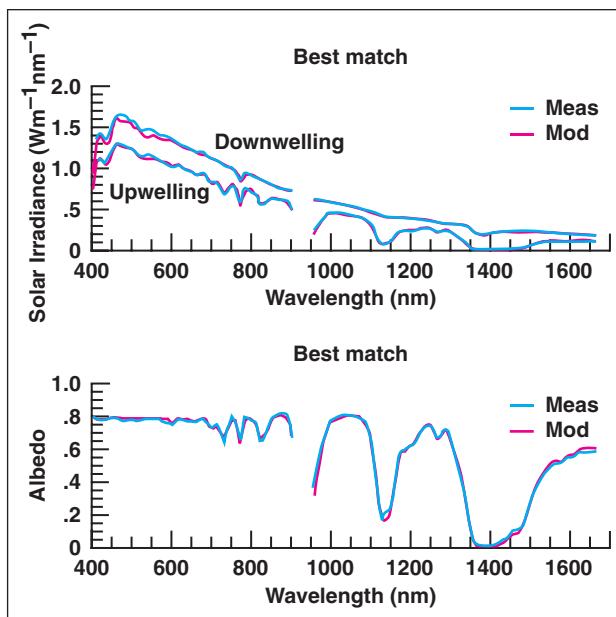


Fig. 2. Upper Panel: Comparison between SSFR measured (blue spectra) and modeled (red spectra) upwelling and downwelling spectral irradiance for the ARESEII case on March 29, 2000. The retrieved cloud optical depth was 45 and the effective droplet radius was 9.5 microns. Lower Panel: Measured and modeled albedo (ratio of upwelling to downwelling) for the same case.

exoatmospheric solar source function rather than the cloud model.

Southern African Regional Science Initiative (SAFARI)-2000

In a manner similar to the analysis of PRIDE spectral irradiance, the spectral absorption properties of dust and smoke aerosol in the atmosphere over the southern African continent has been determined and found to be quite varied. Aerosol radiative properties depend on composition, size, and shape and thus are linked to their origin. During the southern Africa dry season there are various sources of smoke and dust ranging from anthropogenic sources such as industrial and agricultural burning to wind-borne dust linked to agricultural practices. These efforts will aid in determining how these various types of aerosol can affect the radiative energy balance over this region.

Aerosol Characterization Experiment-Asia (ACE-Asia)

ACE-Asia conducted in FY01 was the third in a series of experiments focused on aerosol radiation and chemistry. This latest ACE mission focused primarily on Asian dust. ARC personnel contributed by measuring solar spectral radiative flux throughout the lower troposphere. Twenty flight missions took place over a six-week period in March and April, during which time nearly 200,000 spectra were collected. Data are being analyzed in much the same manner as during PRIDE and SAFARI-2000. Preliminary analysis indicated that the Asian dust absorption is similar in its spectral signature to the Saharan dust that was observed over the western Atlantic.

Collaborators on this project were Maura Rabbette, John Pommier, Steve Howard, and Robert Bergstrom, BAERI.

Point of Contact: P. Pilewskie
(650) 604-0746
Peter.Pilewskie-1@nasa.gov

Discriminating Type Ia and Ib Polar Stratospheric Clouds in POAM Satellite Data

Anthony W. Strawa, Katja Drdla, Rudolf F. Pueschel

A method for discriminating Type Ia and Ib polar stratospheric clouds (PSCs) from Polar Ozone and Aerosol Measurement (POAM) satellite occultation measurements of the aerosol extinction coefficient is described. The method has been validated by applying several statistical tests to the results and by using differential absorption lidar (DIAL) and OLEX lidar observations made during SAGE III Ozone Loss and Validation Experiment/Third European Stratospheric Experiment on Ozone (SOLVE/THESEO) 2000. Type Ia PSCs are believed to be composed of large nitric-acid-containing particles that will sediment out of the stratosphere, causing denitrification and facilitating ozone depletion. Type Ib PSCs are believed to be much smaller and will not sediment out of the stratosphere. Discriminating between these two types of PSCs is significant because it will permit a better understanding of ozone depletion today and predict the fate and effect of PSCs using the more continuous temporal coverage and larger areal coverage that can be obtained from satellites.

The method is made possible by the character of Polar Ozone and Aerosol Measurement (POAM) observations when plotted as normalized extinction versus wavelength dependence. As the extinction increases, observations of Type Ia and Ib PSCs bifurcate. This behavior is also observed in idealized simulations of the formation of Type Ib PSCs and NAT (nitric oxide trihydrate) particles, which are believed to make up Type Ib and Ia PSCs, respectively.

Analysis during FY01 of POAM observations from the 1999/2000 Arctic winter using the PSC

discrimination algorithm revealed that the number of PSC observations peaked in January. In November, December, and January the ratio of Type Ia to Ib PSCs was about 3. In February and March this ratio was about 0.3. The average altitude of Type Ia PSCs descended more than that of the Type Ib PSCs, especially in the spring, when the Type Ia observations were 2 to 3 kilometers (km) below those of the Type Ib observations. This is consistent with observations of denitrification during the 1999/2000 winter.

The PSC discrimination algorithm is applicable to previous winters in both hemispheres, and will work with Stratospheric Aerosol and Gas Experiment (SAGE) III observations as well. This will permit a more extensive study of the statistical significance of some features of the PSCs observed during the 1999/2000 Arctic winter. It is thought that the present method of analyzing satellite data to discriminate Type I PSCs will be of great utility in the study of PSCs and ozone depletion.

Collaborators on this project were M. Fromm, Computational Physics, Inc.; K. W. Hoppel, Naval Research Laboratory; E. V. Browell, NASA/Langley Research Center; P. Hamill, San Jose State University; and David P. Dempsey, San Francisco State University.

Point of Contact: A. Strawa
(650) 604-3437
Anthony.W.Strawa@nasa.gov

Evidence for the Widespread Presence of Liquid-Phase Particles During the 1999-2000 Arctic Winter

Katja Drdla, T. P. Bui, H. Jost, J. Greenblatt

In situ Multiangle Aerosol Spectrometer Probe (MASP) particle measurements have been analyzed to determine the typical behavior of sulphate particles during the SAGE III Ozone Loss and Validation Experiment (SOLVE) campaign. The study has explored variations in the total particle concentration measured by MASP. A new analysis method has been developed that accounts for several known sources of variability in MASP concentrations. In the resulting dataset, variations in MASP concentration reveal the growth characteristics of small particles (those that are smaller than 0.2 micron (μm) in radius at midlatitudes). The method also allows all the MASP measurements made during the SOLVE campaign to be incorporated in a single analysis.

At all levels of the stratosphere, the total MASP concentration varies continuously with temperature. This behavior is well reproduced by assuming that the sulphate aerosols are liquid solutions, but cannot be reproduced if the aerosol is assumed to be frozen. At sufficiently cold temperatures, larger increases in the MASP concentration are consistently seen; the observed onset temperature for this increase is in good agreement with model expecta-

tations for liquid ternary solutions. Liquid-like behavior is apparent for all measurements made during SOLVE, both inside and outside the vortex, and even at the coldest temperatures sampled during the campaign. The only anomalous measurements were made during the flight of January 14, 2001; however, this midlatitude flight was very unlikely to contain sulphuric acid tetrahydrate particles based on the recent warm temperatures experienced by the air. At the levels with the coldest measured temperatures, which cause maximum particle sizes and thus the greatest total MASP concentrations, 90% of the particles grow as liquids. Therefore, the freezing that occurred during the 1999–2000 Arctic winter was selective, causing most of the particles to remain liquid even in the presence of a small number of frozen particles.

B. W. Gandrud and D. Baumgardner, NCAR; J. C. Wilson, University of Denver; D. Hurst, S. M. Schauffler, NCAR; and C. R. Webster, JPL, collaborated with the Ames investigators.

Point of Contact: K. Drdla
(650) 604-5663
Katja.Drdla-1@nasa.gov

Ice Cloud Formation and Dehydration Along Parcel Trajectories in the Tropical Tropopause Layer

Eric Jensen, Leonhard Pfister

Stratospheric water vapor is important not only for its greenhouse forcing, but also because it plays a significant role in stratospheric chemistry. Several recent studies have focused on the potential for dehydration due to ice cloud formation in air ris-

ing slowly through the tropical tropopause layer. These studies showed that temperature variations associated with horizontal transport of air in the tropopause layer can drive ice cloud formation and dehydration.

In this study, a Lagrangian, one-dimensional cloud model is used to further investigate cloud formation and dehydration as air is transported horizontally and vertically through the tropical tropopause layer. Time-height curtains of temperature are extracted from meteorological analyses. The model tracks the growth and sedimentation of individual cloud particles. The regional distribution of clouds simulated in the model is comparable to the subvisible cirrus distribution measured by the Stratospheric Aerosol and Gas Experiment (SAGE) II satellite. The simulated cloud properties depend strongly on the assumed ice supersaturation threshold for ice nucleation. With effective ice nuclei present (low supersaturation threshold), ice number densities are high ($0.1\text{--}10$ per cubic centimeter (cm^{-3})), and ice crystals do not grow large enough to fall very far, resulting in limited dehydration. With higher supersaturation thresholds, ice number densities are much lower ($< 0.01 \text{ cm}^{-3}$), and ice crystals grow large enough to fall substantially; however, supersaturated air often crosses the tropopause without cloud formation. The clouds typically do not dehydrate the air along trajectories down to the temperature

minimum saturation mixing ratio. Rather the water-vapor mixing ratio crossing the tropopause along trajectories is typically 10–50% larger than the saturation mixing ratio.

Figure 1 shows the simulated distribution of water vapor near the tropopause (about 17 kilometers (km)) in the tropics, along with the frequency of clouds from the model calculations. The driest regions are generally displaced to the west of the cloud formation regions because of the rapid horizontal transport of air parcels near the tropopause. Hence, the water-vapor concentration measured in a particular location may be completely unrelated to cloud processes occurring nearby. Multidimensional models, including horizontal transport, vertical transport, and cloud microphysics, are required to investigate dehydration of air entering the stratosphere.

Point of Contact: E. Jensen
(650) 604-4392
Eric.J.Jensen@nasa.gov

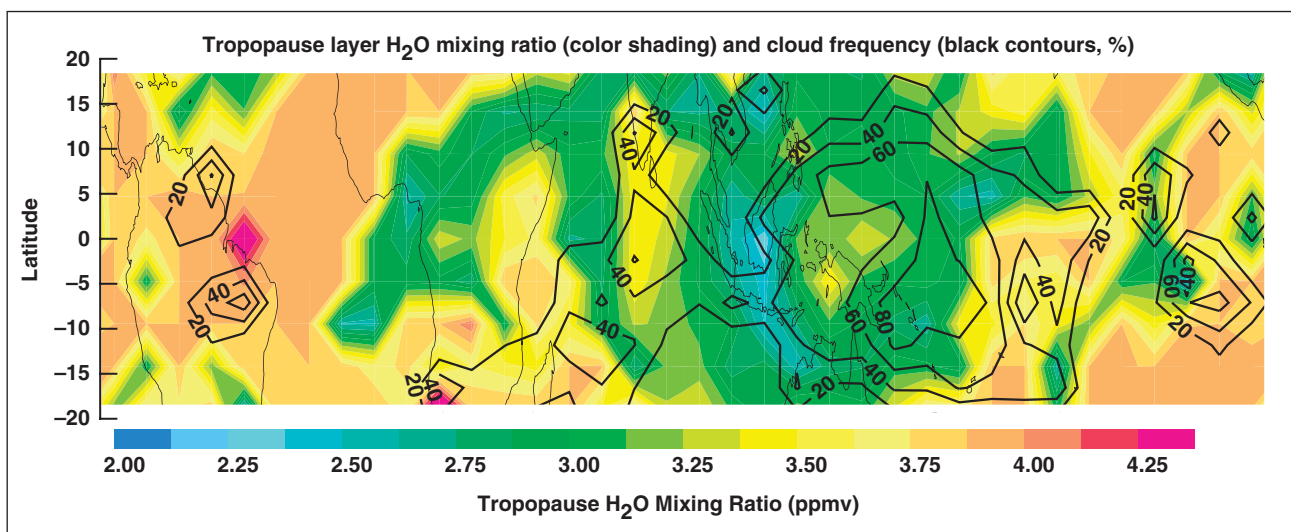


Fig. 1. The distribution of water-vapor mixing ratio (color shading) near the tropopause (about 17 km) is shown for the tropics (within 20 degrees of the equator) based on model calculations. The black contours show the frequency (percentage) of clouds near the tropopause in the model. The clouds form most frequently just east of Indonesia, but the driest regions are displaced to the west because of rapid horizontal transport of air near the tropopause.

In Situ Measurement of Particle Extinction

Anthony W. Strawa

Aerosol optical properties are extremely important in assessing climate change. The lack of sufficient knowledge of aerosol optical properties and their variability in the atmosphere have led the Intergovernmental Panel on Climate Change (IPPC) to rate the effect of aerosol as the most uncertain of all parameters considered important to climate change. Currently, these aerosol properties are obtained from filter samples that measure absorption of black carbon aerosols on a time scale of tens of minutes to hours. Aerosol variability causes significant changes in optical properties on the order of seconds, especially when sampled from aircraft. Thus, the research community is very interested in an instrument that can measure the optical properties of all aerosols, not just black carbon, on a time scale of seconds.

The Ames researchers are working with Informed Diagnostics, Inc. (ID) to develop an innovative instrument using cavity ring-down absorption spectroscopy (CRDS) to measure the extinction and scattering coefficients of aerosol and consequently the single-scatter albedo. The prototype instrument measures the extinction and scattering coefficient at 690 nanometers (nm) and the extinction coefficient at 1550 nm. The instrument itself is small (24 x 19 inches) and relatively insensitive to vibrations. The prototype instrument has been tested in the lab (Figure 1) and used in the field. Although improvements in performance are needed, the prototype has been shown to make accurate and sensitive measurements of extinction and scattering coefficients (Figure 2). If these two parameters are combined, it is possible to obtain the single-scattering albedo and absorption coefficient, both important aerosol properties. The use of two wavelengths also allows a quantitative idea of the size of the aerosol through the Ångström exponent to be obtained. Minimum sensitivity of the prototype instrument is 1.5×10^{-6}

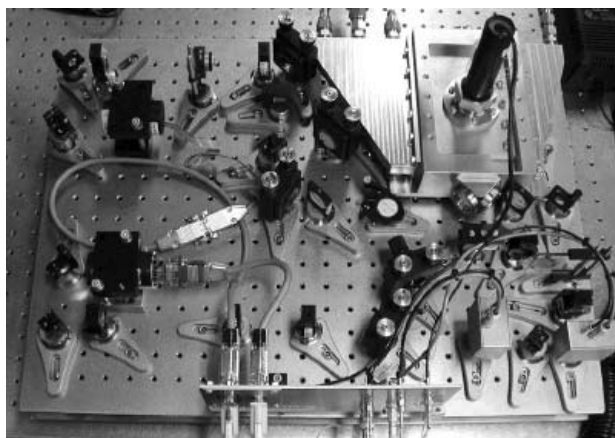


Fig. 1. The prototype instrument in the laboratory. The lasers are in the foreground and the cell is the aluminum block in the rear.

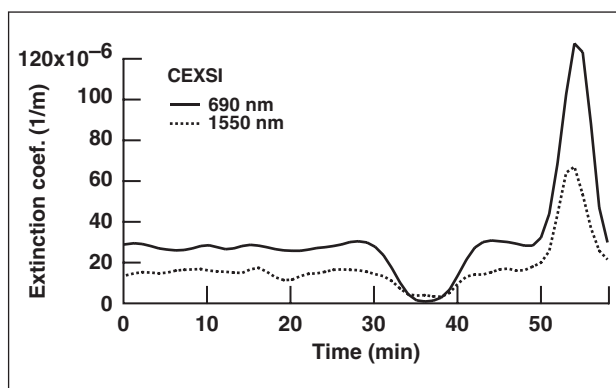


Fig. 2. Measurement of aerosol extinction coefficient at NASA ARC.

per meter (m^{-1}) (1.5 per micron (μm^{-1})). The prototype instrument demonstrates (1) fast and accurate measurement of aerosol extinction, (2) measurement of aerosol scattering in a CRDS system, and (3) simultaneous measurement at two laser wavelengths. The instrument proved capable of measuring the extinction of ammonium sulfate aerosol typical of the mid- to high-troposphere background aerosol. At the same time the scattering of the aerosol was measured, and an estimate of its single-

scatter albedo could be made. Continued development of this technology is expected to lead to a flight-ready instrument.

T. Owano, BlueLeaf Networks, Inc., collaborated with the Ames researchers.

Point of Contact: A. Strawa
(650) 604-3437
Anthony.W.Strawa@nasa.gov

Intensity Measurements of CO₂ Absorption Bands Between 5218 and 5349 cm⁻¹

Lawrence P. Giver, Charles Chackerian, Jr., Richard S. Freedman

Line positions and intensities for several hundred bands of carbon dioxide (CO₂) are tabulated in the high-resolution transmission molecular absorption database (HITRAN) compilation of spectra of atmospheric interest. The intensities of most of the weak bands in this compilation have not been measured; they have instead been determined from “Direct Numerical Diagonalization” (DND) as described in the literature. Many of these bands are significant absorbers in Venus’ hot, dense atmosphere, because it is composed predominantly of CO₂. Some weak bands are prominent absorbers in the Venus near-infrared emission windows. Laboratory measurements were previously made of the band at 4416 per centimeter (cm⁻¹) band, which is prominent in the 4040 to 4550 cm⁻¹ emission window, and, therefore, the correct intensity was important in the modeling work of others.

Measurements have been done on the 01121-00001 perpendicular band at 5315 cm⁻¹ and three of its hot bands. The DND intensity computations for the combination perpendicular bands have not been regarded as reliable, so measurements of several of these bands can be used to improve the computations of the many other bands that cannot be measured. Indeed, the measured intensity for the 5315 cm⁻¹ band is about double the DND computed intensity adopted for the 1992 HITRAN computation.

Linda R. Brown, JPL, collaborated on this project.

Point of Contact: L. Giver
(650) 604-5231
lgiver@mail.arc.nasa.gov

Laboratory Measurements of Near-Infrared Water Vapor Bands Using the Solar Spectral Flux Radiometer

Lawrence P. Giver, Peter Pilewskie, Warren J. Gore, Charles Chackerian, Jr., Richard S. Freedman

Several groups have recently been working to improve the near-infrared spectrum of water vapor in the high-resolution transmission molecular absorption database (HITRAN). The unit-conversion errors found previously have now been corrected in the recently released HITRAN-2000.

But new measurements by other workers show the total intensity of the water-vapor band at 1130 nanometers (nm) about 38% stronger than the sum of the line intensities on the revised HITRAN list in this region.

It was important to quickly determine if the HITRAN intensity values are in error by as much as claimed by others. Only intensity errors for the strong lines could result in the total band intensity being in error by such a large amount. To quickly get a number of spectra of the near-infrared region from 650 to 1650 nm, the solar spectral flux radiometer (SSFR) was used in the laboratory with the 25-meter base path White absorption cell. This moderate-resolution spectrometer is a flight instrument that has flown on the Sandia Twin Otter for the Atmospheric Radiation Measurement Enhanced Shortwave Experiment II (ARESE II). The measured band profiles were then compared to calculated spectra using the latest HITRAN line intensities, convolved with the SSFR instrumental resolution.

The spectra of the 1130-nm band, in fact, have somewhat more absorption than the HITRAN simulations, but not as much as the 38% intensity

increase for this band suggested in the literature. Although not uniform over the entire band, an intensity increase of about 20% on average would be more compatible with the data. The HITRAN line intensities in the 1130-nm band were adopted from values in the literature. It is expected that these measurements of the strong lines have significant errors because the experimental conditions were not optimized to make good intensity measurements of these lines. These lines were typically saturated at the long path lengths used to determine good positions, assignments, and intensities of the many weaker lines.

Prasad Varanasi, SUNY at Stony Brook, collaborated on this project.

Point of Contact: L. Giver
(650) 604-5231
lgiver@mail.arc.nasa.gov

Microphysical Modeling of Chlorine Activation and Ozone Depletion

Katja Drdla

The effect of a range of assumptions about polar stratospheric clouds (PSCs) on ozone depletion during the 1999–2000 Arctic winter were assessed during FY01 using a coupled microphysical/photochemical model. Simulations spanned a large range of denitrification levels, with up to 80% vortex-average denitrification; individual trajectories had even larger denitrification values, and up to 40% dehydration. In addition, the composition of the PSCs was varied (ternary solutions, nitric acid trihydrate, nitric acid dihydrate, or ice) to explore sensitivity to heterogeneous reaction rates.

The presence of PSCs in the lowermost stratosphere during the month of February was found to be critical in causing severe ozone depletion below

500 kelvin (K). Heterogeneous reactions on these PSCs were able to reactivate the chlorine nitrate (ClONO_2) produced as sunlight returned to the vortex. Only to 30% to 40% vortex-average ozone loss, depending on denitrification level, would have occurred without this chlorine reactivation; with chlorine reactivation, an additional 21% to 32% ozone loss is possible. During February (unlike earlier in the winter) the extent of chlorine reactivation and severity of ozone loss were sensitive to the heterogeneous reaction rates; varying the heterogeneous reactivity altered ozone loss by 11%. The heterogeneous chemistry occurred primarily from 0 to 4 K below the nitric acid trihydrate condensation point; however, many uncertainties influence heterogeneous reaction rates at these temperatures.

The chlorine reactivation during February also prevented denitrification from enhancing ozone loss until March: 70% vortex-average denitrification enhanced ozone depletion by only 3% on March 10. The breakup of the vortex at this time probably limited the extent of ozone depletion during the 1999–2000 winter. If the vortex had remained stable until April 15, further ozone loss could have been caused by the observed levels of denitrification. On April 15, 16% ozone loss (out of a total 68% ozone loss) could be caused by 70% denitrification. Ozone

loss intensifies nonlinearly with enhanced denitrification: in individual air parcels with 90% denitrification, more than 40% ozone loss in mid-April can be attributed to denitrification alone.

M. R. Schoeberl, GSFC, collaborated with the Ames investigator.

Point of Contact: K. Drdla
(650) 604-5663
Katja.Drdla-1@nasa.gov

Microphysical Modeling of Polar Stratospheric Clouds, Denitrification, and Dehydration

Katja Drdla

The freezing processes that may lead to the formation of solid-phase polar stratospheric clouds (PSCs) have been examined to assess their winter-long effects, especially denitrification, in a coupled microphysical/photochemical model. Trajectory simulations using data from November 1999 to April 2000 used a large set of trajectories that provided representative coverage of the entire Arctic vortex through the period of PSC formation and ozone depletion.

A freezing process occurring at temperatures above the ice frost point is shown to be necessary to explain both the occurrence of solid-phase PSCs early in the winter and denitrification, especially without dehydration. If freezing occurs only below the ice frost point, the primary contributor to denitrification is actually sedimentation of liquid-phase PSC particles. The mechanism of a second freezing process, occurring above the ice frost point, cannot yet be conclusively determined. Of the cases considered, heterogeneous freezing of the aerosol to form nitric acid trihydrate (NAT) particles best reproduced solid-phase PSC formation and observations of widespread denitrification with limited dehydration. The simulations constrain the number

of frozen particles to be near either 0.02% or 1% of the total aerosol number; values between 0.02% and 1% produce more intense denitrification than observed, demonstrating that small changes in the number of frozen particles could exacerbate denitrification. However, this result was contingent upon assuming that the heterogeneous nuclei remain active, producing PSCs throughout the winter. An idealized homogeneous freezing process was also able to produce NAT PSCs and denitrification (rates of 10^6 – 10^7 per cubic centimeter per second ($\text{cm}^{-3}\text{s}^{-1}$) compared favourably with data), but differed from observations in one key aspect: denitrification was more frequently accompanied by dehydration. Nitric acid dihydrate (NAD) particles were less effective than NAT at denitrification, but heterogeneous freezing of 0.1% of the aerosol yielded results marginally consistent with measurements. An important limitation of all the scenarios considered, however, is that they produced more intense and more widespread dehydration than was observed. This suggests that model minimum temperatures (from United Kingdom Meteorological Organization (UKMO) analyses) were too cold by 1 to 3 K.

Research on this topic continues in order to further characterize the freezing processes. Simulations are being conducted using recent laboratory measurements on the homogeneous freezing rates of liquid solutions to form NAD and NAT. These laboratory rates are also being extrapolated in order to understand in detail how heterogeneous freezing may occur in the stratosphere.

Collaborators on this project were M. R. Schoeberl, Goddard Space Flight Center, and E. V. Browell, Langley Research Center.

Point of Contact: K. Drdla
(650) 604-5663
Katja.Drdla-1@nasa.gov

Precipitation Condensation Clouds in Substellar Atmospheres

Andrew Ackerman

Condensation clouds of silicate and iron in brown dwarfs, and water in extrasolar giant planets likely play a leading-order role in the emitted (and reflected) spectra from these objects. Until now, a theoretical model has not been available to calculate the vertical profile of condensate opacity in the atmospheres of these objects, which is a critical component of any model of their emergent (and reflected) spectra. Such a model has been developed that predicts the vertical profile of condensate mass and its distribution over particle size.

The model assumes a steady-state balance between turbulent mixing (upwards) of vapor and condensate and sedimentation of condensate (downwards), in which the vapor concentration is limited to not exceed the saturation vapor pressure. The sedimentation rate is scaled to the convective velocity scale by a prescribed dimensionless parameter, f_{rain} , which is also tied to the modal radius of condensate particles (assumed to follow a log-normal size distribution). Measurements and model simulations of terrestrial clouds show that f_{rain} is less than unity for stratocumulus, but increases to much greater values for deeper convection such as found in the trade cumulus regime. High values of f_{rain} are expected

for skewed circulations (narrow updrafts, broad downdrafts) and/or small concentrations of condensation nuclei.

Calculations from the model with measurements of the ammonia cloud on Jupiter find agreement for moderate values of f_{rain} (~ 3). The measurements are rather uncertain, but the model is able to fit numerous independent constraints, including cloud physical thickness, optical depth, and average particles size.

Also in this study, theoretical cloudy atmospheres in brown dwarfs and an extrasolar giant planet were computed. The model is able to reproduce the measured color trend (a blueward shift) for the transition between L and (cooler) T dwarfs (see Figure 1). Sedimentation in the model limits the physical thickness of the silicate (and iron) clouds, allowing these clouds to sink below the visible atmosphere (chromosphere) for progressively cooler brown dwarfs. The model fits the data reasonably well for values of f_{rain} between 3 and 5, though the blueward shift in the observations is more extreme than the model is able to reproduce. It is hypothesized that the appearance of holes as the clouds descend into the troposphere (where convection is

expected to be strongest) provides for a more rapid blueward shift than the horizontally homogeneous model is able to explain. A simple treatment of fractional cloudiness will be added to the model to address this issue.

Mark Marley, SST branch, collaborated on this project.

Point of Contact: A. Ackerman
(650) 604-3522
Andrew.S.Ackerman@nasa.gov

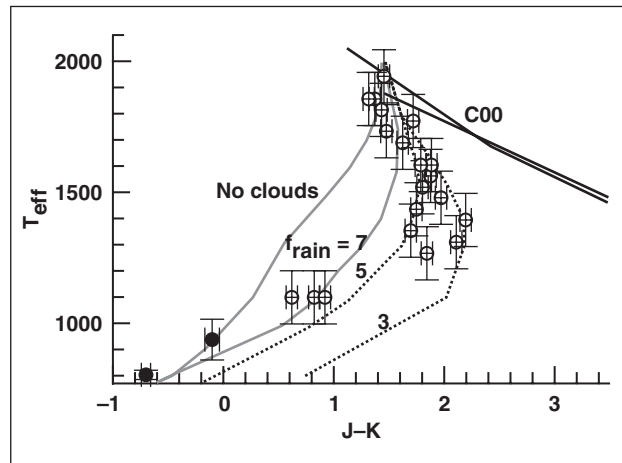


Fig. 1. J-K color of brown dwarfs as a function of effective temperature. Measurements are shown as symbols; the prototypical T-dwarf Gliese 228 B is shown as a filled symbol. Four cases are shown for the present model: evolution with no clouds, and with clouds with different values of the model parameter f_{rain} (as given). Also shown are color trends (for objects of 30 and 60 Jupiter masses) from the Chabrier model, denoted "C00," in which there is no sedimentation. The lack of condensate sedimentation in that model results in an unrealistic redward trend (characteristic of a blackbody) in the transition regime between L and T dwarfs.

Quantitative Spectroscopy of Minor Constituents of the Earth's Stratosphere

Charles Chackerian, Jr., Lawrence P. Giver

The focus of this work has been on determining absolute line intensities for the carbon monoxide (CO) and nitric acid (HNO₃) molecules.

Very accurate measurements of CO have been made on the 3-0 and 2-0 vibrational bands. The results of these measurements have been combined with quantum-mechanical calculations of numerical wave functions to obtain a revised electric-dipole-moment function for CO. This function will soon be used to correct the many thousands of line intensities listed in the high-resolution transmission molecular ab-

sorption (HITRAN) database for normal CO and its important isotopic modifications. The results of this work are used where CO is monitored using infrared spectroscopy, when the sun is used in observations as a background light source, in modeling the atmospheres of cool stars such as brown dwarfs, and in the analysis of combustion sources.

The challenge in obtaining accurate intensity parameters for HNO₃ has been in obtaining a pure sample of gas. The thermal decomposition of HNO₃ occurs in a short period compared to the period

required to record a high-resolution interferogram. A pure gas sample has been obtained by synthesizing HNO_3 at the spectrometer and then flowing this gas through the spectrometer absorption cell while the interferogram was recorded. In this way, a high-quality set of high-spectral-resolution spectra between 800 per centimeter (cm^{-1}) and 3600 cm^{-1} were obtained. Also obtained were low-resolution (0.112 cm^{-1}) spectra over the same spectral region, which were analyzed for spectral absorptivity at

$\sim 0.056 \text{ cm}^{-1}$ intervals. This work on HNO_3 has relevance for its monitoring in the atmosphere and in interpreting the spectral signatures of aerosols and other species, which occur in overlapping spectral regions.

Point of Contact: C. Chackerian, Jr.
(650) 604-6300
cchackerian@mail.arc.nasa.gov

The Effect of Large Volcanic Eruptions on Arctic Ozone Loss and Recovery

Azadeh Tabazadeh, Katja Drdla

Eruptions with a volcanic explosive index (VEI) of 4 or higher produce significant stratospheric injections. Sulfur dioxide, the most important atmospheric component of volcanic emissions, is converted into sulfate aerosols after injection into the stratosphere. More than 100 eruptions with VEIs equal to or greater than 4 are thought to have occurred in the past 500 years. In Figure 1, the historical record of volcanic eruptions is inferred from the aerosol optical depth measurements. However,

only about half of all large eruptions are sulfur rich. Both the 1982 El Chichon (VEI = 4) and 1991 Mt. Pinatubo (VEI = 5) eruptions were sulfur rich, producing volcanic clouds in the stratosphere that lasted for many years. In Figure 2, the time evolution of the Pinatubo volcanic plume is shown 1 day, 1 month, and 2 months after the eruption. It is clear that volcanic aerosols are abundant in the Arctic region within a few months after the eruption. On the other hand, the relatively sulfur-poor eruption of Mt. St. Helens (VEI = 5) in 1980 contributed very little sulfate mass to the stratospheric aerosol layer. Overall, large sulfate-rich eruptions are common. Therefore, it is important to understand to what extent they could affect the Arctic ozone layer in the next 30 years or so while anthropogenic chlorine levels are still sufficiently high (~ 3 parts per billion by volume (ppbv)) to cause severe ozone depletion.

Model simulations have shown that the early rapid growth of the Antarctic “ozone hole” in the early 1980s may have been influenced in part by numerous large volcanic eruptions. The goal of this study is to explore how a large eruption could affect Arctic ozone loss processes, such as chlorine activation and denitrification, in a cold year within the

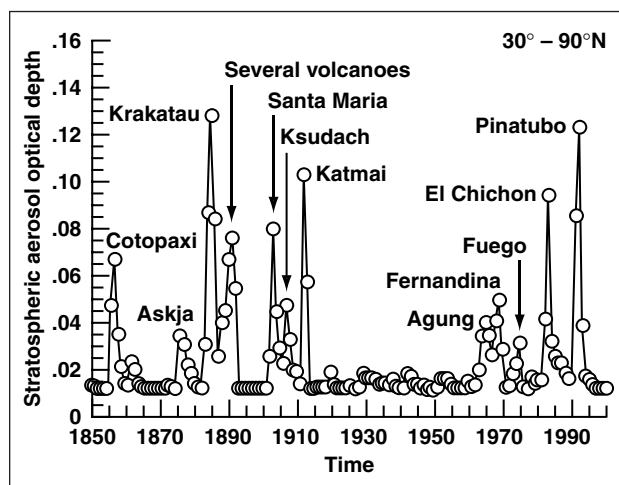


Fig. 1. The stratospheric aerosol optical depth (at $\lambda = 0.55$ micron) over time in the last 150 years.

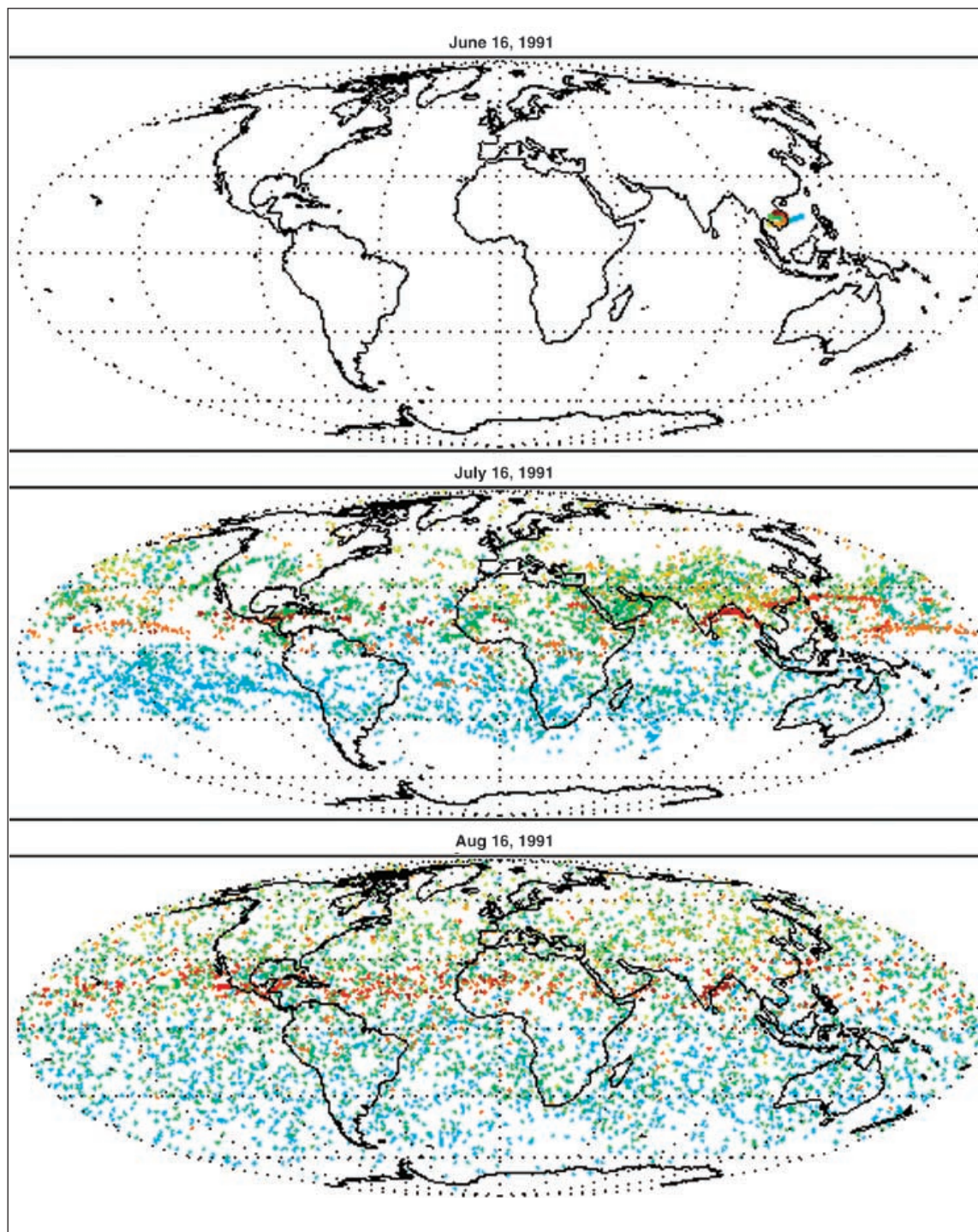


Fig. 2. Dispersal of the Mt. Pinatubo plume 1 day, 1 month, and 2 months after the eruption. It is clear that within a few months of the eruption, volcanic material (particularly at lower altitudes) was globally distributed in both hemispheres. The red and orange colors show plume dispersion at higher altitudes (above 20 kilometers (km)), whereas the green and blue colors show plume dispersion at lower altitude (below 18 km).

current range of natural variability. It is projected that the Arctic climate may be colder in the future as a result of greenhouse gas emissions and their buildup in the lower troposphere. Thus, investigated here is how a possible large eruption could affect ozone loss in a colder Arctic climate. In this project, a chemistry-microphysics model (the Integrated MicroPhysics and Aerosol Chemistry on Trajectories (IMPACT) model) is used to investigate how the

continuous presence of volcanic cloudy-like conditions in the Arctic can affect ozone loss processes, such as chlorine activation and denitrification, in a cold year such as the winter of 1999–2000.

Point of Contact: A. Tabazadeh
(650) 604-1096
Azadeh.Tabazadeh-1@nasa.gov

The Effect of Nitric-Acid Uptake on the Deliquescence and Efflorescence of Binary Ammoniated Salts in the Upper Troposphere

Jin-Sheng Lin, Azadeh Tabazadeh

Up to now laboratory experiments under upper tropospheric conditions have measured only the deliquescence and efflorescence relative humidities of binary ammoniated salts in the absence of gas-phase nitric acid. In this research a thermodynamic electrolyte model is used to examine how nitric acid (HNO_3), which is abundant in the atmosphere, can affect the deliquescence and efflorescence properties of binary ammoniated salts in the upper troposphere.

Traditionally the deliquescence relative humidity (DRH) for a binary salt is defined as the relative humidity at which a dry salt particle instantaneously turns into an aqueous solution droplet. In fact, many laboratory observations at or near room temperature show that binary salts do abruptly change phase at a fixed RH known as the DRH. However, in the atmosphere such a definition is too simple because a dried-up salt particle is exposed to other gaseous components (besides just H_2O vapor, which determines the RH) such as gas-phase HNO_3 . For example, previous research has shown that HNO_3 is not only highly soluble in an aqueous solution of ammonium sulfate ($(\text{NH}_4)_2\text{SO}_4$) at cold upper tropospheric temperatures, but it can interact with

ammonium and sulfate ions in the aqueous salt solution to form $(\text{NH}_4)_3\text{H}(\text{SO}_4)_2$ (letovicite). Letovicite is a new salt that cannot form in a pure aqueous $(\text{NH}_4)_2\text{SO}_4$ solution that is exposed only to gas-phase H_2O , because this salt formation requires the presence of H^+ in solution.

In Figure 1(a) the variation of the DRH is shown for the $(\text{NH}_4)_2\text{SO}_4$ system both in the presence and in the absence of gas-phase HNO_3 . The HNO_3 concentration ranges from zero to background (100 parts per trillion by volume (pptv)) and polluted (up to 2 parts per billion by volume (ppbv)) levels in the upper troposphere. The green line shows the standard DRH where the gas-phase HNO_3 is set to zero in the calculations, which is the condition used in all the laboratory experiments to date. The black lines show the effect on the DRH after HNO_3 is introduced into the gas phase. It is clear from the results shown in Figure 1(a) that HNO_3 can strongly affect the DRH behavior of the $(\text{NH}_4)_2\text{SO}_4$ system. Similar results are shown in Figure 1(b) for the ammonium hydrogen sulfate (NH_4HSO_4) system. Overall, the more HNO_3 gas phase in the atmosphere, the more it can affect the DRH behavior of the binary ammoniated aerosol system. In addition, as shown

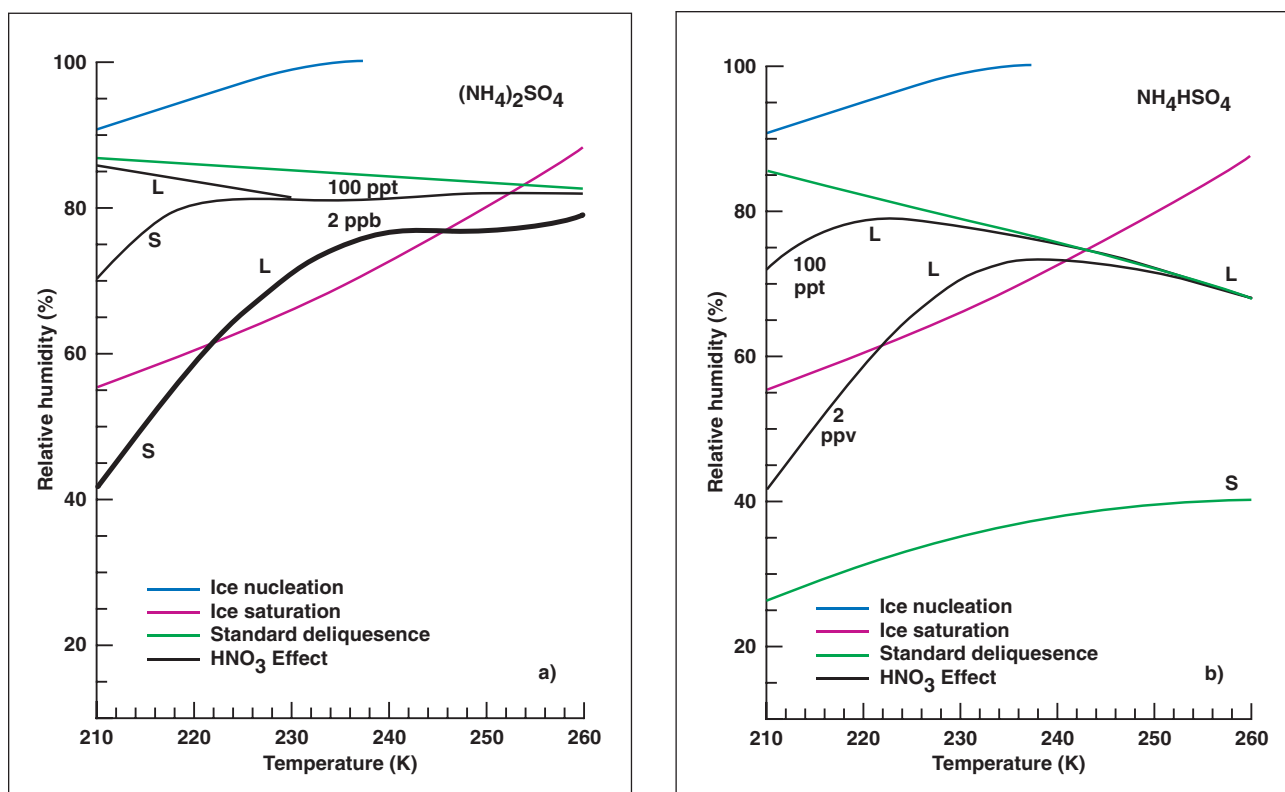


Fig. 1. The effect of HNO_3 uptake on the deliquescence of $(\text{NH}_4)_2\text{SO}_4$ (a) and NH_4HSO_4 (b) in the upper troposphere. The ice nucleation and ice saturation lines are marked on the plot. The green lines show the standard DRH behavior in the absence of HNO_3 . The black lines show the effect of HNO_3 uptake for a gas-phase mixing ratio of ~ 100 pptv and 2 ppbv. Lines marked as S show the point where the aqueous solutions first appears. Line L (in panels a and b) marks the point where letovicite will fully dissolve in the aqueous solution. Between the lines S and L the equilibrium system is mixed phase. Below the line labeled as S the dry salt will be composed of letovicite plus NH_4NO_3 and NH_4HSO_4 in panels a and b, respectively. See the text for more detail. Model calculations were performed using a fixed binary salt concentration of 10^{-9} mole per cubic meter (m^{-3}) (~ 100 ppt at 200 millibars (mb)) for all panels. The HNO_3 concentration was set to zero for the standard calculations and was varied from 1 (~ 100 ppt at 200 mb) to 20 (~ 2 ppbv at 200 mb) $\times 10^{-9}$ moles m^{-3} in the HNO_3 simulations. Note that in order to obtain the results shown, neither H_2SO_4 nor HNO_3 hydrates were allowed to form during the model simulations.

in Figure 1, there is no abrupt change in the physical state of the thermodynamic system (instantaneous change of a dry salt particle into an aqueous solution) at the deliquescent point, behavior typical for such a phase transition in the presence of only water vapor.

Exposure of ammoniated salts to nitric acid can also affect the efflorescence relative humidity (ERH) of binary ammoniated salts in the upper troposphere. Efflorescence is the RH at which a binary aqueous solution of a salt instantaneously turns into the crys-

talline state. Figure 2 illustrates how saturation ratios (crystalline) for $(\text{NH}_4)_2\text{SO}_4$ and NH_4HSO_4 , both at background mixing-ratio levels, change with relative humidity and HNO_3 concentration at 230 K. Crystalline states of a salt in solution can form only when the saturation ratio (SR) of the salt exceeds unity. As shown in Figure 2, SR of letovicite is higher than that of either of the binary salts in the aqueous solution by a factor of over 10 for RHs above 50%, indicating that the likelihood for letovicite to crystallize from these solutions is favored over the binary salts.

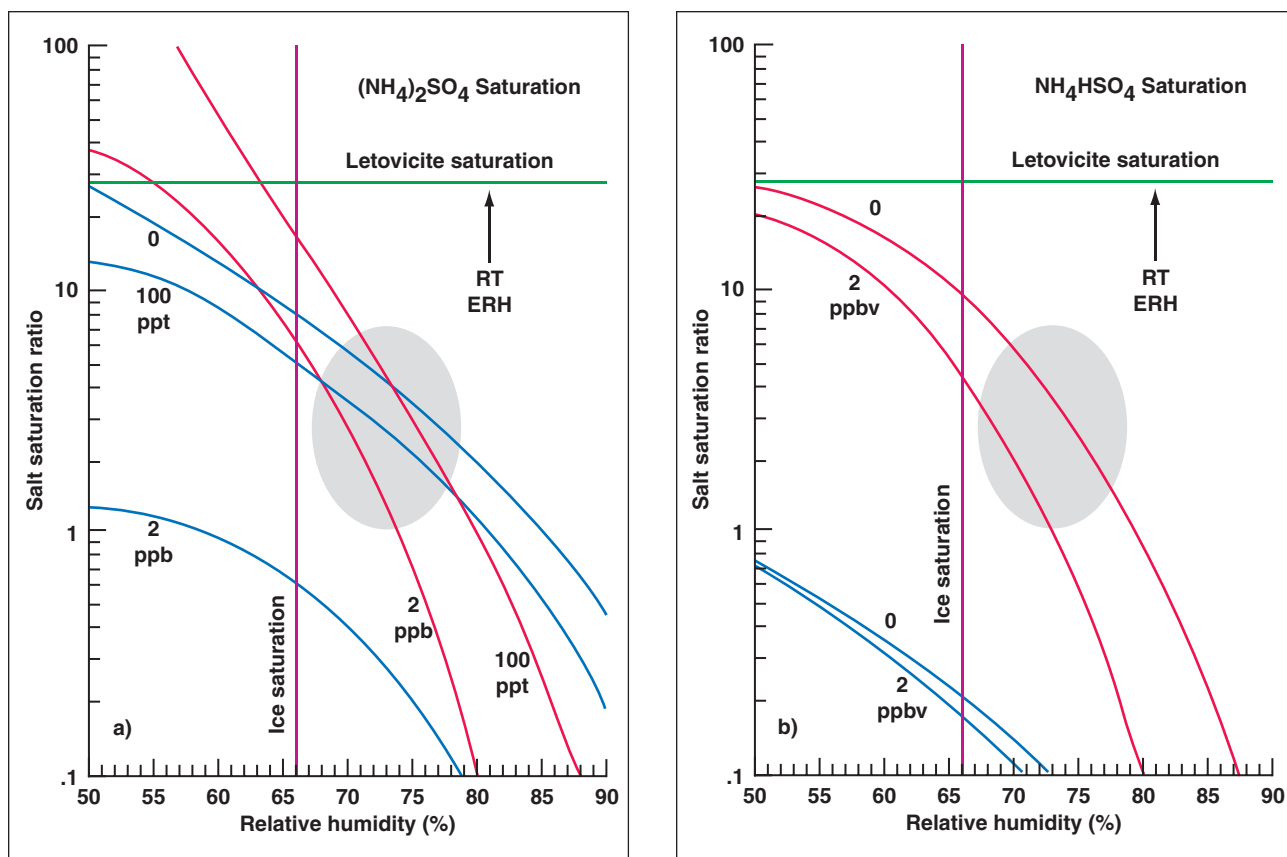


Fig. 2. The effect of HNO_3 uptake on the efflorescence of $(\text{NH}_4)_2\text{SO}_4$ (a) and NH_4HSO_4 (b) solution in the upper troposphere at 230 K. The variations in the salt saturation ratio as a function of RH are also shown. The room temperature (RT) ERH for both $(\text{NH}_4)_2\text{SO}_4$ and letovicite is shown as a dashed line. The ice saturation line at 230 K is also marked. The shaded area marks the region where both ice and ammoniated salts are saturated in the aqueous solution. See text for more detail. The model conditions used for binary salts and various HNO_3 concentrations are described in the caption for Figure 1. In order to obtain salt saturation ratios in solution, it is assumed that the solution was supercooled and, therefore, neither salts nor ice were allowed to form during the simulations.

The results of this work show that both the DRH and ERH of binary ammoniated salts in the upper troposphere are significantly impacted by gas-phase HNO_3 . The DRH cannot occur via the standard abrupt change in the physical state of the system (a salt particle quickly turning into an aqueous solution droplet). In addition, it will be unlikely for either $(\text{NH}_4)_2\text{SO}_4$ or NH_4HSO_4 to crystallize in upper tropospheric aerosol solutions. Instead, the crystalline state of both salts in the upper troposphere is letovicite, which can then coexist with an aqueous solution. Thus, the state of aerosols (containing both ammonium and sulfate ions) is

often mixed in the upper troposphere. Both the ice nucleating properties and the heterogeneous reactivity of upper tropospheric particles are dependent upon the aerosol solution phase and composition and, therefore, the effect of HNO_3 should be considered to accurately predict the physical state of ammoniated aerosol particles in the upper troposphere.

Point of Contact: J. Lin
(650) 604-5505
jlin@mail.arc.nasa.gov

The Runaway Greenhouse Effect on Earth and Its Implication for Other Planets

Maura Rabbette, Peter Pilewski, Christopher McKay (Code SST), Richard Young (Code SST)

The primary greenhouse gas in the Earth's atmosphere is water vapor, which is an efficient absorber of outgoing longwave infrared radiation. When surface temperature increases, increased evaporation of water from the surface further increases water vapor in the atmosphere, causing more of an atmospheric greenhouse effect. This in turn further increases the surface temperature. If this cycle continues unchecked, a runaway greenhouse effect occurs. Venus is thought to be an example where the runaway greenhouse caused the loss of essentially all water from the planet. The runaway greenhouse effect is also a factor in determining the habitable zone of extrasolar planets. Planet habitability is a principal topic in Astrobiology, a field for which Ames has major responsibilities. There is observational evidence that the runaway greenhouse effect may occur locally on Earth. Using Earth science satellite data and other in situ data, it is possible to model the signature of the runaway greenhouse effect. This will allow determination if, in fact, the

runaway greenhouse effect does occur locally on Earth. If so, key insights will be gained into the Earth's climatology, as well as the processes involved in determining planet habitability.

The process involves combing the vast oceanic and atmospheric data archives to retrieve measurements acquired with instruments and sensors on various platforms, including buoys, ships, radiosondes, high altitude aircraft, and satellite platforms. The retrieved global datasets give both spatial and temporal observations (including daily, weekly, and monthly averages) of sea surface temperatures, top of the atmosphere outgoing infrared flux to space, atmospheric humidity, and temperature profiles (Figure 1). The region that was considered covers a large area of the Pacific Ocean: longitude 150°E to 110°W, latitude 35°S to 35°N, subdivided into 2.5° x 2.5° grid boxes. This region is important because it includes the Pacific Warm Pool where the highest sea surface temperatures occur.

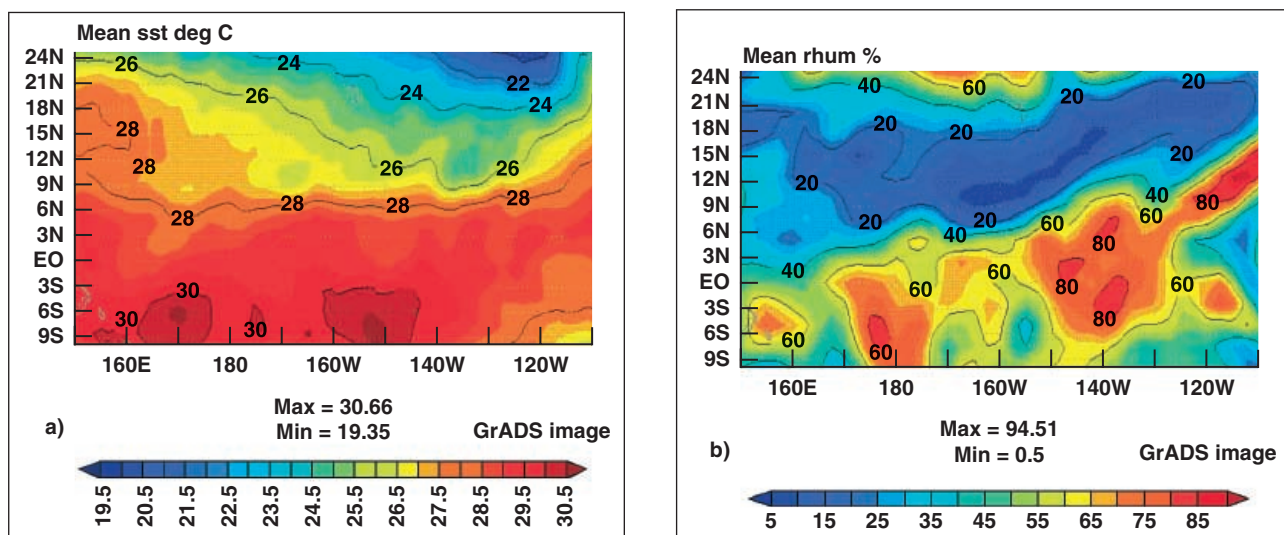


Fig. 1. A sample of satellite and in situ data used to model the runaway greenhouse effect. (a) Mean sea surface temperature, (b) Mean relative humidity for various atmospheric altitudes.

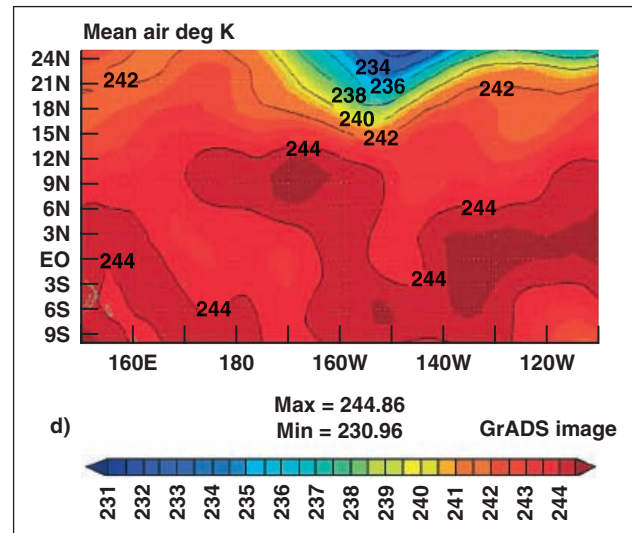
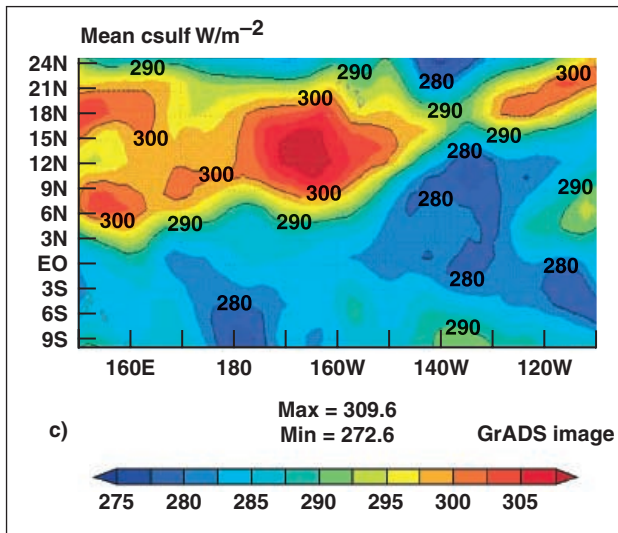


Fig. 1. Concluded. (c) Mean clear-sky upward longwave flux, (d) Mean air temperature for various atmospheric altitudes.

Point of Contact: M. Rabbette
(650) 604-0128
mrabbette@mail.arc.nasa.gov

REPORT DOCUMENTATION PAGE			Form Approved OMB No. 0704-0188	
Public reporting burden for this collection of information is estimated to average 1 hour per response, including the time for reviewing instructions, searching existing data sources, gathering and maintaining the data needed, and completing and reviewing the collection of information. Send comments regarding this burden estimate or any other aspect of this collection of information, including suggestions for reducing this burden, to Washington Headquarters Services, Directorate for Information Operations and Reports, 1215 Jefferson Davis Highway, Suite 1204, Arlington, VA 22202-4302, and to the Office of Management and Budget, Paperwork Reduction Project (0704-0188), Washington, DC 20503.				
1. AGENCY USE ONLY (Leave blank)		2. REPORT DATE June 2003		3. REPORT TYPE AND DATES COVERED Technical Memorandum
4. TITLE AND SUBTITLE Ames Research Center Research & Technology Report 2001			5. FUNDING NUMBERS	
6. AUTHOR(S) Ames Investigators				
7. PERFORMING ORGANIZATION NAME(S) AND ADDRESS(ES) Ames Research Center Moffett Field, CA 94035-1000			8. PERFORMING ORGANIZATION REPORT NUMBER A-0208287	
9. SPONSORING/MONITORING AGENCY NAME(S) AND ADDRESS(ES) National Aeronautics and Space Administration Washington, DC 20546-0001			10. SPONSORING/MONITORING AGENCY REPORT NUMBER NASA/TM-2003-211405	
11. SUPPLEMENTARY NOTES Point of Contact: Dr. Stephanie Langhoff, Chief Scientist, Ames Research Center, MS 230-3, Moffett Field, CA 94035-1000 (650) 604-6213 or contact the person(s) designated as the point of contact at the end of each article.				
12a. DISTRIBUTION/AVAILABILITY STATEMENT Unclassified — Unlimited Subject Category 99 Distribution: Nonstandard Availability: NASA CASI (301) 621-0390			12b. DISTRIBUTION CODE	
13. ABSTRACT (Maximum 200 words) This report highlights the research accomplished during fiscal year 2001 by Ames Research Center scientists and engineers. The work is divided into accomplishments that support four of NASA's Strategic Enterprises: Aerospace Technology, Space Science, Biological and Physical Research, and Earth Science. The primary purpose of this report is to communicate knowledge—to inform our stakeholders, customers, and partners, and the people of the United States about the scope and diversity of Ames' mission, the nature of Ames' research and technology activities, and the stimulating challenges ahead. The accomplishments cited illustrate the contributions that Ames is making to improve the quality of life for our citizens and the economic position of the United States in the world marketplace.				
14. SUBJECT TERMS Aeronautics, Space transportation, Space science, Earth science, Life science, Information technology, Research and technology.			15. NUMBER OF PAGES 240	
			16. PRICE CODE	
17. SECURITY CLASSIFICATION OF REPORT Unclassified	18. SECURITY CLASSIFICATION OF THIS PAGE Unclassified	19. SECURITY CLASSIFICATION OF ABSTRACT Unclassified	20. LIMITATION OF ABSTRACT	